The development of biomedical instrumentation using backscattered laser light

Nicholas J. Barnett (1990)

THE DEVELOPMENT OF BIOMEDICAL INSTRUMENTATION USING BACKSCATTERED LASER LIGHT

NICHOLAS JAMES BARNETT

A thesis submitted in partial fulfilment of the requirements of the Council for National Academic Awards for the degree of Doctor of Philosophy

October 1990

Oxford Polytechnic in collaboration with
I.C.I. Pharmaceuticals, Alderley Edge, Cheshire.

ACKNOWLEDGEMENTS

I would like to thank all my family, friends and colleagues who have supported me during the last three years of research.

I am grateful for all the help provided by the Cardiovascular Group at I.C.I Pharmaceuticals. All in vivo surgery and animal preparation was performed by ICI employees with appropriate Home Office licenses. My special thanks to Steve Pettinger for his enthusiastic supervision throughout the project.

I greatly appreciate the thoughtful guidance given by Dr. Geoff Dougherty, Director of Studies, especially his valuable comments during the writing of this thesis.

I would also like to thank Dr. Dave Boggett, Geoff Ward, and Dr. Andy Obeid for the interest they have shown and the many useful discussions and ideas.

Thanks also to Moor Instruments, Nellcor, and Perimed for allowing me to borrow certain items of equipment for my studies.

Finally, I am indebted to Anna for her support, encouragement and understanding throughout the project.

ABSTRACT

This thesis is concerned with the measurement of blood flow and oxygen saturation in the microcirculation using the techniques of laser Doppler flowmetry and pulse oximetry.
An investigation of the responses of Doppler flowmeters using different signal processing bandwidths and laser sources revealed two major findings. Firstly, that careful choice of processing bandwidth is required in order to sample the whole range of possible Doppler frequencies present in the backscattered light. Secondly, that the choice of laser source is important in governing the output stability of a flowmeter. Another investigation focused on the evaluation of a dual channel laser Doppler flowmeter using both *in vitro* and *in vivo* models. It was demonstrated that the instrument permitted a useful method of obtaining flow information by comparing simultaneous responses at experimental and control sites.
The choice of laser wavelength was investigated in a study to determine whether blood flow measurements are obtained from different depths within the skin tissue. The results indicate that some depth discrimination is obtainable using instruments operating at different wavelengths, however it is difficult to demonstrate the effect *in vivo*.
In a separate study it was shown that pressure applied to the skin surface greatly affects the underlying blood flow. It is recommended that care has to be taken when positioning Doppler probes on the skin.

A reflection pulse oximeter was developed using laser light backscattered from the skin. The instrument was evaluated *in vitro* and *in vivo* by comparing desaturation responses with a commercial transmission pulse oximeter. The reflection oximeter was demonstrated to reliably follow trends in oxygen saturation but several problems prevented instrument calibration.
Finally, a device combining laser Doppler flowmetry with reflection pulse oximetry was developed and used *in vivo* to follow trends in blood flow and oxygen saturation from the same tissue sample.

TABLE OF CONTENTS

CHAPTER 1

Introduction

1.1 A Guide To The Thesis

This thesis investigates non-invasive optical techniques for monitoring microvascular blood flow and oxygenation by detecting laser light backscattered from the skin. In **Chapter One** emphasis is placed on the need for non-invasive monitoring techniques and consideration given to applications where they may be of most use. There follows a general introduction to the techniques of laser Doppler flowmetry and pulse oximetry describing how they may provide information concerning skin nutrition. The basic structure and physiology of skin tissue is introduced then finally an outline of the optical properties of the tissue volume sampled by the monitoring techniques is presented.

Chapter Two concentrates on methods of monitoring tissue blood flow. There is a brief review of microvascular flow measurement techniques. A literature review describes how the laser Doppler technique has developed over the last two decades. The final section covers the theory of the laser Doppler technique.

The next three chapters cover several laser Doppler flow studies. The objective of **Chapter Three** is to evaluate a dual channel Laser Doppler system using an *in vitro* model and by monitoring the vaso-dilating effects of a drug *in vivo;* **Chapter Four** investigates the effect of applying pressure on the skin surface and monitoring the consequent changes in blood flow; and **Chapter Five** aims to demonstrate the possibility of obtaining depth discrimination in laser Doppler measurements by using different wavelength lasers.

Chapter Six considers measurements of blood oxygenation. There is a brief overview of some of the methods used to measure either the partial pressure of oxygen or the oxygen saturation of blood. The theory of pulse oximetry is

explained and a literature review covering the major developments in pulse oximetry technology is presented.
The objective of **Chapter Seven** is to demonstrate the design and development of a pulse oximetry system incorporating two different wavelength lasers. Measurements are described using transmission and backscattered modes of operation and methods of improving instrument sensitivity are investigated.
The aim of **Chapter Eight** is to develop an instrument that combines the two techniques of laser Doppler flowmetry and pulse oximetry permitting measurements from the same tissue sample volume.
Finally, **Chapter Nine** contains a summary of the thesis and recommendations for further research.

1.2 The Motivation For Monitoring Microvascular Blood Flow And Oxygenation

Non-invasive methods for quantifying skin blood flow and tissue oxygenation on a regional basis are required for both general clinical measurements and medical research studies.
Skin blood flow measurements may provide useful information in a variety of experimental studies concerning the investigation of peripheral vascular disease. Cardiovascular disease is the largest single cause of deaths in the majority of the developed countries. This includes diseases which affect the heart directly and others which predominantly affect the vascular system. Hypertension (high blood pressure) may lead to heart failure, coronary heart disease, or kidney failure whereas arteriosclerosis (hardening of the arteries) may lead to arterial wall damage and result in vessel occlusion. Arterial occlusion or narrowing of the arteries in the legs and feet results in claudication or even gangrene; in the heart, it results in myocardial ischaemia or infarction; and in the brain, it results in a stroke.
Peripheral arterial disease develops due to a reduction of

arterial blood flow to the legs and feet. It manifests itself by severe leg pains, intermittent claudication (where the increased demand for blood during exercise cannot be met), resting pain, and in the more advanced stages, the onset of ulceration and finally gangrene. If cases of such occlusive diseases go undetected for a long period of time the affected tissue may have to be amputated. To avoid this, the disease has to be detected in its early stages so that patients can be treated effectively.

Although there is no general theory for the development of vascular disease the disease process is often manifested in the peripheral microvascular circulation. Changes in red blood cells, vessel wall properties and nervous innervation of vessels due to disease are likely to be displayed by changes in the ability of the blood to perfuse the microcirculation and this can be revealed by transcutaneous monitoring techniques.

By monitoring the perfusion at the skin surface techniques can often be used to predict the onset of disease. The effects of both drug and physical interventions can be monitored and the measurements used to predict the severity of disease.

Microvascular disorders may sometimes be caused by some other generalized illness. For example, one of the major complications with diabetes mellitus is the occurrence of peripheral arterial disease. In diabetics the red blood cells become less flexible than usual, there is increased friction between the blood cells and vessel walls, and the blood becomes less able to flow through the capillary network. Together with the neuropathy often associated with diabetes, this can lead to small vessel disease and vascular damage.

Several skin diseases may be investigated by observing the effect of external influences, procedures and manoeuvres on the microvascular perfusion. For example, by studying changes in peripheral perfusion due to changes in posture, monitoring techniques have been used to discriminate between

different stages of peripheral arterial disease such as claudication and impending gangrene (Belcaro et al., 1989).

In addition to investigating peripheral vascular disease the monitoring of the microcirculation can also be used to assess drug reactions and study tissue blood flow control mechanisms. It may be used to investigate a number of other diseases such as psoriasis, sickle cell disease and Raynaud's phenomenon. There are also a number of applications in assessment of tissue viability in areas of burn injury, plastic surgery, and general wound healing.

The transport of oxygen to the tissue cells is vital for the tissue to remain healthy. Several monitoring techniques have been developed to measure blood oxygenation which can be indicated either by the partial pressure of oxygen (pO_2) or by the oxygen saturation of haemoglobin (SO_2). Arterial pO_2 and SO_2 (written as p_aO_2 and S_aO_2 respectively) are both good indicators of blood oxygenation. Generally the partial pressure determines the diffusion of oxygen to the tissues whereas the oxygen saturation indicates the degree of binding of oxygen onto haemoglobin.

Measurements of blood oxygen saturation have become routinely available using pulse oximetry. The application of the technique has been mainly in situations where there may be sudden unexpected changes in the blood oxygenation. Examples include, monitoring during anaesthesia, in intensive care units, and in preterm and neonatal special baby care units.

Preterm infants are especially susceptible to respiratory illness since their breathing mechanisms are not fully developed. In such cases oxygen levels may fall to such a level that brain damage may result or the child may die. Large variations in blood oxygenation may occur within a matter of a few minutes and intermittent measurements by blood gas machines may miss hypoxic events. Pulse oximetry allows continuous monitoring and hence improved detection of

hypoxic events.
As a diagnostic tool, measurement of the blood oxygen saturation in the peripheral arterioles rather than the main arteries would provide an indication of localized blood oxygenation and would greatly increase the nutritional information available to the clinician. By combining measurements of perfusion and oxygenation a better understanding of microcirculation physiology and nutritional supply mechanisms would be provided which would help in diagnostic procedures. The general understanding of both normal and diseased skin states may be enhanced aiding disease management.
A combined instrument may also have applications in other areas of research, for example, as well as SO_2 monitoring there is also a clinical need for continuous blood flow assessment during acute patient care where both oxygenation and perfusion are of primary concern.

1.3 A General Introduction To The Optical Techniques

1.3.1 The laser Doppler technique

Laser Doppler flowmetry is a non-invasive method for monitoring the flow of red blood cells (rbcs) in tissue microcirculation.
Low power laser light (usually < 5 mW) is directed toward the tissue using an optical fibre. Some of the light incident on the tissue is reflected off the top surface. However the majority enters the tissue where a complex process of scattering and absorption takes place. Photons scattered by moving rbcs undergo a shift in frequency that is proportional to the speed of the rbc movement as described by the Doppler effect. Backscattered laser light is collected by a second optical fibre which directs the light onto the surface of a sensitive photodetector. A process of optical mixing takes place on the surface of the photodetector creating a range of beat frequencies which are

apparent in the photocurrent signal.
The range of optical (Doppler) beat frequencies can be observed using a spectrum analyser or can be processed electronically to generate a continuous output signal related to blood flow within the measuring volume. Several laser Doppler flowmeters are commercially available allowing laboratory investigations and clinical bedside monitoring of microvascular blood flow. These laser Doppler flowmeters produce a real-time output that is sensitive and responsive to the flux (viz. the mean rbc velocity multiplied by the mean rbc concentration) of moving rbcs.

1.3.2 Pulse oximetry

Pulse oximetry is a non-invasive optical technique for monitoring the oxygen saturation of arterial blood. Measurements are usually performed by transilluminating a volume of tissue such as the ear or finger. The technique essentially measures the change in light transmitted through the skin as a consequence of the pulsation of arterial blood through the tissue.
Usually the optical probe consists of two different wavelength light emitting diodes and a photodetector. The intensity of the light passing through the tissue depends on the attenuating properties of the tissue and blood constituents within the illuminated volume. The detected signal can be separated into pulsatile and non-pulsatile components. It is assumed that the arterial blood is the only contributor to the pulsating component and can therefore be uniquely identified.
Light attenuation depends to a great extent on the apparent colour of the blood passing through the sample volume which in turn depends on its state of oxygenation. By comparing the amplitudes of the different wavelength pulsatile signals the arterial oxygen saturation can be calculated.

1.3.3 Combining laser Doppler and pulse oximetry measurements

Laser Doppler flowmetry has been demonstrated to be a useful method for monitoring microvascular blood flow. It can be used to provide information of the blood perfusion at a specific measuring site and therefore indicate the general state of health of the tissue volume under investigation.
One of the most important functions of the blood circulation is to transport oxygen from the alveolar capillaries to the peripheral tissue capillaries where it is required for metabolism. For an area of tissue to survive a good nutritional supply has to be maintained. This depends on both the perfusion of blood and the oxygen-carrying capability of the rbcs. Laser Doppler measurements give an indication of microvascular blood flow alone and no indication of the amount of oxygen being transported to the tissue bed. A better indicator of nutritional supply to tissues would be obtained if both blood perfusion and oxygenation were to be monitored simultaneously, ideally from the same volume of tissue.
This thesis is concerned with the optical techniques of laser Doppler flowmetry and pulse oximetry and their application to monitoring blood flow and oxygenation.
Laser Doppler flowmetry has been used in several studies to record fetal scalp blood flow during labour (Smits et al., 1989; Smits and Aarnoudse, 1984). One application of a combined reflection mode instrument would be to simultaneously monitor the blood flow and oxygenation from the fetal scalp.

1.4 Skin Structure And The Microcirculation

The skin functions as a tough, flexible and waterproof layer on the surface of the body. It provides protection for the underlying tissue and a means of controlling body temperature. The thickness and structure of the skin varies

considerably with age, sex, race, degrees of nutrition and region on the body. Nevertheless, some general comments can be made about its construction.
There are two main layers of skin tissue - the epidermis and the dermis, figure 1.1.

1.4.1 Epidermis

The epidermis is the uppermost layer of skin consisting predominantly of a thick keratin region free from any blood vessels. The epidermis can be differentiated into different layers, the most superficial being the stratum corneum which has an average thickness of 30 μm and consists mainly of dead cells. The deepest region of the epidermis, where it borders with the dermis, is called the basal layer. This layer consists of a row of actively dividing cells containing some melanin pigment responsible for the colour of the skin. This basal layer continually renews living cells which are slowly pushed outwards towards the stratum corneum. The thickness of the epidermis varies widely from region to region on the body, often thickest at the fingertips where it may exceed 350 μm (Whiton and Everall, 1973).

DIAGRAM ON THIS PAGE IS EXCLUDED UNDER INSTRUCTION FROM THE UNIVERSITY

Figure 1.1. Cross-section through the skin showing the main tissue layers and blood vessels (from Obeid (1989)).

1.4.2 Dermis

The dermis is a region of connective tissue rich in collagen and elastic fibres that lies directly beneath the epidermis. It provides strength and elasticity to the skin and brings nutrients to the epidermis through its complex vasculature. The dermis may also be divided into two layers - the papillary layer and the reticular layer. The papillary layer contains the dermal papillae, a number of connective tissue fibrils containing the capillary network. The papillae form a pattern of undulating ridges on the underside of the epidermis allowing the nutrients carried by the blood to be passed to the basal layer where new cells are formed. The reticular layer is deeper and made up of dense collagenous connective tissue. It contains the vessels that supply and drain the highly profuse network of arterioles, capillaries and venules.
Below the dermis is subcutaneous tissue the onset of which may be identified by large blood vessels, nerves, fat and muscular layers that it contains.

1.4.3 Skin vasculature

Blood carries oxygen and other nutrients to the tissues, and carbon dioxide and other waste products away from them. It is transported around the body by a vast network of arterial and venular vessels, the general pattern and structure of which are now described.
Arteries, approximately 100 μm in diameter pass through the deep dermis of the skin. These vessels have a continuous muscle coat and thick elastic walls. The inside walls are lined with endothelial cells which minimize frictional resistance to blood flow. As they pass through the lower dermis each artery divides into smaller diameter vessels running vertically into the mid-dermis where they divide again. In the mid-dermis the vessels are about 50 μm in diameter and have only a single layer of smooth muscle

cells. This muscle layer gradually becomes discontinuous and the vessels are then defined as arterioles. When the upper dermis is reached the vessel diameter is reduced to approximately 15 μm, the vessels have no muscle coating and are defined as capillaries. The capillaries branch out horizontally such that they lie parallel to the skin surface. In some cases two layers of vessels may be distinguished - a superficial and deep horizontal plexus. Vertical capillary loops branch out from the sub-papillary plexus and supply blood to the papillae. Typically each papilla contains only one such capillary. Each papillary loop is between 0.2 and 0.4 mm long and supplies nutrients to between 0.04 and 0.27 mm^2 of skin surface (Ryan, 1973). Moving away from the papillae the vessels increase in diameter and lead to a system of venules. The venules are more numerous than arterioles within the upper dermis and have a range of different diameters. In the upper and mid-dermis the diameters are usually between 40 and 60 μm whereas in the deeper tissues they may range from 100 to 400 μm. As the venules increase in diameter the amount of muscle coating increases and once a continuous muscle coating is formed the vessels are defined as veins. Generally the veins are thinner walled than arteries of the same diameter.

1.4.4 Properties and constituents of blood

The blood serves as a transport medium carrying nutrients from the digestive tract to the tissues, end products of metabolism from the cells to the organs of excretion, oxygen from the lungs to the tissues and carbon dioxide from the tissue to the lungs. It helps to regulate body temperature, maintain a constant concentration of water and electrolytes in the cells and defend against microorganisms.
The blood consists of white blood cells (leucocytes) , red

blood cells (erythrocytes) and platelets (thrombocytes) suspended in a fluid called plasma. The red blood cells are biconcave, circular discs with a mean diameter of 5 μm. They are flexible and capable of undergoing changes in shape while passing through some of the smaller diameter capillaries. White blood cells (wbcs) are larger but much less numerous than the rbcs, with approximately 550 rbcs to one wbc. Various kinds of white cell exist carrying out separate functions mainly to defend the body from harmful bacteria.

The haematocrit of blood is defined as the percentage volume of packed cells in whole blood after a blood sample has been centrifuged. Values are typically between 38 and 45% in the major vessels. The packed cell volume (p.c.v.) or volume fraction of cells is similar to the haematocrit but defines the percentage of the tissue volume occupied by rbcs. The majority of skin tissue has a p.c.v. of less than 0.5%.

1.4.5 Haemoglobin and oxygen transport

Haemoglobin is the normal pigment of rbcs. The haemoglobin molecule is able to undergo a reversible reaction with oxygen allowing oxygen to be absorbed where the oxygen concentration is high and released where the concentration is low. During the passage of rbcs through the pulmonary capillaries surrounding the alveoli haemoglobin combines with oxygen to produce oxyhaemoglobin. The oxygen is carried through the vascular network until it passes into the systemic capillaries in areas of tissue where it is required for metabolism. The oxygen is released and the oxyhaemoglobin reverts to haemoglobin. The colour of the blood depends on the concentration of haemoglobin and oxyhaemoglobin present. When oxygenated blood appears bright red but reduced haemoglobin causes it to appear dark red.

Other haemoglobin derivatives exist. Carboxyhaemoglobin is formed due to the carbon monoxide present in inhaled air. The affinity of haemoglobin for carbon monoxide is 250 times

greater than for oxygen. Its formation prevents oxygen from being taken up and thus interferes with the oxygen supply to tissues. Methaemoglobin is sometimes present due to hereditary factors or may be induced by a number of drugs including local anaesthetics (benzocaine), nitrates (nitroglycerin), nitrites or sulfonamides. Levels of carboxyhaemoglobin are significantly higher in cigarette smokers than in non-smokers. Also since tobacco smoke contains both nitric oxide (NO) and nitrogen dioxide (NO_2) higher levels of methaemoglobin have been reported in subjects that smoke. Typical levels of dyshaemoglobins in smokers and non-smokers measured using a CO-oximeter have been reported by Imbriani et al. (1987).

Mean values and standard deviations () for levels of dyshaemoglobins reported by Imbriani et al. (1987).

parameters	non-smokers	smokers
%MetHb	0.56 (0.3)	0.63 (0.3)
%COHb	1.82 (0.8)	4.17 (2.2)
%OxHb	96.1 (1.2)	93.8 (2.3)
No. of subjects	479	377

The presence of either methaemoglobin or carboxyhaemoglobin influences the optical absorption of blood and is therefore of special interest in pulse oximetry as they can lead to overestimation of the oxygen saturation (Barker et al., 1989).

1.4.6 Blood flow in the microcirculation

The life of every body cell depends on an adequate blood supply. In order to force blood throughout the whole capillary system a high pressure must be developed by the heart. The arterial side of the vascular system has a pressure of between 30 and 120 mmHg whereas the venous side has a lower pressure of between 5 and 10 mmHg.
The flow can be regulated either via nerve fibres

controlling smooth muscle cells in the walls of the arterial vessels, or by locally released compounds such as histamines and catecholamines. The capillaries are non-muscular and therefore have no major control of flow. Instead capillary flow is regulated by precapillary sphincters, elongated muscle cells coiled around the arterioles. Blood flow to the capillary beds may be increased by widening the cross sectional area of the arterial vessels (vaso-dilation) or decreased by vessel narrowing (vaso-constriction).

In a number of tissue beds apparently spontaneous abrupt changes in the rate of blood flow may be observed. This process of vasomotion is defined by the maximum number of changes in flow rate per minute. There are usually between 2 and 6 changes per minute but in disorders such as hypertension the rate may be higher.

Thermoregulation may also be controlled using a shunting network that exists in the dermis of the extremities such as the hands and feet. Heat loss may be controlled by shunting blood through vessels called arteriovenous anastomoses (AV shunts) connecting arterioles directly to venules. Opening the AV shunts diverts blood away from the capillaries and the volume of flow through the AV shunts is increased. In this way a large volume of blood passes close to the skin surface and there is increased heat loss. Alternatively, to prevent heat loss the AV shunts close and the volume of blood flowing near the skin surface is reduced, figure 1.2.

Blood is transported rapidly to and from the capillaries but the flow rate in the capillary network is only a fraction of the rate in large arteries. Capillary blood flow is slow (usually less than 4 mms^{-1}) and non-uniform. The rbcs can hardly pass through some of the smallest vessels and usually pass through in bolus flow where they orient themselves into single file separated by volumes of plasma. The volume fraction of rbcs to blood volume is much less in the capillaries than in the larger blood vessels. Lipowsky et al. (1980) demonstrated a fall in haematocrit from

approximately 31.3% in the 70 μm arterioles to 8.4% at the "true capillary" level in the microcirculation of the cat. The excess of plasma may be due to the remaining rbcs passing through AV shunts or other preferential flow channels.

There is a close packed capillary network allowing every tissue cell to be close to slow moving blood. A large surface area exists for the exchange of materials from the blood to the tissue. Nutrients leave the blood and enter the tissues through the thin walls of the capillaries by diffusion and ultrafiltration. At the same time waste products leave the tissues and enter the blood by diffusion and osmosis.

A process of autoregulation takes place within the microvascular network depending on the metabolic requirement at individual tissue sites. For example, microcirculatory control may be observed when the blood supply to a tissue bed is totally occluded for a brief interval. The increase in blood flow in the post occlusion period (reactive hyperaemia) is due to the deficiency of nutrient supply caused by the occlusion. The accumulation of waste products and the depletion of oxygen have to be remedied so there is an increase in blood flow to the region when the occlusion is released. The intensity and duration of the hyperaemia are directly related to the duration of occlusion.

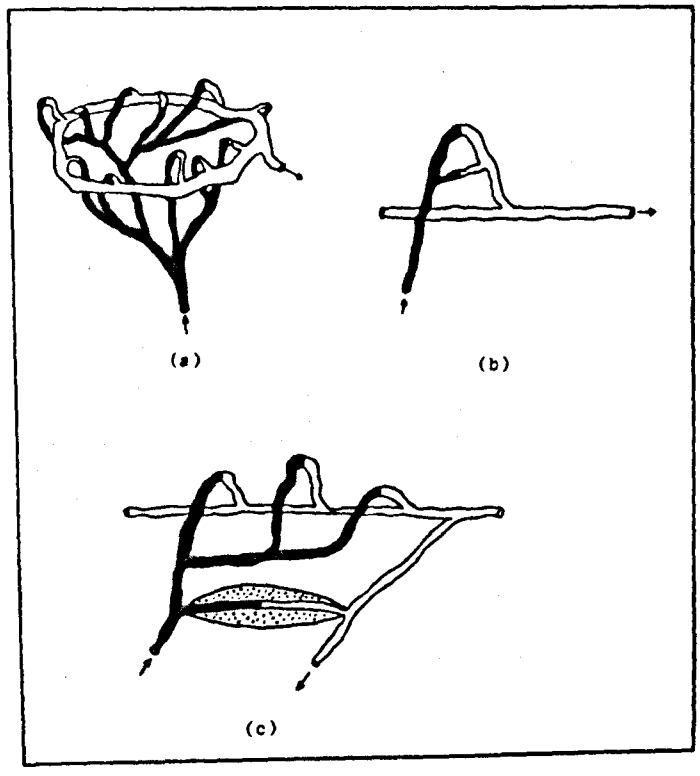

Figure 1.2. Blood can be shunted through several preferential channels including, (a) the subpapillary plexus, (b) a simple capillary alternative channel and, (c) a muscle controlled arteriovenous shunt.

1.4.7 Velocity of blood flow

Quantitative blood flow statistics have been collected by several investigators using a variety of techniques. Asano and Branemark (1970) used direct observation to investigate the subcutaneous microcirculation through a special transparent window inserted into the skin of human subjects. Figures for flow rates were reported as

vessel	velocity range (mm/s)	mean velocity
arteriole	0.68 - 3.87	1.50
capillary	0.23 - 1.48	0.74
venules	0.32 - 1.21	0.66
AV shunts	0.38 - 2.22	1.37

Lipowsky and Zweifach (1977) measured velocities in a range of vessels in the cat mesentery as

vessel	diameter (μm)	average rbc velocity (mm/s)
arteriole	45	20.8
arteriole	23	23.2
capillary	7	0.7
venule	17	2.0
venule	54	7.5

Other researchers have reported mean resting capillary blood cell velocities for humans between 0.5 ± 0.3 and 0.8 ± 0.5 mms^{-1} (Ostergren and Fagrell, 1986; Bollinger et al., 1974; Fagrell et al., 1977) depending to a great extent on the dimensions of the vessels being studied. Maximum capillary blood cell velocities have been reported to be as high as 3.5 mms^{-1} in the nailfold capillaries (Bollinger et al., 1974).

1.5 Optical Properties Of The Skin

The structure of the skin may vary enormously not only from subject to subject but also for different body sites on an individual subject. This makes it difficult to make a detailed prediction of the optical properties at any one skin site. However general statements can be made about the interaction of light and skin tissue and these can then be applied to specific tissue locations.

When light radiation strikes the skin, part is backscattered, part is absorbed, and part is transmitted into successive layers of cells until the energy of the incident beam is dissipated, figure 1.3.

The total fraction of the incident radiation backscattered from the skin is called the remittance, a combination of that reflected from the top surface of the skin and that backscattered from deeper tissue.

The first optical interaction is at the stratum corneum where a small portion of incident light is reflected due to the change in refractive index between air and skin. This reflection is called regular reflectance as it is described by Fresnel's law of reflection. By taking the refractive index of the stratum corneum layer as 1.55, and that of air as 1.00, it can be calculated that approximately 5% of normally incident light will be reflected in this manner. The majority of the remittance from Caucasian skin is not from regular remittance but from radiation that transverses the epidermis and backscattered from the deeper dermal layers. The light not returned by regular reflection enters the tissue and undergoes processes of scattering and absorption.

The skin tissue has a complex structure containing many physical inhomogeneties that cause the incident light to be scattered. The strength and distribution of scattering depend on the size and shape of the inhomogenities relative to the wavelength of the light. Scattering by molecules or particles that have dimensions less than one tenth of the

wavelength (Rayleigh scattering) is weak, isotropic and varies inversely with the 4th power of the wavelength. Particles that have dimensions of the same order of magnitude as the incident wavelength have a stronger scattering effect. The light is mainly scattered in the forward direction and again varies inversely with wavelength but not by such a strong inverse function (Rayleigh-Gans-Debye scattering). When the scattering particle has dimensions that are larger than the incident wavelength the scattering (Mie scattering) becomes weak again and mainly forward directed. The scattering remains inversely related to the wavelength.
All these scattering processes take place in skin tissue but Mie scattering dominates over the others due to the relative quantity of scattering particles and molecules with dimensions larger than the incident wavelength.

There are distict differences in the optical properties of the epidermis and dermis.
The epidermis is a strongly forward scattering layer. The degree of epidermal absorption depends to a great extent on the wavelength of the incident light and the melanin content of the layer. There is moderate absorption in the visible but substantial absorption in the ultra-violet.
In the dermis the scattering is of great significance in determining the depth of penetration of light. Mie scattering is dominant due to the quantity of relatively large scattering structures such as collagen fibres therefore the scattering is inversely related to the wavelength. The scattering is mainly forward directed but due to the extent of scattering events the photons are eventually scattered through an overall wider range of angles. Some of the photons are scattered back towards the skin surface where they add to the total remittance.
Dermal absorption is determined mainly by the presence of haemoglobin, oxyhaemoglobin, bilirubin and cytochrome.

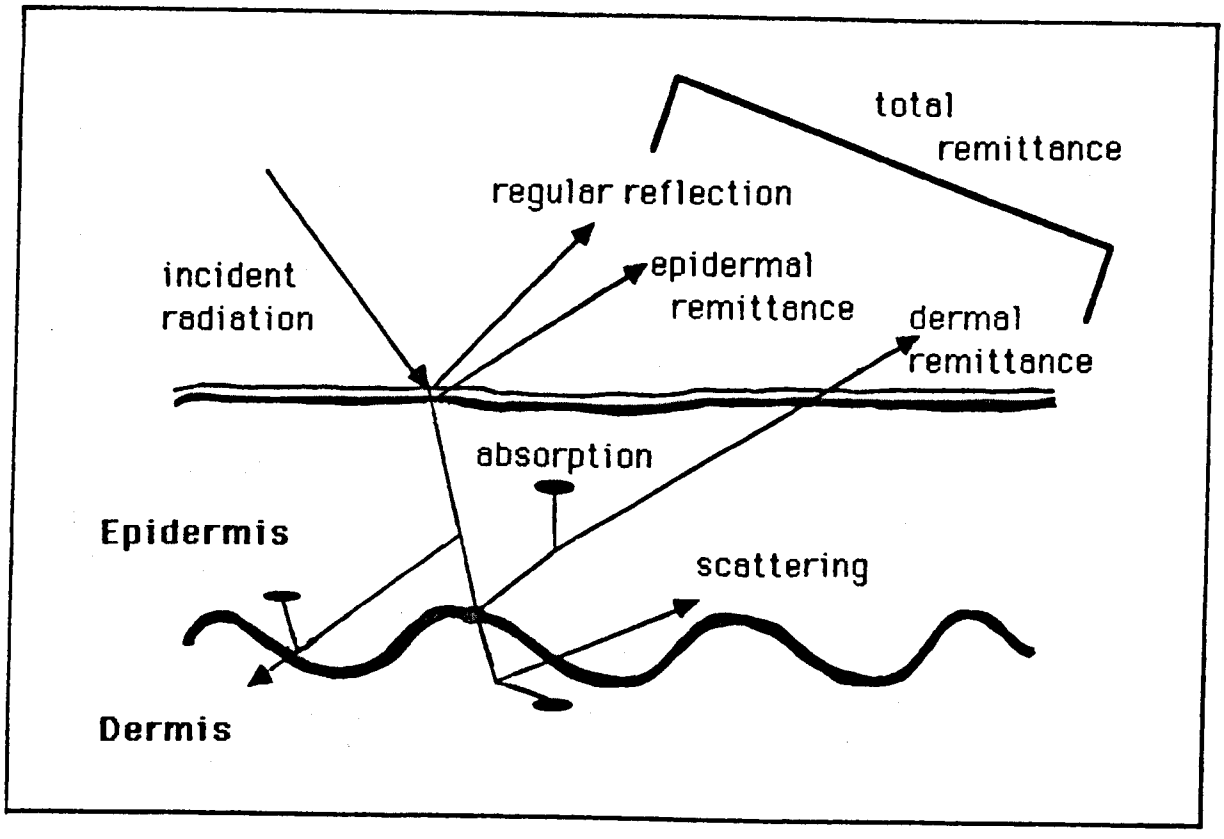

Figure 1.3. Scattering, absorption and reflection of radiation incident on the skin surface.

1.5.1 Absorption spectra of skin and blood chromophores

Absorption processes in a diffusing medium such as skin depend on two processes. These are the characteristic absorption of the tissue components containing pigment such as melanin and haemoglobin, and the attenuation produced by multiple scattering as a result of the structural inhomogenities of the skin.

In general it can be observed that between the wavelengths of 600 and 1000 nm an optical window exists where light can be transmitted through the skin. However, the absorption process has a distinct wavelength dependency which is determined by the presence of several different pigments. At wavelengths less than 320 nm there is a great increase in absorption within the epidermis due to the amino acids of the epidermal protein, keratin. Absorption bands exist within the visible and near ultraviolet due to haemoglobin, oxyhaemoglobin, bilirubin, cytochrome and melanin. At the other end of the spectrum, absorption of near infrared wavelengths is mainly due to the presence of water. The overall absorption depends on the combined absorption effects of all the pigments contained within the volume of illuminated skin. Absorption spectra of the major skin pigments are shown in figure 1.4.

The combined effect of absorption and scattering on the penetration depth of light into the skin has been studied by several investigators including Anderson and Parrish (1981) who produced a table of penetration depths in Caucasian skin for a range of wavelengths. Large differences in penetration depths between blue and near infrared wavelengths were observed. Red and near infrared wavelength radiation are transmitted deepest into the skin, in some instances reaching the subcutaneous tissue. In certain regions such as the finger-tips a fraction of red light may be visibly seen to pass through several millimetres of tissue. Conversely the blue and green wavelength ranges are strongly scattered and absorbed penetrating only a few microns into the dermis.

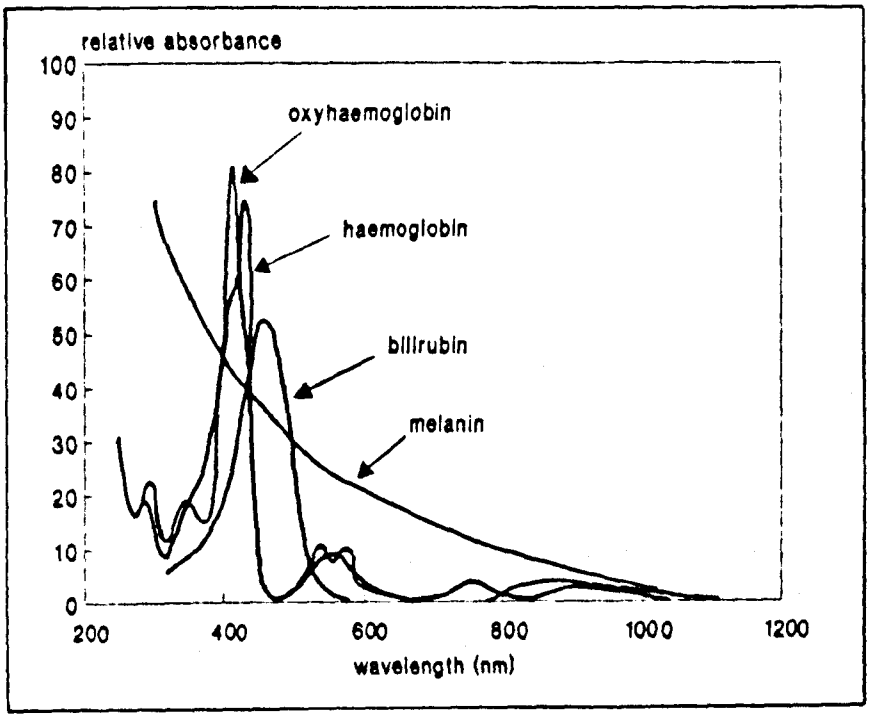

Figure 1.4. Absorption spectra of the major chromophores within the skin tissue

1.5.2 Skin reflection and backscattering

Several studies have investigated the reflectance of living human skin (Jacquez et al., 1954; Anderson et al., 1981). Skin reflection is not merely a surface effect but is affected by backscattering and absorption processes within the deeper tissue layers. There is considerable variation in skin reflectance due to pigmentation, skin blood flow and blood oxygenation. The absorption bands of haemoglobin, oxyhaemoglobin, bilirubin and cytochrome appear strongly in the reflection spectra. Consequently, by monitoring the backscattered radiation information may be obtained on the blood oxygenation within the skin tissue. Reflectance spectra of laboratory animals frequently used in optical radiation studies (e.g. rats and rabbits) are similar to those of Caucasian human skin (Dimitroff et al., 1955).

CHAPTER 2

Laser Doppler Studies

2.1 Introduction

In this chapter the wide variety of techniques for monitoring microvascular blood flow are examined and their limitations are indicated. The development of the laser Doppler technique is reviewed and some of the studies describing recent advances are reported. Finally the different processing algorithms are explained.

2.2 Microvascular Blood Flow Measuring Techniques

Although the skin is the most accessible tissue, devising a technique for measuring the blood flow within it has proved to be a perplexing task. Many different techniques have been shown to be good indicators of skin blood flow, but no one method fulfils the requirements to such an extent that it has been accepted as the "gold standard".
Skin blood flow monitoring techniques should be simple-to-use, non-invasive, inexpensive, and supply a continuous, reproducible measurement of the parameters in the microcirculation. Ideally this measurement should be an absolute measure of the microvascular blood flow.
Extensive reviews of microvascular flow measuring techniques have previously been undertaken (Swain and Grant, 1989; Tooke and Smaje, 1985). This section concentrates on the more recent advances in the techniques showing most promise for future skin blood flow assessment.

2.2.1 Video capillary microscopy

Capillary microscopy provides a non-invasive technique for investigating microvascular blood flow. The tissue is normally illuminated by blue (540 nm) light and observed through a microscope with a magnification of between x12 and x25. The volume of tissue sampled usually permits between 2 and 30 capillaries to be viewed at one time depending on the focusing power of the microscope lens. One of the problems with the technique is that the examining procedure requires the blood vessels to run parallel to the skin surface and therefore is limited to specific skin sites. Measurements are usually taken from the nail fold capillaries, however useful information may sometimes be obtained from other areas of abnormal vasculature surrounding tissue wounds. Using this technique the clinician can observe the distribution of rbcs as they flow through the capillaries and detect changes in blood vessel diameter. However, these simple microscopy techniques provide only qualitative information about capillary flow.

Absolute measurement of rbc velocities can be calculated using video film which may be analysed retrospectively (Fagrell et al., 1977). Flynn et al. (1989) described the separate components required for videomicroscopy systems and reviewed several methods of video analysis. Absolute velocities can be calculated by measuring the distance travelled by each rbc or plasma gap between successive video frames (Bollinger et al., 1974; Fagrell et al., 1977; Tooke et al., 1983).

Continuous real-time measurements of blood cell velocity can be obtained by photodensitometry measurements using cross-correlation techniques (Ostergren and Fagrell, 1986). It is also possible to monitor individual rbc oxygenation using videomicroscopy techniques (see section 6.2.3).

2.2.2 Temperature measurements

Mechanisms controlling skin blood flow are used to a large extent to regulate the temperature of the body. As the blood passes through the peripheral circulation there is an exchange of heat from the body to the surrounding environment. Consequently it has been suggested that temperature measurements are a good indication of either local or regional blood perfusion. Techniques based on skin temperature measurements include infrared radiometry, thermography, microwave radiometry and thermal clearance techniques.

Radiometry and thermography apply basic thermodynamic laws relating the emission of radiation to surface temperature in order to determine the energy emitted from the skin. Radiometry uses Wein's law which relates the frequency at which the maximum energy is radiated to the temperature of the emitting object, in this case the body's surface. The human body emits radiation in the infrared range between 2 and 25 μm, and non-invasive measurements of skin surface temperature can be obtained using an infrared radiometer. Radiometry can also be applied in the microwave region of the electromagnetic spectrum between 1 and 10 GHz. Using microwave measurements of human tissue temperatures to a depth of up to 2 cm can be determined. Both these techniques have been used effectively in several clinical studies to assess peripheral vascular disease (Henderson and Hackett, 1978; Spence et al., 1981; Manson et al., 1985). The techniques give an indication of flow at a localized site, but absolute flow values are not obtainable.

Thermography uses the Stefan-Boltzmann law which relates the emitted radiation flux to the skin surface temperature. Traditionally the detectors used with this technique have had to be cooled using liquid nitrogen in order to achieve good signal-to-noise ratios. However recent improvements in detector technology have produced detectors that operate at

normal temperatures and are compatible with conventional television technology. The technique produces an image of the regional distribution of temperature over the surface of the body (Love, 1980). Thermography measurements are sensitive to changes in environmental temperature and the thermoregulatory status of the patient. Due to these limitations a dynamic thermography method was devised by Wilson and Spence (1989). Skin blood flow was derived from measurements where skin temperature changes were induced by application of a cooling device. The subsequent rate of tissue reheating was recorded permitting qualitative measurements of regional dermal perfusion.

Thermal clearance techniques provide a local indication of blood flow by measuring the transfer of heat through the skin by the circulating blood. The thermal clearance probe usually consists of a central copper heating disc surrounded by a copper ring on the outermost edge of the probe. Thermocouples measure the temperature difference from the heater to the outer edge of the probe. It is assumed that as the blood flow increases more heat is removed from the central disk; but when blood flow decreases less heat is removed and the temperature increases. Hence changes in blood flow can be detected by monitoring the temperature difference across the thermocouple. Many groups have claimed that the thermal clearance technique provides a very good indication of skin blood flow (Holti and Mitchell, 1978; Manson et al., 1985). It has also been demonstrated that by altering the geometry of the probe it is possible to obtain flow measurements from different depths of tissue (Thalaysingam and Delpy, 1989: Britton et al., 1984).
The main problems encountered with temperature measuring techniques are due to the assumption that the conduction of heat away from the body is due to perfusion alone. The temperature is also affected by the thermal conductivity of the tissue and the heat generated by metabolism. Care has to be taken with measurements taken on a local scale as

temperature readings will be greatly affected by major blood vessels near the skin surface. It must also be remembered that readings taken with the thermal clearance technique are of the perfusion when the skin has been heated and may not be representative of "normal" skin blood flow.

2.2.3 Isotope clearance techniques

Extensive blood flow studies have been performed measuring the wash-out of radioactive isotopes from the microcirculation. Isotopes such as ^{133}xenon and ^{99}technetium are injected subcutaneously and the rate of clearance is detected at a specified skin site. Absolute measurement of tissue blood flow in ml min^{-1} $100g^{-1}$ is obtained from the half-life indicated on the wash-out curve.

Xenon has been the most widely adopted isotope (Sejrsen et al., 1969) but it is known to have a great affinity to subdermal fat which can create misleading blood flow measurements. More recent studies have investigated the use of ^{125}I-4-iodoantipyrine as a clearance marker isotope since it is much less fat soluble than xenon and diffuses well in the subcutaneous tissue (McCollum et al., 1985; Forrester et al., 1980).

One of the main disadvantages of the isotope clearance technique is that it is invasive. It has been demonstrated that the subcutaneous injection causes a dramatic increase in the blood flow of the surrounding tissue (Holloway, 1980). Also, the measurements are of an intermittent nature and from a very localised area of tissue. Nevertheless the technique is thought to have advantages in some applications since it can be used to measure the nutrient flow within the upper dermis (Young and Hopewell, 1983).

2.2.4 Photoplethysmography

Photoplethysmography is a non-invasive technique that provides indication of both the pulsatile flow and the total blood content within the peripheral microcirculation by measuring the intensity of light either transmitted through or reflected from a sample of skin tissue. Of these two options, light reflection can be applied to a wider number of skin sites. Light is directed towards the skin where it undergoes a process of absorption and scattering. A portion of the light is eventually scattered back to a detector placed alongside the light source. The photodetected signal is then analysed to provide information concerning the blood flow. Hertzman and Speakman (1937) determined that the detected photoplethysmogram signal is composed of two components, one a slowly varying DC component due to the total blood volume, and the other AC component due to the blood volume changes within the illuminated tissue volume. Several researchers have attempted to model the complex scattering processes that determine the backscattered intensity (Weinman et al., 1977; Challoner, 1979; de Trafford and Lafferty, 1984; Roberts, 1982). However the processes are difficult to predict since the light attenuation depends on the presence of fibrous tissue and blood vessel walls, as well as total blood volume. Recent studies have suggested that probe design can improve the quality of the photoplethysmography measurements (Almond et al., 1988).

Several problems exist with photoplethysmography. If light used in the monitoring probe is not at an isobestic wavelength between haemoglobin and oxyhaemoglobin the measurements are affected by changes in blood oxygenation. Also the technique cannot distinguish between nutritional flow and deeper dermal flow.

2.2.5 Ultrasound

Doppler ultrasound has been used extensively to measure the velocity of blood flowing in major arteries such as the aorta. For these measurements the ultrasound transducers have to operate at frequencies of up to 10 MHz. The technique has also been used for non-invasive assessment of peripheral vascular disease by examining peripheral arteries such as the superficial femoral artery (Rosenfield et al., 1989). The system used by Rosenfield and coworkers combined colour flow Doppler and two-dimensional ultrasound, and produced a simultaneous display of anatomic as well as physiological data.

Doppler ultrasound blood flow measurements have been reported to collect data from predetermined levels within the skin (Payne et al., 1985). This application is promising but many problems exist when applying it to such small vessels. For measurements of skin microcirculation much higher transducer frequencies of between 70 and 90 MHz are required (Frew and Giblin, 1985). Also, the blood flow is at a much lower velocity than that in the large arteries so the Doppler shift is smaller and consequently signal-to-noise ratios are lower. If these problems can be overcome the technique may become a very useful diagnostic tool.

2.2.6 Fluorometry

Fluorometry may be used as an indicator of regional blood flow (Lange and Boyd, 1942). Sodium fluorescein is injected intravenously into the circulation and the tissue is exposed to blue or ultraviolet light (450 to 500 nm). Ground state electrons of the fluorescein dye are excited into higher energy levels by the blue light and when they return to their ground state photons are emitted in the green-yellow (530 to 660 nm) wavelength range. By monitoring this green-yellow fluorescence areas of non-perfused skin can be identified (Myers and Donovan, 1985). Fluorescein dye accumulates in the extracellular fluid by diffusing across the capillary walls so that fluorescence is a good method for indicating nutritional blood flow (Spence et al., 1985). Levels of tissue perfusion may be monitored by measuring the intensity of the fluorescence at different sites and comparing it with normally perfused tissue. Silverman et al. (1980) developed a optical fibre dermofluorometer and the technique was used clinically to accurately discriminate between full and partial thickness burns (Gratti et al., 1983).

Existing problems with this technique include the fact that readings can be affected by skin pigmentation. The measurements are very useful for tissue viability assessment but are not non-invasive since they require an injection of fluorescein dye into the bloodstream.

2.2.7 Transcutaneous oxygen tension measurement

As blood circulates through the capillary beds it supplies oxygen to the surrounding tissue. Consequently an indication of blood supply may be obtained by measuring the oxygen content of a tissue bed. (Section 6.2.1 gives a thorough description of the transcutaneous technique).

The problems encountered with this technique for assessing blood flow include a dependency on skin thickness, tissue

cell metabolism, and skin heating profile. In a study of Raynaud's phenomenon transcutaneous oxygen measurements were found to be of limited value in discriminating between different subject groups (Wollersheim and Thien, 1988). In the same study the non-invasive nature of the technique was hampered by the heated probe causing skin injuries in some of the subjects. Nevertheless the technique has been successfully used to assess peripheral circulation in ischaemic skin sites prior to amputation (Dowd, 1983) and also to discriminate between normal patients and patients with claudication, ischaemia and gangrene (Dowd, 1982; Linge et al., 1988).

Bader and Grant (1985) and Spence et al. (1985) proposed that dynamic changes in transcutaneous oxygen measurements induced by breathing oxygen may provide an improved indication of tissue viability. This technique was later shown to be useful for determining levels of amputation (Oishi et al., 1988).

2.3 Laser Doppler Literature Review

In 1888 a German astronomer, H.C. Vogel, demonstrated that the motion of distant stars could be calculated by measuring the "red shift" of their emission spectra (Sandage, 1956). Smaller scale measurements using the Doppler shift of light were not possible until the invention of the laser (Schawlow and Townes, 1958) which provided a bright light source with a narrow spectral width suitable for use in optical heterodyne detection techniques.

2.3.1 Initial laser Doppler measurements

Cummins et al. (1964) predicted that the speed of macromolecules in solution could be measured by analysing the photodetector current produced by detecting the laser light backscattered from the solution. Later that year the technique was demonstrated by observing light scattered from

a suspension of polystyrene latex spheres in water flowing through a tube (Yeh and Cummins, 1964). The scattered laser light was combined with a reference beam from the same laser source to produce an optical beating effect on the surface of a square-law photodetector where the output current is proportional to the intensity of the incident light. Photocurrent spectrum and autocorrelation analysis techniques were used to calculate the range of velocities present.

A similar technique, the differential Doppler technique, was later developed. It used two laser beams of equal intensity simultaneously illuminating the moving objects. Using this method absolute values of the velocity can be calculated directly from the Doppler shift once the photodetector position and the and other fixed parameters are known. The differential Doppler technique has become the standard non-contact technique for studying flow fields. Known as laser Doppler anemometry the technique is used for a variety of applications such as designing fuel-efficient turbines, studying turbulence and measuring speeds of rotating machinery (Stevenson, 1982).

Riva et al. (1972) applied the detection technique used by Cummins to measure blood flow through fine capillary tubes of 200 μm internal diameter (i.d.). The unshifted (10 mW Helium Neon (HeNe)) laser light backscattered from the glass tubes was used as the reference beam. Photocurrent power spectra were obtained using a spectrum analyser and it was shown that a linear relationship existed between the maximum shifted frequency and the observed flow. They used the technique to measure the blood flow in the retinal vessels of a rabbit. Tanaka et al. (1974), using a much less powerful HeNe laser (18 μW) demonstrated that similar retinal flow measurements could be obtained from humans using short recording times of 10 seconds. Further results were presented by Feke and Riva (1978) using the Doppler frequency spectra to investigate suspensions of polystyrene spheres and rbcs flowing through glass capillary tubes.

These spectra were compared with spectra obtained from human retinal vessels and maximum rbc speeds calculated directly from the maximum cut-off frequencies of the spectra. A laser Doppler system capable of obtaining absolute values of the speed of rbcs flowing in individual retinal vessels was presented by Riva et al. (1979). This was achieved by obtaining Doppler frequency spectra from two different scattering angles.

The measurements up to this point were limited to sites easily accessible to the laser light. Optical fibre delivery and collection of laser light for Doppler flow measurements was introduced by Tanaka and Benedek (1975). By developing a narrow optical fibre catheter (0.5 mm diameter) flow velocity measurements in the femoral vein of a rabbit were reported.

Another application of the laser Doppler technique was proposed by Mishina et al. (1974) who suggested that measurements were possible through a microscope using the differential Doppler arrangement. The system was built into a microscope using a photomultiplier as a detector and measured flow velocities in an area of approximately 5 μm diameter. Flow velocity measurements were obtained from capillaries in the web of a frog's foot (Mishina et al., 1976). Further laser Doppler microscopy measurements were reported by Einav et al. (1975 a, b) who applied the system to the examination of blood flow in small arteriole vessels in the hamster cheek pouch. They showed that there were parabolic flow profiles in the smaller 65-98 μm diameter arterioles and velocities of up to 6.84 mms^{-1} were measured at the centre of the vessels. Le-Cong and Zweifach (1979) subsequently used the system to accurately measure flow velocity, velocity profiles and vessel dimensions which allowed them to calculate volume flow in microvessels.

2.3.2 Cutaneous microvascular blood flow

Laser Doppler measurements of cutaneous microvascular blood flow differ from measurements from single vessels or tubes because the light is diffusely scattered by the overlying skin and all the directional information is lost. Stern (1975) was the first to report that cutaneous microcirculation may be continually studied by applying optical heterodyning. He recognised that the complex scattering of laser light within the skin tissue prevented a quantitative measurement of microvascular blood velocity. However, by using a 15 mW HeNe laser and a photomultiplier detector he demonstrated that it was feasible to detect changes in the photocurrent spectra obtained from the fingertip under various interventions. Noticeable changes to the spectra were observed for flow before and after occlusion of the brachial artery.

Stern at al. (1977) demonstrated the feasibility of the monitoring technique using a simple analogue instrument. By considering the bandwidth of the Doppler spectrum to scale proportionally with rbc velocity an empirical algorithm was presented where the flux parameter was based on the unnormalized root-mean-square bandwidth of the Doppler signal. Normalisation by the mean photocurrent was used to ensure that the flux parameter was independent of laser light intensity and the reflectivity of the skin. The flux parameter was compared with measurements using ^{133}xenon washout method for skin blood flow in volunteers subjected to ultraviolet-induced erythema. An approximately linear response to changes in skin blood flow was demonstrated.

The system designed by Stern incorporated a complex optical arrangement that limited it to laboratory investigations. In 1977, Holloway and Watkins produced a portable analogue blood flow instrument (Holloway and Watkins, 1977; Watkins and Holloway, 1978). By using photodiode detection instead of a photomultiplier tube the overall size of the instrument was reduced and the need for a high voltage source was

eliminated. A 5 mW HeNe laser with a optical fibre delivery and collection system was used and a flow parameter obtained by dividing the root-mean-square (rms) of the amplified heterodyned signal by a dc intensity term. This rms value provided a method of monitoring blood flow without requiring a spectrum analyser or a real-time autocorrelator. The response of the instrument was demonstrated to have a good linear relation with the technique of ^{133}xenon clearance in the human arm. Problems were encountered with the instability of the laser output causing fluctuations in the flux output from the instrument.

Williams et al. (1977) successfully used the laser Doppler instrument to map regional blood flow distribution on the surface of the cerebral cortex in Rhesus monkeys. A stroke was produced on one side by ligation of the middle cerebral artery. The region of stroke was easily mapped and its progression with time was observed.

Stern et al. (1979) then applied the technique to measuring blood flow in the renal cortex and medullary ampulla of rats. The flow was varied by aortic constriction or administration of norepinephrine or angiotensin. Reproducible results were obtained and compared well with measurements using an electromagnetic flow probe and a technique using radioactive microspheres.

In a later report Holloway (1980) used a portable instrument to investigate the effect of intracutaneous injections on skin blood flow. A sevenfold increase in resting flow was measured due to the insertion of a needle, questioning the validity of some invasive blood flow monitoring techniques such as radioisotope clearance. The instrument was also used by Piraino et al. (1979) and Enkema et al. (1981) to simultaneously measure skin perfusion with transcutaneous oxygen measurements.

In 1980, Nilsson et al. (1980 a) introduced a new differential detection technique to reduce the problems of laser mode competition reported by Watkins and Holloway. By using two photodiode detectors it was shown that common mode

terms such as fluctuations in the laser output intensity and external lighting factors could be suppressed to a negligible level increasing the sensitivity of the instrument. Their instrument also used a different signal processing algorithm. The laser Doppler flowmeter produced an output proportional to the normalized first moment of the power spectral density (Nilsson et al., 1980 b).

The instrument was evaluated over a range of blood volume fractions and rbc velocities in a mechanical fluid model providing a fixed flow geometry. A linear relationship between flowmeter response and flux of rbcs was demonstrated for almost all of the range of fractional values of red cells investigated. However as the red cell concentration was increased it was observed that the flowmeter response became nonlinear. For concentrations above about 0.3% volume fraction of rbcs the flux output underestimated the true blood flux. It was suggested that this was due to an increase in homodyne mixing processes which was in turn due to multiple scattering of photons.

The first moment of the spectrum was also chosen by other researchers as a flow indicator. Bonner and Nossal (1981) published work that analysed the theory of scattering of photons by the microvasculature. A general model of the tissue matrix was devised allowing a guide to the design of laser Doppler instrumentation. Several assumptions had to be made due to the uncertainty of the vascularized tissue under investigation but the derived equations showed a good representation of flow behaviour in living tissues. It was shown that where heterodyne mixing was dominant the first moment of the detected spectrum varied proportionally with relative blood flux.

For higher concentrations there was an increase in the number of homodyne mixing processes occurring. In that case the first moment was still sensitive to changes in flow but varied approximately as the square root of the degree of multiple scattering and linearly with rms rbc speed. Bonner et al. (1981) described an analogue processor based on the

theory of light scattering that had been developed. A real-time output of the mean Doppler frequency was produced by the flowmeter which was demonstrated in studies of reactive hyperaemia and Valsalva manoeuvre responses.

By 1983 there were two commercial laser Doppler flowmeters available: the LD5000 Laser Doppler Perfusion Monitor (Med Pacific Corporation) designed by Holloway and Watkins, and the Periflux Laser Doppler Flowmeter (Perimed) designed by Nilsson and associates. Both instruments used the Doppler shift of laser light but incorporated different signal processing algorithms. Fischer et al. (1983) compared the two flowmeters simultaneously monitoring blood flow changes in the skin of an island flap. The study concluded that the responses of the two instruments had a high degree of correlation with arterial and venous occlusion, and also with each other ($r=0.92$, $p<0.001$). These results were confirmed when Obeid (1989) used an in vitro model to compare the different processing algorithms used in the analogue instruments. His results suggested that both frequency-weighted algorithms respond linearly to average velocity changes within the physiological range typically present in skin tissue. Both algorithms were shown to underestimate blood flow as the rbc concentration increased above 0.2% p.c.v. However the algorithm using the first moment of the power spectrum appeared to be less likely to underestimate changes in rbc concentration when measuring from highly perfused tissue.

Nilsson (1984) described a signal processor that increased the range of rbc concentrations over which the Periflux flowmeter responded linearly with microvascular blood flow. The nonlinear response of the original signal processor at high rbc volume fractions had been shown to be due to multiple photon scattering. A hard-wired linearizer was added to the signal processor which operated by multiplying the unadjusted flowmeter flux output by a correction factor related to the concentration of rbcs present. The performance of the improved signal processor was evaluated

on a fluid model and the performance further demonstrated by recording in vivo reactive hyperaemia responses. Ahn et al. (1987) compared the performance of the improved signal processor developed by Nilsson with the original instrument. Evaluation was carried out using an in vivo model comprising of a segment of feline intestinal wall. The advanced signal processor was shown to be linear over the entire range of blood flow investigated (0 to 300 ml min^{-1} $100g^{-1}$) whereas the original instrument underestimated the highest flow rates. It was also noted that the linearity depended on the bandwidth chosen for the study. The response of the processor was most linear when recording in its wideband (12 kHz) operating mode.

With the increasing availability of small and inexpensive infrared laser diodes several researchers have changed to using these light sources rather than the bulkier HeNe gas lasers originally used in Doppler flowmeters. Boggett et al. (1986) compared *in vitro* results for Doppler flowmeters using both types of laser sources demonstrating that both produced linear flow responses over the typical microvascular flow range.

Shepherd et al. (1987) described a commercial laser Doppler flowmeter (Laserflo, TSI) using an infrared laser diode source and a microprocessor for signal analysis rather than the previously used analogue circuitry. The linearity and reproducibility of the flux response were tested using a rotating disk model to simulate microvascular perfusion. *In vivo* evaluation was carried out in isolated perfused rat livers and canine gastric flaps where linear relationships were observed between total flow and laser Doppler flow ($r = 0.98$ both for the liver and the gastric mucosa correlations).

2.3.3 Other processing techniques

The photodetector current produced by backscattered laser light can be interpreted by obtaining either the frequency power spectrum or the photon correlation spectrum. Initial studies by Feke and Riva (1978) were performed by direct observation of the maximum cut-off frequency of the power spectra. Fujii et al. (1985) considered the light scattering effect in terms of time varying laser speckle rather than laser Doppler shifts. They suggested that the speckle pattern produced by skin tissue consisted of two components, (i) the fast speckle fluctuation due to the blood flow in the capillaries, and (ii) the slowly changing speckle field due to the movement of the outer skin surface. Using a HeNe laser and a photomultiplier system the power spectral distribution of the detected signals was observed using a fast-Fourier-transform spectrum analyser. A simple signal processor was constructed measuring the gradient of the power spectral density by measuring its amplitude at two arbitrary frequencies, namely 40 Hz and 640 Hz. The response of the signal processor was demonstrated by monitoring the blood flow during occlusion and subsequent reactive hyperaemia.

Processing algorithms used in commercial flowmeters are described in terms of power spectra. However a number of researchers have used photon correlation spectroscopy (Palmer et al., 1980; Hamilton et al., 1982; Gush et al., 1984). The system used by Gush et al. (1984) used optical fibres, a photomultiplier detector, a photon correlator and a mini-computer to investigate microvascular perfusion. In these studies the flow-related parameter was produced by obtaining the reciprocal of the autocorrelation function time constant.

2.3.4 Problems associated with Doppler measurements

Movement artefact

A persistent problem with laser Doppler measurements is that sudden movements of the optical fibres can cause fluctuations in the flowmeter output due to intensity fluctuations as the speckle pattern on the skin surface changes. The problem of movement artefact was addressed by Gush and King (1987) and Newson et al. (1987). In their studies the region of the photocurrent spectrum most affected by fibre induced noise was identified as between 0 and 3 kHz, and several methods of reducing movement artefact were suggested. One method of reducing movement artefact problems replaces the optical fibres with a probe head containing both a laser diode and a photodiode detector. Several research groups have developed such fibreless probes (de Mul et al., 1984; Boggett et al., 1986; Obeid et al., 1990).

Absolute units versus relative changes

Usually when using laser Doppler flowmeters the blood flow responses are measured as relative changes. Recently a number of studies have suggested that absolute flow values may be provided by using certain calibration factors. The calibration factors are obtained by determining the correlation between the Doppler flow parameter with values obtained by ^{133}Xe and H_2 clearance and microsphere deposition in various tissues. In fact some commercial LDF monitors suggest that quantitative measurements are always obtained by displaying flow in units of (ml min^{-1} $100g^{-1}$). Rendell et al. (1989) used such an instrument to map skin blood flow, microvascular volume and erythrocyte velocity on diabetic and non-diabetic subjects. Of these measurements only the velocity parameter was not calibrated. Blood volume was quoted in numbers of moving erythrocytes/mm^3 of tissue and flow in ml min^{-1} $100g^{-1}$.

Ahn et al. (1985) and Feld et al. (1982) reported that they had been successful in establishing calibration factors to convert Doppler readings to absolute flow units in their studies on intestinal mucosa. However absolute measurements of blood flow have been severely criticized by some other researchers. Dirnagl et al. (1989) found that for measurements in the rat cortical microcirculation absolute flow values were meaningless, and highly dependent on probe placement and position. These findings were recently supported by Obeid et al. (1990).

Probe design

The laser Doppler technique is usually implemented using small diameter optical fibre probes which restrict the sampled volume of tissue to a hemisphere of approximately 1 mm radius. In some studies this may cause problems since both spatial and temporal variations in tissue blood flow may lead to local measurements being unrepresentative of flow in other adjacent areas (Tenland et al., 1983; Salerud et al., 1983).

Salerud and Nilsson (1986) recognised that in many situations an average skin blood flow may be a better diagnostic parameter and introduced an integrating probe for the Perimed instrument. The probe received light from seven different scattering volumes simultaneously and produced an integrated signal taken to represent an average flow value over an area of approximately $1cm^2$. A similar integrating probe has been recommended and demonstrated to be of value for diagnosing patients with obliterative arteriosclerosis (Kvernebo et al., 1988; Ostergren et al., 1988).

In other situations deep tissue perfusion measurements may be required. By designing an optical fibre probe with an overall diameter of 0.5 mm Salerud and Oberg (1987) demonstrated that perfusion at different depths in a variety of organs can be obtained by inserting this "needle probe" into the tissue.

2.3.5 Applications of the laser Doppler technique

The ability to measure microvascular blood flow is of great importance in a wide range of medical and physiological studies. The contribution that laser Doppler has made to increasing the general understanding of tissue perfusion is demonstrated by the number of studies that have used the technique.

Peripheral vascular disease

Laser Doppler flowmeters have been used in the general assessment of skin blood flow in peripheral vascular disease and have been shown to be able to discriminate between patient groups with intermittent claudication, critical ischaemia and control groups (Karanfilian et al., 1984; Kvernebo et al., 1988; Cochrane et al., 1986; van den Brande and Welch, 1988). Studies have also shown that it may be a useful technique for determining appropriate amputation levels in lower limb atherosclerosis (Kvernebo et al., 1989) or for predicting healing after amputation (Gebuhr et al., 1989).

Diabetes

As a consequence of diabetes, regulation of microvascular blood flow is often altered. The affect of diabetic microangiopathy on retinal blood flow was demonstrated by Grunwald et al., (1984). Impairment of skin blood flow is also regularly demonstrated consequently a large number of studies have been performed with diabetic patients (Rayman et al., 1986). A recent study by Rendell et al. (1989) investigated flow responses in diabetic and non-diabetic patients to temperature interventions at several locations on their bodies. They found that both rbc volume fraction and velocity were generally decreased in the diabetic subjects.

Psoriasis & Raynaud's disease

Other skin diseases investigated using the laser Doppler technique include psoriasis (Hull et al., 1989), and Raynaud's disease (Wollersheim et al., 1988; Kristensen et al., 1983).

Drug monitoring

The application of vasodilating drugs represent one of the most widely used medical procedures in the treatment of peripheral vascular diseases. Accordingly Laser Doppler flowmeters have been used to monitor the effects of several vasoactive drugs (Bisgaard et al., 1986; Li Kam Wa et al., 1989; Leonardo et al., 1986).
Woolfson et al., (1989) used a laser Doppler flowmeter to monitor the effect of local anaesthesia on skin blood flow. A significant increase in peak blood cell flux resulted from the application of amethocaine percutaneous anaesthetic preparations, the magnitude of the increase correlating with an increase in drug concentration. These results confirmed the vasodilating properties of amethocaine.

Burns and intensive care

In intensive care it is extremely important to be able to predict the depth of burn wounds and the probability that they will heal. Micheels et al. (1984) demonstrated how the method may be used with burned patients, patients in shock and patients with hypothermia. The technique has also been used to select patients who require skin grafts (Waxman et al., 1989). It was shown to be able to predict both whether healing would occur and also the quality of the healing in terms of scar formation.

Other tissues

Blood flow measurements have been performed on many tissues other than skin.
Gastric mucosal blood flow is of great importance in controlling secretion and consequently has been monitored in many studies (Kvernebo et al., 1986; Ahn et al., 1988; Lunde et al., 1988; Christoforidis et al., 1989). Laser Doppler measurements may be performed either during operation or by using an optical fibre incorporated into an endoscope.
Several studies have examined the blood flow in the microcirculation of the brain (Haberl et al., 1989; Fasano et al., 1988; Williams et al., 1977). Recent studies by Arbit et al. (1989) used the laser Doppler technique to demonstrate the different states of perfusion that exist in brain tumours compared with normal brain tissue. It was observed that blood flow is reduced in most cerebral tumours.

The laser Doppler technique has also been used in studies of microvascular flow in bone, on the surface of the heart, kidney, liver, muscle and pancreas tissue.

2.4 Laser Doppler Theory

The laser Doppler technique is based on the Doppler shift of light caused during interactions between photons and rbcs. The situation is complicated by the scattering properties of the skin tissue.
In general, laser light directed on to a tissue surface penetrates the epidermal layers and reaches into the dermis. Complex reflection and refraction processes within the superficial tissue cause strong scattering effects that randomize the direction of the incident photons. Consequently, the rbcs may be assumed to be illuminated from all directions (Bonner and Nossal, 1981).
Photons scattered by moving rbcs undergo a shift in

frequency proportional to the speed of the rbc movement described by the Doppler effect (Chu, 1974).
The frequency shift (figure 2.1) is given by :

$$\delta\varpi = \bar{q} \cdot \bar{v} = (\bar{k}s - \bar{k}i) \cdot \bar{v} \qquad (2.1)$$

ϖ = angular frequency = $2\pi f$

$\bar{v}$ = velocity vector of the rbc

$\bar{k}i$ = wavevector of the incident light

$\bar{k}s$ = wavevector of the scattered light

$\bar{q}$ = scattering vector

$\delta\varpi$ = shift in angular frequency

when,

$$|v| << c \quad , \qquad |ks| \approx |ki| = \frac{2\pi n}{\lambda} \qquad (2.2)$$

where, n = refractive index of the medium

λ = wavelength of laser light <u>in vacuo</u>

c = speed of light

The magnitude of the scattering vector, $\bar{q}$, is calculated from figure 2.2 using Pythagoras theorem,

$$\bar{q} = 2ki \sin(\theta/2) \qquad (2.3)$$

Now,

$$\delta\varpi = \bar{q} \cdot \bar{v} = 2kiv \sin(\theta/2) \cos\phi$$

$$= \frac{4\pi nv}{\lambda} \sin(\theta/2) \cos\phi \qquad (2.4)$$

For backscattered light $\sin(\theta/2) \approx 1$, therefore,

$$\delta\varpi = \frac{4\pi nv}{\lambda} \cos\phi \qquad (2.5)$$

The optical frequency spectrum of the light scattered from the microvasculature contains frequency contributions from ϖ_i to $\varpi_i + \delta\varpi_{max}$, where ϖ_i is the angular frequency of the incident laser light and $\delta\varpi_{max}$ is the largest frequency shift from the sampled rbc population. From equation (2.5) the maximum frequency shift is produced when colliding photons and rbcs travel in parallel directions.
Then,

$$\delta\varpi = \frac{4\pi n v}{\lambda} \quad , \quad \delta f = \frac{2nv}{\lambda} \qquad (2.6)$$

By substituting typical values into this equation
(λ = 632.8 nm, n = 1.4) a photon scattered by a rbc moving at 1 mms^{-1} would undergo a maximum frequency shift of approximately 4.4 kHz. This is many orders of magnitude smaller than the frequency of the incident laser light which is approximately 4.7 x 10^{14} Hz. The heterodyne mode of optical mixing spectroscopy is used to detect such relatively small Doppler frequency shifts.

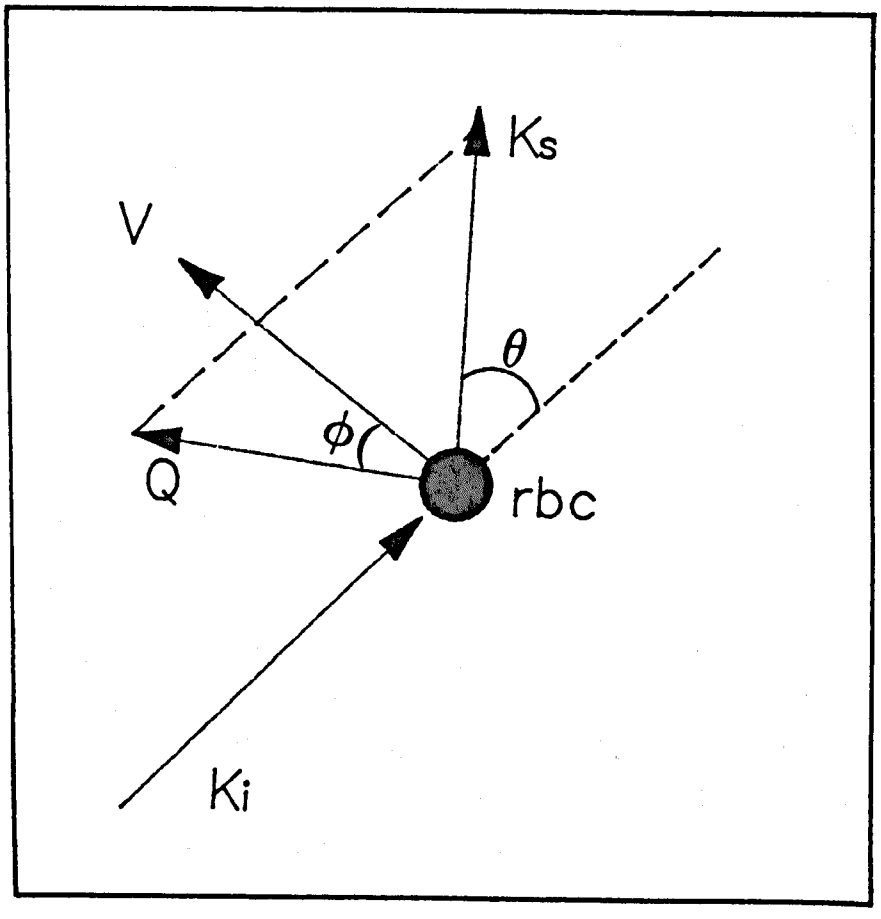

Figure 2.1 The Doppler shift

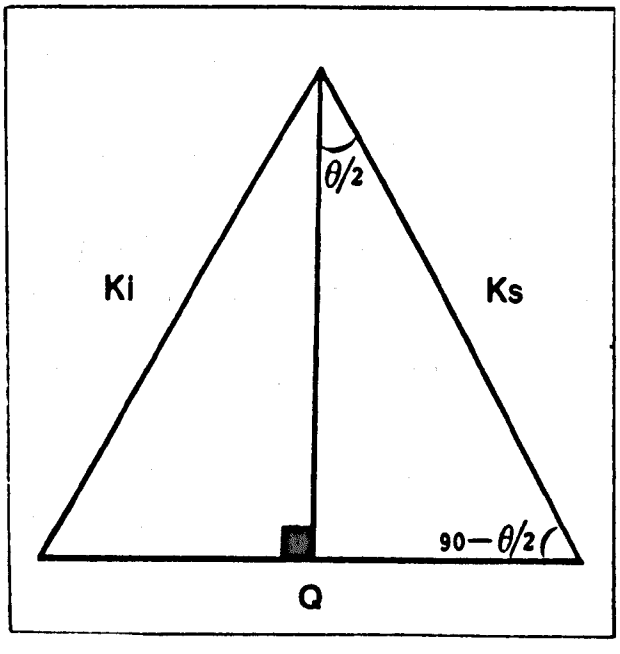

Figure 2.2 The magnitude of the scattering vector may be obtained using the Pythagoras theorem.

2.4.1 Optical beating and heterodyne detection

Light backscattered to the skin surface contains a number of photons that have been scattered by collisions with static tissue and moving rbcs (Doppler shifted) and a number that have been scattered by static tissue alone (non-shifted). Light directed on to the surface of a non-linear photodetector produces interference effects by the mixing of frequency shifted and non-shifted photons leading to a range of optical beat frequencies being produced. In this heterodyne detection mode the non-shifted light is used as the local oscillator or reference beam. The beat frequencies produced are at frequencies equal to the difference between the local oscillator and Doppler shifted frequencies. For measurements from the tissue microvasculature these "Doppler beat frequencies" are usually confined to the low audio range between 0 and 12 kHz. For some well perfused tissue the range may extend beyond 20 kHz.
The output of the non-linear photodetector is a current $i(t)$ which is proportional to the absolute square of the total electric field $E_T(t)$ impinging on its surface.

$$i(t) = C|E_T(t)|^2 \qquad (2.7)$$

Where C is an instrumentation constant.

The electric field $E_T(t)$ has components due to both the non-frequency-shifted and the Doppler frequency-shifted photons.

$$E_T(t) = E_R(t) + \sum_{v=0}^{vmax} E_{Sv}(t) \qquad (2.8)$$

where $E_R(t)$ is the local oscillator (reference) field and $E_{Sv}(t)$ is the scattered field due to a rbc moving at a speed v.

$$E_R(t) = A \exp(-i\varpi_i t) \quad (2.9)$$

$$E_{sv}(t) = B \exp(-i(\varpi_i \pm \varpi_v)t) \quad (2.10)$$

A and B are electric field amplitude terms
ϖ_i is the incident light angular frequency
ϖ_v is the Doppler shifted angular frequency

The photocurrent can be rewritten as,

$$i(t) = C|E_T(t)|^2$$

$$= C\left|E_R(t) + \sum_{v=0}^{vmax} E_{sv}(t)\right|^2$$

$$= C\left(|E_R(t)|^2 + 2\left|E_R(t) \sum_{v=0}^{vmax} E_{sv}(t)\right| + |E_{sv}(t)|^2\right)$$

$$= i_R(t) + i_s(t) + 2CE_R \sum_{v=0}^{vmax} E_{sv}(t) \exp(i\delta\varpi_v t)$$

...(2.11)

The first term is a dc component due to the non-frequency shifted components. The second term is a homodyne component and the third term is the heterodyne component which contains the Doppler frequencies.

Heterodyne processes occur when frequency-shifted light mixes with non-shifted (local oscillator) light. For pure heterodyne detection the magnitude of the local oscillator must be much greater than the magnitude of the scattered field. Usually, light backscattered from the tissue microvasculature contains only a small percentage, approximately less than 0.1% (Bonner and Nossal, 1981), of Doppler shifted photons and therefore heterodyne processes dominate.

Homodyne or self-beating processes occur when frequency shifted-light mixes with other frequency-shifted light

(figure 2.3). For low perfusion levels this self-beating term is insignificant compared to the larger proportion of heterodyne components. However as the tissue perfusion increases the relative number of frequency shifted photons in the backscattered light also increases and the homodyne processes become more significant.

As the tissue perfusion increases multiple photon scattering events also become more frequent. The average number of times that a photon is scattered by moving rbcs increases. Each time a photon-rbc interaction occurs the photon undergoes an additional Doppler frequency shift. Multiple scattering and increased homodyne processes tend to produce a wider spread of detected Doppler frequencies and cause laser Doppler instruments to become non-linear with increasing rbc concentrations.

Analysis of the photodetector current may be performed either in the time domain using the autocorrelation function or in the frequency domain using the power spectrum. The autocorrelation function is derived in Appendix 1. In order to convert from the autocorrelation function to the power spectrum the Wiener-Khintchine transform is used. The final power spectrum contains a light beating spectrum covering the Doppler-shifted frequency range.

$$P(\varpi) = \frac{e\langle i\rangle}{\pi} + \langle i\rangle^2\delta(\varpi) + \frac{\langle i\rangle^2}{\pi}\int_0^{\infty} |g^{(1)}(\tau)|^2 \exp(i\varpi\tau)\,d\tau$$

$$= \frac{e\langle i\rangle}{\pi} + \langle i\rangle^2\delta(\varpi) + S(\varpi) \qquad (2.12)$$

$S(\varpi)$ = power spectrum containing the Doppler information

$P(\varpi)$ = photocurrent power spectrum

$g^{(1)}(\tau)$ = the Fourier transform of the normalized optical spectrum

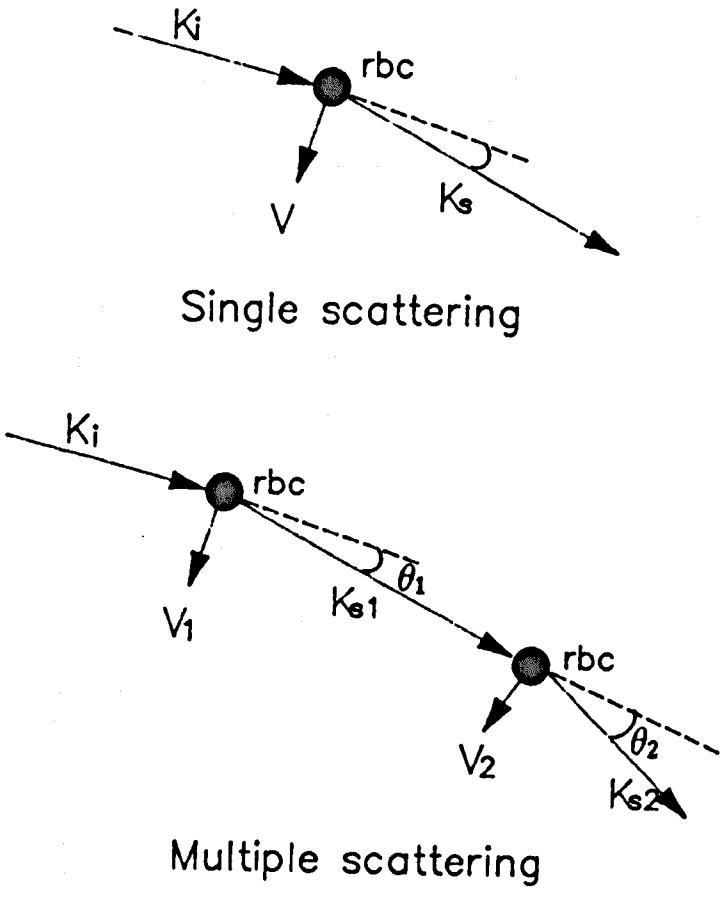

Figure 2.3 Multiple photon scattering increases the range of frequency shifts obtained.

2.4.2 Signal processing algorithms

Theoretical background

To obtain a flow parameter from the Doppler information within the photocurrent power spectrum $P(\varpi)$ the initial step is to find a parameter related to the rbc velocity. The Doppler effect produces a frequency shift proportional to the velocity of the moving scatterers. For a spectral distribution of velocities a velocity-related parameter may be obtained (figure 2.4) either from the root-mean-square frequency, $(\varpi^2)^{\frac{1}{2}}$ or the average frequency, $\langle\varpi\rangle$.

$$(\overline{\varpi^2})^{\frac{1}{2}} = \left[\frac{\int \varpi^2 \, P(\varpi) \, d\varpi}{\int P(\varpi) \, d\varpi} \right]^{\frac{1}{2}}$$

$$\langle\varpi\rangle = \overline{\varpi} = \frac{\int \varpi \, P(\varpi) \, d\varpi}{\int P(\varpi) \, d\varpi}$$

A blood flow parameter can be obtained by defining blood flux as,

$$\text{Blood flux} = \text{average speed of rbcs} \times \text{number concentration of rbcs}$$

The area under the power spectrum is proportional to the number of scattering rbcs (figure 2.5), so that,

$$\text{number concentration of rbcs} \propto \int P(\varpi) \, d\varpi$$

A flux parameter should be obtained from the product of the velocity-related parameter and the number concentration-

related parameter.

For the term derived from the root-mean-square frequency,

$$\text{Blood flux} = (\varpi^2)^{\frac{1}{4}} \int P(\varpi)\, d\varpi$$

$$= \left[\frac{\int \varpi^2 P(\varpi)\, d\varpi}{\int P(\varpi)\, d\varpi} \right]^{\frac{1}{2}} \int P(\varpi)\, d\varpi$$

$$= \left[\int \varpi^2 P(\varpi)\, d\varpi \int P(\varpi)\, d\varpi \right]^{\frac{1}{2}}$$

$$= \left[\int \varpi^2 P(\varpi)^2\, d\varpi \right]^{\frac{1}{2}}$$

For the term derived from the average frequency,

$$\text{Blood flux} = \langle \varpi \rangle \int P(\varpi)\, d\varpi = \frac{\int \varpi P(\varpi)\, d\varpi}{\int P(\varpi)\, d\varpi} \int P(\varpi)\, d\varpi$$

$$= \int \varpi P(\varpi)\, d\varpi$$

The area under the power spectrum is affected by the intensity of the laser light incident on the skin tissue as well as the number concentration of scatterers. Therefore the concentration parameter has to be normalized by a term proportional to the incident laser power. The power spectrum is normalized by the square of the mean photocurrent (I_{dc}^2).

$$\text{Normalized concentration of rbcs} = \frac{\int P(\varpi)\ d\varpi}{I_{dc}^2}$$

Similarly since the flux terms include a concentration term they have to be normalized.
The normalized flux derived from the average frequency term is given by,

$$\text{flux} = \frac{\int \varpi\ P(\varpi)\ d\varpi}{I_{dc}^2}$$

and the normalized flux derived from the rms frequency term is given by,

$$\text{flux} = \frac{\left[\int \varpi^2\ P(\varpi)^2\ d\varpi\right]^{1/2}}{I_{dc}^2}$$

$$= \frac{(\varpi^2)^{1/4} \int P(\varpi)\ d\varpi}{I_{dc}^2}$$

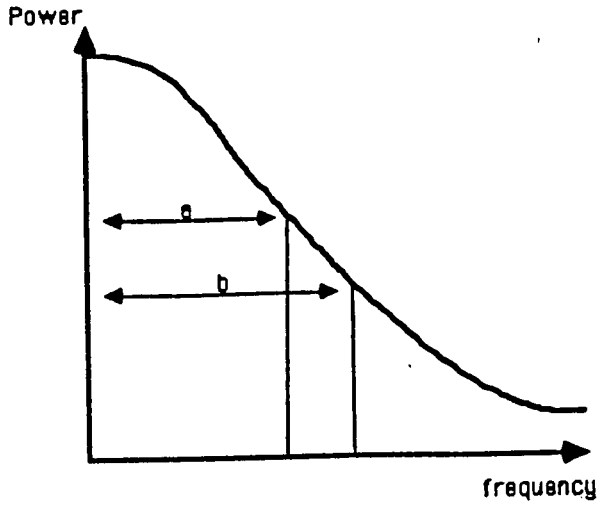

Figure 2.4 Velocity related parameters obtained from the Doppler power spectrum. (a) the average frequency and (b) the root-mean-square frequency

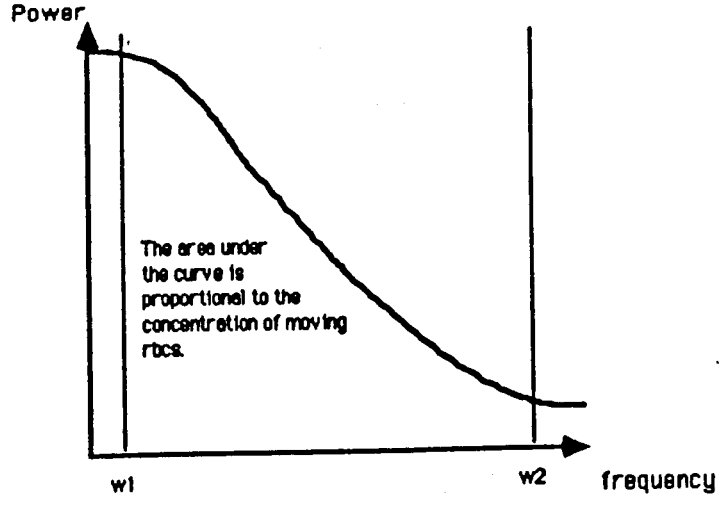

Figure 2.5 A term related to the number concentration of rbcs is obtained from the Doppler power spectrum

Algorithms used in Doppler instrumentation

Several investigators have developed laser Doppler instruments permitting real-time evaluation of the flow by calculating flow parameters from the photocurrent using simple analogue electronics.
The two common approaches to signal processing are based on the root-mean-square and average frequency shift present in the photocurrent. The algorithms can be thought of as being weighted estimates of the Doppler frequency spectrum. The algorithm based on the root-mean-square frequency is known as ϖ^2-weighting (Stern et al., 1977) and the algorithm based on the average frequency is known as ϖ-weighting (Bonner and Nossal, 1981; Nilsson et al., 1980a). The latter of these is the more sensitive algorithm at low flux rates.

Stern algorithm (ϖ^2-weighting)

The photocurrent signal processing algorithm developed by Stern et al. (1977) is based on a dimensional argument that the bandwidth of the Doppler spectrum should scale in proportion to the red cell velocities. Also, the magnitude of the Doppler signal should increase with the number of red cells in the sampled volume of tissue. However it was noted that this is not a linear relationship when there is a large proportion of multiple scattering events.
The blood flux is defined as the unnormalized root-mean-square (rms) bandwidth of the Doppler signal,

$$\text{Flux} = \left(\int (\varpi^2 P(\varpi)\, d\varpi)\right)^{1/4}$$

Normalization to correct for changes in laser output power was performed by dividing by the mean photocurrent.

$$\text{Flux} = \frac{\left(\int (\varpi^2 P(\varpi)\, d\varpi)\right)^{1/4}}{I_{dc}}$$

This algorithm is based on the rms frequency shift but is

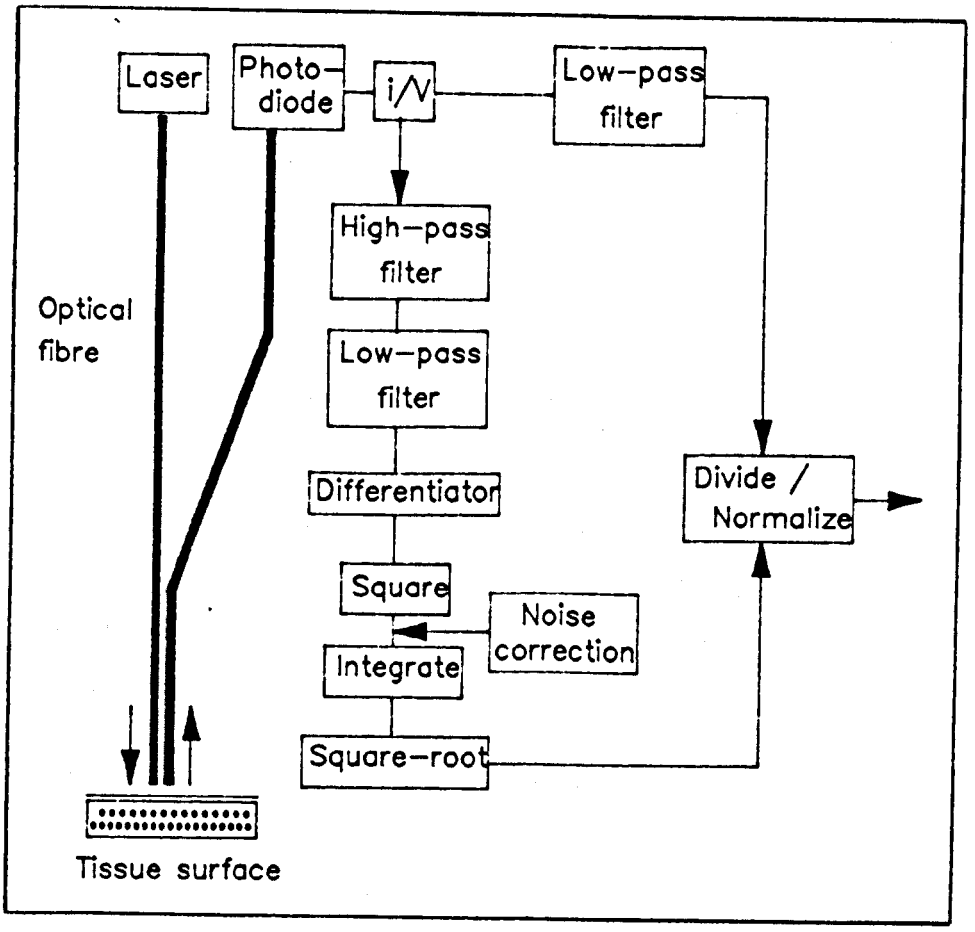

Figure 2.6 Block diagram of the Stern processing algorithm

not exactly consistent with theory. In this case normalization by I_{dc} rather than I_{dc}^2 is used because the top line of the equation contains the square root of the power spectrum.

Analogue implementation of the Stern algorithm

A block diagram illustrating the Stern processing algorithm is presented in figure 2.6.
Light backscattered from the tissue is directed on to a photodetector producing a current containing a dc component and a fluctuating ac component. The photocurrent is converted to a voltage and then ac-coupled to remove the dc-component. The signal is then passed through a bandpass filter that allows the Doppler frequency range through.
At this point the signal can be written as

$$\int_{\varpi_1}^{\varpi_2} F(\varpi)\ d\varpi$$

where $F(\varpi)$ is a Fourier component of the photocurrent and ϖ_1 and ϖ_2 are the lower and upper cut-off frequencies of the bandpass filter.
The Fourier component can be expressed as,

$$F(\varpi) = A \exp(i\varpi t) + B \exp(-i\varpi t)$$

where A and B are constants.
When the signal is differentiated with respect to time a ϖ-weighting factor is produced,

$$\int_{\varpi_1}^{\varpi_2} \varpi\ F(\varpi)\ d\varpi$$

The signal is then passed through an rms-to-dc converter.

The square of the absolute Fourier component is given by,

$$|F(\varpi)|^2 = P(\varpi) + aI_{dc}$$

where a is a constant depending on the photodetector gain. Hence the output of the rms converter (R) is,

$$R = \left[\int \varpi^2 P(\varpi)\, d\varpi + aI \int \varpi^2 d\varpi \right]^{\frac{1}{2}}$$

The flow parameter is obtained by subtracting a noise correction term and normalizing by the average photocurrent.

$$F = \frac{(R - N)^{\frac{1}{4}}}{I_{dc}}$$

Bonner and Nossal algorithm (ϖ-weighting)

The algorithm developed by Bonner and Nossal (1981) was based on the average frequency shift in the Doppler power spectrum. By making several assumptions about the light-tissue interaction a theoretical model was developed for analysing light scattering in the microvasculature (Appendix 2). They showed that the average Doppler shift, $\langle\varpi\rangle$, is related to the rms speed of the moving rbcs by the relationship,

$$\langle\varpi\rangle = \frac{\langle v^2\rangle^{\frac{1}{4}}}{(12\varepsilon)^{\frac{1}{4}}a}\, \beta\, f(m)$$

where,
$\langle\varpi\rangle$ is the average Doppler frequency shift
$\langle v^2\rangle^{\frac{1}{4}}$ is the rms speed of the moving rbcs
a is the radius of a spherical scatterer representing a rbc
ε is a factor related to cell shape
β is an instrumentation factor
f(m) is a function depending on the average number of collisions that photons make with moving rbcs (m)

For low rbc concentrations, m < 1, the first moment of the spectrum was shown to vary directly with the rbc flux. For higher rbc concentrations, m > 1, the first moment of the spectrum remained sensitive to changes in flow but varied approximately as the square root of m. In this case the first moment still changed linearly with the rms speed of the rbcs.

Analogue implementation of the Bonner and Nossal algorithm

A block diagram illustrating the Bonner and Nossal algorithm is presented in figure 2.7.
An output relating to the concentration of rbcs is produced by bandpass filtering the photocurrent and then squaring the output.

$$\int_{\varpi 1}^{\varpi 2} P(\varpi)\, d\varpi$$

The output related to the speed of rbcs is obtained by bandpass filtering the photocurrent over the same bandwidth as the concentration term but the signal is then passed through a $\varpi^{1/4}$-weighting filter producing a signal represented by,

$$\int_{\varpi 1}^{\varpi 2} \varpi^{1/4} F(\varpi)\, d\varpi$$

The signal is then corrected for noise contributions and passed through a squarer. The speed parameter is produced by dividing this output by the concentration term.

$$\frac{\int_{\varpi 1}^{\varpi 2} \varpi P(\varpi)\, d\varpi}{\int_{\varpi 1}^{\varpi 2} P(\varpi)\, d\varpi} = \langle \varpi \rangle$$

The flux term is produced by multiplying the concentration by the speed,

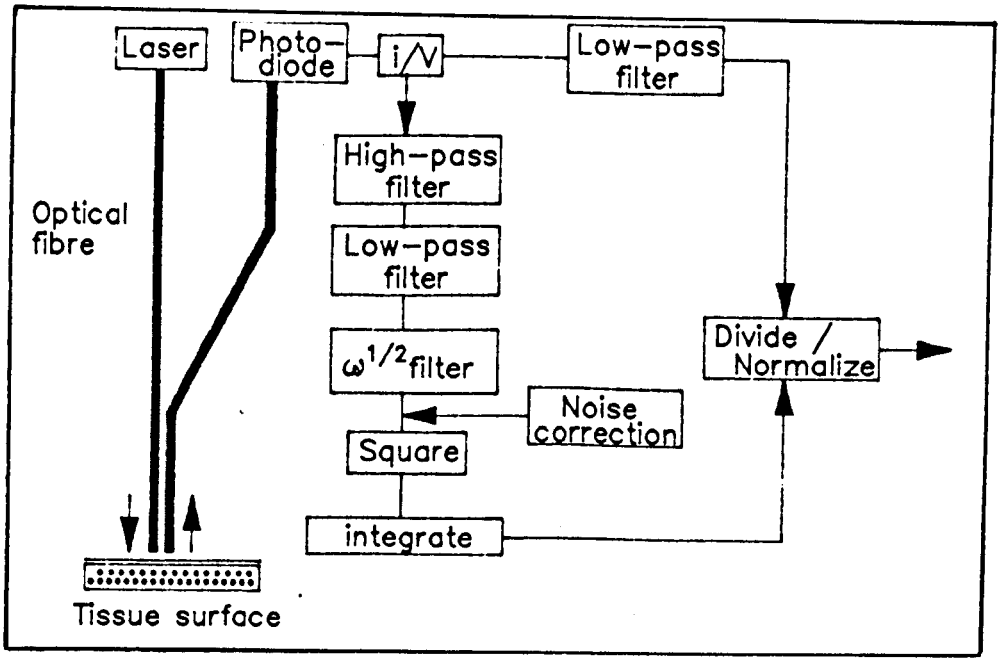

Figure 2.7 Block diagram of Bonner and Nossal processing algorithm

$$\text{flux} = \langle\varpi\rangle \int_{\varpi 1}^{\varpi 2} P(\varpi)\, d\varpi$$

Normalization is performed by dividing by a term proportional to the incident laser power.

$$\text{normalized flux} = \frac{\langle\varpi\rangle \int_{\varpi 1}^{\varpi 2} P(\varpi)\, d\varpi}{I_{dc}^{\,2}}$$

$$\text{normalized concentration} = \frac{\int_{\varpi 1}^{\varpi 2} P(\varpi)\, d\varpi}{I_{dc}^{\,2}}$$

CHAPTER 3

Evaluation Of Dual Channel Laser Doppler Flowmetry

3.1 Introduction

The aims of this chapter were to investigate developments in laser Doppler instrumentation and methodology. In the first section two commercial instruments were used to determine the differences in recorded responses due to different laser sources and processing bandwidths. Then a dual channel laser Doppler flowmeter was evaluated using an *in vitro* model and a method of applying the dual channel instrument was demonstrated *in vivo*.
Some of the results from this chapter have been published in a paper (Barnett et al., 1990).

3.2 Comparative Study Of Two Laser Doppler Flowmeters

Laser Doppler flowmeters can differ in many ways - including the choice of laser source, probe construction, processing algorithm and bandwidth options used in their design. In this study two commercial laser Doppler flowmeters, Perimed PF3 (Perimed, Stockholm, Sweden) and Moor MBF3 (Moor Instruments Ltd., Axminster, England), were compared to determine the effects that various design choices have on the instrument response.

3.2.1 Description of instruments

The Perimed PF3 uses a 2 mW HeNe gas laser (Siemens LGR 7621S) emitting light at a wavelength of 632.8 nm. The laser light is directed towards the skin via a single delivery fibre such that a maximum of 1 mW is radiated from the probe tip. The backscattered light is collected by two fibres and directed back to two separate photodetectors. A differential detection system (Nilsson et al., 1980a) is used to produce

a photocurrent which is processed using analogue electronics to yield an output voltage representing blood flux. The blood flux is digitally displayed on an LED display in arbitrary perfusion units. Blood flux, concentration of moving blood cells and total backscatter values are all available in digital form for external computer processing or analogue form for displaying on a chart recorder. There are two options of processing bandwidth either 20 Hz to 4 kHz (narrowband), to which the instrument automatically defaults, or 20 Hz to 12 kHz (wideband mode). Other options on the instrument include a movement artefact filter, a low light level indicator and adjustable alarms for low perfusion levels.

The Moor MBF3 uses a 3 mW semiconductor laser diode operating at a wavelength between 780 and 810 nm. The laser diode emits a diverging beam so a lens system is used to couple the laser light into the delivery fibre. The laser diode drive current is electronically stabilized and the temperature controlled using Peltier devices which can both heat and cool the lasers. Two glass fibres are used in the standard probe, one to transmit light to the tissue and one to collect the backscattered light. Differential detection is not used. The laser radiation power at the probe tip is 1 mW, similar to that of the PF3. A combination of analogue and digital processors are used to process the photodetector current. Blood flux, rbc concentration, average rbc velocity and dc backscattered intensity are all displayed digitally and a large liquid crystal display allows changes in these parameters to be observed in real-time. All parameters may also be obtained in digital or analogue form for external use and data is automatically stored for later analysis and print-out.

The MBF3 also has different processing bandwidth options - either 20 Hz to 15 kHz (wideband) or 20 Hz to 3.1 kHz (narrowband), with the instrument defaulting to the former of these.

Both flowmeters have their individual motility standards

that permit flowmeter calibration at the start of a set of measurements. The calibration standards consist of a solution of latex spheres undergoing Brownian motion. When a Doppler probe is immersed in the solution the subsequent flowmeter output can be used as a reference level to compare any further measurements. In this way measurements should be reproducible from day to day and from machine to machine.

3.2.2 Study one: Differences due to laser sources

Whereas the Perimed PF3 flowmeter operates by detecting red light originating from a HeNe laser, the Moor MBF3 detects infrared light from a semiconductor laser diode. Due to the construction of the gas-filled HeNe laser when the laser is switched on the laser warms up and the cavity expands causing the output intensity to fluctuate for a period of time (Fairs, 1988). The effect of these fluctuations on laser Doppler measurements were investigated and compared to the measurements obtained using the laser diode system over the same time period.

Experimental procedure

The two flowmeters were fitted with standard probes which were placed in their respective motility standards. The flux response was displayed on a chart recorder (Kipp and Zonen BD9) over a period of 1 hour after switching on the power supplies. Room temperature was 23°C throughout the measuring period.

Results

Figure 3.1 shows the traces of the flux output from the two flowmeters. The flux output from the PF3 has a periodic fluctuation with a peak-to-peak amplitude of approximately 4% of the mean flux signal. The frequency of the fluctuation decreases with time. At 10 minutes after switching on the

power supply there are approximately 4 fluctuations min^{-1}, at 25 minutes there are 1.5 min^{-1}, at 40 minutes there are 0.5 min^{-1} and at 55 minutes there are 0.3 min^{-1}.
There were no regular fluctuations in the MBF3 flux output. However there was some output variation particularly within the first 10 minutes (approximately 2.5% of the mean flux signal) after that any change in output intensity produced less than 1% change of the flux output.

Discussion

The results shown in figure 3.1 demonstrate the effects of the warming of the gas-filled HeNe laser used by the PF3 Doppler flowmeter. Fluctuations in the laser intensity are caused by mode hopping as the laser cavity heats and expands. The laser requires a long warm-up period before the light output stabilizes and throughout this period regular oscillations in the flux reading were observed. The manufacturers recommend a warm-up time of 30 minutes before measurements are made (Periflux PF3 Users handbook), but in this study fluctuations in laser intensity continued up to a period of at least 60 minutes. The differential detection circuit does not totally eliminate the fluctuations. The presence of these intensity fluctuations is dependent on the model of HeNe laser used. In particular, cheap lasers are usually more susceptible to intensity fluctuations.
Differential detection is not used by the MBF3 nevertheless the flux output from the flowmeter has a significantly shorter warm-up period compared to the PF3 flowmeter. The manufacturers recommend that measurements using the MBF3 should not be used for a period of 15 minutes after switching on the laser power supplies. These results show that the flux output is stable after this time period. From these results it is suggested that the laser diodes are potentially ideal light sources for laser Doppler instrumentation. As well as their output stability the devices are small, inexpensive, reliable and less fragile

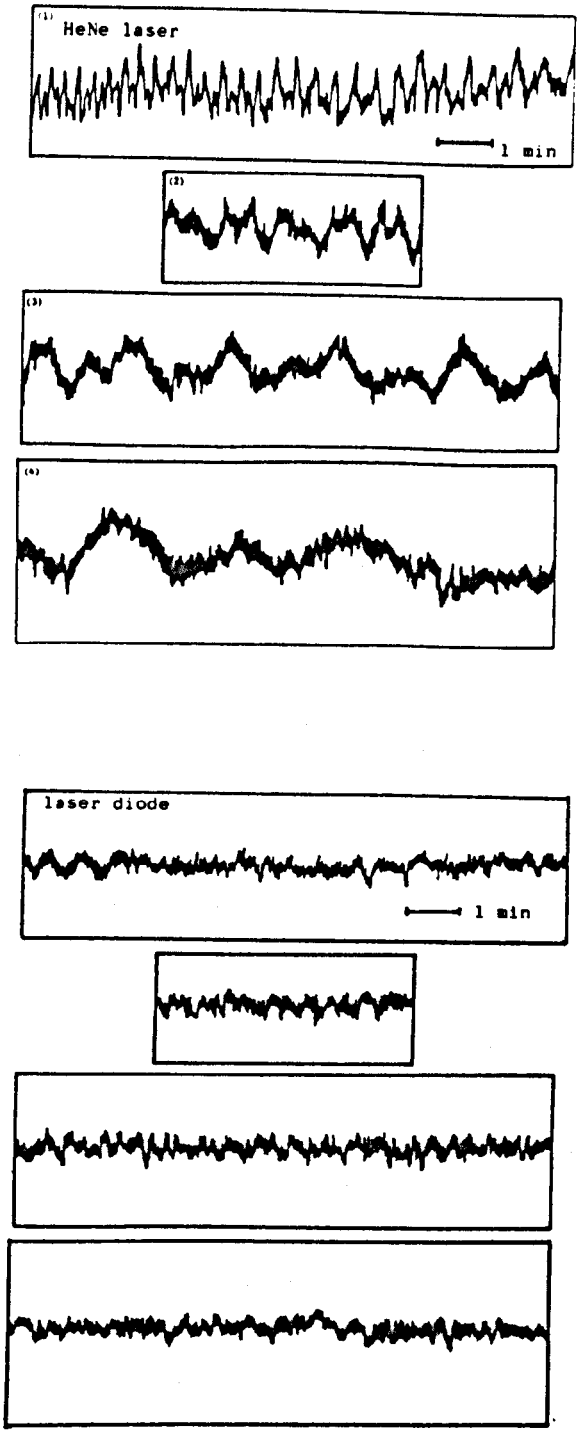

Figure 3.1 The Flux responses of the Perimed (HeNe) and Moor (laser diode) instruments (1) 1 to 10 minutes, (2) 20 to 25 minutes, (3) 30 to 40 minutes, and (4) 45 to 55 minutes after switching on the laser power supplies

than the HeNe lasers (Kolari, 1985). But there are some technical problems with the use of laser diodes. Output instabilities due to optical feedback in the laser cavity and diode heating have to be overcome by a well designed front-end optical arrangement. Also the majority of laser diodes operate at infrared wavelengths so the volume of tissue sampled by the radiation will be slightly larger than with the red systems.
The introduction of motility standards greatly improves Doppler measurements permitting some comparison between measurements. Reliable calibration producing reproducible flux values from day to day depends on the use of the motility standards therefore care has to be taken when using the standards. For example, the calibration temperature must be kept constant since the average velocity of moving particles is proportional to the square-root of temperature.

3.2.3 Study two: Effects of signal processing bandwidth

The signal processing algorithm used by both flowmeters is based on the average Doppler frequency shift (Bonner and Nossal, 1981), but the blood flux response of the flowmeters is dependent on the bandwidth over which the processing is performed. In this study the flux response was examined over a range of conditions created using an *in vitro* flow model and the effect of choosing different processing bandwidths on the linearity of the flux response was investigated.
The choice of processing bandwidth limits the range of frequency shifts processed and consequently the range of speeds of rbcs monitored. From the standard Doppler equation the maximum frequency shift, δf_{max}, of a photon when in collision with a rbc moving at a velocity v (figure 3.2) is,

$$\delta f_{max} = \frac{2nv}{\lambda}$$

for λ = 632.8 nm $\quad \delta f_{max} = 4.4$ kHz $(mms^{-1})^{-1}$
for λ = 780 nm $\quad \delta f_{max} = 3.6$ kHz $(mms^{-1})^{-1}$
assuming that the low pass filters controlling the

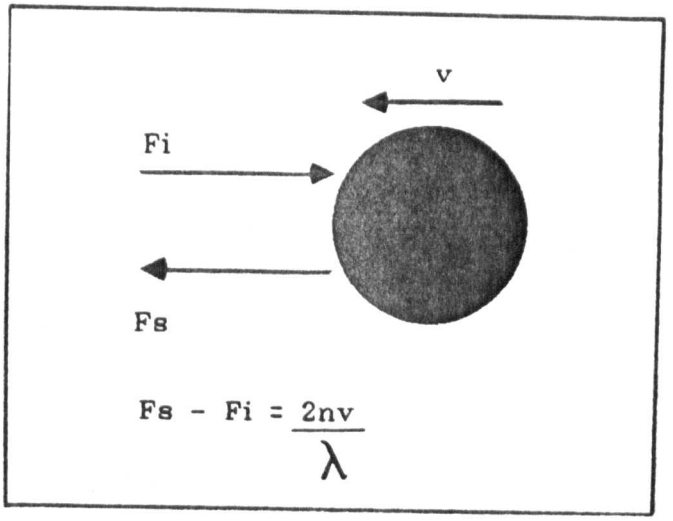

Figure 3.2 Conditions producing the largest Doppler frequency shift due to the collision between a photon and a moving rbc.

processing bandwidth of both Doppler instruments have a sharp cut-off characteristic.
Thus, in wideband mode, the PF3 (λ = 632.8 nm, bandwidth = 12 kHz) should cover a velocity range from 0 to 2.7 mms^{-1} comprehensively, whilst the MBF3 (λ = 780 nm, bandwidth = 15 kHz) should cover a velocity range from 0 to 4.2 mms^{-1} comprehensively. In the narrowband mode the velocity ranges are reduced. Both the PF3 (with a bandwidth of 4 kHz), and the MBF3 (bandwidth of 3.1 kHz) would be expected to cover a velocity range from 0 to 0.9 mms^{-1}. Velocities outside these ranges will create some frequency shifts outside the processing bandwidth. At least some part of the information from the faster moving rbcs will be lost and consequently the blood flux reading will underestimate the actual blood flow. In cases where the concentration of rbcs is high, multiple scattering will also tend to produce higher frequency shifts outside the processing bandwidth.

Experimental procedure

A simple *in vitro* model was constructed to investigate the blood flux responses of the two laser Doppler instruments, figure 3.3. The model comprised of a length of polythene tubing (i.d. = 3 mm, o.d. = 5 mm) set in a Silastic base (2 mm thick) with a diffusing layer of plastic (0.1 mm thick) covering the top surface. The diffusing layer was used to randomize the direction of the photons incident on the moving rbcs. Blood flow was controlled by a Harvard withdrawal/infusion pump holding either a 50 ml or 20 ml glass syringe. The average rbc velocity was calculated by collecting a volume of blood over a period of time as it was pumped through the model. Both laser Doppler instruments were fitted with standard probes and calibrated using their respective motility standards. The probe tips were placed on the surface of the model separated by a distance of approximately 5 cm to prevent cross-detection of backscattered light. This arrangement allowed a simultaneous

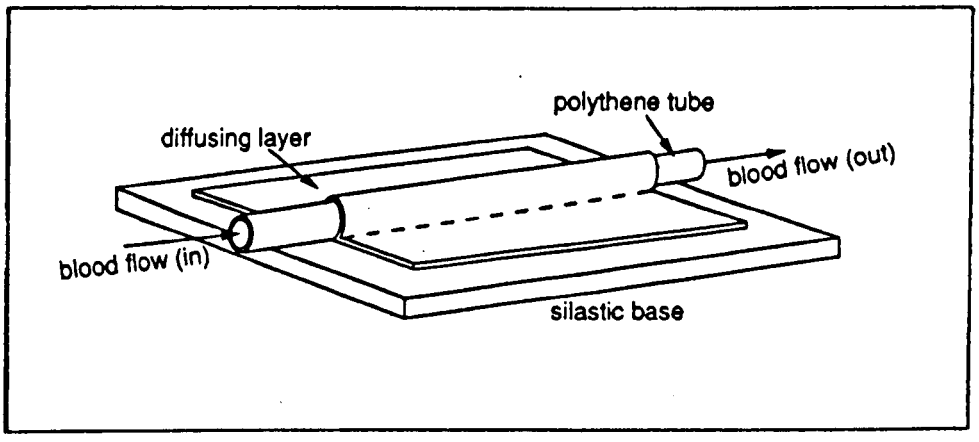

Figure 3.3 The *in vitro* model

comparison of the two instruments for almost identical flow conditions.

Fresh canine blood was heparinised and diluted with physiological saline solution to obtain values for rbc volume fraction equivalent to the typical values expected in the microcirculation. The maximum volume fraction of whole blood in the skin capillary layer is approximately 0.5% (Tenland, 1983), whilst the fraction of rbcs (p.c.v.) is lower and depends on the microcirculatory haematocrit. Rbc velocities in a resting skin capillary bed have been measured using video microscopy to range from 0 to 3.47 mms^{-1} (Bollinger et al., 1974). A wide range of rbc velocities, including those expected physiologically, were obtained in the *in vitro* model by using several different settings on the infusion pump. The instruments were tested over a range of blood flow conditions using both wideband and narrowband bandwidth options.

Results

Wideband mode

The laser Doppler flowmeter responses in wideband mode for various flow conditions are shown in figure 3.4.

There was a strong correlation, ($r=0.96$, $p<0.001$), between the responses of the PF3 and MBF3 instruments over the whole range of blood flow conditions in the wideband mode figure 3.5. The responses were linear over a large range of velocities including those expected in most microcirculatory conditions. The MBF3 appears to be linear over a larger range of velocities than the PF3, most probably due to the larger bandwidth employed in the MBF3 processing.

Narrowband mode

When the instruments were in narrowband mode the linearity of response was over a much smaller velocity range, figure

3.6. Above a velocity of approximately 1.2 mms^{-1} the flux measurements underestimate the blood flow to various extents.

Discussion

The *in vitro* investigation demonstrates that the two laser Doppler instruments have similar flux response characteristics over a variety of flow conditions. In wideband operation the responses of both instruments are strongly correlated ($r=0.96$, $p<0.001$). Both instruments in their wideband modes have linear flow responses over the expected microvascular blood flow range, but are linear over a smaller velocity range in the narrowband mode. In some conditions, such as reactive hyperaemia and skin flushing or where the laser light is incident on a number of arterioles and venules, the microcirculatory flow may fall outside the narrowband linear range. In such cases the instruments underestimate blood flow.

Both instruments had linear responses that extended beyond the velocity ranges predicted for each mode of operation. The PF3 was linear for velocities from 0 to 4.5 mms^{-1} in wideband mode and 0 to 1.2 mms^{-1} in narrowband mode, whilst the MBF3 was linear over the range 0 to 6 mms^{-1} in wideband mode and 0 to 1.2 mms^{-1} in narrowband mode. This extended linearity was probably due to only a small percentage of collisions between photons and rbcs producing large (near maximum) frequency shifts. A large portion of the incident light is scattered in the forward direction (Tenland, 1982) consequently the percentage of high frequency shifts occurring at each velocity may be smaller than expected and those occurring outside the processing bandwidth may only become apparent at higher velocities.

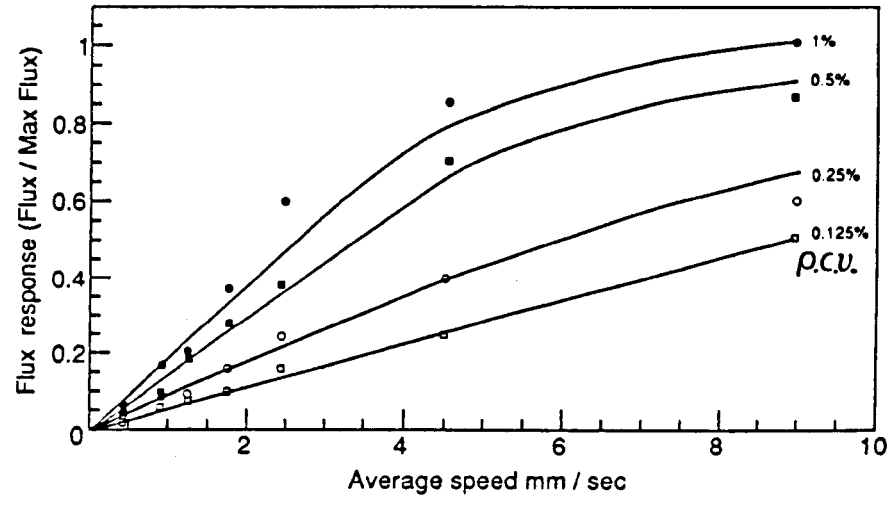

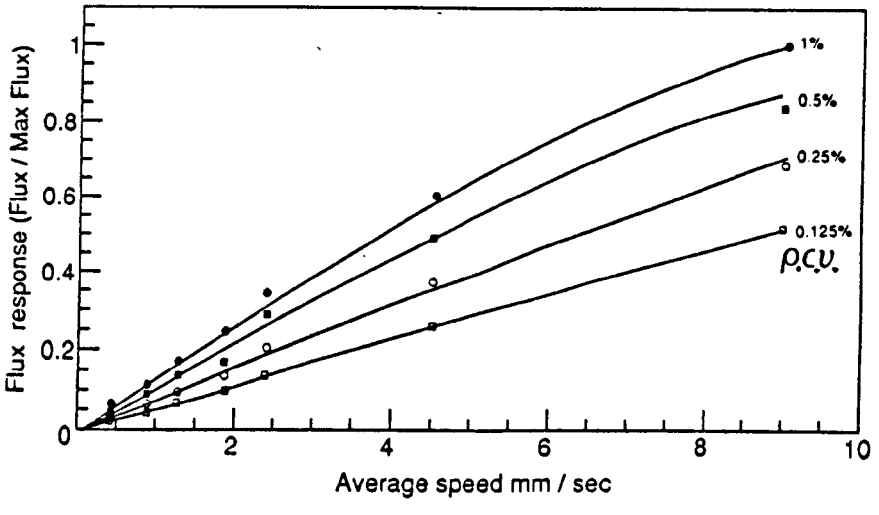

Figure 3.4 Wideband flux responses for the Perimed PF3 (top) and the Moor MBF3 (bottom).

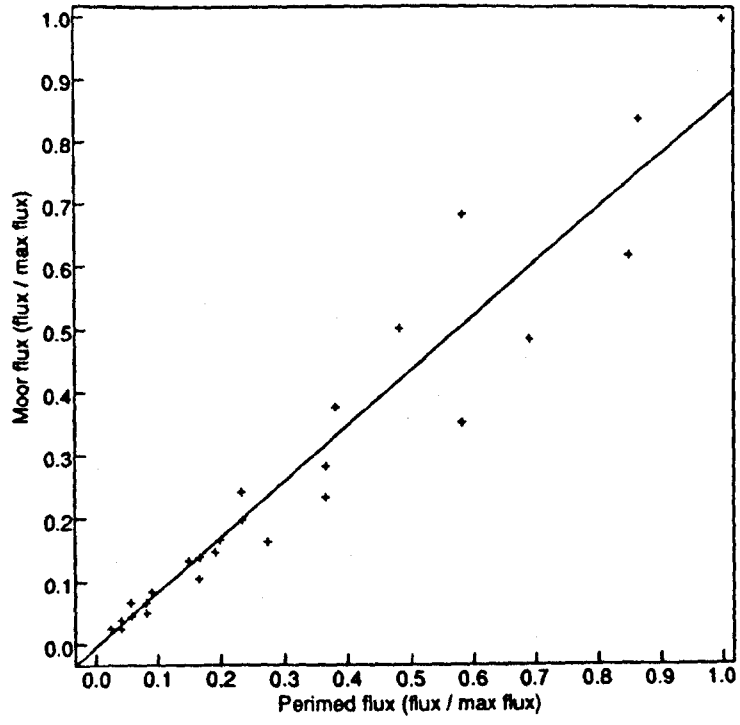

Figure 3.5 Comparison between the two Doppler flowmeter responses in wideband mode.

An important feature to notice is that the responses of both instruments in narrowband mode appear to become non-linear at low values of blood flux. This occurs because, even at relatively low values of blood flux, some of the individual Doppler shifts are outside the instruments' processing bandwidth in this mode. The PF3 defaults to narrowband mode when switched on. Although this range covers most states ofmicrocirculatory blood flow, whenever levels of high perfusion are expected the wideband mode of operation should be selected. Measurements made using the narrowband mode should not be directly compared with values measured using the wideband mode because limiting the bandwidth significantly reduces the signal level. This is due to the loss of the Doppler shifts in the 4 to 12 kHz range in the narrowband mode. The MBF3 defaults to wideband mode which is more appropriate because its response is then linear for all velocities expected in the microcirculation. There was no significant decrease in signal-to-noise by choosing this mode rather than the narrowband mode.

In summary the processing bandwidth of the laser Doppler instruments has a significant effect on the responses to blood flow. This is especially noticeable for large rbc volume fractions and for fast moving cells. For both instruments the wideband mode of operation should be used in the majority of perfusion studies.

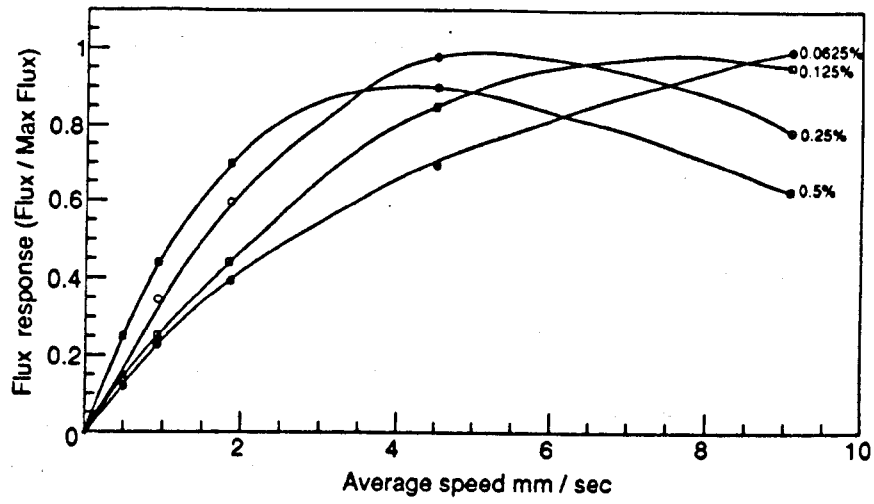

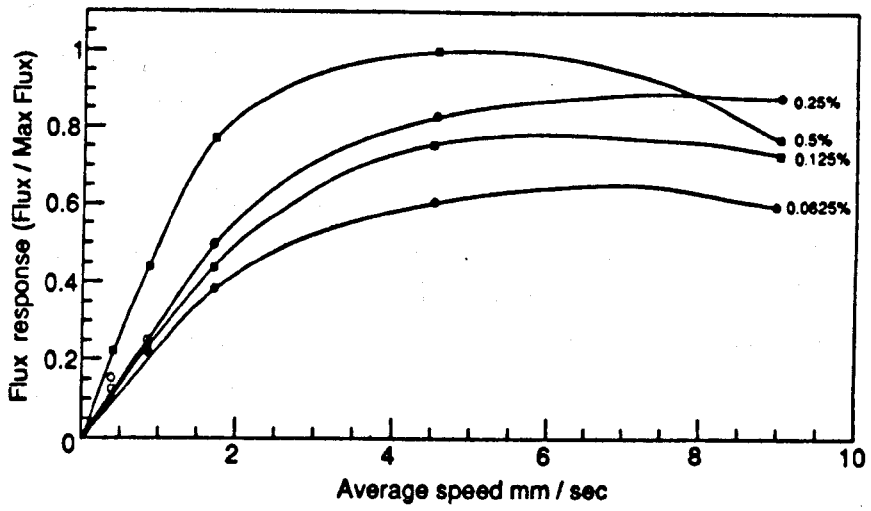

Figure 3.6 Narrowband flux responses for the Perimed PF3 (top) and Moor MBF3 (bottom).

3.3 Dual Channel Measurements

One limitation of the laser Doppler technique is that in order to compare two perfusion sites either two separate monitors are required (Hirkaler and Rosenberger, 1989) or one probe has to be moved between sites. The first option can become expensive while the second only allows discrete, non-continuous measurements at the two sites. The Moor MBF3D is a dual channel laser Doppler instrument that allows blood flow studies to be performed simultaneously at two separate measuring sites. Each channel of the MBF3D is similar to the MBF3 single channel flowmeter used in the earlier studies. Ideally for a dual channel system the two channels should respond identically for identical flow conditions. In this investigation the flux responses for both channels were compared to the flow in an *in vitro* model. The monitor was then used in an *in vivo* study to demonstrate a method of using the dual channel measurements.

3.3.1 *In vitro* study

The dual channel device was evaluated using the *in vitro* model from the previous study. Both probes were initially placed in the Moor motility standard and calibrated so that the flux responses from each channel would be similar when placed on the model. Percentage changes in response were compared for changes in flow as the pump speed was altered in steps from 0.18 mms^{-1} to 4.5 mms^{-1} and for rbc volume fractions of 0.125% to 2%. The wideband processing bandwidth was used throughout the study.

Results

The two channels of the MBF3D respond almost identically for changes in blood flow over a range of rbc velocities and concentrations, figure 3.7. There was strong correlation ($r=0.999$, $p < 0.001$) between the two measurements of flux

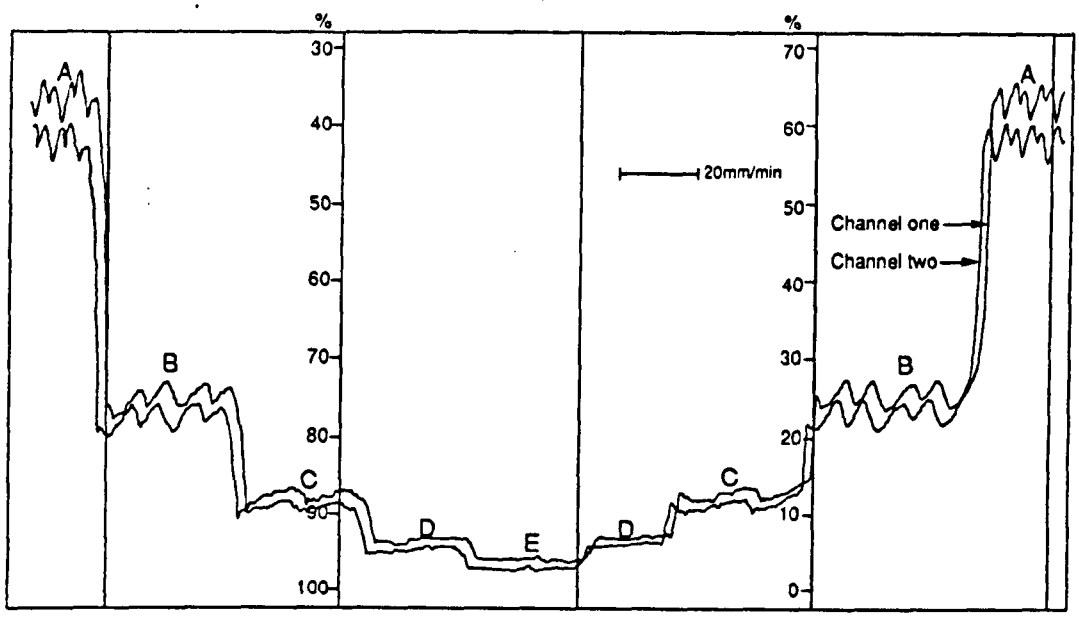

Figure 3.7 Blood flux responses for both channels of the Moor MBF3D for a p.c.v. of 0.5% and average rbc speed of; (A) 4.5, (B) 1.8, (C) 0.9, (D) 0.45 and (E) 0.18mms^{-1}.

from the two channels, figure 3.8, and also between the measured flux and the known blood flux in the model over the whole range of flows investigated ($r=0.94$, $p < 0.001$, for both channels).

Discussion

The dual channel capability of the Moor MBF3D was evaluated by placing the probes from both channels on the *in vitro* model where they sampled almost identical flow. By previously calibrating the two probes in the motility standard they produced very similar responses for changes in flow. Both channels demonstrated a strong correlation ($r=0.94$, $p<0.001$ for both channels) between the flux measurements and the known flow in the model. The strong correlation between the channels ($r=0.999$, $p<0.001$) justify the use of the dual channel instrument in investigations where changes in blood flux are compared at different sites. Pre-measurement calibration using the motility standard ensures that similar flux values are obtained for similar scattering conditions.
In figure 3.7 there is a small offset between the two flux measurements. This may be due to the two probes sampling slightly different flow volumesdue to positioning on the model. Otherwise it may be due to incorrect calibration of probes at the start of the experiment.

3.3.2 *In vivo* study

All *in vivo* investigations were performed with the aid of the Cardiovascular Group at I.C.I. Pharmaceuticals, Macclesfield, Cheshire, England. All animal preparation was performed by employees of I.C.I.
The aim of this study was to demonstrate how the dual channel flowmeter may be used to monitor local drug effects on skin blood flow at a test site compared to a control site and to demonstrate that global (or systemic) changes in blood flow affect both blood skin sites. In this study

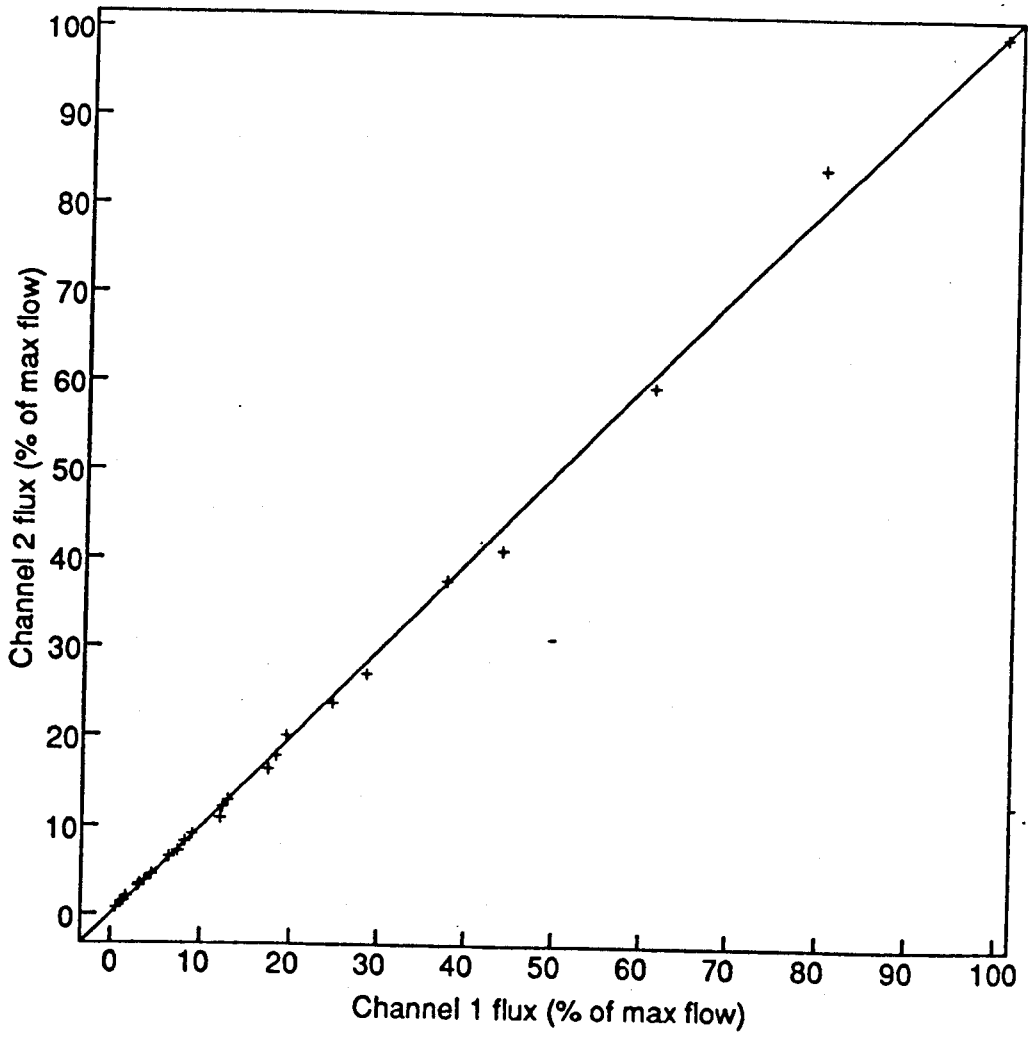

Figure 3.8 Comparison between flux responses obtained from channel one and channel two.

measurements were taken from a subject group of 4 animals. Male beagle dogs 12 - 17 kg were anaesthetised with an intravenous injection of Sagatal (30 mg kg^{-1}) and anaesthesia maintained with a continuous perfusion of a Sagatal-saline mixture (Sagatal : saline = 1:12). The left femoral vein and artery were cannulated, the former for maintenance of anaesthesia and the latter for blood pressure measurement via a pressure transducer and a chart recorder (Graphtec, Thermal Arraycorder WR3600). A jugular catheter was inserted for administration of test substances and a tracheal cannula inserted to respire the animal using a Harvard pump.

An area on the inside hind leg of the dog was shaved and the two Doppler probes carefully placed on the skin surface (figure 3.9). Small right-angled Doppler probes were held at the measurement sites using strips of transparent adhesive dressing (Tegaderm, 3M, St. Paul). Continuous tracings of the flux responses from both channels were recorded using a dual channel chart recorder (Kipp and Zonen BD9).

After a steady baseline flux measurement had been obtained for both channels an intradermal injection of a vasodilator (beta stimulant) was given locally near to one of the measuring sites. Care was taken when injecting the drug not to disturb the Doppler probe position on the skin but it was difficult to avoid some movement which was observed as artefact on the flux output. Flux measurements were recorded for a period of approximately 20 minutes after the injection then the flux responses at the two sites were compared (figure 3.10). The probe situated at the injection site was then moved to another area on the hind leg and a baseline measurement of blood flux obtained over a period of 5 minutes. At this point, an intravenous injection of the vasodilator was given through the jugular catheter. The flux responses of the two flowmeter channels were similarly recorded and compared over a period of 20 minutes (figure 3.11).

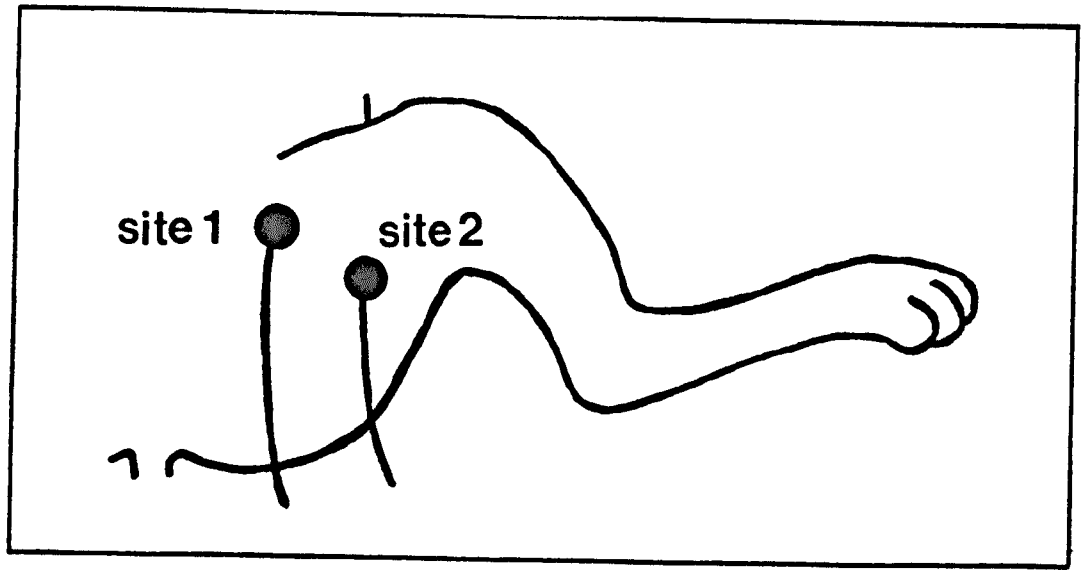

Figure 3.9 Position of Doppler probes on the hind leg of the dog.

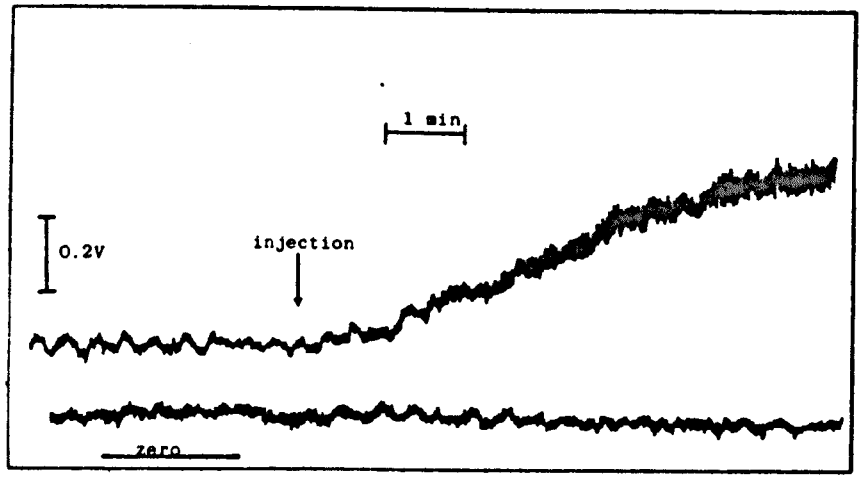

Figure 3.10 Typical chart recording of flux responses at a control site and drug site after an intradermal injection of vasodilator.

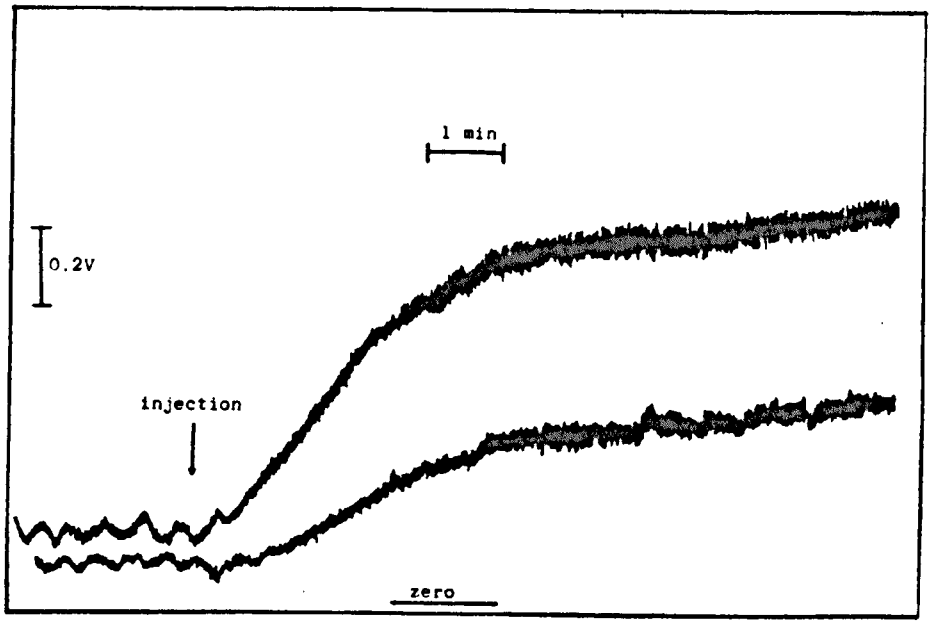

Figure 3.11 Typical chart recording of flux responses at a two skin sites after an intravenous injection of vasodilator.

Results

The drug response curves for each animal were combined to show the general drug effect when given either locally or systemically. In the case of the local injection the skin became visibly reddened and the blood flux increased dramatically for the flowmeter channel monitoring at that site. At the other measurement site, the control site, the flux remained close to the baseline measurement (figure 3.12).

When the drug was injected through the jugular catheter a global skin flushing was observed and blood flux increased dramatically at both measurement sites. When the flux responses were calculated as a percentage of the maximum flux response obtained in each test then the response at the two sites were very similar (figure 3.13).

Discussion

Investigations where the probe is moved between sites are unsatisfactory due to the difficulties of repositioning the probes and the non-continuous nature of the results. A better method of performing measurements is to continuously monitor two separate tissue sites and compare dynamic changes at those two sites simultaneously.

This study demonstrated that local changes can be monitored using the dual channel flowmeter using one of the channels as a control-site measurement. Global changes in blood flow were seen to affect both channels to the same extent. Dual channel systems used in this way can greatly improve the scope of experiments carried out using laser Doppler measurements.

Global changes such as increases in body temperature should generally affect two healthy skin sites similarly and therefore should be seen to affect both flux measurements equally. There will be some site dependency in the measurements but generally the technique is an improvement

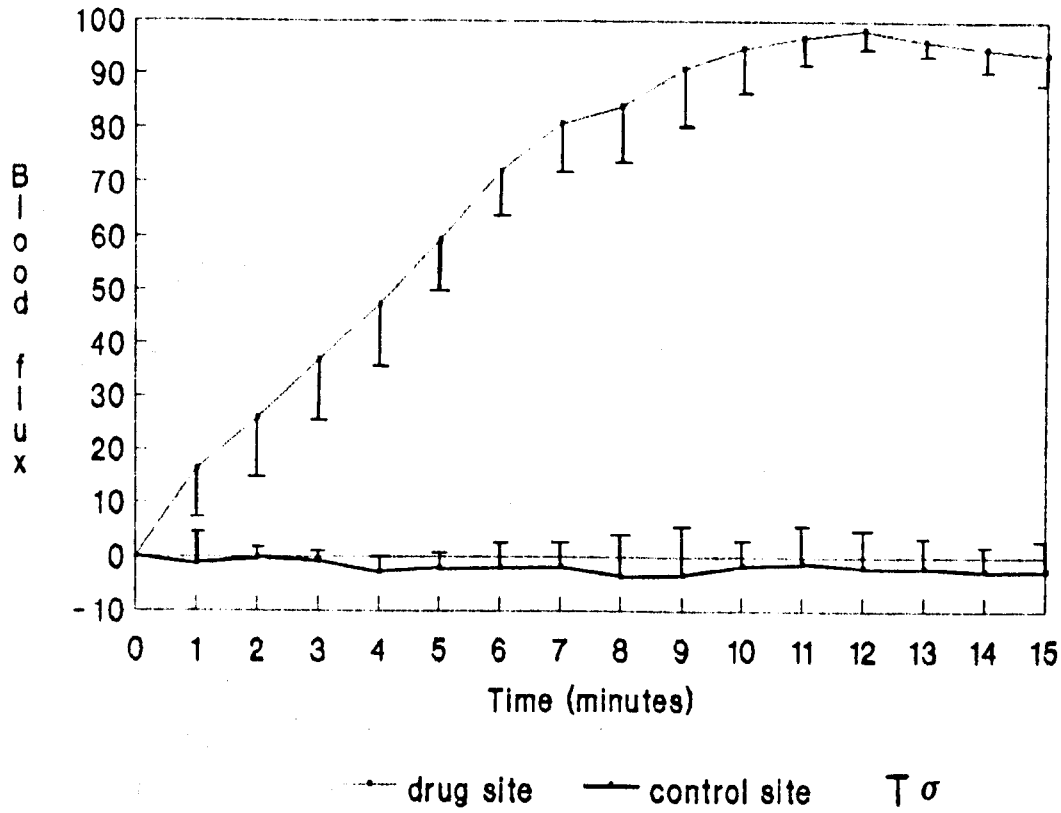

Figure 3.12 Blood flux responses at a control site and drug site after an intradermal injection of vasodilator.

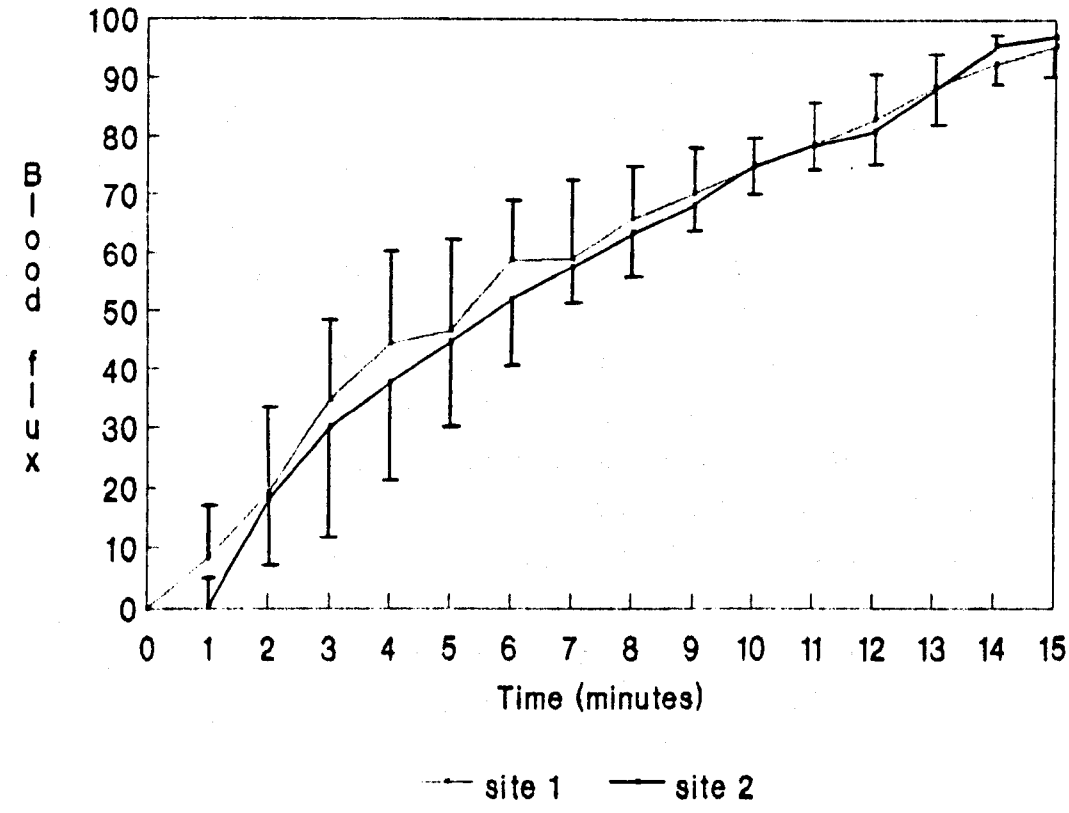

Figure 3.13 Blood flux responses at a two skin sites after an intravenous injection of vasodilator.

on earlier methods where the probe has to be frequently moved.

There are several applications where the dual channel device improves the methodology of obtaining blood flow information. For example, the flowmeter may be used to compare measurements from diseased skin sites with measurements from control sites displaying different flux responses due to either global or local interventions.

Conclusions

Two commercial laser Doppler flowmeters using similar processing algorithms but different laser sources and processing bandwidths were evaluated *in vitro*. The laser diode was shown to have a shorter warm-up time than the gas HeNe laser before the output intensity stabilised. This short warm-up time and the small size of the diode indicate that the laser diode is a better choice of light source for Doppler instrumentation. As the two flowmeters operate with different wavelength lasers the sample volume of tissue is different for each. Theory indicates that the infrared laser diode light will sample a larger volume of tissue than the HeNe red light.

The choice of processing bandwidth was shown to have a dramatic effect on the flux response of the instruments. Wideband mode should be chosen in applications where fast moving rbcs (> 1 mms^{-1}) may be sampled.

The introduction of dual channel Doppler instrumentation was demonstrated to improve the method of obtaining measurements *in vivo* by simultaneously monitoring blood flux at drug and control skin sites. Increased multiple site measurements may have further advantages in a number of applications to simultaneously monitor changes in blood flow at several sites.

CHAPTER 4

Depth Discrimination In Laser Doppler Measurements By Choice Of Wavelength Source

4.1 Introduction

Skin blood flow measurements performed using either red or infrared lasers are usually assumed to measure from a tissue volume reaching down into the dermis and subcutaneous levels. The approximate depth from which measurements are obtained has been quoted by different authors to be anywhere from 0.6 mm to 3 mm (Nilsson et al., 1980; Bonner and Nossal, 1981). Deeper measurements have been reported in other tissues Johansson et al. (1989), for example, suggested that a measurement depth of 6 mm was obtained in gastrointestinal tissue. (This is presumably due to the absence of the strong absorbing layers usually found in the epidermal layers of skin). As a result transcutaneous laser Doppler measurements are of a total skin blood flow within the dermal vasculature sampled at that specific measurement site. Capillary flow information is not distinguished from the thermoregulatory flow in the deeper lying vessels.
There is considerable interest in obtaining depth discrimination in laser Doppler measurements. The basal layer containing the capillary network is where the exchange of nutrients and waste products takes place. In a number of diseased states it is primarily the superficial skin layers, including the basal layer, that are affected. For example, in psoriasis the capillary blood vessels become dilated and tortuous. A technique with the ability of monitoring nutritional flow to the skin without being affected by the deeper dermal flow would provide a valuable tool for clinical investigation of such skin diseases. It would also aid in the understanding of general blood flow physiology and treatment by topically applied drugs.

In techniques concerned with the interaction of light with skin tissue one method of obtaining depth discrimination is by choice of wavelength. The aims of the studies in this chapter were primarily to determine whether the depth of laser Doppler measurements are different when red or infrared wavelengths are used. Preliminary studies investigating the Doppler information obtained using a green laser system are also presented.

4.1.1 Wavelength dependence of skin absorption and scattering:

Many researchers have investigated the processes involved as different wavelengths pass through the skin tissue (Anderson and Parrish, 1981; Hardy et al., 1956) but an extensive model of radiation transfer that can be applied to all tissue has not been established. The task is made more demanding because the radiation is scattered and absorbed by structures and chromophores which are continuously changing with time and vary from site to site and subject to subject. Generally melanin is the major epidermal absorber and blood chromophores such as haemoglobin and oxyhaemoglobin are the main contributors to absorption in the dermis. Scattering by collagen fibres within the dermis also has a great influence on the depths to which optical wavelengths penetrate the skin. As a result red and near infrared radiation may penetrate several millimetres or more into the skin whereas blue and green wavelengths only penetrate several micrometers. It follows that by using shorter wavelength radiation only the superficial blood vessels, the capillaries and venous plexus will be sampled.
Several investigators have reported the depth of penetration of different wavelengths into the skin. Recent studies have estimated that red wavelengths penetrate deeply into the dermis and reach the subcutaneous fat (Anderson et al., 1981). Anderson and Parrish (1981) analysed the transmittance spectra of human dermis and epidermis *in vitro*

Using a simple radiation transfer model with various thicknesses of fresh skin. The data estimating the depth of penetration is presented in table 4.1.

Table 4.1. Approximate depth for penetration of optical radiation in fair Caucasian skin to a value of 37% of the incident energy density (Anderson & Parrish, 1981).

Wavelength (nm)	Depth (μm)
250	2
280	1.5
300	6
350	60
400	90
450	150
500	230
600	550
700	750
800	1200
1000	1600
1200	2200

Such results provide only a limited indication of the measurement depth. In Doppler measurements it is the backscattered light that is detected. Although a substantial portion of light may reach into the subcutaneous layers this penetrating light will be less likely to be backscattered to the skin surface.

4.1.2 Previous studies using choice of wavelength to provide depth discrimination

A photoplethysmography study by Giltvedt et al. (1984) demonstrated that by using infrared (950 nm) and green (560 nm) wavelength light emitting diodes it is possible to record vascular changes in different layers of the skin. The detected green light signal was reported to derive from the shallow arteriole vessels while the infrared signal was reported to originate from deeper small arteries.

Duteil et al. (1985) performed a series of laser Doppler studies to discriminate between total and superficial skin blood flow based on a two wavelength system (argon ion laser at 548 nm and a HeNe laser at 632.8 nm). The frequency power spectra of the detected photocurrent were examined by fitting Lorentzian curves to the spectral data and a flow parameter - the mean Doppler shift - was obtained from the half-width at half-height of the spectra. Measurements from blood flowing through a range of different diameter glass tubes (50 μm to 1 mm i.d.) demonstrated no significant difference between the rbc velocities sampled by the two wavelengths. This was expected since there were no major wavelength-dependent scattering layers in the *in vitro* model.

In vivo results suggested that the blue wavelength was sampling a shallower tissue volume. Both wavelengths were demonstrated to be monitoring blood flow by observing the Doppler frequency power spectra change in response to performing forearm occlusions in a human volunteer. Responses to intradermal injections of noradrenaline and nicotinic acid ester were obtained using both the HeNe and argon ion laser sources. The subsequent vasoconstriction and vasodilation were observed by gradual changes in the half-width of the Doppler spectra and statistical evidence demonstrated that the blue light was sampling a more superficial level within the skin.

Obeid et al. (1988) performed *in vitro* studies using red (HeNe laser at 632.8 nm), infrared (laser diode at 780 nm) and green (HeNe laser at 543 nm) wavelengths. Solutions of either latex spheres or blood flowing through a large (1 mm i.d.) polythene tube were used. Each wavelength was found to sample the same velocity cross section using solutions of latex spheres. However for solutions of blood the green wavelength light was found to sample a slower moving population of scatterers. This was attributed to the longer wavelengths penetrating further into the tube and sampling the faster moving rbcs at the tube centre. As there were no

major scattering layers within the tube model these results credit some of the depth discrimination to the absorption by the chromophores present in the blood.

4.2 *In Vivo* Studies

There is considerable difficulty demonstrating depth discrimination using either *in vitro* or *in vivo* models. *In vitro* models present problems in replicating the scattering and absorption properties of the skin tissue. On the other hand, *in vivo* measurements are difficult because of the problems of controlling flow at different skin depths. Several *in vivo* tests were devised in an attempt to demonstrate the depth of measurement of different wavelength laser sources.

4.2.1 Study one: Occlusion responses using red and infrared wavelengths

As all commercial laser Doppler flowmeters use either red or near infrared wavelengths the first three studies aimed to detect whether there were any significant differences between the tissue volumes sampled by these different lasers. In the first study red and infrared wavelengths were used to observe femoral artery occlusion responses in the rat.

Experimental Procedure

Female Alderley Park Wistar rats (250 g) were anaesthetised using sagatal (Pentobarbitone 60 mg kg^{-1}). An area of the hind leg was shaved so that two laser Doppler probes could be placed at separate measurement sites. The femoral artery was exposed and a cotton tie placed loosely around it. The tie was then hooked over a height-adjustable clamp. The laser Doppler probes were held in manoeuvrable stands and placed on the skin with negligible external pressure applied

to the surface. The two optical fibre probes were attached to two separate laser Doppler flowmeters (Moor Instruments Ltd., MBF1), one of which was operating using a HeNe laser at 632.8 nm (Melles Griot) and the other a semiconductor diode laser at 780 nm (Sharp LT022MC0). The laser output powers at the tip of the optical fibre probes were matched at 1 mW.
The probes were placed on the skin with a separation of at least 3 mm to prevent any cross-detection of laser light (figure 4.1).
A series of femoral occlusions were then performed while continuously monitoring blood flux at both measuring sites. Each occlusion was performed for 3 minutes. The tie was then released for a period of 5 minutes or longer if the blood flow had not reached a steady level. After the first occlusion response had been recorded the optical fibres were changed over and a second occlusion performed. In this way an occlusion response at both measurement sites was recorded for both wavelength laser source. The process of changing over optical fibres then performing occlusion responses was repeated a number of times and in several different animals (n = 6).

Statistics and results

In each rat six femoral occlusions were performed while measuring the blood flux at two different skin sites with two different laser wavelengths. Typical chart recordings of the occlusion responses is shown in figure 4.2.
The measurement of occlusion response was taken to be the difference between the average preocclusion level minus the average signal level during the occlusion.

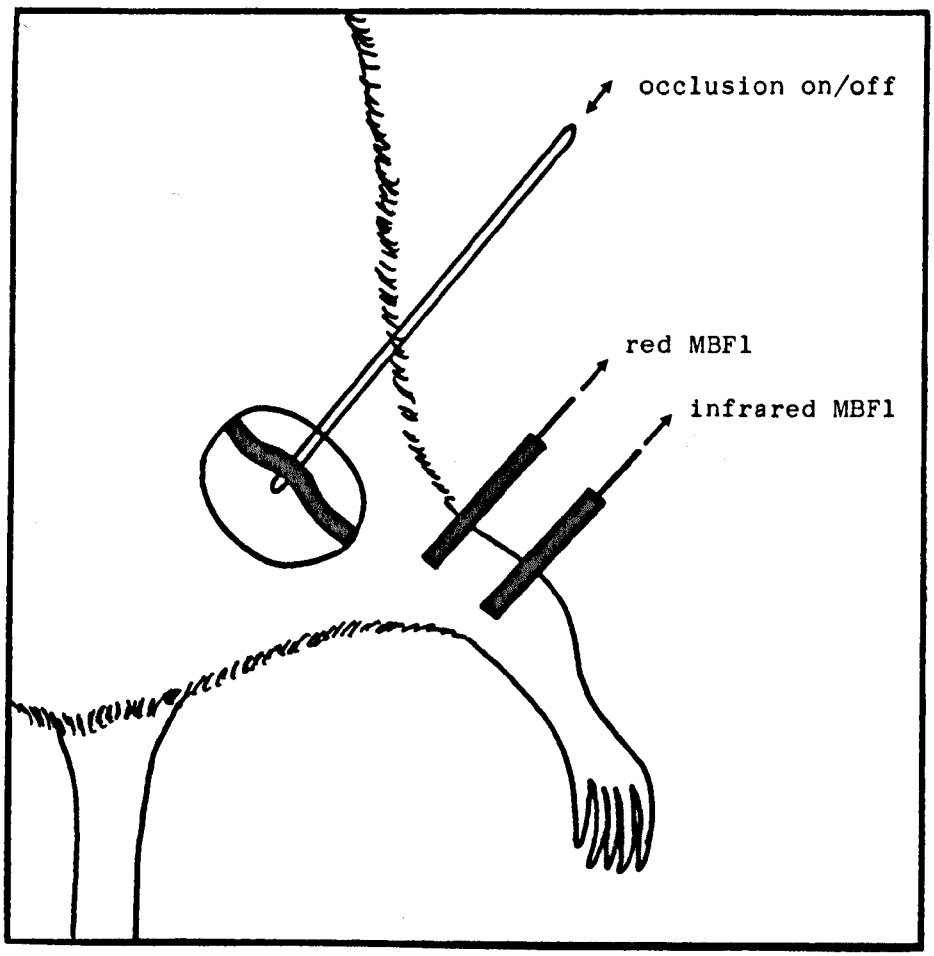

Figure 4.1 Approximate positions for the two laser Doppler probes on the hind leg of the rat.

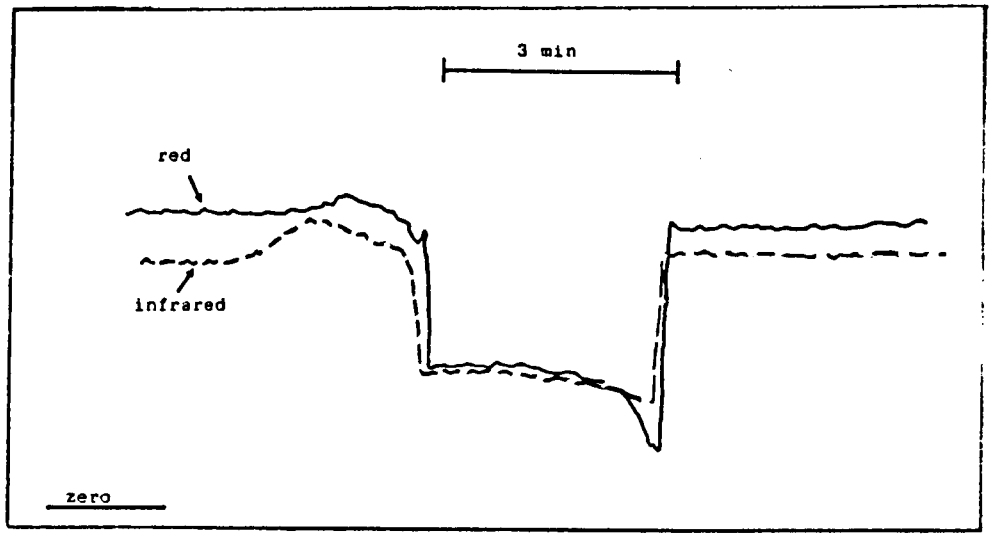

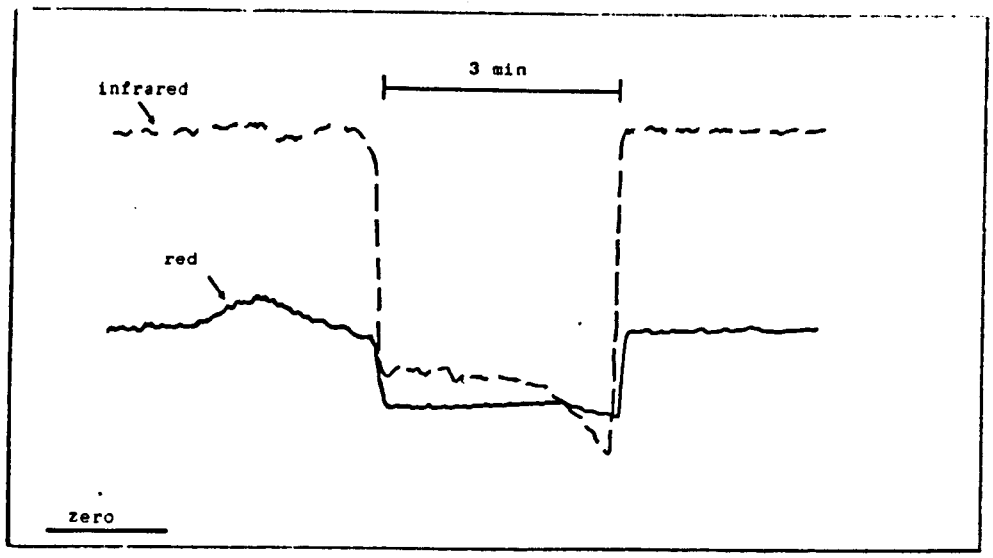

Figure 4.2 Consecutive occlusion responses using the laser Doppler flowmeters. The red and infrared sources were swapped over between the two responses.

The wavelength sources were not swapped after each occlusion but the following procedure was followed:

	site one	site two
occlusion 1	R11	I21
occlusion 2	I12	R22
occlusion 3	I13	R23
occlusion 4	R14	I24
occlusion 5	R15	I25
occlusion 6	I16	R26

(Zxy, Z is the wavelength light R = red, I = infrared)

In the majority of the animals it was apparent that there was a difference between responses recorded at the two different measurement sites. This was presumably due to the expected variability in skin perfusion from region to region on the skin surface.

Statistical analysis was used to demonstrate whether consecutive occlusions using a specific wavelength were reproducible. The responses I_{12} with I_{13}, I_{24} with I_{25}, R_{14} with R_{15} and R_{22} with R_{23} for each rat were used in the analysis. A strong correlation ($r = 0.96$, $p < 0.001$) was observed between these consecutive occlusion responses (figure 4.3). A Student t-test (SPSS/PC Base Manual, 1988) demonstrated that for occlusion responses using the same wavelength at a specific measurement site there was no significant difference between the consecutive measurements ($t = 1.58$, $df = 23$, $p = 0.13$)[1].

Statistical analysis was then performed to establish whether there was any difference between consecutive occlusion responses performed at the same site but with different wavelengths. A Student t-test using responses R_{11} with I_{12}, R_{14} with I_{13}, R_{15} with I_{16}, R_{22} with I_{21}, R_{24} with I_{23} and R_{25} with I_{26} demonstrated that there was a significant difference

[1]t is the difference in means divided by the standard error, df is the degrees of freedom, and p is the level of significance.

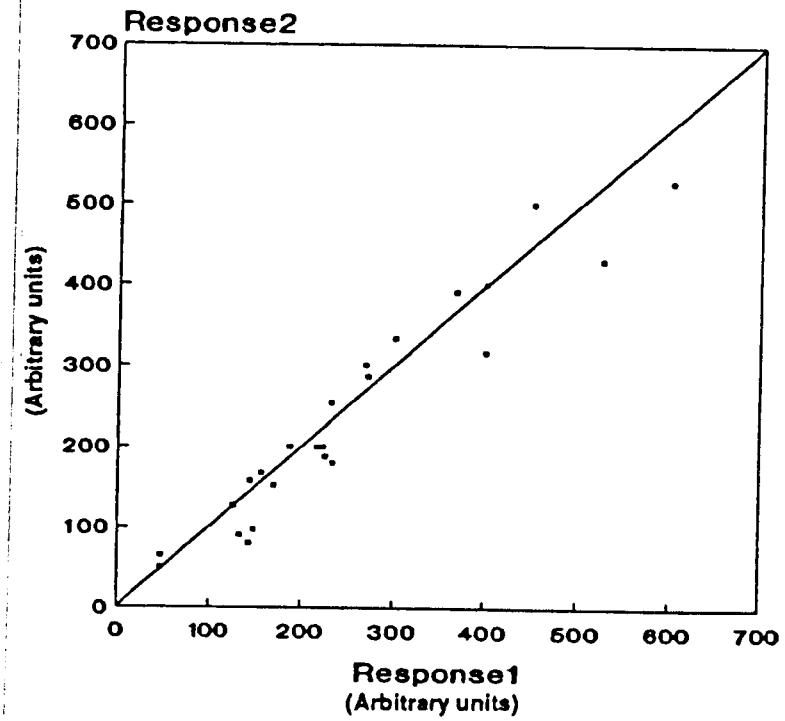

Figure 4.3 Comparison between consecutive occlusion responses with no change in operating wavelength.

between the measurements made at each wavelength ($t = 5.67$, $df = 35$, $p < 0.0001$). The mean infrared response was 1.5 times larger than the mean red response. There was a strong correlation ($r = 0.82$, $p < 0.001$) between the red and infrared responses (figure 4.4).

Discussion

The results suggest that the red and infrared wavelengths measure similar blood flow responses, but that the infrared measures from a larger tissue sample volume sampling some faster moving rbcs.

4.2.2 Study two: Occlusion responses detected through skin flaps

The objective of this study was to investigate the thickness of skin tissue through which laser Doppler measurements can be obtained.

Experimental procedure

Female Alderley Park Wistar rats (250 g) were anaesthetised using sagatal (Pentobarbitone 60 mg kg^{-1}). Each rat was placed on its back, the femoral artery was exposed and a cotton tie placed loosely around it. An area of the hind leg below the incision was shaved as preparation for siting the laser Doppler probe. Care was taken when placing the probe to prevent excess skin contact pressure.
Blood flux was recorded continuously using a Moor MBF1 flowmeter connected to a chart recorder. The laser sources (HeNe red at 632.8 nm and infrared laser diode at 780 nm) were interchangeable without altering the position of the laser Doppler probe.
After allowing the blood flux reading to establish a steady level the femoral artery was occluded for one minute by raising the cotton tie. Then the occlusion was released by

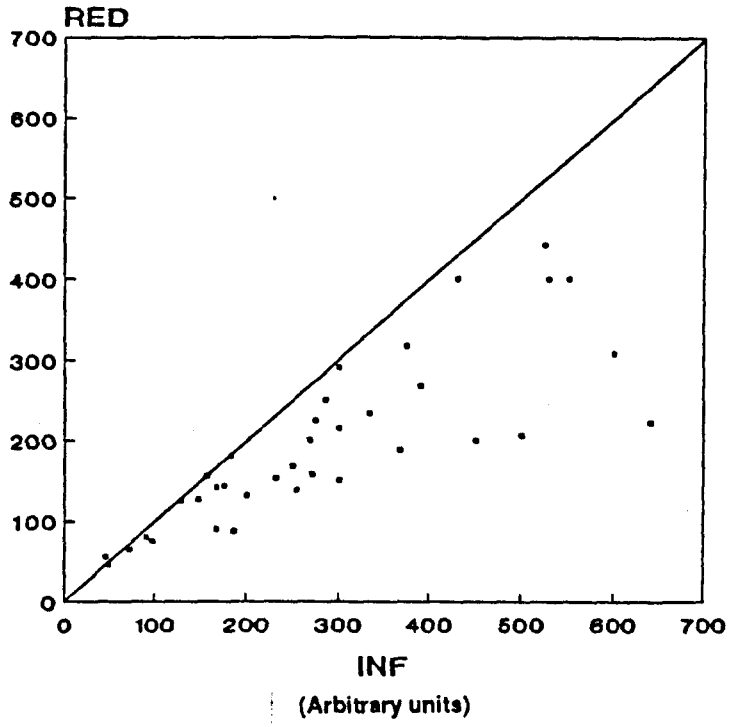

Figure 4.4 Comparison between consecutive occlusion responses with different wavelengths.

loosening the tie allowing blood flow to resume. Once the procedure had been completed using the HeNe laser source the blood flux reading was allowed to re-establish a steady level. The occlusion response was then repeated using the infrared laser source at the identical measurement site. The time between consecutive occlusion responses was approximately 5 minutes. After an occlusion response had been obtained at each wavelength the Doppler probe was moved away from the measurement site.

A layer of skin was placed over the measurement site on the hind leg. It was found that the optical properties of the skin stored for 24-48 hours prior to the experiment were different to that of freshly removed skin. When stored in physiological saline the skin flaps became thicker and opaque. To avoid this fresh skin flaps were removed from the abdomen or neck of the anaesthetised rats. Skin flap thickness was measured using a micrometer calliper.

The Doppler probe was repositioned over the new layer of skin directly above the previous measurement site (figure 4.5) and the occlusion responses repeated for both laser sources. The process was then repeated for a range of different thicknesses of skin. For a direct comparison between the HeNe and infrared lasers the output powers were matched at the start of the study using an optical power meter (AQ-2101, Ando Electric Co. Ltd.) and adjusting the laser diode drive current until the output powers were equal.

Results

The results are presented in figure 4.6.

There was a gradual decrease in the occlusion response for both wavelengths as the skin thickness was increased. Occlusion responses were observable through 2.0 mm of excised skin using the infrared laser but were undetected by the red laser.

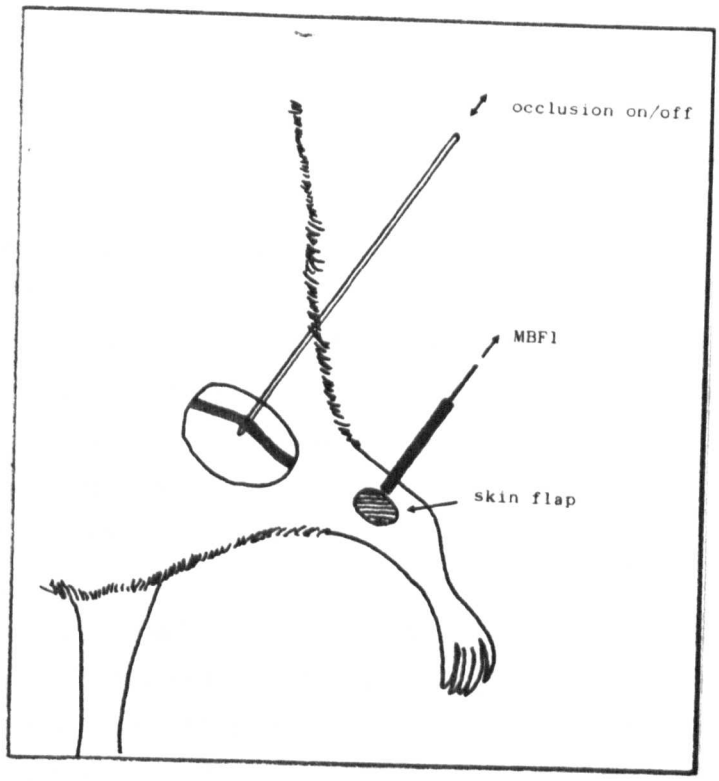

Figure 4.5 Position of the Doppler probe above the skin flap on the hind leg of the rat.

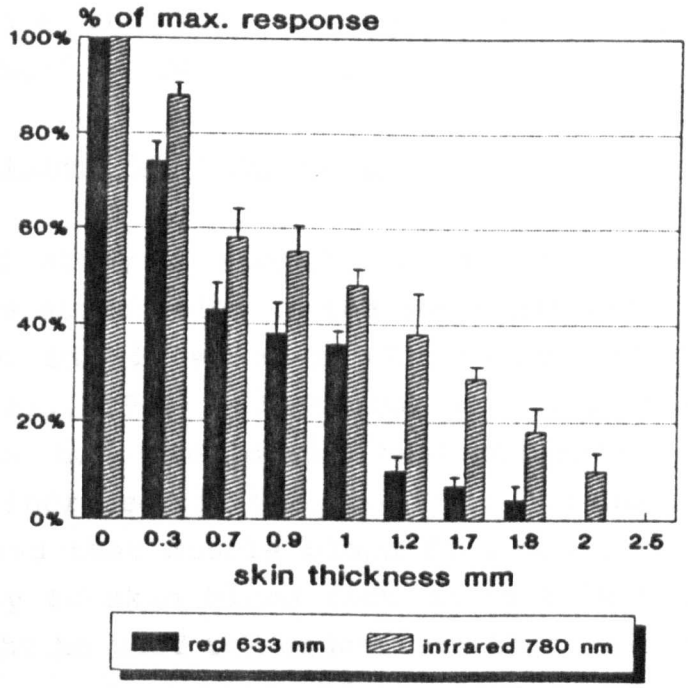

Figure 4.6 Relative magnitude of occlusion responses through various thicknesses of skin.

Discussion

The results suggest that in laser Doppler measurements wavelengths in the infrared region sample a larger tissue volume than that of red wavelengths. It is difficult to quantify the difference in measurement depth since it depends on the exact tissue components and structure at the measurement site.

The *in vivo* model used in this study consisted of a series of skin layers placed on top of the original measurement site. By using fresh skin rather than layers of tape as used by some other researchers (Gush et al., 1984) a closer resemblance to the true tissue structure, scattering and absorption properties were obtained. However a number of problems with the model still exist. By adding extra layers on to the original measurement site extra optical interfaces were introduced, leading to an increase in the overall scattering properties of the model. Also, since the tissue layers had been removed from the animal there was no blood flowing through them. These almost bloodless samples of tissue did not have the same absorption properties as perfused tissue and most probably caused the values of measurement depth to be overestimated.

4.2.3 Study three: Exploratory test using pithed rat model

In the third study a simple *in vivo* model was set up permitting the stimulation of the autonomic outflow from the spinal column in pithed rats (Gillespie and Muir, 1967; Gillespie et al., 1970). Electrical stimulation at the base of the spine had previously been observed to produce reproducible increases in the blood flow to the hind limbs[1]. It was proposed that muscle blood flow would be stimulated preferentially to skin blood flow using this technique and that this might be used to demonstrate that infrared samples a deeper tissue volume than red wavelengths.

[1]ICI Pharmaceuticals. Unpublished observations

Experimental procedure

Female Alderley Park Wistar Normotensive rats (200-350 g) were anaesthetised with 2% Halothane and respired artificially through a tracheal cannula. The animals were quickly pithed by inserting a short pithing rod (a flexible, partially insulated steel electrode) through the orbit and down to the base of the spine. A steel rod inserted through an incision below the ear and pushed down alongside the spine acted as an indifferent electrode.

Immediately after pithing the rats were attached to a Harvard pump and artificially respired at 3 cm^3 stroke volume at 53 cycles per minute. The right jugular vein and left common carotid artery were cannulated, the former for the administration of drugs (Atropine @ 1 mg kg^{-1}) and the latter for the measurement of blood pressure and heart rate using a pressure transducer connected to a chart recorder (Devices Instruments Ltd. MX2). The temperature of each pithed rat was maintained at 37.5°C by a heating blanket and monitored with a rectal thermometer (digi-thermo, SOAR corporation). The hind limb was shaved and loosely restrained then the laser Doppler probes were carefully positioned on the skin surface (figure 4.7). Two laser Doppler flowmeters (Moor Instruments Ltd, MBF1) were used for the flow studies using either red (HeNe at 632.8 nm) or infrared (semiconductor diode at 780 nm) lasers.

Electrical stimulation was performed using a stimulator (Grass S88 stimulator, Grass Instruments, USA) attached between the pithing rod and the indifferent electrode. The pithing rod was carefully moved up and down the spinal cord until stimulation produced an increase in hind limb blood flow without affecting either heart rate or blood pressure. Blood flux was monitored continuously for both flowmeters using a 2-channel recorder (Kipp and Zonen BD9).

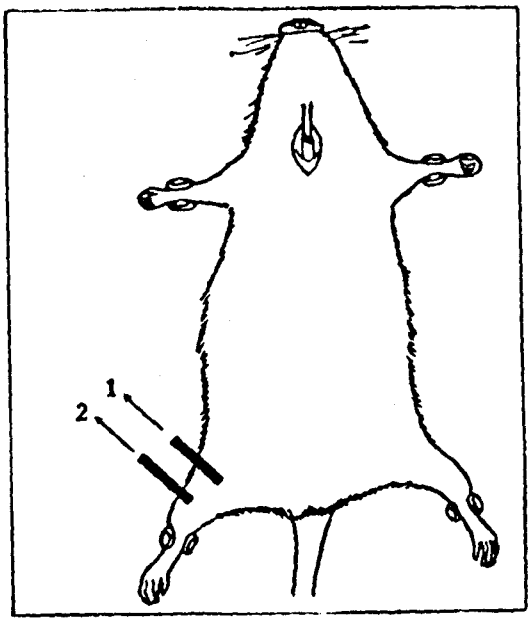

Figure 4.7 Approximate positioning of Doppler probes on the hind leg for the investigations using the pithed rat model.

A cycle of electrical stimulation was applied such that a voltage response curve was obtained. The stimulation rate was set at 5 pulses per second with a pulse duration of 0.05 ms. Stimulation was performed for 1.5 minutes then switched off for 5 minutes before applying the next cycle of stimulation. During each cycle the blood flux rapidly increased with each pulse to a maximum response which was maintained for the remaining period of stimulation. When the stimulation was stopped the blood flux returned towards the previous baseline level.

There is considerable variation in the thickness of the skin at different sites on a rat. On the hind limb the thickness was usually found to be less than 1 mm. Therefore it was assumed that Doppler measurements using either red or infrared wavelengths were from a sample volume including skin and some deeper muscle tissue.

Initially both flowmeters were operated with HeNe laser sources. A small incision was made at one of the measurement sites and a thin metal plate positioned between the skin and hind muscle, limiting flow measurements to the skin layers. The two Doppler probes were then placed on the skin surface approximately 3 mm apart, one sampling skin and deeper muscle blood flow but the other limited to measuring skin blood flow alone. Several voltage response curves were generated to determine whether there was a different response between the skin measurement and the skin and muscle measurement. In a number of runs the measurement sites were changed to investigate whether the difference in responses was due to the different areas of skin sampled. No site dependency was found.

In a second experiment a series of voltage response curves were obtained using the two flowmeters operating with different wavelengths: red at 632.8 nm and infrared at 780 nm. In this case both skin sites were left undisturbed as measurements of skin blood flow alone were not required.

Results

It was not possible to pool the data from individual rats because the voltage response curves demonstrated large variations from animal to animal.

Several voltage response curves showing blood flux increases with increasing stimulating voltage are presented in figure 4.8. In the experiments using HeNe laser sources for both flowmeters a general trend was observed for the blood flux measurements. As the voltage was increased the blood flux increased at a faster rate in the undisturbed skin site compared to the site containing the metal plate. It is suggested that this increased response was due to preferential stimulation of muscle blood flow with respect to skin blood flow.

Blood flux measurements using the two different wavelengths also exhibit a general trend. In these response curves the infrared measurement was seen to increase at a faster rate than the red measurements as the stimulating voltage was increased. It is suggested that these measurements demonstrate that the infrared wavelength samples from a deeper tissue volume when used in laser Doppler studies. The muscle flow influences the infrared measurement to a greater extent than it does the red.

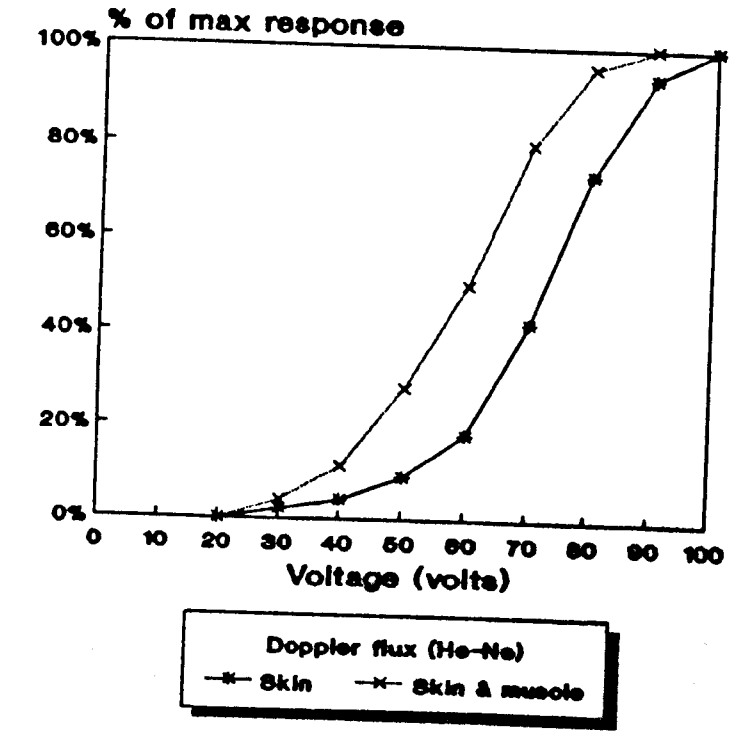

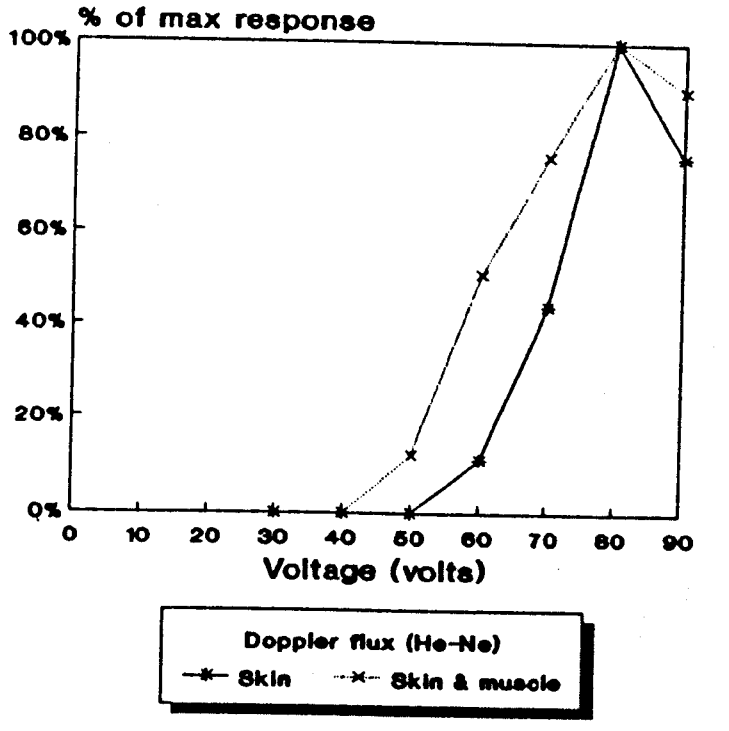

Figure 4.8a Voltage response curves at skin and skin and muscle sites.

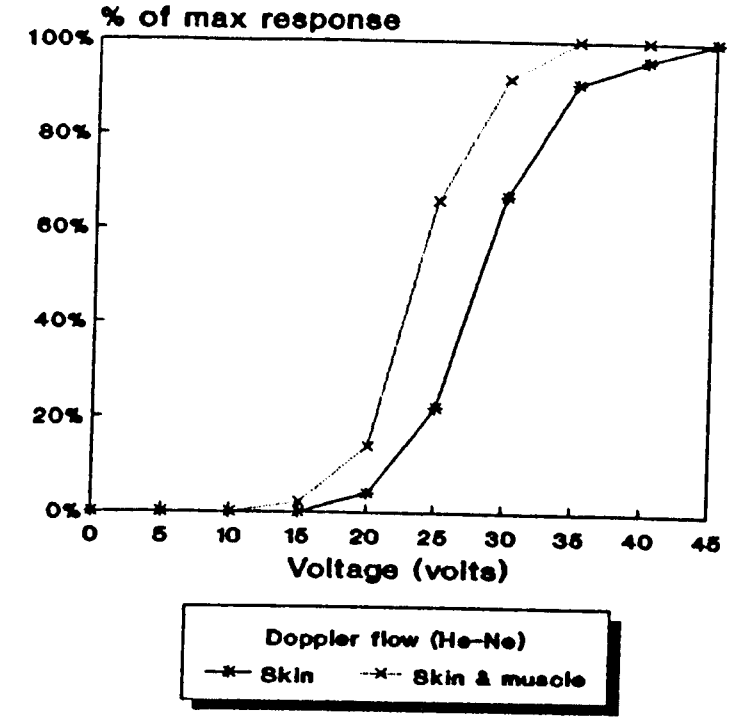

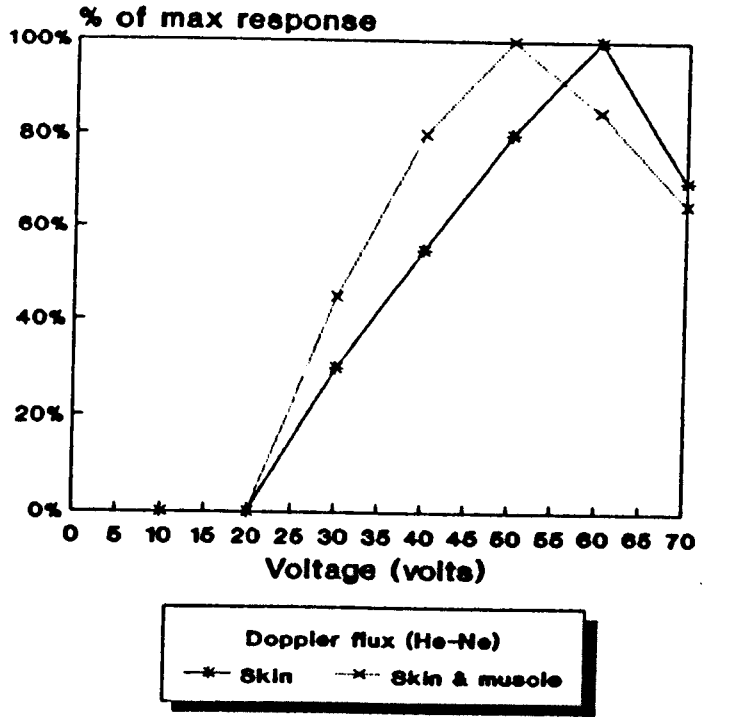

Figure 4.8b Voltage response curves at skin and skin and muscle sites.

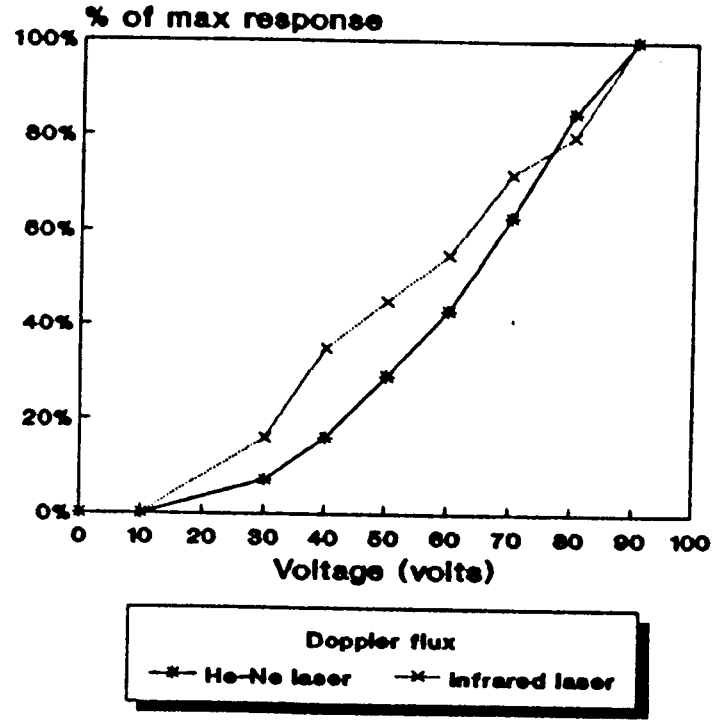

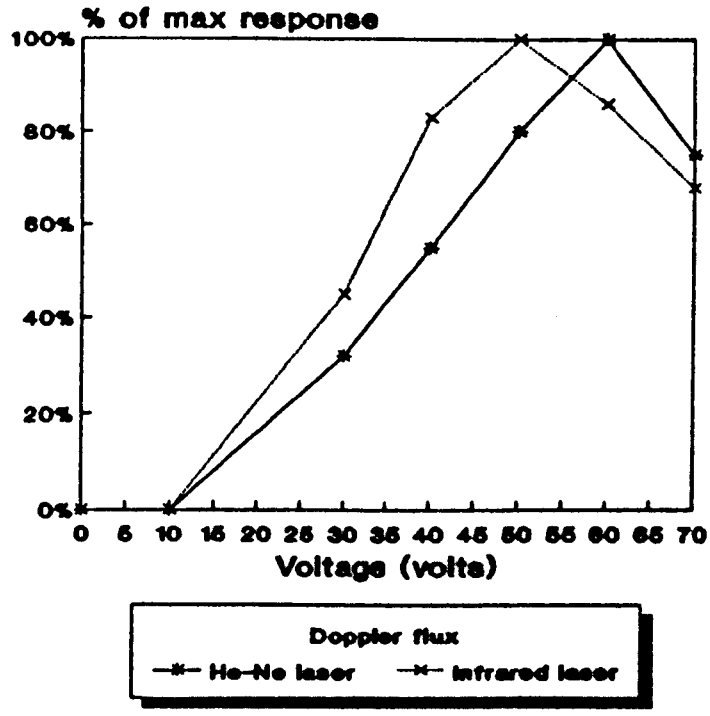

Figure 4.8c Voltage response curves using the red and infrared lasers.

Discussion

The pithed rat model was used as an investigative study to demonstrate the wavelength dependence of laser Doppler measurements *in vivo*. In this study the differences between flow measurements using red and infrared wavelengths were explored.
By stimulating the nerve fibres at their origin the technique avoids the confusing picture due to the mixing of sympathetic and parasympathetic responses which often take place within the periphery making *in vivo* measurements difficult to analyse.
The preliminary results suggest that the infrared wavelength samples from deeper levels within the tissue.
Several problems existed with the pithed rat model which precluded further investigations. Firstly, it was not fully understood why the voltage stimulation preferentially increased muscle blood with respect to skin blood flow. Also, the voltage range over which response curves were obtained varied widely from animal to animal reducing analysis to individual cases.
Difficulties due to twitching limbs were also encountered producing movement artefact on the Doppler flux measurements but these were reduced by loosely restraining the limb using adhesive tape.

4.2.4 Study four: Laser Doppler measurements using a green wavelength source

Introduction

The previous studies concentrated on blood flow measurements using red or infrared wavelength laser light. This section reports on *in vivo* measurements made while investigating a method of selecting capillary flow in isolation from dermal flow by using a shorter wavelength green laser.

Apparatus and signal processing

For these studies a 1.5 mW HeNe green laser (Melles Griot) was chosen, emitting light at a wavelength of 543 nm. Fluctuations in the laser output were reduced by using a dc-dc power supply (Model 101, Laser Drive Inc., Pennsylvania) rather than a mains supply. Due to the low power of the backscattered laser light and fluctuations in the output light intensity analysis of the Doppler signal was performed by directly observing the Doppler photocurrent spectra obtained from the light backscattered from the skin.
Laser light was directed to the skin surface through a 1 mm diameter plastic optical fibre. A portion of the backscattered light was collected by two fibres that led to two separate photodiode detectors (BPX 65, RS Components Ltd.). A differential detection circuit, figure 4.9, was used as proposed by Nilsson et al. (1980 a). After current-to-voltage conversion the photodetector signals were passed through a differential op-amp to reject noise signals common to both inputs (laser noise and mains (50 Hz) harmonics). The signal was then amplified and low pass filtered using a seventh-order switched capacitor programmable filter (AMI S3528, Gould Inc.). Filter cut-off frequencies of either 1 or 5 kHz were selected. Doppler power spectra were obtained by passing the output of the filter to an FFT Analyser (AD3522, Hakuto Co. Ltd.) which allowed averaging over several (16 or 64) spectra.

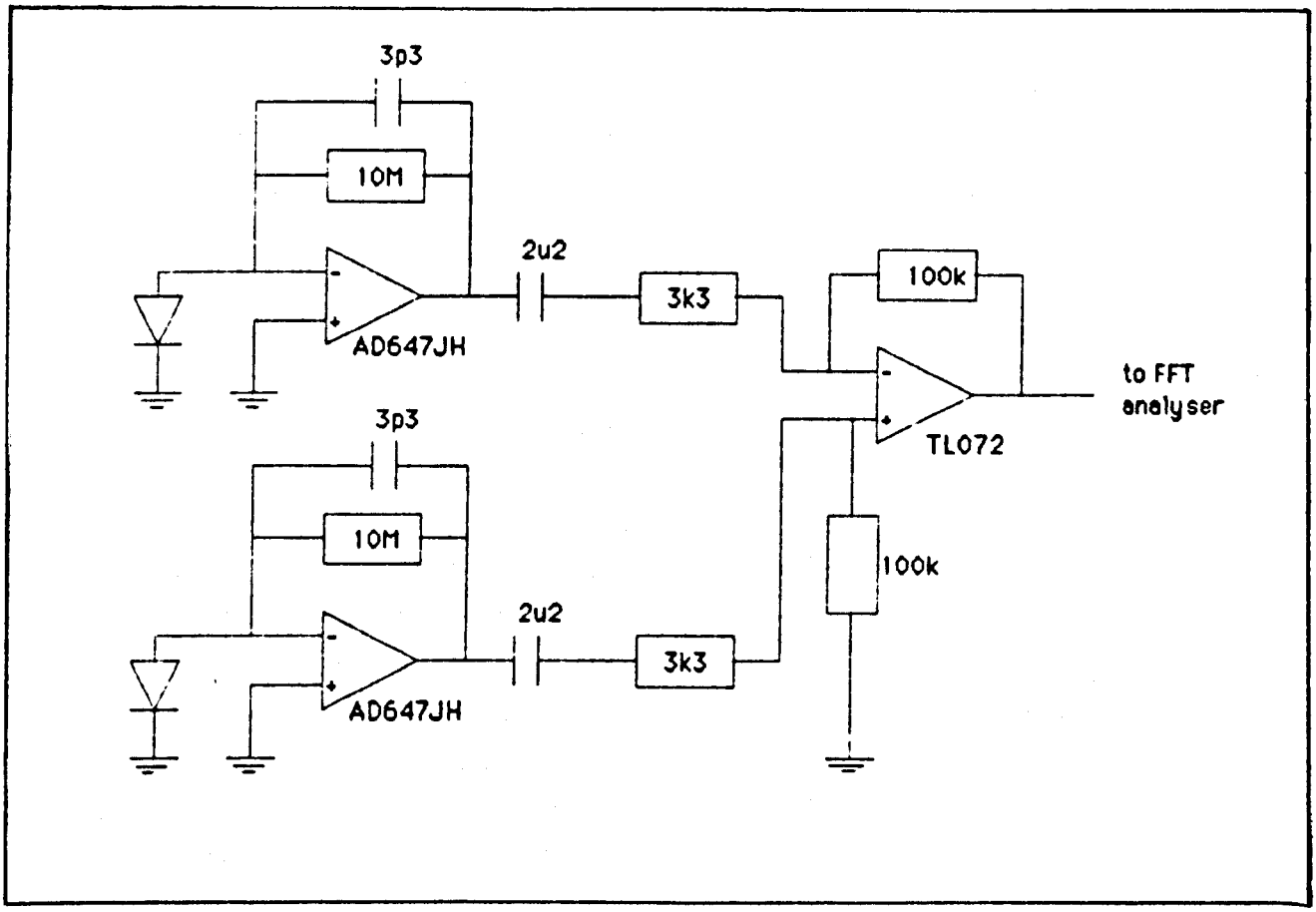

Figure 4.9 The differential detection circuit

In vivo observations

The aim of these tests was to determine whether blood flow measurements were obtainable by detecting green laser light backscattered from the skin.

The first test was to determine whether a blood flow response would be detected by the green system during a femoral occlusion performed in the hind limb of a rat. An Alderley Park Wistar rat was anaesthetised using Sagatal (Pentobarbitone 60 mg kg^{-1}), placed on its back and a cotton tie fastened loosely around the exposed femoral artery. An area of the hind leg below the incision was shaved and the Doppler probe carefully placed on the skin surface. A control power spectrum was recorded using the FFT analyser with the bandwidth set at 5 kHz. The recorded spectrum was averaged over 64 individual spectra calculated over a period of approximately 70 seconds. The femoral artery occlusion was performed and a second power spectrum recorded. A third power spectrum was recorded immediately after releasing the occlusion. There was very little difference between the control measurement and the measurement obtained during the femoral occlusion. However during the post occlusion hyperaemia the power spectrum was observed to increase in magnitude particularly across the lower range of frequencies. The increase across the spectrum was as a result of the expected increase in the blood flow within the tissue. A power spectrum obtained 2 minutes after the occlusion showed the spectrum settling back towards the control measurement.

A further series of spectra were obtained for a second occlusion response with the bandwidth of the power spectrum limited to 1 kHz. Again, there was no significant difference between the control measurement and the measurement obtained during the femoral occlusion but the post occlusion hyperaemia response was observed by an increase in magnitude across the whole 1 kHz bandwidth. The spectrum settled back towards the control measurement with time. A selection of

the recorded spectra are presented in figure 4.10.
The observed changes in power spectra may be explained if the green laser light samples the superficial skin layers. There was little difference between the control and occlusion spectra because in the anaesthetised animal there is poor peripheral flow[2]. However on the release of the occlusion the blood rushes throughout the microvasculature including the capillary vessels. The increase in peripheral flow was observed by the changes in the magnitude of the green spectra within the first 1 kHz bandwidth which suggests that the rbcs are slow moving within the green sample depth. The spectra have to be compared with Doppler spectra obtained for similar occlusion responses using infrared or red laser light. For these wavelengths the occlusion response affects the magnitude of the Doppler spectrum over a much wider frequency range, sometimes up to 15 kHz. Changes are observed both during and after occlusion, which implies that the flow information is obtained from a deeper tissue sample than with the green.
The second test was to investigate the effect of a topically applied drug on the Doppler power spectra recorded with the green laser. Control power spectra measurements were taken from the forearm of a human subject and compared with spectra obtained from the same skin site after administration of a local vasoconstrictor (Xylocaine spray (containing lignocaine), Astra Pharmaceuticals Ltd., Kings Langley, England). The probe remained in position as the spray was administered. The process was then repeated using an infrared wavelength source. An indication of the reproducibility of the spectra at both green and infrared wavelengths is given by the standard deviation error bars shown on the spectra at 0.5kHz. A series of typical spectra are presented in figure 4.11.

[2]ICI Pharmaceuticals. Unpublished observations.

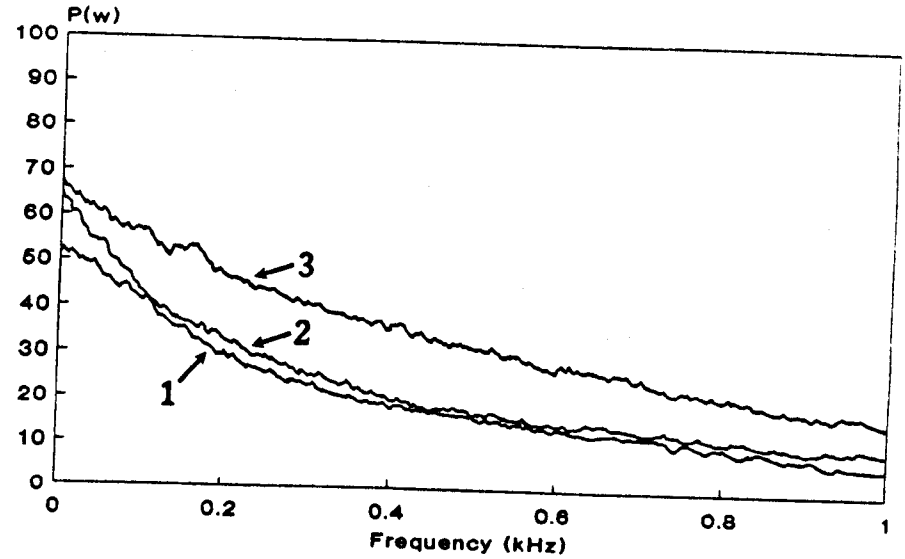

Figure 4.10 Femoral occlusion responses observed via the Doppler spectra. (1) control measurement, (2) measurement during occlusion, and (3) post occlusion response.

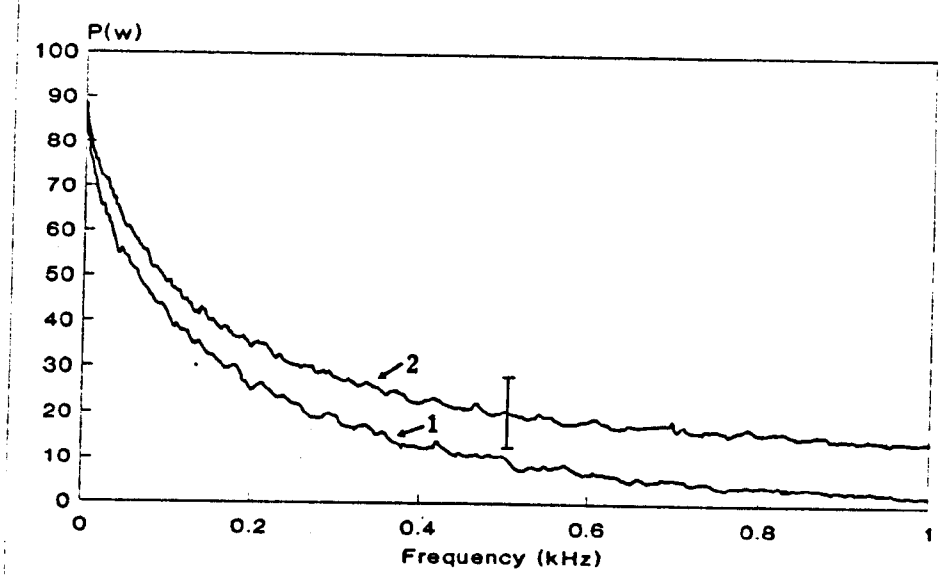

(A)

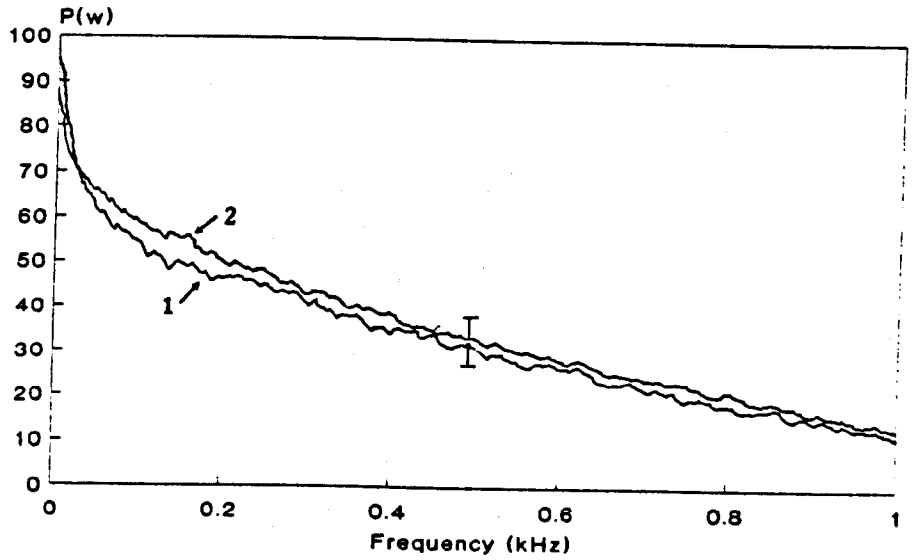

(B)

Figure 4.11 Doppler spectra for the green (A) and infrared (B) wavelengths (1) after and (2) before administration of the Xylocaine spray.

The local effect of the vasoconstrictor produced a significant reduction in the magnitude of the green spectra but had little effect on the infrared spectra. This may be explained by the vasoconstriction causing a reduction of blood flow in superficial skin layers. Since the infrared wavelength samples a larger tissue volume, the reduction in capillary flow has little overall effect on the Doppler signal. The green wavelength obtains Doppler information predominantly from the capillary vessels so the green spectra was greatly affected by the application of the drug.

Discussion

These observations demonstrate that Doppler flow information can be obtained using green laser light and indicate that the measurement is of capillary blood flow.
Due to the low power of the signal backscattered from the skin and fluctuations in the laser output intensity measurements using the green system are restricted to examinations made directly from the power spectra. The development of a more powerful green laser source is required to improve the photocurrent signal-to-noise ratio. Also, further work is required to find the optimum method of processing the green photodetected signal and to develop a functional laser Doppler flowmeter.

Conclusions

Results from a number of *in vivo* models indicate that infrared wavelengths used in laser Doppler measurements obtain measurements from a slightly larger volume of tissue than the red wavelengths.
By choosing a shorter wavelength laser source in the green wavelength range blood flow measurements appeared to be obtained from a shallower tissue sample but the low power output of the laser restricted examinations to the direct observation of the Doppler power spectra.

CHAPTER 5

Effects Of Externally Applied Pressure On Tissue Blood Flow Measurements

5.1 Introduction

When a laser Doppler probe is placed on the skin surface the pressure applied to the tissue can affect the magnitude of the flow parameters obtained. This pressure effect has previously been overlooked in many studies. It is important to quantify to what extent the blood flow is influenced by externally applied pressure in order to determine the degree of care required when positioning probes on the skin.
Externally applied pressure may cause problems in some laser Doppler applications but in other studies it is useful to observe the changes in blood flux as the external pressure is increased. For example, perfusion pressure within the tissue can be measured by observing the reduction in blood flow as external pressure is applied and this can be a valuable parameter when selecting the level of amputation (Holstein and Lassen, 1977) or predicting the healing of diabetic ischaemic ulceration (Castronuovo et al., 1987).
Studies of pressure dependent skin blood flow also provide valuable information in the study of bed sores. Prolonged externally applied pressure at a tissue surface impairs the blood flow and consequently the nutritional supply to that tissue volume eventually leading to tissue cell necrosis. In immobile or chronically ill patients special care has to be taken since the pressure applied to the body surface due to the patients own body weight against a hard surface frequently leads to tissue breakdown (Daly et al., 1976; Bader and Gant, 1988; Schubert and Fagrell, 1989).
In this chapter the effect of externally applied pressure on blood flux measurements was investigated in detail.

5.2 Study One: Effects On The Doppler Spectra

The aim of this study was to observe the influence that increased pressure on a laser Doppler probe has on the measured Doppler frequency spectrum.

Schubert and Fagrell (1989) investigated the change in skin perfusion with increasing external pressure using a laser Doppler probe positioned in the centre of a circular pressure ring. As the ring was lowered on to the skin surface an initial increase in skin blood flux was recorded, but with further pressure increases the flux steadily decreased. This initial increase in flow was probably due to the blood beneath the pressure ring being pushed towards the Doppler measuring volume. To avoid this increase at small pressures a laser Doppler probe was designed such that a measurement of applied pressure was obtained from the probe surface.

A probe was constructed that contained three optical fibres, one for light delivery and two for backscattered light detection. Adjacent to these fibres was a water-filled tube leading to a pressure transducer (Gould P-50), figure 5.1. Pressure measurements were recorded via a pre-amplifier (Devices Instruments Ltd., Welwyn Garden City, England) on to a flatbed chart recorder (Kipp and Zonen BD9). Pressure transducer calibration was regularly performed using a mercury sphygmomanometer. A 3 mW infrared laser diode (Sharp LTO22MCO) was connected to the delivery optical fibre and backscatter detection was performed using a differential photodiode detection system (described in 4.2.4). The photocurrent signal was then sampled using a digital FFT spectrum analyser (Hakuto International, AD3522) which processed the photocurrent over a 5 kHz bandwidth and produced an average spectrum from 64 separate frames (each frame sampling for 200 ms). The Doppler probe was held in a height-adjustable stand and placed above the subjects forefinger. By gradually lowering the probe onto the skin surface the probe pressure was slowly increased from 0 to

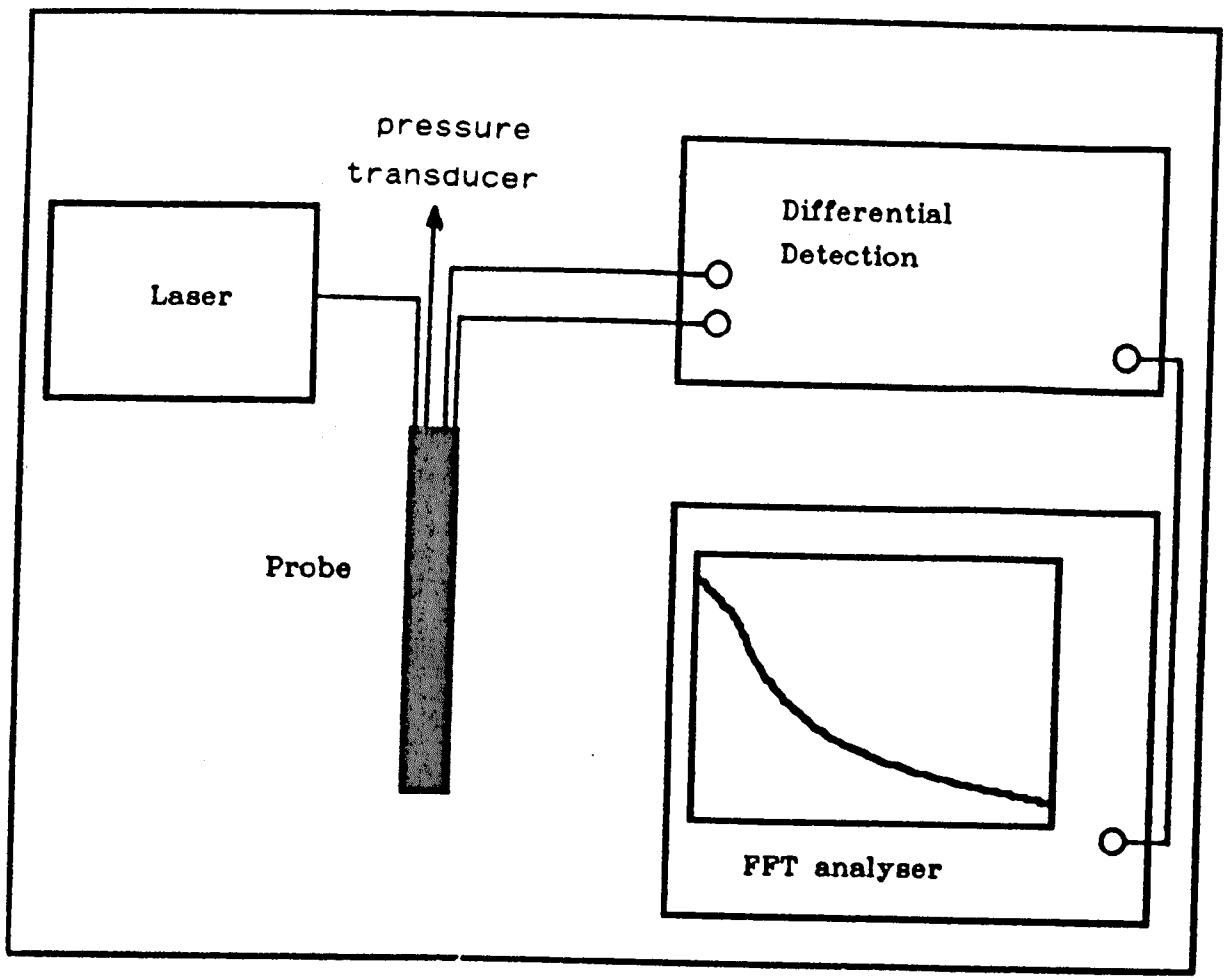

Figure 5.1 Apparatus for studying the changes in the Doppler spectra at different applied pressures

20 mmHg and the Doppler power spectra analysed for different levels of applied pressure. Interpretation of these spectra was qualitative but large changes in the shape of the spectra were observed for changes in probe pressure.

Results

By directly observing the changes in Doppler spectra detailed qualitative information about the distribution of rbc speeds can be obtained which in some cases may be of more use than quantitative flux values. A selection of amplitude spectra for different levels of applied pressure are shown in figure 5.2.
The first spectrum shows the Doppler frequencies present with no pressure applied to the skin surface. The spread of frequencies is approximately constant throughout the 5 kHz bandwidth.
As pressure was applied to the skin there was a shift in the amplitude of the Doppler spectrum towards the low frequencies. For 1 mmHg the amplitude between 0 and 3 kHz was significantly increased while the amplitude at higher frequencies remained relatively unchanged. Further increases in pressure produced a reduction in the amplitude of the spectrum within the high frequency range (3 to 5 kHz).

Discussion

There are dramatic changes in the shape of the Doppler spectrum as pressure is applied to the skin surface. With no pressure applied to the skin the shape of the Doppler spectrum indicated a wide spread of rbc speeds in the sample volume of tissue. By applying a small pressure (< 1 mmHg) there was an increase in the amplitude at low frequencies, implying a general increase in the number of rbcs moving at slow speeds. Further increases in applied pressure produced a decrease in the amplitude at the high frequency end of the spectrum which can be attributed to a reduction in the

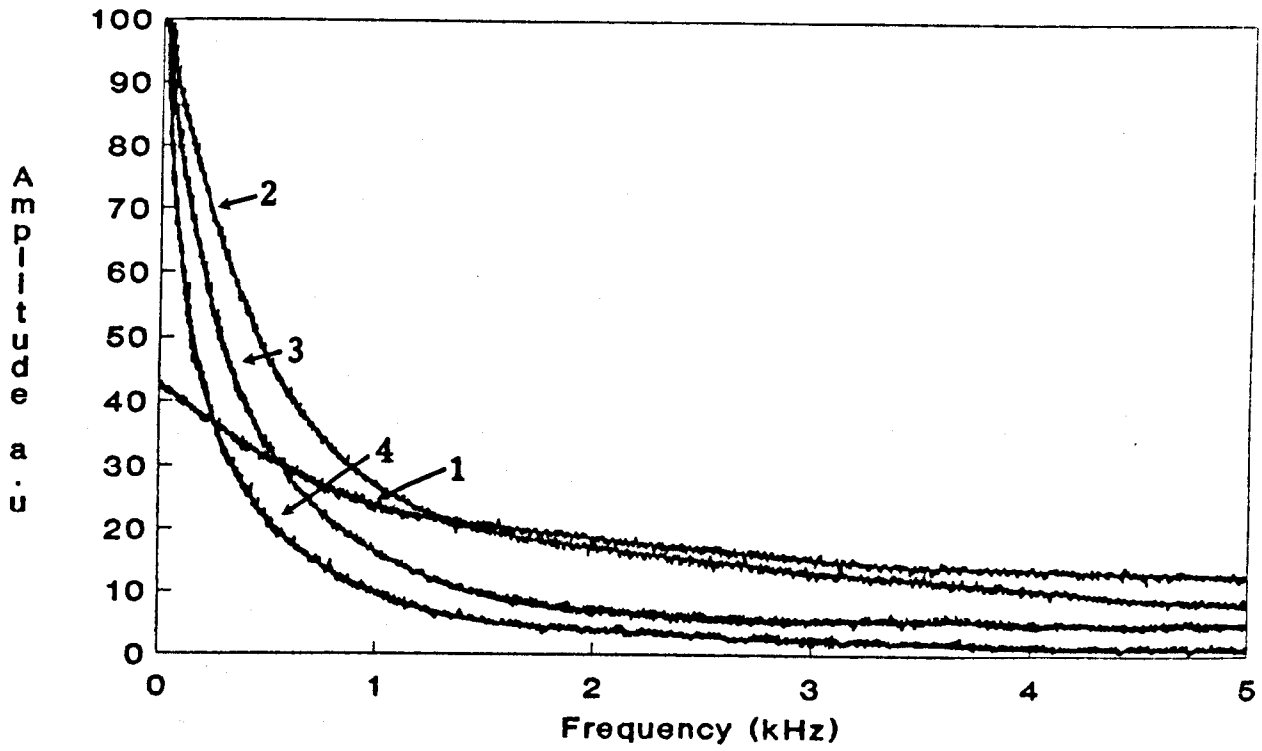

Figure 5.2 Amplitude spectra for pressures of (1) 0 mmHg, (2) 1 mmHg, (3) 5 mmHg and (4) 10 mmHg.

number of fast moving rbcs. The large increase in amplitude at the low frequency end of the spectrum is mainly due to the increased number of slow moving rbcs. Reduction in the concentration of moving rbcs can be observed by the decrease in the total area beneath the spectra as the applied pressure was gradually increased.

5.3 Study Two: Local Pressure Effects

A two fibre Doppler probe was constructed and blood flux measured using a commercial Doppler flowmeter (Moor MBF1), figure 5.3. Dark and shot noise adjustments were made at the beginning of the experiment and a baseline zero flow measurement was taken off a static scatterer. The first reading of skin blood flux was obtained with the Doppler probe just touching the skin surface without any measurable pressure exerted on the tissue. Then probe pressure was increased gradually in a step-wise manner until no further decrease in blood flux was obtained. Simultaneous recordings of Doppler flux and probe pressure were made on a chart recorder and the blood flux reading allowed to settle to a steady level after each incremental pressure change (figure 5.4). The pressure was then gradually reduced by lifting the probe away from the skin in small increments. The whole process was repeated several times for both HeNe (632.8 nm) and infrared semiconductor (780 nm) laser sources.

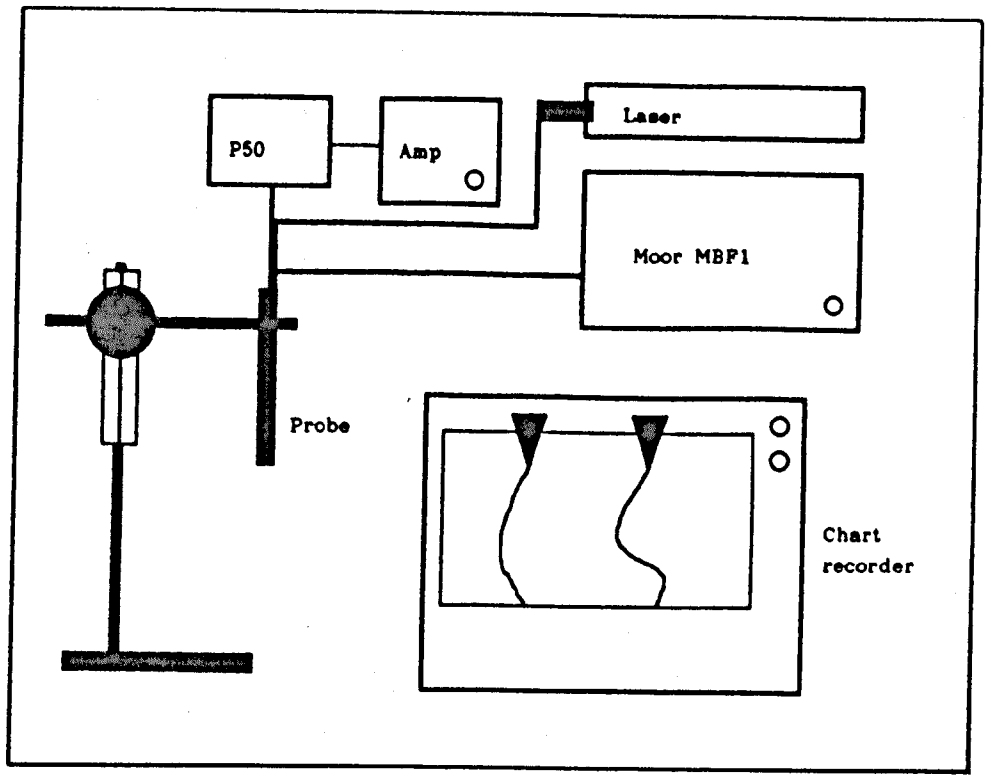

Figure 5.3 Apparatus used for studying the change in blood flux for locally applied pressure.

Results

The change in blood flux with increasing applied pressure is shown in figure 5.5. It was observed that there is a dramatic reduction in skin blood flow when pressures of between 0 and 10 mmHg are applied to the optical fibre probe. At pressures greater than 10 mmHg the rate at which the blood flow changes is significantly reduced. Further decreases in flow were recorded until the applied pressure reached approximately 30 mmHg.

Discussion

External pressure applied to a specific skin site compresses the tissue and vessels underlying the skin surface. The applied pressure eventually causes occlusion in the smaller vessels and the pressure required for this depends to a great extent on the perfusion pressure within the vessels. A study of the distribution of pressures in the microcirculation using direct micropuncture techniques (Zweifach, 1974) found that typical capillary blood pressures were between 30 and 40 mmHg. This corresponds with the observation that the laser Doppler flux measurements approach zero at these pressures.It also demonstrates that the majority of the Doppler signal is obtained from the capillary vessels. If the deeper larger vessels were sampled then higher pressures would be required to reduce the measured blood flux to the baseline level.
In general laser Doppler usage great care has to be taken with the pressure applied to the measuring probe. Measurements recorded in one study may vary from another similar study due to differences in the pressure applied on the probe-tissue interface. Pressure may be minimized by attaching the Doppler probes to the skin surface using double sided adhesive tape, in which case the pressure on the tissue depends solely on the weight of the probe head. In some instances blood flux measurements can be obtained

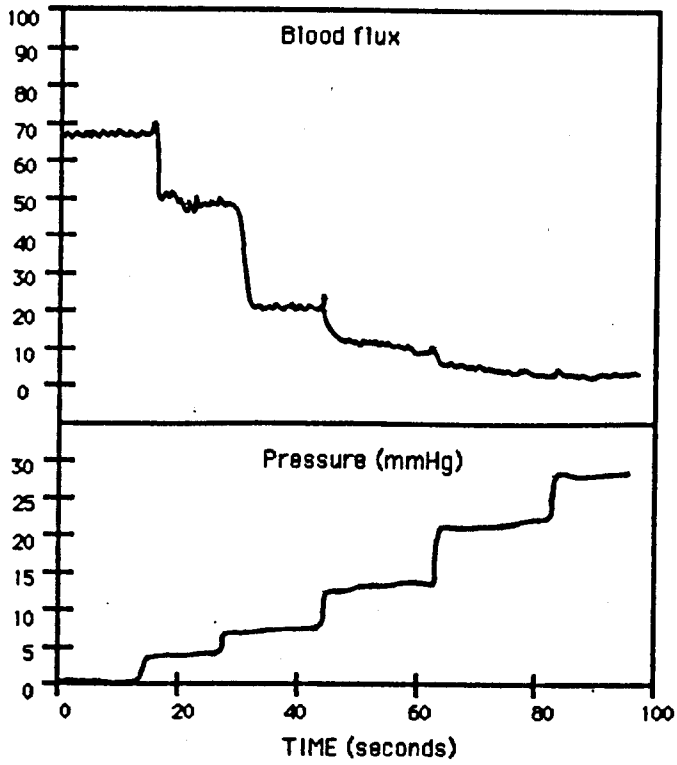

Figure 5.4 Simultaneous traces of blood flux and applied pressure.

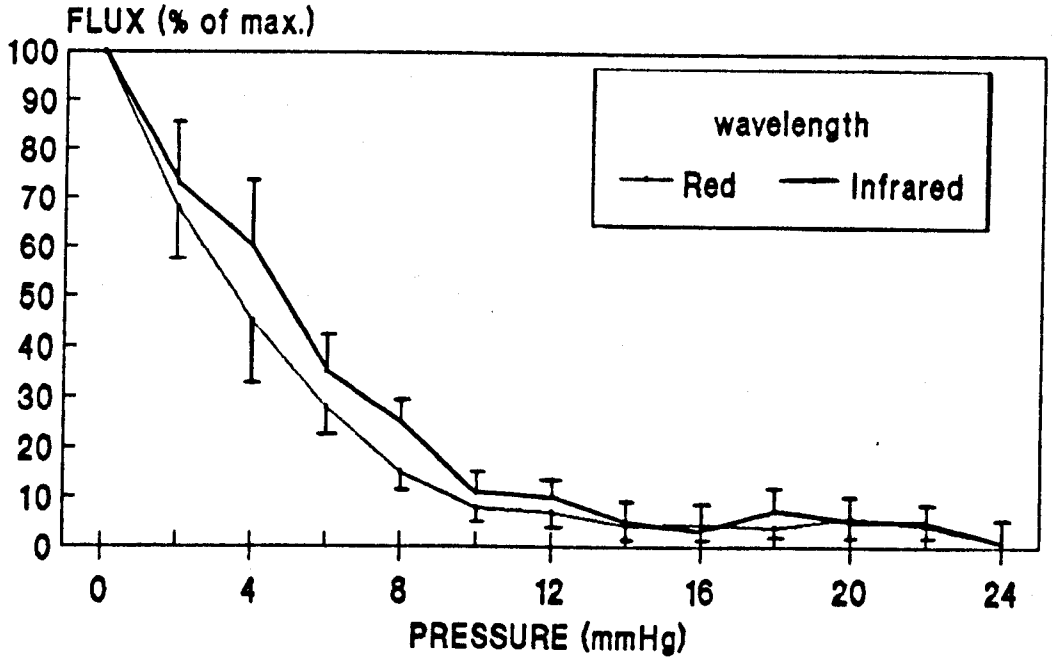

Figure 5.5 Results demonstrating the effect of pressure applied to the skin on the underlying tissue blood flow.

with no contact and therefore no pressure between the probe and the skin tissue. However any slight movement between the probe and skin surface causes large movement artifact signals that render the flux recording unreadable. Measurements are most successful when the Doppler probe tip is just in contact with the skin surface, touching the skin surface but exerting a minimum of pressure to the underlying vessels.

5.4 Study Three: Global Pressure Effects

In a third study the effects of pressure on the skin blood flow were investigated by placing the Doppler probe under a pressure cuff wrapped around the subjects forearm (figure 5.6). By increasing the pressure in the cuff the blood flow to the lower arm and hand was gradually reduced. A small right-angled probe (Moor Instruments Ltd.) was placed under the cuff in contact with the skin. The time constant on the Moor MBF3D was set to 3 s to reduce any movement artifact on the flux output. Pressure readings were made using a mercury sphygmomanometer. Measurements were started with the pressure cuff deflated, then after 30 s of steady baseline readings the cuff was inflated in 10 mmHg steps up to a pressure of 110 mmHg. At each step a steady blood flux response was recorded for approximately 25 s before the next increase in pressure.
Using the Moor MBF3D, flux, speed and concentration were monitored throughout the study. The test was repeated six times and mean measurements at each pressure calculated.

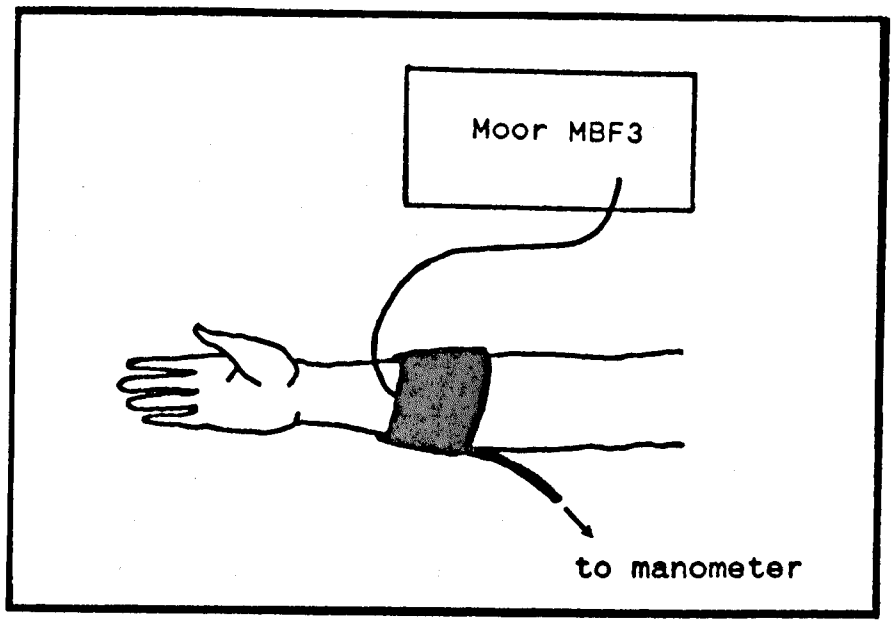

Figure 5.6 The Doppler probe was placed on the forearm under the pressure cuff.

Results

The measurements are displayed in figure 5.7.
Unlike the results for locally applied pressure blood flux did not start to decrease until 30 mmHg. As further pressure was applied the blood flux measurement rapidly decreased. The fastest change in flux was between 30 mmHg and 70 mmHg, where the flux reading was less than 40% of the starting baseline flux value.

Discussion

The results from this study differ from the previous ones in that a larger applied pressure is required to reduce the blood flux measurement. This may be interpreted as follows; in the previous study the external pressure was applied locally and therefore only affected the blood vessels within the immediate surrounding tissue. The rbcs perfusing through that area of tissue were diverted through preferential capillary flow channels and did not produce a flux reading as they were outside the volume sampled by the laser light. In this study a pressure cuff was applied to the forearm. When the cuff was inflated, equal pressure was applied to all areas of skin lying beneath it. The tissue was compressed over a large cross-section of the forearm which resulted in all the peripheral capillary vessels within that cross-section being restricted. As there were no preferential capillary pathways for the blood to pass through the arterial pressure forced the blood through the compressed vessels. Reductions in blood flux were not observed until the applied pressure approached the systemic arterial pressure. A slight increase in concentration of rbcs was observed between 25 and 40 mmHg. As this is the typical range for systemic venous pressure the increase may be attributed to the blood pooling in the capillary vessels as the veins become occluded.

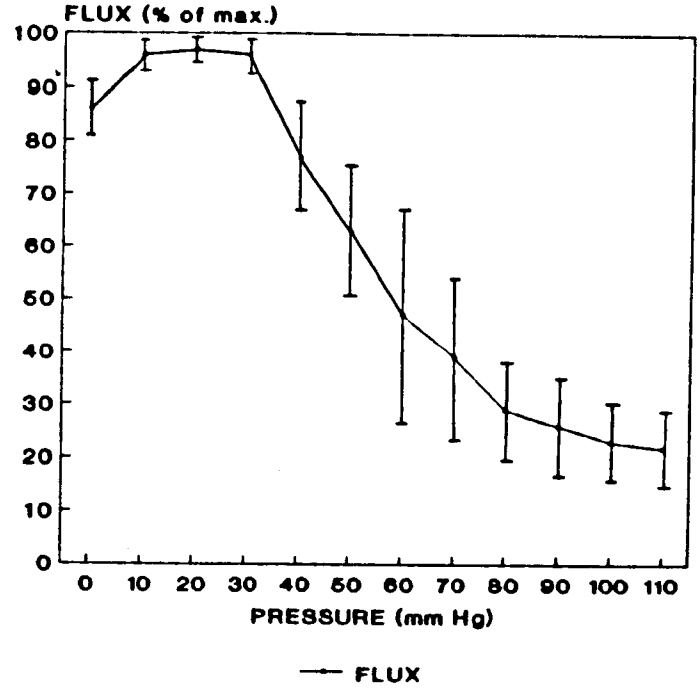

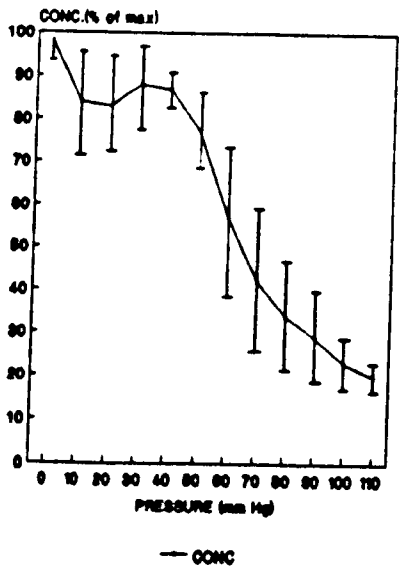

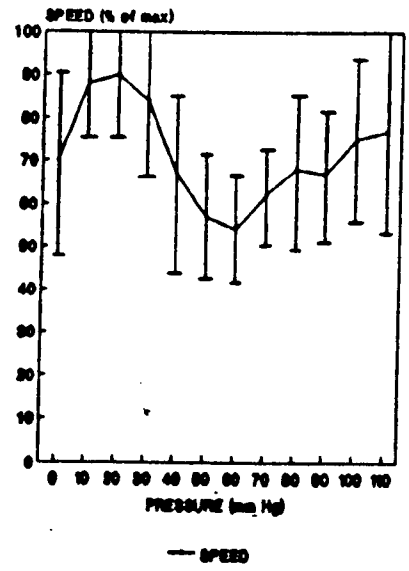

Figure 5.7 Effects of applied pressure on the skin blood flux, rbc concentration and rbc speed.

5.5 Summary

The results indicate that the reduction in skin blood flow as external pressure is applied depends to some extent on the way in which the pressure is applied. In laser Doppler measurements pressure is usually applied locally by the probe tip on the skin surface, so that the results from the first two studies should apply. The measurements indicate that even small amounts of locally applied external pressure (> 2 mmHg) greatly affect the flux reading obtained. Standard probes are usually held in the investigators hand or in a probe holder where the degree of applied pressure is unknown. By using small right angled probes attached with double sided adhesive the pressure exerted onto the tissue sample depends on the weight of the probe head alone and has little affect on the blood flow.

CHAPTER 6
Introduction To Oximetry

6.1 Introduction

In this chapter several non-invasive oxygen monitoring techniques are reviewed and the developments leading to the introduction of pulse oximetry are outlined. A section on pulse oximetry theory describes the methods used to calculate arterial oxygen saturation.

6.1.1 Oxygen transport

A supply of oxygen to the tissue is vital for the processes of metabolism and the production of new cells. Oxygen is carried into the lungs with each breath of air where it is distributed throughout a fine network of alveoli. The transport of oxygen from the lungs to the tissue is one of the main functions of the blood circulation. The oxygen diffuses from the alveoli to the pulmonary capillaries and is transported in the blood by either dissolving in the plasma or combining with the haemoglobin contained by the rbcs. The majority of the oxygen combines with haemoglobin to form oxyhaemoglobin, whilst only a small percentage, usually less than 4%, is carried by the plasma.
There are two parameters that are frequently used in describing oxygen transport: the partial pressure of oxygen pO_2 (sometimes referred to as oxygen tension) describes the comparative pressure or concentration of oxygen in a solution; and, the oxygen saturation SO_2 describes the concentration of oxyhaemoglobin as a percentage of the total haemoglobin (including all haemoglobin derivatives such as carboxyhaemoglobin and methaemoglobin).

$$SO_2 = \frac{[\text{oxyhaemoglobin}]}{[\text{total haemoglobin}]} \times 100 \qquad (6.1)$$

When referring to arterial blood the partial pressure is written as p_aO_2 and the oxygen saturation written as S_aO_2.

The most important factor affecting gas diffusion is the partial pressure gradient of the oxygen. Values of pO_2 usually range from about 100 mmHg in the blood leaving the pulmonary veins to 40 mmHg at the peripheral tissue. In general the haemoglobin molecule absorbs oxygen where the oxygen tension is high (for example surrounding the lungs), and releases oxygen where the tension is low (at the capillaries). In terms of oxygen saturation, under normal circumstances blood leaving the lungs is 95-98% saturated with oxygen and remains in this state until it reaches the capillaries. The saturation falls to about 70% in venous blood. The relationship between oxygen saturation and the partial pressure of oxygen is described graphically by the distinctive sigmoid (S-shaped) oxyhaemoglobin dissociation curve.

6.1.2 The oxyhaemoglobin dissociation curve

Figure 6.1 shows the dissociation curve under normal resting conditions, with a blood pH of 7.4 and temperature of 37°C. At rest the p_aO_2 is 100 mmHg. By referring to the dissociation curve at this point the haemoglobin is approximately 97.5% saturated with oxygen. It should be noted that the upper part of the curve is almost flat, demonstrating that for this part of the curve a large change in pO_2 is associated with only a small change in the oxygen saturation. In the steeper part of the curve (below pO_2 = 60 mmHg, SO_2 =90%) a small change in pO_2 is associated with a large change in oxygen saturation.

Carbon dioxide, pH and temperature all affect the dissociation curve. The curve is displaced to the right by increases in temperature or carbon dioxide (CO_2) or decreases in pH. Such a shift to the right causes the oxygen to be released more readily by the haemoglobin. For example, in

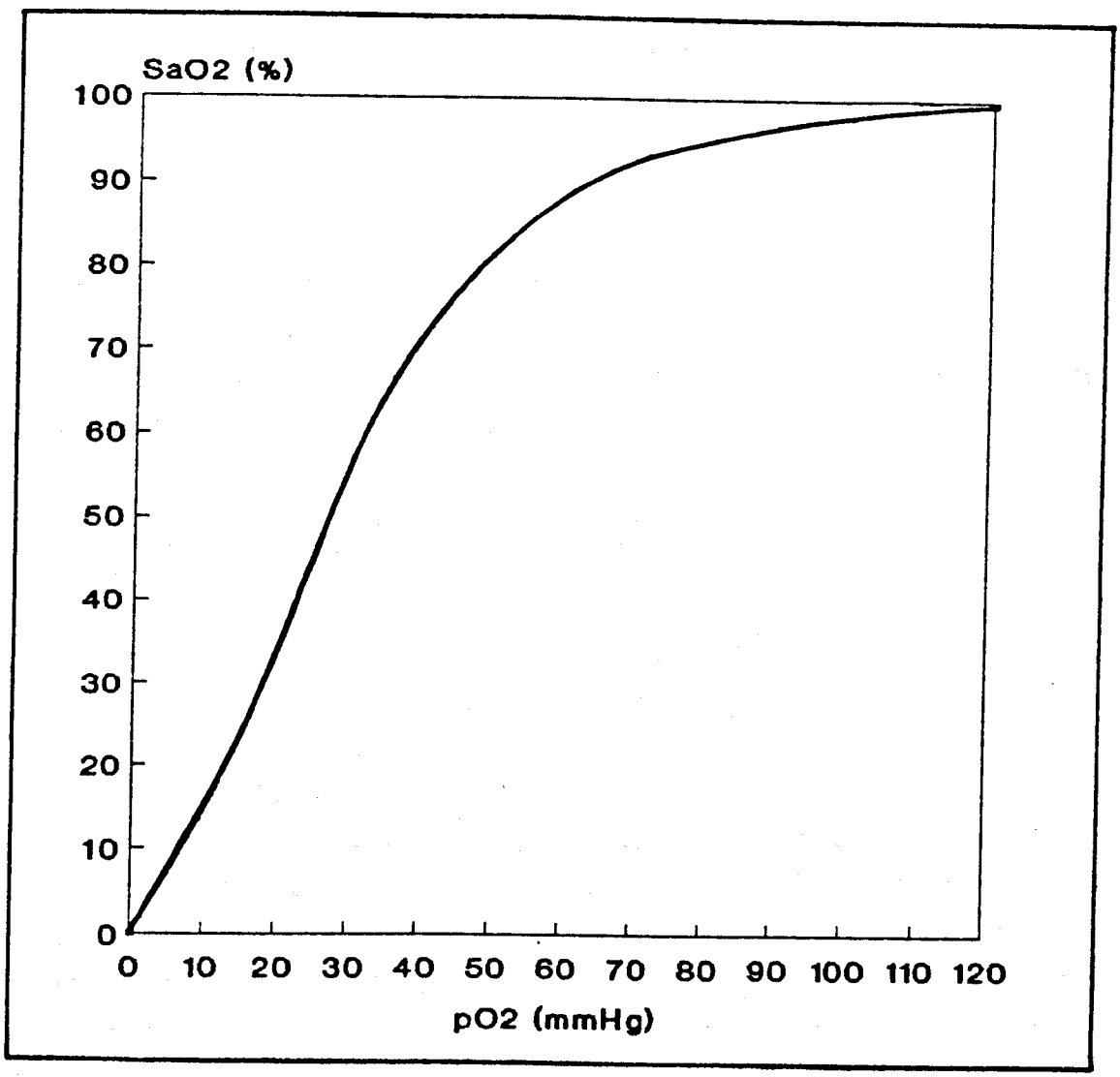

Figure 6.1 The oxyhaemoglobin dissociation curve

areas of tissue where the level of CO_2 increases, the shift in the dissociation curve leads to an increase in the partial pressure gradient and therefore a greater availability of oxygen for the tissue.

6.1.3 The motivation for developing a non-invasive oximeter.

There are many situations where a continuous measure of the oxygen saturation of blood is a critical parameter to be monitored. It is of particular importance in procedures where the airway may become blocked, for example, during general anaesthesia. Comroe and Bothelho (1947) performed a study that determined the accuracy with which clinicians could assess degrees of cyanosis and arterial oxygen desaturation. They concluded that a level of saturation as low as 75% may be undetected by the human eye indicating the need for reliable oxygen monitoring techniques to be developed. In another report Zorab (1988) stated that,

> "A knowledge of the patients arterial saturation is arguably the single most important piece of information needed during anaesthesia".

However, until recently anaesthesiologists relied on crude clinical signs such as the patients colour, heart rate and blood pressure to determine the patients arterial oxygenation (Fairley, 1989).
Knowledge of blood oxygenation levels are also useful in non-critical situations such as in studies of ischaemic tissue damage or general diagnosis of blood and nutritional transport. For example, Graham et al. (1986) used measurements of oxygen saturation to assess the vascular integrity of replanted digits. Five out of 16 patients had S_aO_2 values under 85%, and all 5 were found to have venous occlusion of the graft.

6.2 Non Invasive Methods For Monitoring Tissue And Blood Oxygenation

Introduction

Several methods for monitoring both blood and tissue oxygenation have been developed. The following section reviews some non-invasive techniques.

6.2.1 Transcutaneous oxygen tension measurements

Transcutaneous oxygen measurements were made possible by the development of the Clark electrode (Clark, 1956). The transcutaneous device consists of a small heated polarographic electrode attached to the skin surface that measures the oxygen partial pressure in the underlying tissue. The oxygen sensor consists of a platinum cathode and a silver anode that is coated with silver chloride (Ag/AgCl). The electrodes are separated by an electrolyte solution containing potassium chloride and are covered by an oxygen permeable membrane. There is a continuous flow of charge between the cathode and anode, the rate of which is determined by the supply of oxygen to the electrode. The current produced in the external circuitry is proportional to the pO_2 within the tissue.

Transcutaneous oxygen measurements are based on the principle that oxygen diffuses from the capillaries to the surface of the skin where it may be detected by the sensor. Using a small heater the skin temperature can be increased. This has three main effects:

1. Vasodilation of the capillaries producing "arterialization" of the capillary blood.
2. A rightwards shift in the oxyhaemoglobin dissociation curve leading to an increase in pO_2 at the electrode site.
3. An increase of oxygen diffusion through the epidermis.

Transcutaneous measurements were first used to monitor arterial oxygen in neonates (Huch et al., 1973). Accurate

measurements of the p_aO_2 of newborn infants were made by careful choice of sensor/skin temperature such that the over-reading due to heater-induced vasodilation balanced out the reduction in pO_2 caused by tissue metabolism that occurs across the uppermost layers. For newborn infants a temperature of 43°C was found to be sufficient to reach this balance. Adults have thicker skin tissue and even with an electrode temperature of 44°C the transcutaneous measurements have been demonstrated to significantly underestimate the actual arterial pO_2 (Eikhoff and Jacobson, 1980). Other researchers have shown that better correlations between surface and arterial partial pressure measurements in adults may be made using a topically applied metabolic inhibitor at the skin/sensor interface (Engel et al., 1979; Patel et al., 1989).

There are a number of problems with the technique of transcutaneous oxygen pO_2 monitoring, depending to some extent on the application. Generally there are problems with sensor drift which means that calibration is required before use (Tremper and Barker, 1987). False-negative measurements are sometimes made when the sensor becomes detached from the skin and reads room-air pO_2 values and there is the potential of causing a small skin burn with the heated pO_2 electrode. (For an electrode temperature of 44°C an electrode may be placed at the same site on an adult for 6 to 8 hours before there is a risk of burn (Tremper and Barker, 1987). Also, care has to be taken when interpreting results since the transcutaneous pO_2 measurement is affected by a number of parameters including blood flow. In order to decide whether a change in pO_2 is of circulatory or respiratory origin additional measurements are required (Mindt and Eberhard, 1982; Barker et al., 1986).

6.2.2 pO_2 measurement by fluorescence and phosphorescence techniques

When light strikes a photoluminescent dye, electrons within the dye can be excited to higher energy levels. The excited electrons later decay back to the ground state by emitting a photon of a wavelength greater than that of the absorbed light. For certain dyes the emission of photons is "quenched" (inhibited) by the presence of oxygen molecules. Methods of obtaining accurate and rapid measurements of oxygen concentration have been developed using the quenching of the fluorescence of pyrene butyric acid (Knopp and Longmuir, 1972; Opitz and Lubbers, 1984). Further development has recently produced invasive "optodes" (optical blood gas "electrodes") that are capable of measuring pO_2, pCO_2 and pH simultaneously. The technique is not noninvasive but a combined device can be made very small and placed on the tip of a flexible optical fibre (Tremper and Barker, 1989; Shapiro et al., 1989).

Photoluminescent quenching has been used to monitor oxygenation (Rumsey et al., 1988). Palladium (Pd)-coproporphyrin dye has a phosphorescence lifetime and intensity that are both dependent on the oxygen concentration. Using a video camera Rumsey and co-workers mapped the oxygen distribution over the surface of a perfused rat liver. The videotape displayed well oxygenated tissue as dark areas and regions with less oxygen as brighter areas. The problems with this technique are that it is not completely non-invasive since the photoluminescent dye has to be introduced into the blood circulation, and care has to be taken with the analysis of the fluorescence intensity measurements since the intensity depends on several other parameters apart from oxygen concentration (for example, other quenching agents).

6.2.3 Videomicroscopy

Videomicroscopy is mainly used for measuring rbc velocities within the microcirculation. However, by implementing optical techniques it has been demonstrated that measurements of oxygen saturation may also be obtained. Using a computer-aided spectrophotometric method Ellsworth et al. (1987) demonstrated that networks of capillaries can be analysed to determine the oxygen saturation gradients along capillaries. The technique was previously used by Pittman and Duling (1975a, b) who obtained measurements from individual microvessels.

Videomicroscopy uses Twersky's theory (Twersky, 1970) for the transmission of light through a suspension of rbcs . The vessels are illuminated by a xenon lamp with two different wavelength interference filters (for example, 431 nm and 420 nm). By careful choice of wavelengths a linear relationship between the ratio of the two optical densities and the oxygen saturation is produced. The technique has successfully been used in studies of capillary networks in the hamster cheek pouch retractor muscle to simultaneously determine values of rbc velocity, rbc frequency, oxygen saturation, oxygen flow, oxygen saturation gradient and capillary diameter (Ellsworth et al., 1988; Ellis et al., 1990).

There are several limitations to the technique. For example, real-time measurements cannot be obtained, the videotaped scenes have to be analysed off-line and, the measurements are restricted to specific tissue sites that may be transilluminated.

6.2.4 Near infrared spectroscopy (NIRS)

Cytochrome-c oxidase (cytochrome aa) is the terminal enzyme in the oxidative metabolic pathway and is therefore the most direct indicator of tissue oxygen sufficiency. Unlike haemoglobin, the cytochrome is fixed in the tissue where it

exists in either an oxidised or reduced state. Near infrared spectroscopy is a noninvasive multiwavelength technique for the continuous measurement of the oxidation state of cytochrome-c oxidase. In the wavelength range from 700 nm to 1000 nm (near infrared) a significant amount of radiation can be transmitted through several centimetres of biological tissue. Cytochrome-c oxidase has an absorption maximum at 830 nm therefore as the cytochrome becomes increasingly oxidised there is an increase in absorption at that wavelength. Most near infrared systems use four different wavelength light sources. Haemoglobin and oxyhaemoglobin also have absorption bands within the near infrared range so that careful choice of monitoring wavelengths permits changes in the oxidative state of haemoglobin and cytochrome to be measured.

Jobsis-VanderVliet and coworkers (Jobsis, 1977) pioneered the study of near infrared absorption in tissue. The majority of measurements have studied brain tissue, but some skeletal muscle measurements have been reported (Piantadosi et al., 1986). Developments in instrumentation have led to the possibility of taking measurements across a headsize of between 9 and 10 cm diameter or a muscle thickness of 6 to 7 cm (Cope and Delpy, 1988).

Until recently only relative changes in the measured parameters have been obtained but this has partially been resolved by using ultrashort picosecond pulses of laser light across the tissue bed. This technique allows the optical pathlength of the light to be determined for specific tissue-probe geometries and quantitative results to be calculated using a modification of Beer's Law (Delpy et al., 1989).

6.2.5 Multiwavelength oximetry

Conventional optical oximeters use two different wavelengths of light in order to measure levels of blood oxygen saturation. However these instruments (not including pulse

oximeters) are affected by skin pigmentation and inhomogeneities in skin structure and can therefore only monitor relative changes in oxygenation. Instruments using additional wavelengths of light produce self-calibrated systems unaffected by pigments other than those of interest ie. haemoglobin and oxyhaemoglobin. The Hewlett Packard ear oximeter is an 8 wavelength oximeter based on Beer's law which produces an indicator of blood oxygen saturation (Merrick and Hayes, 1976). Using a rotating wheel containing eight optical filters and optical fibre for light delivery and collection this instrument became a "gold standard" for other oximeters to be compared against. The oximeter was shown to be accurate (Douglas et al., 1979) but was not accepted for clinical monitoring because of the large earpiece and the expense of the instrument.

6.3 Pulse Oximetry

6.3.1 Development of classical oximetry

Transmission Mode

Spectrophotometric analysis of oxygen saturation was introduced by applying Beer's law to the transmission of light through the human hand to study the dynamics of tissue oxygenation (Nicolai, 1932). The first optical devices for measuring oxygen saturation were developed in 1935. Kramer used a single wavelength device to demonstrate that the transmission of red light depended on the oxygen saturation in the blood vessels but was only able to follow trends in saturation levels (Kramer, 1935). Matthes constructed the first two wavelength device measuring oxygen saturation by transmitting light across the ear pinna (Matthes, 1935). The two wavelengths were chosen such that one was sensitive and the other insensitive to changes in oxygen saturation (red and green wavelengths respectively). Unknown to Matthes the green filter also transmitted infrared light. It was later

demonstrated that very little of the green wavelength light penetrated the ear and the detected wavelengths were in fact in the infrared and red wavelength range (Wood, 1950). Further attempts were made to produce two wavelength oximeters (Squire, 1940; Millikan, 1942) but since the transmission of light was dependent on skin pigmentation of each subject only relative changes in oxygen saturation were obtainable. Improvements to the transmission technique were made by Squire (1940) and Goldie (1942) who obtained a zero oxygen measurement by compressing the ear such that the tissue became void of blood. This gave a baseline measurement against which further measurements were compared. The zero measurement was originally obtained by manually squeezing the ear pinna but the oximeter earpiece was later modified to include an inflatable balloon which was used to compress the tissue (Wood and Gracie, 1949).

Reflection

The prospect of non-invasive reflection oximetry was originally demonstrated in an investigation showing that Beer's law applied to red light reflected from the skin (Brinkman and Zijlstra, 1949). The oximeter used a small photocell to detect backscattered light at a wavelength of 650 nm. A two wavelength oximeter (the "Cyclops") was later constructed detecting light reflected from the subjects forehead. Another two wavelength system was later developed to obtain measurements from the forehead and fingertip (Cohen and Wadsworth, 1972) but absolute measures of oxygen saturation were unobtainable due to the unknown optical properties of the skin at the measuring site. Several wavelengths have to be used in order to eliminate the absorption effects of all the pigments present in the skin. Takatani et al. (1980) developed a noninvasive tissue reflectance oximeter using five different wavelength LEDs. But problems existed with the the pressure

applied on the transducer head affecting measurements, and calibration of the instrument still required reflectance data at a known value of oxygen saturation and for the tissue void of haemoglobin (Takatani, 1978).
All the classical oximetry devices rely on measurements of absolute intensity transmitted or reflected from a volume of tissue. Measurements cannot be defined as originating from arterial blood alone but are also influenced by any venous blood within the measuring volume. To minimize this problem many researchers heated the skin to "arterialize" the blood. The skin heating causes vasodilation which brings the capillary blood oxygenation closer to that in the arteries. The problem of obtaining only relative changes in S_aO_2 remain.

6.3.2 Development of pulse oximetry

A great advance was made in oximetry by combining photoplethysmography with classical oximetry. By including the photoplethysmogram pulsatile arterial blood can be distinguished from non-pulsatile venous blood.
Transmission pulse oximetry was originally proposed in Japan by Nakajima et al. (1975), developed by Minolta and tested by Asari and Kesmotsu (1976), Suzukawa et al. (1978) and Yoshiya et al. (1980). The device used filtered light sources and optical fibres to detect the light transmitted through the ear. By using the pulsatile arterial flow an absolute measurement of oxygen saturation was obtained. However this first pulse oximeter was marketed with little success due to its large size and sensitivity to movement.
The first clinically acceptable pulse oximeter was developed by making two basic changes from the Minolta design. Light emitting diodes and photodiode detectors were used to produced a lightweight probe, and a digital microprocessor was incorporated to store a calibration algorithm based on *in vivo* measurements. The device was marketed by Biox Corporation in the early 1980's and since then many other

commercial pulse oximeters have become available using similar designs.

In 1983 Mendelson and co-workers proposed that measurements of blood oxygen saturation may be made by applying pulse oximetry to the light backscattered from the skin (Mendelson et al., 1983; Mendelson et al., 1984). A skin reflection pulse oximeter was developed using two LEDs and one photodetector in close proximity on the skin surface. The accuracy of the oximeter was demonstrated over a range of blood oxygenation levels from 72% to 100% by comparing measurements taken from the forearm with transmission pulse oximetry measurements taken from the ear (Mendelson and Ochs, 1988). More recently a few commercial systems utilizing backscattered light have been introduced by oximeter manufacturers (Ciba-Corning 310 Pulse Oximeter).

6.3.3 Evaluation of pulse oximeters

The first pulse oximeters based on Beer's Law were shown to be inaccurate at levels of oxygen saturations below 90% (Sarnquist et al., 1980; Shimada et al., 1984). It has been known for some time that Beer's Law does not apply to whole blood but the relationship depends to a great extent on the scattering properties of the rbcs (Kramer et al., 1951). For this reason, more recent pulse oximeters use empirical algorithms based on *in vivo* calibration and are accurate over a much wider range of oxygen saturation.

Several investigations have compared the accuracy of pulse oximeters by comparing measurements with oxygen saturation measurements of arterial blood samples measured by a CO-oximeter blood gas analyser (Taylor and Whitwam, 1988). Accuracy is usually specified by the manufacturers as between 1.5 and 3%, decreasing as S_aO_2 decreases. In most studies a very strong correlation is usually found between 70% and 100% saturation (Yelderman and New, 1983; Shippy et al., 1984; Chapman et al., 1986; Nickerson et al., 1988) but under certain conditions the oximeters have been shown to

give inaccurate results.

Pulse oximetry measurements have been shown to be dependent on the presence of dyshaemoglobins such as carboxy- or methaemoglobin. As the pulse oximeter uses only two wavelengths of light it can only determine the concentration of two haemoglobin species, oxyhaemoglobin and reduced haemoglobin. Other dyshaemoglobins present in the blood cause inaccuracies in the resulting measurement of oxygen saturation. Barker et al. (1989) demonstrated that high levels of methaemoglobin induced by local anaesthetics caused pulse oximeters to overestimate oxygen saturation levels. High levels of carboxyhaemoglobin acts like a mixture of about 90% oxyhaemoglobin and 10% reduced haemoglobin when sampled by the two wavelength technique, and therefore oximeters have a tendency to overestimate in heavy smokers. Sickle cell haemoglobin has also been shown to cause inaccuracies in pulse oximetry measurements (Keifer et al., 1989) however, high bilirubin plasma levels and differences between adult and fetal haemoglobins have been demonstrated to have very little effect (Mendelson and Kent, 1989; Veyekemons et al., 1989).

Some researchers have questioned whether the photoplethysmogram results mainly from arterial blood. Kim et al. (1986) demonstrated the presence of a venous pulse that would cause the pulse oximeters to become inaccurate under certain conditions. This followed from earlier work (DeBakey et al., 1947) that claimed that changes in veins and venules had some contribution to the pulse volume amplitude.

Other difficulties include movement artefact, interference from external lighting and problems obtaining measurements in the presence of low perfusion.

The introduction of a noninvasive technique of measuring oxygen saturation has found widespread clinical application despite the above mentioned problems. Dorlas and Kuipers (1987) reported the usefulness of pulse oximetry during anaesthesia to detect desaturation occurring during

operations. Pulse oximeters are frequently used in intensive care units (Galdun et al., 1989), managing patients with respiratory distress, monitoring during patient transport (Elling and Hanning, 1986) and in special baby care units (Bucher et al., 1989; Hay et al., 1989; Swedlow, 1989). In some American states regulations have been proposed that require pulse oximeters to be used during anaesthesia (Brahams, 1989) and this has made their use almost mandatory in the operating theatre.

6.4 Transmission Pulse Oximetry Theory

6.4.1 Absorption of light and Beer's law

When blood is oxygenated it is a bright red colour due to the presence of oxyhaemoglobin. As the haemoglobin molecules are reduced the blood changes colour to a dark red-blue colour. The basic principle of oximetry is to monitor these changes in blood colour by detecting two different wavelengths of light that have passed through the blood.Light is transmitted across a volume of skin and detected on the opposite side using a photodiode detector. As the light passes through the tissue it is scattered and absorbed by various structures and pigments within the measuring volume. The absorption of light can be modelled using the Beer's law (figure 6.2) which relates the intensity of the light transmitted through the solution to the concentration of a solute in suspension.

Beer's Law can be written as:

$$I_T = I_0 \exp(-\alpha c d) \qquad (6.2)$$

Where I_T = transmitted intensity
I_0 = incident light intensity
α = extinction coefficient of the solute (a function of wavelength)
c = concentration of solute
d = distance travelled through liquid

The extinction coefficients for the different skin tissue absorbers vary continuously throughout the entire visible and near infrared wavelength range. At least n wavelengths would be required to identify any one absorber of light out of a system of n absorbers. Therefore for measurements of oxygen saturation in the tissue microcirculation a multiwavelength system would usually be required to differentiate between the main absorbers oxyhaemoglobin, haemoglobin, melanin, water and carotene.
The pulse oximeter can calculate arterial oxygen saturation using just two wavelength sources. The photodetected signals from the two wavelength sources both comprise of two components (figure 6.3). The first component varies slowly with time and is called the DC component; the second component fluctuates with every heart beat and is called the AC component. The DC component is due to absorption and scattering effects caused by tissue and bone structures and also the non-pulsatile venous blood within the sampled volume. The AC component is due to the extra volume of blood that passes through the tissue with every beat of the heart. The majority of this signal is derived from the arterial blood so that by isolating the AC component the arterial blood can be uniquely identified. By identifying the arterial blood the number of absorbers and therefore the number of wavelengths required to measure blood oxygen saturation is reduced to the main absorbers within the

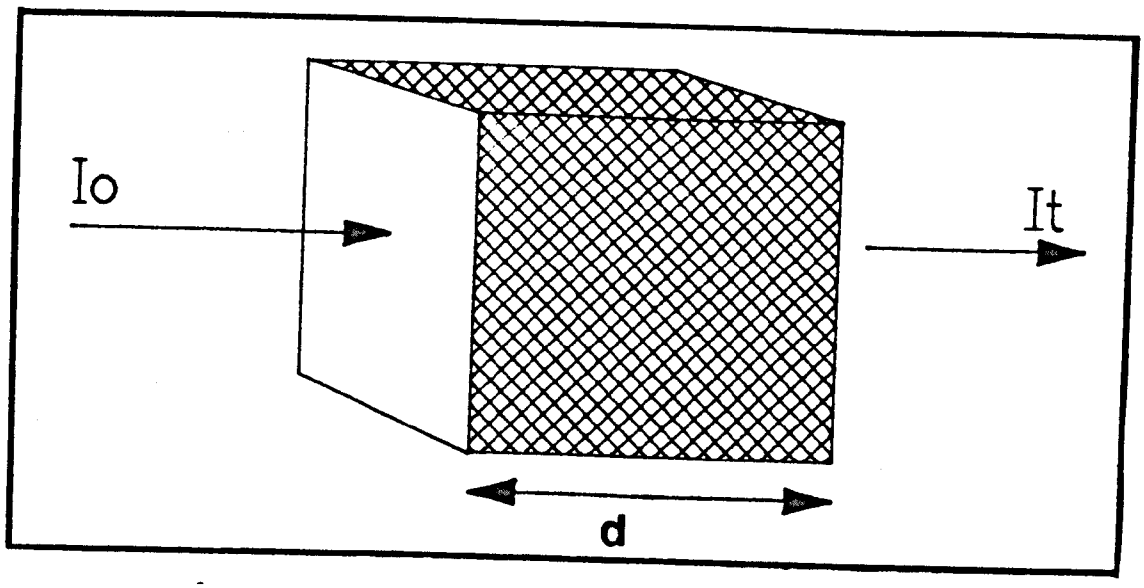

Figure 6.2 Beer's Law

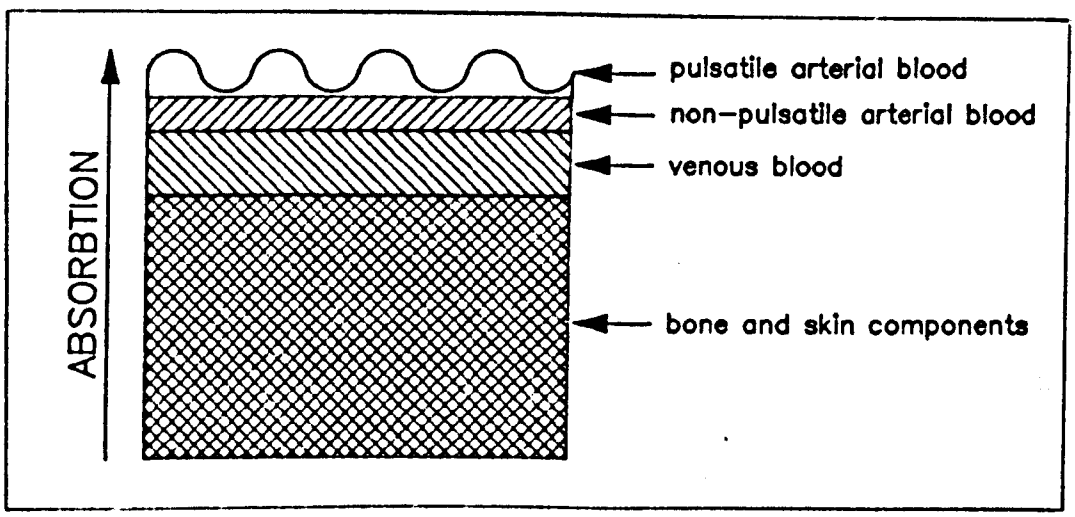

Figure 6.3 The absorption of light in the skin showing the fluctuating component due to the pulsatile arterial blood.

blood. Tissue pigmentation effects can be eliminated from the calculation.

There are two main absorbers in blood; oxyhaemoglobin and reduced haemoglobin. By observing the absorption spectra for these two pigments the two measuring wavelengths can be chosen. Usually one wavelength is chosen from the spectral region where the difference between the two absorption curves is greatest at approximately 660 nm. The second wavelength can be chosen at the isobestic point where the absorption of haemoglobin and oxyhaemoglobin are equal (805 nm) or from a longer wavelength (805-1000 nm).

From Beer's Law the transmitted intensities at each wavelength can be written as,

$$I_{T1} = I_{o1} \exp(-\alpha_1 cd) \quad (6.3)$$

$$I_{T2} = I_{o2} \exp(-\alpha_2 cd) \quad (6.4)$$

rearranging these equations an expression for optical density (OD) can be obtained,

$$\frac{I_{T1}}{I_{o1}} = \exp(-\alpha_1 cd) \quad (6.5)$$

$$OD_1 = \alpha_1 cd \quad (6.6)$$

For blood it is assumed that there are two absorbers at each wavelength (haemoglobin and oxyhaemoglobin) and the two absorption effects are additive (figure 6.4). Then the optical density is written as,

$$OD_1 = \alpha_{11} c_1 d + \alpha_{12} c_2 d \quad (6.7)$$

$$OD_2 = \alpha_{21} c_1 d + \alpha_{22} c_2 d \quad (6.8)$$

where, α_{11} = extinction coefficient for haemoglobin at wavelength 1

α_{12} = extinction coefficient for oxyhaemoglobin at wavelength 1

α_{21} = extinction coefficient for haemoglobin at wavelength 2

α_{22} = extinction coefficient foroxyhaemoglobin at wavelength 2

c_1 = concentration of haemoglobin

c_2 = concentration of oxyhaemoglobin

Equations (6.7) and (6.8) are simultaneous equations that can be solved by Cramer's rule using matrices and determinants (Appendix 3).

$$\delta = \begin{vmatrix} \alpha_{11} & \alpha_{12} \\ \alpha_{21} & \alpha_{22} \end{vmatrix} = a_{11}a_{22} - a_{21}a_{12} \qquad (6.9)$$

$$c1 = \frac{\begin{vmatrix} OD_1 & \alpha_{12} \\ OD_2 & \alpha_{22} \end{vmatrix}}{\delta} \qquad c2 = \frac{\begin{vmatrix} \alpha_{11} & OD_1 \\ \alpha_{21} & OD_2 \end{vmatrix}}{\delta} \qquad (6.10)$$

Then,

$$c1 = \frac{OD_1\alpha_{22} - OD_2\alpha_{12}}{\alpha_{11}\alpha_{22} - \alpha_{21}\alpha_{12}} \qquad c2 = \frac{OD_2\alpha_{11} - OD_1\alpha_{21}}{\alpha_{11}\alpha_{22} - \alpha_{21}\alpha_{12}} \qquad (6.11)$$

Oxygen saturation is given by,

$$S_aO_2 = \frac{[\text{oxyhaemoglobin}]}{[\text{total haemoglobin}]} \times 100 \qquad (6.12)$$

$$\approx \frac{[\text{oxyhaemoglobin}]}{[\text{oxyhaemoglobin}] + [\text{reduced haemoglobin}]} \times 100$$

For pulse oximetry the calculated oxygen saturation does not take the dyshaemoglobins into account therefore it is often denoted by S_pO_2 (Payne and Severinghaus,1986).

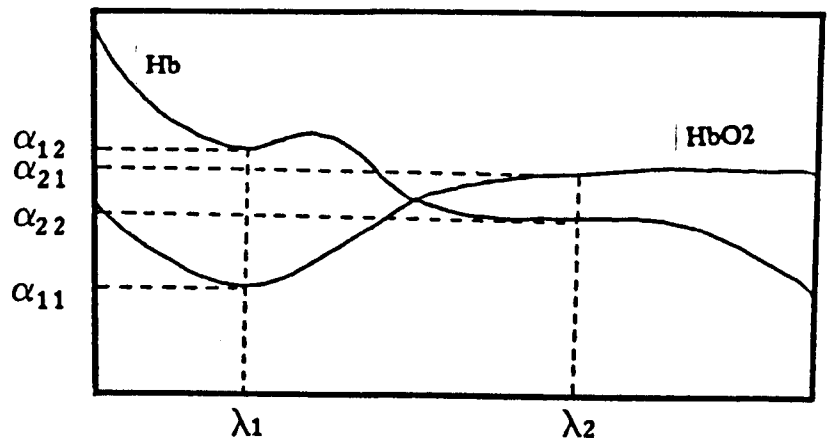

Figure 6.4 The absorption spectra of haemoglobin and oxyhaemoglobin

$$S_pO_2 = \frac{c_2}{c_1 + c_2} = \frac{OD_2\alpha_{11} - OD_1\alpha_{21}}{OD_1\alpha_{22} - OD_2\alpha_{12} + OD_2\alpha_{11} - OD_1\alpha_{21}}$$

$$= \frac{\alpha_{11}OD_2 - \alpha_{21}OD_1}{OD_2(\alpha_{11} - \alpha_{12}) + OD_1(\alpha_{22} - \alpha_{21})}$$

$$= \frac{\alpha_{11} - \alpha_{21}(OD_1/OD_2)}{(\alpha_{11} - \alpha_{12}) + (\alpha_{22} - \alpha_{21})(OD_1/OD_2)} \qquad (6.13)$$

By choosing wavelength 2 at the isobestic point or a wavelength where there is only a small difference between the absorption of haemoglobin and oxyhaemoglobin,

$$\alpha_{22} - \alpha_{21} \approx 0 \qquad (6.14)$$

Therefore,

$$S_pO_2 = \frac{\alpha_{11} - \alpha_{21}(OD_1/OD_2)}{(\alpha_{11} - \alpha_{12})}$$

$$= A - B(OD_1/OD_2) \qquad (6.15)$$

6.4.2 Implementation of transmission pulse oximetry theory

Signal processing

The Minolta pulse oximeter used a signal processing algorithm based directly on equation (6.15). Optical density values were obtained by measuring the AC component of the detected light at each wavelength and dividing by the corresponding AC+DC signal. The logarithm of this division was used as the optical density which was than used in equation (6.15) to obtain a value of SpO_2 (Yoshiya et al., 1980).

$$S_pO_2 = A - B \left[\frac{\log ((AC+DC)/DC)_1}{\log ((AC+DC)/DC)_2} \right] \qquad (6.16)$$

Several investigators have demonstrated that Beer's Law is only accurate over a small range of oxygen saturation (Kramer et al., 1951; Anderson and Sekelj, 1967; Sarnquist et al., 1980). Sarnquist et al. showed that the oximeters grossly overestimated oxygen saturation for levels below 90%. The reason for this inaccuracy was first demonstrated by Kramer et al. (1951) who reported that *in vitro* measurements using Beer's Law were more accurate if the blood was haemolysed. The principal difference between whole blood and haemoglobin solutions is the presence of strong scattering where the rbcs are intact.

Shimada et al. (1984) corrected for the oximeter overestimation by applying light scattering theory to derive a new equation for calculating the oxygen saturation that was linear over a larger range of oxygenation.

$$S_pO_2 = A' - B' (OD_1/OD_2)^2 \qquad (6.17)$$

The values of A′ and B′ were determined empirically.

More recent pulse oximeters are not based on Beer's Law but use empirically based algorithms basing their calculations on calibration curves derived from healthy volunteers. Several pulse oximeters use the ratio of the normalized AC components at the two measuring wavelengths to calculate S_pO_2 (Pologe, 1987). By dividing the AC component by the corresponding DC component the technique corrects for any changes in the intensity of the incident light.

$$S_pO_2 = A - B \left[\frac{AC_1/DC_1}{AC_2/DC_2} \right] \qquad (6.18)$$

This relationship can be seen to approximate from the

relation used by Yoshiya, equation (6.16).

$$\log\left[\frac{AC + DC}{DC}\right] = \log\ (1 + (AC/DC)) \qquad (6.19)$$

This may be expanded as,

$$\log\ (1 + x) = x - (x^2/2) + (x^3/3) - (x^4/4) + \ldots \qquad (6.20)$$

therefore,

$$\log\left[\frac{AC + DC}{DC}\right] = \left[\frac{AC}{DC}\right] - \frac{1}{2}\left[\frac{AC}{DC}\right]^2 + \frac{1}{3}\left[\frac{AC}{DC}\right]^3 - \frac{1}{4}\left[\frac{AC}{DC}\right]^4 + \ldots$$

$$\approx \frac{AC}{DC} \qquad (6.21)$$

The error introduced by using equation (6.18) rather than (6.16) is given by,

$$\text{error} = -\frac{1}{2}\left[\frac{AC}{DC}\right]^2 + \frac{1}{3}\left[\frac{AC}{DC}\right]^3 - \frac{1}{4}\left[\frac{AC}{DC}\right]^4 + \ldots \qquad (6.22)$$

Light sources

All commercial pulse oximeters use two different wavelength LEDs, one emitting in the red and the other in the infrared. Photodetection is performed using a single photodiode which measures the intensity of the light as the LEDs are switched on and off. Typically three different light levels are measured; the red intensity, the infrared intensity and the ambient intensity. To achieve this the LEDs are turned on and off sequentially. Each time the red LED is on, the infrared LED is off and a red intensity signal is detected. Similarly an infrared intensity is recorded with both the

infrared LED on and red LED off. The LEDs are sequenced at a rate equal to an integer multiple of the electrical supply mains frequency to avoid fluctuations due to flickering of room lights (figure 6.5). The calculation of oxygen saturation is then performed by either beat-to-beat analysis or running average analysis techniques.

Beat-to-beat analysis uses peak detection to measure changes in light intensity from the maxima and minima points of the pulse wave, figure 6.6. For each arterial pulse changes in red and infrared intensity are recorded and used in equation (6.18) to calculate a value for oxygen saturation. The value obtained is then averaged over a number of beat cycles.

Running average analysis (Wutkitsch et al., 1988) calculates the changes in detected red and infrared light intensities for every pulse of the LEDs. In this way multiple measurements of oxygen saturation are made throughout each arterial pulse. The values of oxygen saturation can be selectively weighted then averaged to enhance the stability of the calculated saturation level.

Of these methods of analysis the running average usually has the faster response time but is more susceptible to movement artefact.

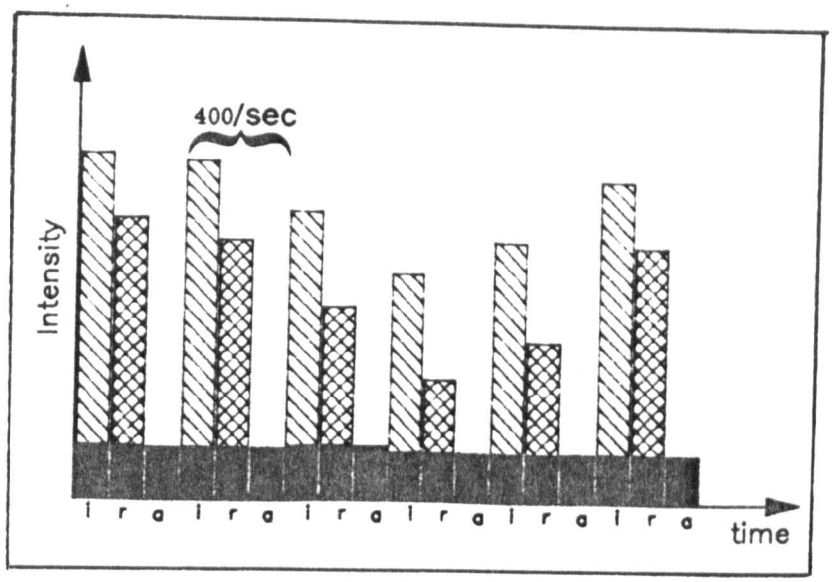

Figure 6.5 Sequencing of the LED's to avoid interference due to room lighting

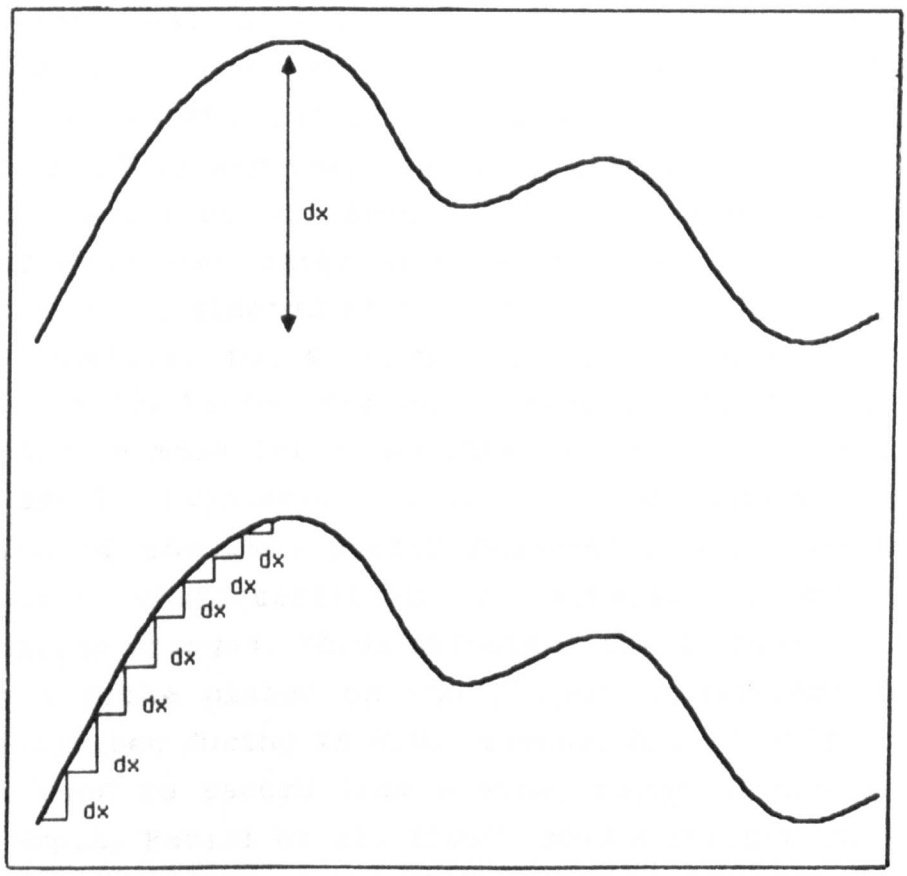

Figure 6.6 Changes in light intensity can be measured from the maxima to the minima of the pulse wave or many times along the wave.

CHAPTER 7

Development Of A Pulse Oximeter Using Backscattered Laser Light

7.1 Introduction

Measurement of arterial oxygen saturation provides an indication of the general oxygenation status of the patient. However, the final destination of the blood-borne oxygen is the cells of the body and since oxygen diffuses into the cells from the capillaries it would be useful to monitor the blood oxygenation in these small vessels. By developing a pulse oximeter that detects light backscattered from the skin surface it is proposed that oxygenation information may be obtained predominantly from the peripheral capillaries and arterioles. Several investigators have demonstrated experimentally that the pressure pulse generated by the heart reaches the capillaries (Intaglietta et al., 1970; Zweifach, 1974; Lipowsky and Zweifach, 1977; Smaje et al., 1980). These findings suggest that pulse oximetry can be applied even when large arterial vessels are not situated within the illuminated skin volume.

Most commercial pulse oximeters (e.g. Ohmeda Biox 3700, Nellcor N-100, Novametrix 500, Criticare CSI 501) operate in transmission mode using two LEDs and a photodiode detector in a small, lightweight optical probe. Rapid sequential flashing of the LEDs permit measurements of the changing absorption characteristics of arterial blood as the oxygenation changes. These oximeters are designed to operate with the probe placed on the finger or ear-lobe and have been evaluated during *in vivo* studies. A reflection oximeter may be used to record from a wider range of tissue sites. For example, Hariri et al. (1990) used a reflection oximeter to assess cerebral oxygenation.

This chapter explains the factors taken into account during the development of a pulse oximetry system operating by

detecting laser light backscattered from skin tissue. Details of the instrument design are presented including the choice of specific optical components, and the oximeter is tested *in vitro*. The response of the oximeter is compared with that of a commercial transmission system both *in vitro* and *in vivo* to determine its sensitivity to changes in saturation.

7.2 Pulse Oximeter Design Considerations

7.2.1 Choice of light source

One of the goals of this thesis was to determine the possibility of developing an instrument combining laser Doppler flowmetry with pulse oximetry. Commercial pulse oximeters and laser Doppler flowmeters operate using very different front-end optical systems which prevent them being used together on the same tissue sample. In order to develop a pulse oximeter operating in parallel with a laser Doppler flowmeter certain aspects of instrument design have to be considered. The ideal system would use the same optical sources and detectors for both monitoring techniques, so that at least one of the oximetry wavelengths has to be provided by a laser. The laser light output has to be of a continuous nature because this is a requirement for the laser Doppler technique. Two laser sources were chosen for the optical front-end, both operating in continuous mode but at different wavelengths. Photodetection was performed using two filtered photodiodes.

By using laser light sources rather than LEDs several improvements in light output stability were made. Typically an LED has a bandwidth of between 20 and 50 nm (half power width) and the output intensity indicates some weighted average signal over that frequency band (Shephard et al., 1984; Pologe, 1987). Lasers have much narrower spectral output. For example the half power width for the HeNe 632.8 nm transition is approximately 0.002 nm (Wilson and

Hawkes, 1983). For a laser diode the spectral width is approximately 0.08 nm (Sharp laser diode user's manual, 1989).
The LED is sensitive to temperature, both with regard to its wavelength and light intensity. For example, the variability in intensity and wavelength for an ultra bright intensity LED are 2 $\%°C^{-1}$ and 3 $nm°C^{-1}$ respectively (R.S. Components catalogue, 1990). For a laser the temperature dependence of the output wavelength is approximately 0.2 $nm°C^{-1}$ (Sharp laser diode user's manual, 1988).

7.2.2 Choice of wavelengths

For a dual wavelength pulse oximeter the choice of wavelengths determines the sensitivity and linearity of the output signal to changing oxygenation. The majority of devices use one wavelength in the red region where the extinction coefficients for oxyhaemoglobin and haemoglobin are very different and one wavelength in the infrared region where the extinction coefficients are approximately equal. Beer's law is additive when there are several absorbing solutes in a solution. Therefore the optical density at any specific wavelength can be written as,

$$OD = \alpha_1 c_1 d + \alpha_2 c_2 d + \ldots + \alpha_n c_n d \qquad (7.1)$$

where n is the number of different absorbers within a mixture
α_n is the extinction coefficient of absorber n
c_n is the concentration of absorber n
d is the length of the optical path through the solution.

If arterial blood is assumed to essentially consist of haemoglobin and oxyhaemoglobin the optical density can be written as,

$$OD_1 = \alpha_{11} c_{Hbo2} d + \alpha_{12} c_{Hb} d \quad (7.2)$$

$$OD_2 = \alpha_{21} c_{Hbo2} d + \alpha_{22} c_{Hb} d \quad (7.3)$$

Oxygen saturation can be expressed as,

$$S_pO_2 = 100 \times \frac{C_{Hbo2}}{C_{Hbo2} + C_{Hb}} \quad (7.4)$$

which in turn can be expressed in terms of optical density (equation 6.15).

Using equations (7.2) and (7.4) the relative optical densities over a range of oxygen saturation levels were calculated for different wavelengths. Several theoretical optical densities are shown in figure 7.1.

These were combined to obtain theoretical graphs of oxygen saturation against the optical density ratio of two oximeter wavelengths (OD_1/OD_2) thus demonstrating how changes in device wavelengths can alter the response of the oximeter to changes in saturation . Combinations of several laser wavelengths (670 nm, 633 nm, 780 nm, 805 nm and 810 nm) were tested for linearity and sensitivity to saturation changes. Various combinations of the wavelengths are shown in figure 7.2. A linear oximeter response would be expected if the graph of optical density versus saturation were linear. The sensitivity of the oximeter depends on the gradient of the graph.

From the sample of wavelengths investigated the best combination of wavelengths are 633 and 810 nm. These wavelengths produce a straight line graph with a shallow gradient producing a large change in optical density ratio for a small change in oxygen saturation. These wavelengths were chosen for the initial oximetry studies using a HeNe red laser (at 632.8 nm) and an infrared laser diode (at 810 nm).

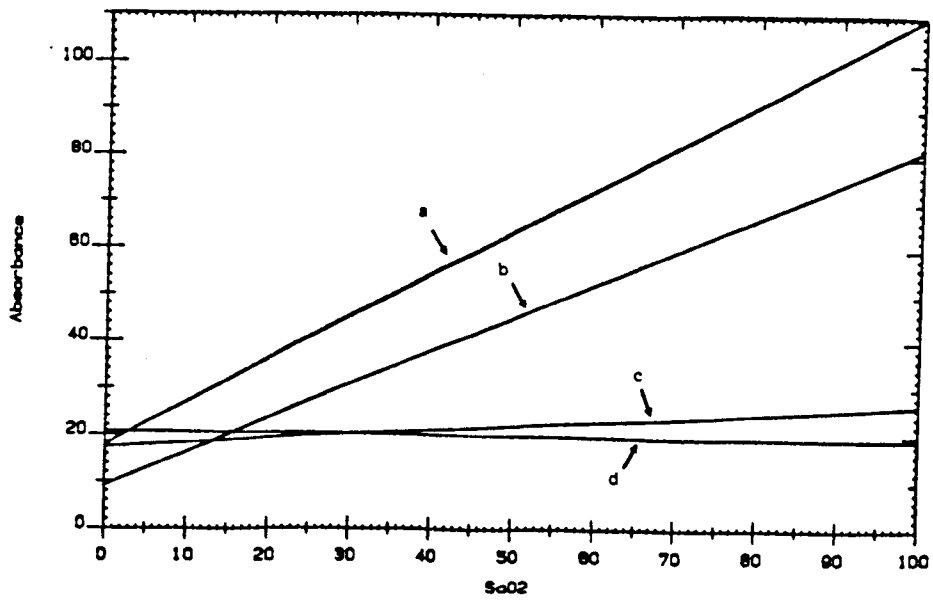

Figure 7.1 Optical densities calculated using Beer's law for different wavelengths, (a) 633 nm, (b) 670 nm, (c) 780 nm and (d) 810 nm, as the blood oxygen saturation varies between 0 and 100%.

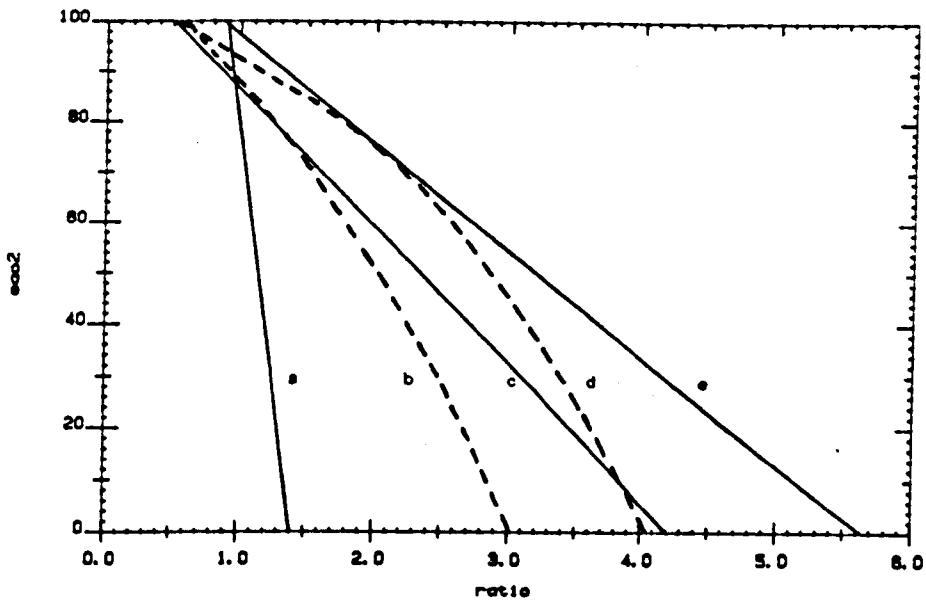

Figure 7.2 Theoretical curves for the oximeter ratio R using various two wavelength combinations, (a) 780 and 810 nm, (b) 670 and 780 nm, (c) 670 and 810 nm, (d) 633 and 780 nm, and (e) 633 and 810 nm.

Choice of oximeter wavelength is also determined by the absorption effects of methaemoglobin and carboxyhaemoglobin. Both have an increasing absorption effect as the wavelength decreases through the red region of the spectrum (figure 7.3). By choosing the red wavelength at 670 nm rather than 633 nm inaccuracies in oximeter measurements due to high levels of carboxyhaemoglobin and methaemoglobin can be reduced. Within the infrared wavelength range the absorption due to methaemoglobin increases and that due to carboxyhaemoglobin reduces as the wavelength is increased. Of these dyshaemoglobins, high levels of carboxyhaemoglobin are more frequent so it is best to choose the infrared wavelength in a region where absorption by carboxyhaemoglobin is insignificant.

7.2.3 Front-end optics laser sources, detectors and filters

The prototype oximeter used two laser sources, a 5 mW infrared (at 810 nm) laser diode (Sharp LT010MC0) and a 3 mW red HeNe (at 632.8 nm) laser (Melles Griot). Four plastic optical fibres (core diameter 1 mm), each 1 metre long, were used for delivery and collection of the laser light. The output power at the tip of each delivery fibre was limited to 1.0 mW.

Photodetection was performed using two photodiodes (DF series photodiodes, EG&G Photon devices, Salem, MA, USA) fitted with interference filters at the two wavelengths (width at half power = 10±2 nm). The filters have a minimum transmission of 45% at the centre wavelength, with maximum discrete wavelength transmission outside the bandpass quoted as $< 10^{-6}$ of the peak value. The photodetector response has a temperature coefficient of less than 0.03% $°C^{-1}$.

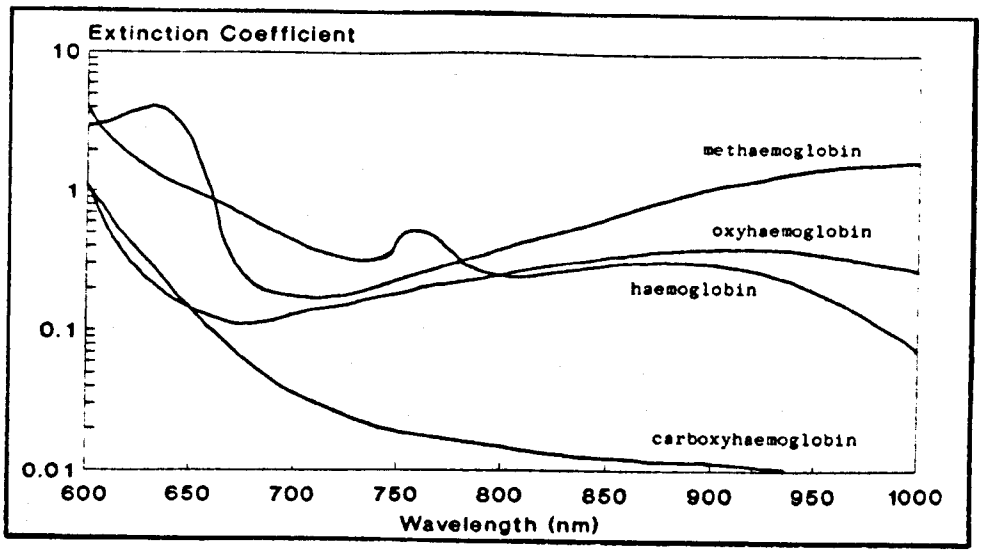

Figure 7.3 Absorption spectra of haemoglobin, oxyhaemoglobin, methaemoglobin and carboxyhaemoglobin.

7.2.4 Circuit design

The reflection oximeter had two modes of operation, either as a pulse oximeter or as a dc oximeter. The processing algorithm adopted for the pulse oximeter was that described by Pologe (1987). For each wavelength the photocurrent was passed through a current-to-voltage converter, amplified then separated into AC and DC components. The DC component was obtained by passing the signal through a low-pass filter (f_c = 0.6 Hz). The AC component was selected by passing the signal through a high-pass filter (f_c = 0.5 Hz) followed by a low-pass filter (f_c = 3.3 Hz). Two-pole Bessel filters were chosen rather than Butterworth or Chebyshev filters because they gave the shortest settling time and lowest overshoot filter characteristics. The AC signal was then amplified, rectified and integrated over a period of 5 seconds (figure 7.4). Circuit diagrams are presented in Appendix 4.
The two wavelength channels had identical gain settings and time constants. The integrated AC signal from the red wavelength channel was divided (using a MPY634 multiplier \divider integrated circuit) by the equivalent signal from the infrared channel. The DC signal on the infrared channel was divided by the red DC signal. This dc ratio was used as the dc oximeter output.

$$\text{dc oximeter output} = \left[\frac{DC_i}{DC_r}\right] \qquad (7.5)$$

The pulse oximeter output (R) was given by the product of the AC ratio with the dc ratio.

$$\text{pulse oximeter output, } R = \left[\frac{AC_r}{AC_i}\right] \times \left[\frac{DC_i}{DC_r}\right]$$

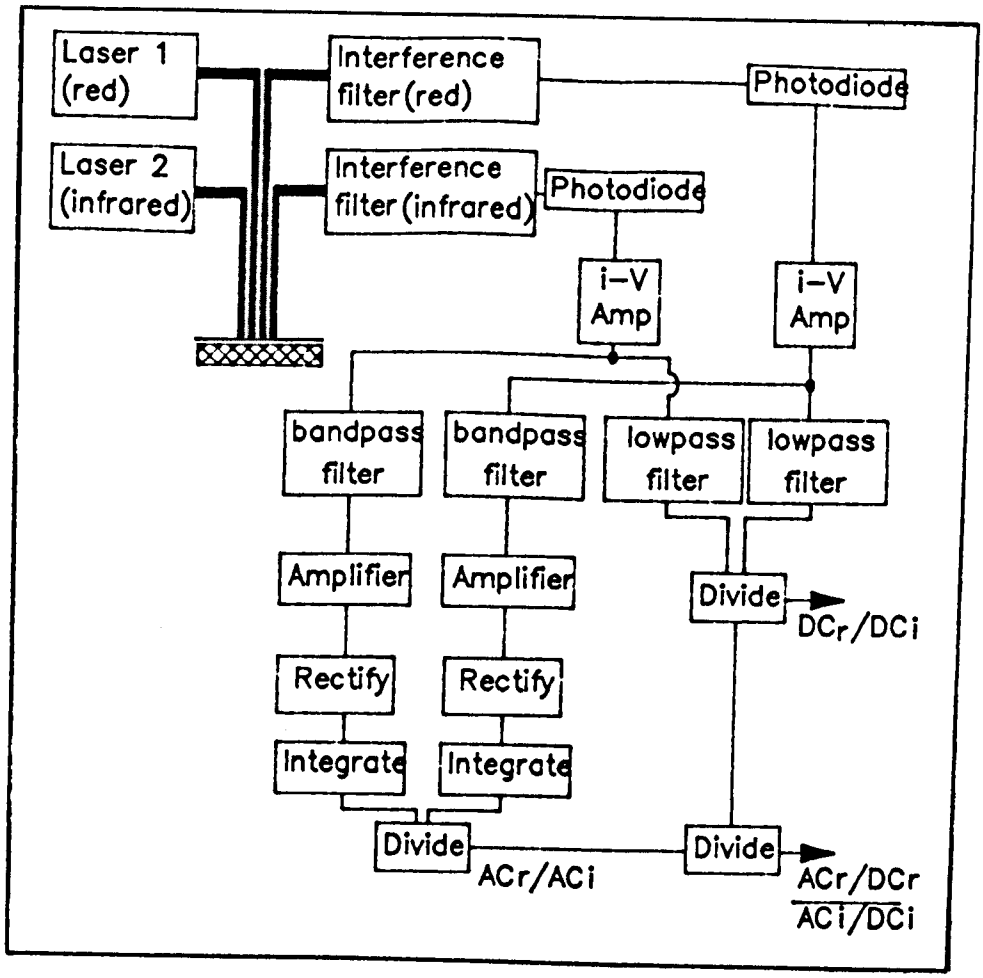

Figure 7.4 Block diagram of the oximeter processing

$$= \frac{(AC_r/DC_r)}{(AC_i/DC_i)} \qquad (7.6)$$

An output related to oxygen saturation was obtained from the equation,

$$S_aO_2 = A - BR \qquad (7.7)$$

where A and B were selected by two potentiometers.

7.3 *In Vitro* Testing

Several *in vitro* studies were performed using the oximeter. The *in vitro* models permitted the instrument to be evaluated over a wide range of blood oxygen levels both in transmission and reflection mode. Studies were also performed to determine whether the response of the reflection oximeter was affected by the configuration of the optical fibre probe. At this stage in the investigations the oximeter probe consisted of two parts, the 2 delivery fibres and the 2 collection fibres. The pulse oximeter output was uncalibrated because it was found that each probe configuration required different values for A and B in order to give an absolute measure of S_aO_2.

Canine blood was used both in the *in vitro* and *in vivo* models in these studies. Pulse oximeters have been developed primarily for measurements on human subjects and therefore commercial instruments are calibrated using human haemoglobin derivatives. However it has been demonstrated that for the wavelength range used in pulse oximetry (600-940 nm) the spectra of canine and human haemoglobin derivatives are almost identical (Sendak et al., 1988). The pulse oximeters should therefore be as accurate for measurements taken from dogs as from humans.

7.3.1 Study one

In vitro model

The *in vitro* model provided a simple system permitting gradual changes in blood oxygen saturation to be investigated, figure 7.5. A small glass beaker acted as a blood reservoir containing a solution of canine red blood cells diluted with physiological saline. Blood temperature was maintained at 37°C by placing the beaker in a thermostatically controlled water bath. Blood oxygenation was controlled by varying the gas mixture of nitrogen and oxygen bubbled through the blood reservoir using flow regulators on the appropriate gas cylinders. A peristaltic pump (Watson Marlow 502S) produced pulsatile blood flow (1 beat s^{-1}) through a tissue model comprising of Silastic tubing (1 mm i.d.) and a small chamber, made of 1 mm thick Silastic sheeting (Dow Corning Corporation, Michigan, USA) where the oximeter probe was positioned. For this study the oximeter processing was performed using a microprocessor (Tandon Plus) which calculated both the average dc ratio and the pulse oximeter ratio R over a 3 s time period. The calculated ratio values from the oximeter were updated every 10 seconds, and compared with blood samples taken from the outflow side of the blood chamber. The blood samples were immediately analysed for oxygen saturation using a blood/gas analyser (STAT Profile, NOVA Biomedical). Throughout this experiment the blood haematocrit was maintained at 33±1%. The design of the tissue model allowed the oximeter to be used both in transmission and reflection mode. In transmission mode the two delivery and two collection optical fibres were placed directly facing each other on either side of the chamber. In reflection mode all the fibres were placed on the same side of the chamber and positioned a few mm apart, figure 7.6.

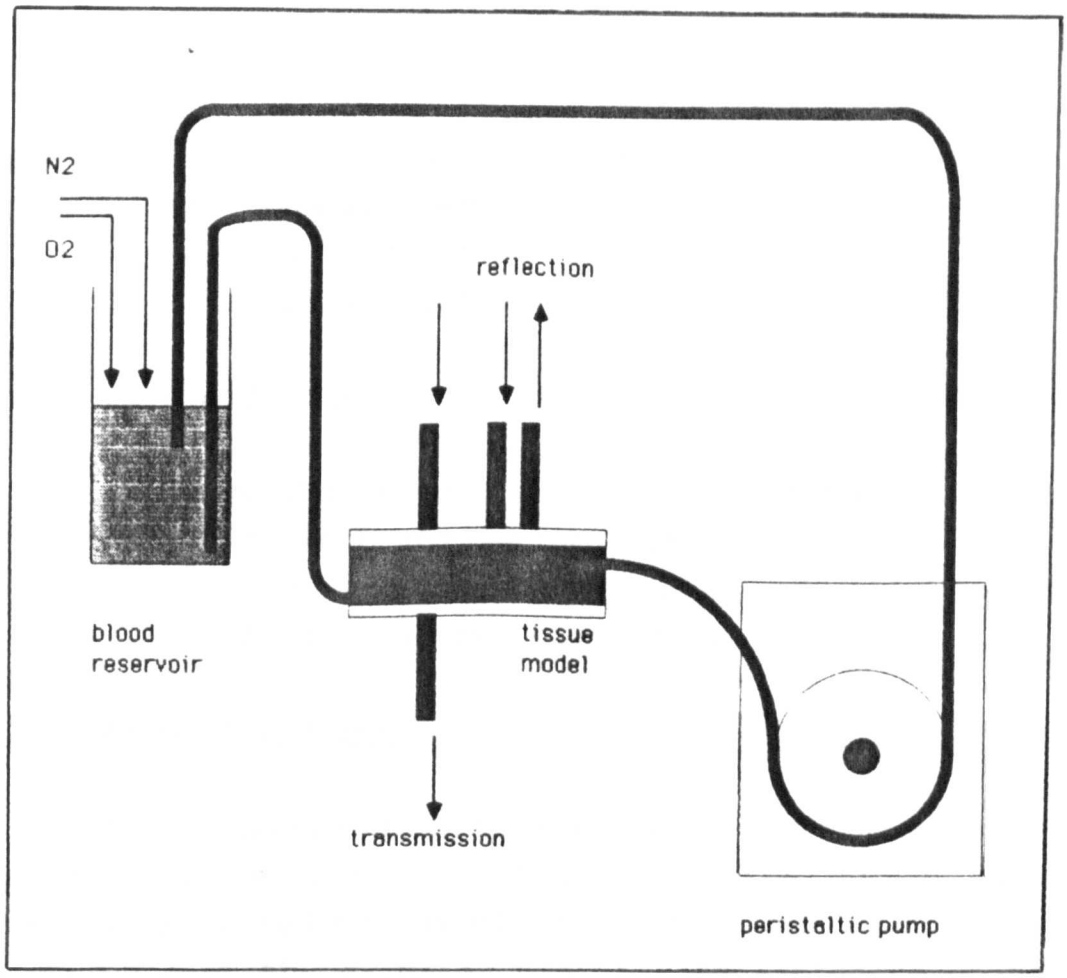

Figure 7.5 The *in vitro* model.

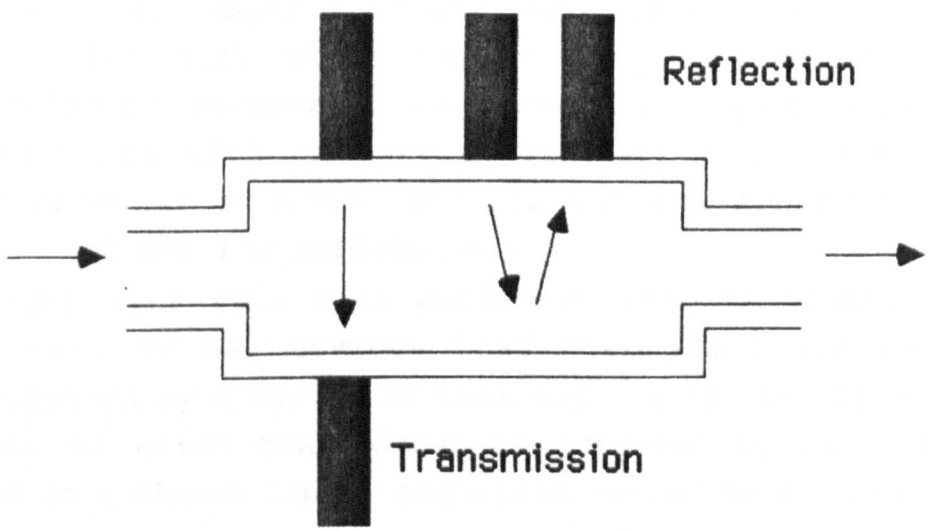

Figure 7.6 Transmission and reflection measurements using the prototype oximeter.

The oximeter response was evaluated by obtaining measurements over a range of oxygen saturation levels both in transmission and reflection. Throughout the studies the photoplethysmogram waveforms were observed on an oscilloscope (Gould digital storage oscilloscope OS1420).

Transmission mode results

Figure 7.7 shows the oximeter response for changes in blood oxygen saturation in transmission mode.
There was a strong correlation ($r = 0.99$, $p<0.001$) between the oximeter response and the blood oxygen saturation.

Reflection mode results

The oximeter response using backscattered light was strongly correlated ($r = 0.93$, $p<0.001$) with the blood oxygen saturation measured by the blood gas machine.
The response of the oximeter was less sensitive to changes in blood oxygenation in reflection mode than in transmission mode as can be seen from the range of values spanned on the axes in figure 7.8.
The dc ratio response of the oximeter was also tested for correlation with blood oxygenation. The reflection and transmission responses are shown in figure 7.9. Strong correlations with the oxygen saturation were obtained in both cases ($r = 0.986$, $p<0.001$ for transmission and $r = 0.936$, $p<0.001$ for reflection).
Straight line fits were performed for all graphical data even when it was obvious that the data would be better represented by a curve. In this way one is able to judge the margin of error that would be produced by an instrument based on a direct linear algorithm rather than *in vivo* data.

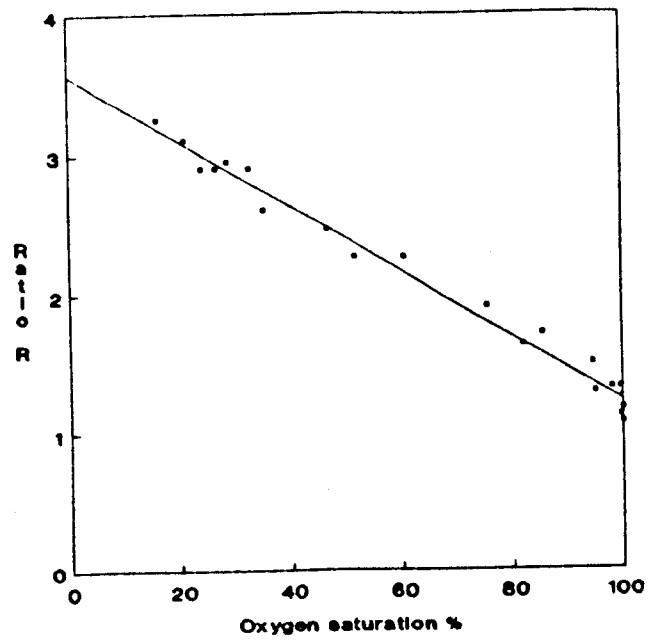

Figure 7.7 Oximeter response in transmission mode.

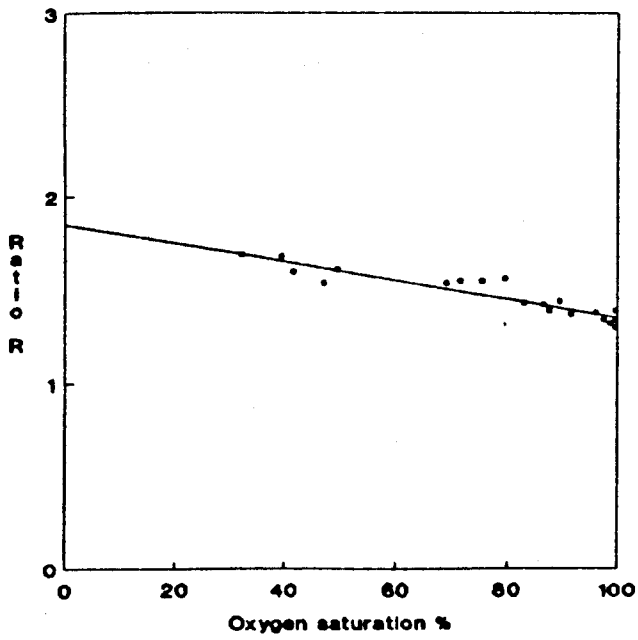

Figure 7.8 Oximeter response in reflection mode.

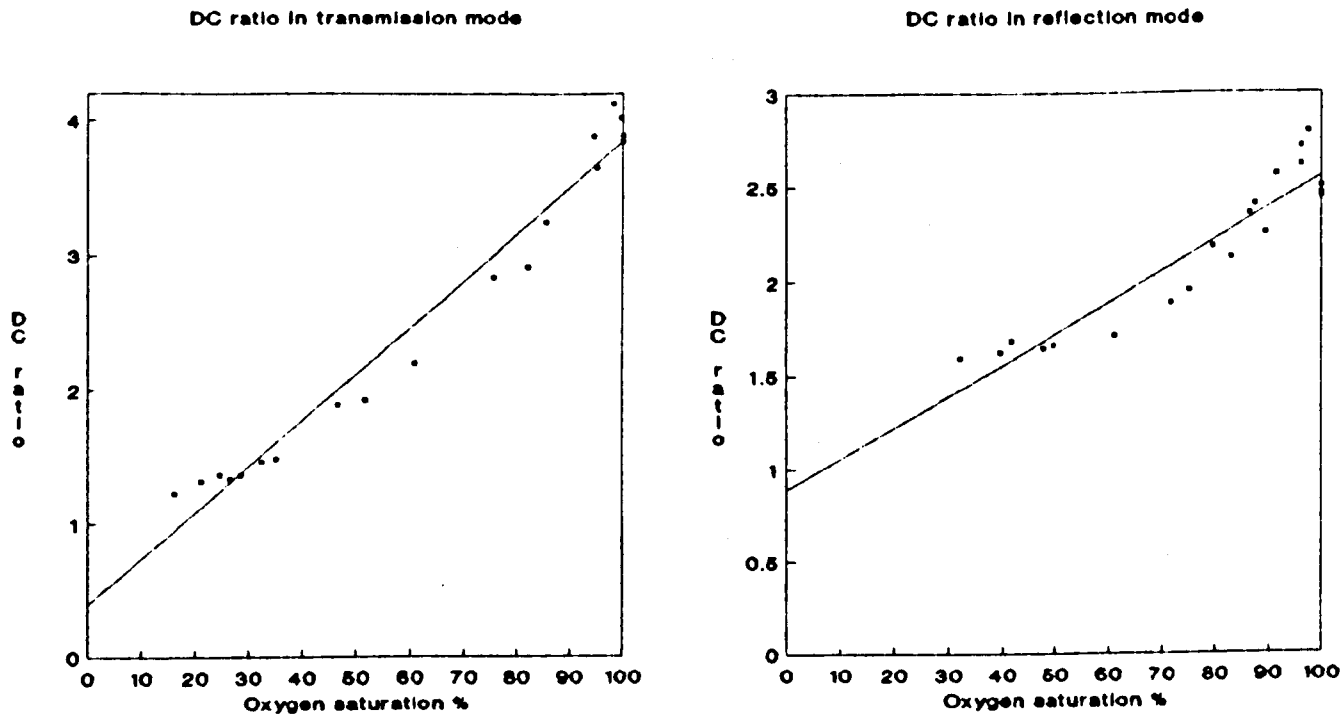

Figure 7.9 DC oximeter response (a) in transmission and (b) in reflection mode.

Discussion

Figures 7.7 and 7.8 show that the pulse oximeter responds well to changes in oxygen saturation both in transmission and reflection. However the response does not follow the calibration line predicted by direct application of Beer's law. The results indicate that instruments using the Beer's law calibration line would be inaccurate especially at low values of S_aO_2. Previous research has shown this discrepancy to be due to the light scattering effects of the rbcs which are not taken into account by Beer's absorption theory. Manufacturers have overcome the problems associated with the implementation of Beer's law by calibrating oximeters using data points obtained *in vivo*. The measurements are incorporated into a microprocessor based look-up table within the oximeter. Such empirical calibration extends the range of accuracy of the S_aO_2 measurements over the total expected range of oxygenation.

7.3.2 Study two

An improved tissue model was designed for the second *in vitro* study. Blood was pumped through two concentric Silastic tubes (10 mm i.d., 14 mm o.d. and 6 mm i.d., 8 mm o.d.) arranged such that the only blood volume was situated on the outer portion of the model, figure 7.10. This provided a simple representation of the perfused tissue and bloodless bone structure of a finger. The oximeter processing was performed by analogue electronics producing an output voltage relating to ratio R and the dc ratio. Initially the oximeter response was tested in reflection mode by comparing measurements with oxygen saturation levels calculated using a separate multiwavelength oximeter. Several blood samples were taken at various levels of oxygenation and immediately analyzed using an IL282 CO-oximeter.

Both the ratio R and the dc ratio responses of the oximeter

operating in reflection mode were compared with the response obtained simultaneously from a commercial transmission pulse oximeter (Nellcor N-100). The *in vitro* model was designed to permit measurements from both oximeters by placing the Nellcor N-100 across the model and the reflection oximeter probe on the top surface, figure 7.11.
The reproducibility of the oximeter response was determined by performing successive desaturations in the *in vitro* model and comparing the change in oximeter output during each response.

Results

Comparisons with the IL282 CO-oximeter demonstrated a strong correlation ($r = 0.979$, $p<0.001$) between the pulse oximeter response and the oxygen saturation over a range 100% to 40%, figure 7.12.
Both the ratio R and the dc ratio responses of the oximeter resembled that of the Nellcor N-100, figure 7.13. Strong correlations were demonstrated for both the pulse oximeter ratio R ($r = 0.884$, $p<0.001$) and the dc response ($r = 0.860$, $p < 0.001$), figure 7.14.
Successive desaturation responses were monitored by the oximeter with the collection and delivery fibres fixed in one position. The fibres were moved to a different model site and the desaturation response repeated. Using a paired t-test it was demonstrated that initially there was no significant difference between two successive desaturation responses ($t = 2.6$, $df = 17$, $p = 0.018$). But when the collection and delivery fibres were moved to a different site on the surface of the model the desaturation response was significantly different from those performed previously ($t = 7.53$, $df = 17$, $p < 0.0001$). There was still a strong correlation between the pulse oximeter response and the S_aO_2 calculated by the Nellcor N-100 ($r = 0.993$, $p < 0.001$) but the voltage range covered by the reflection oximeter differed from previous desaturations (figure 7.15).

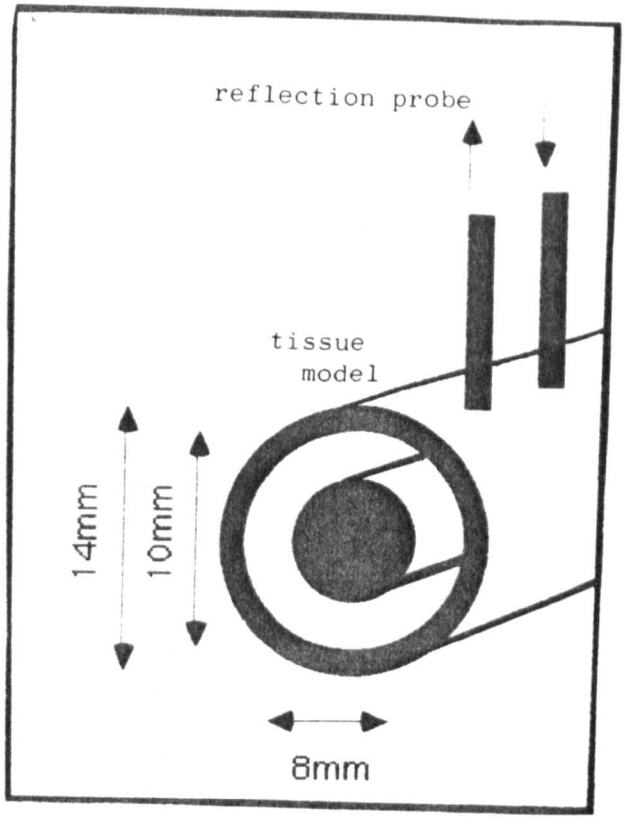

Figure 7.10 The *in vitro* tissue model

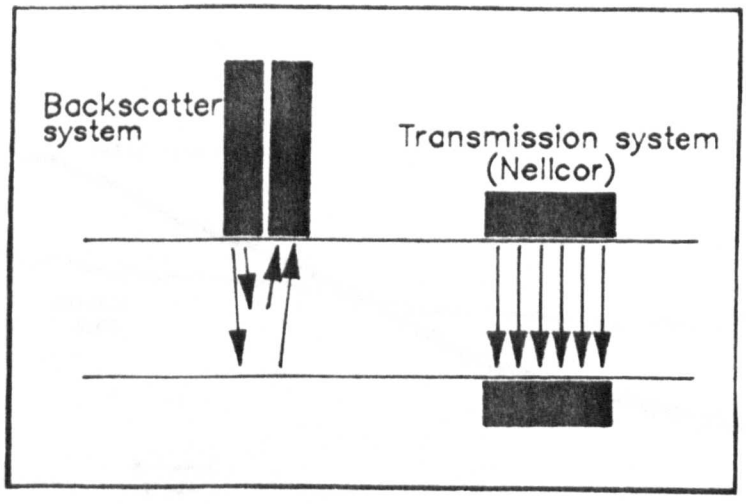

Figure 7.11 Simultaneous measurements were made by placing the reflection probe and Nellcor probe side by side on the model.

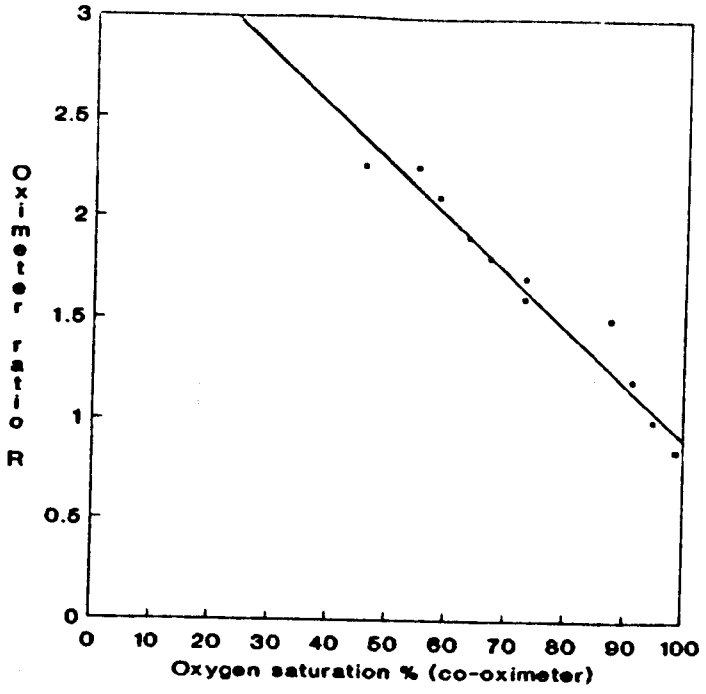

Figure 7.12 The oximeter response compared with measurements obtained from an IL282 CO -oximeter.

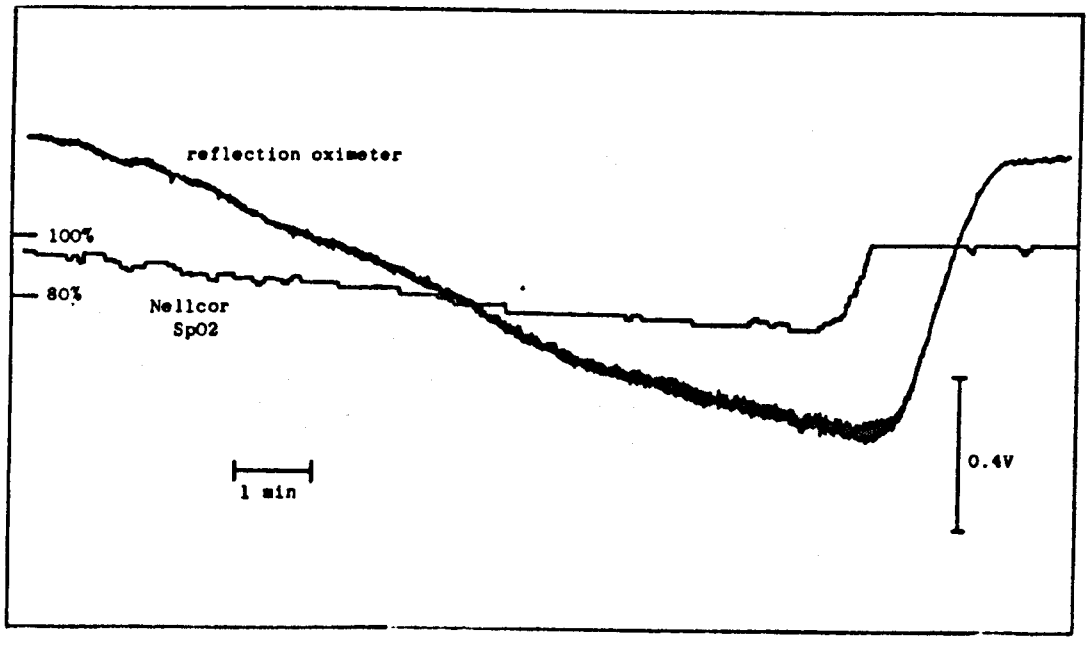

Figure 7.13 Desaturation responses simultaneously recorded using the reflection oximeter and the Nellcor transmission oximeter.

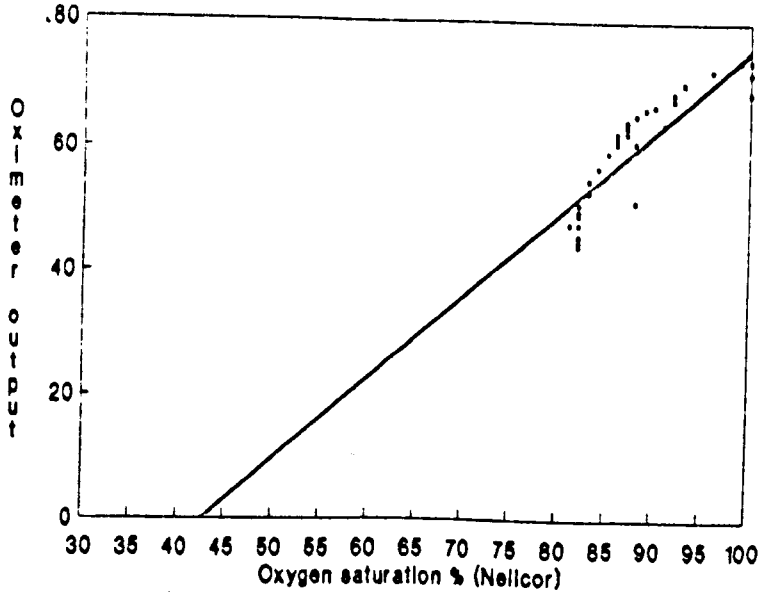

Oximeter output is shown in arbitrary units

(a)

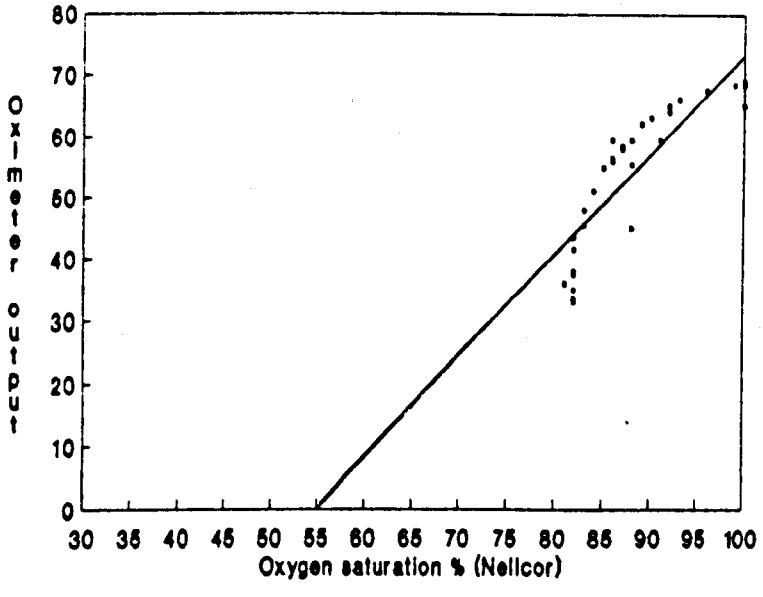

Oximeter output is shown in arbitrary units

(b)

Figure 7.14 Comparison of the (a) ratio R and (b) DC ratio responses with the Nellcor response.

Discussion

The reflection oximeter responses correlate strongly with changes in blood oxygenation measured by a CO-oximeter and a commercial transmission pulse oximeter. The CO-oximeter measures the transmission of four wavelengths (535, 585, 594 and 626 nm) through a blood sample *in vitro* to obtain percent concentrations of haemoglobin, oxyhaemoglobin, carboxyhaemoglobin and methaemoglobin (Operator's Manual IL282 CO-oximeter 79282, Lexington, MA: Instrumentation Laboratory).

In vitro measurements during desaturation were also shown to be reproducible for a fixed probe configuration at any individual model site. However if the oximeter probe was repositioned between desaturations the oximeter response was significantly altered. For each desaturation response the oximeter reliably followed changes in blood oxygenation but the output voltage was different for each probe configuration. This was attributed to the delivery and collection fibres being moved with respect to each other and was further investigated in later studies. These findings indicate that the oximeter cannot be calibrated unless the optical fibres are fixed within the probe and would require new calibration constants for any different probes used.

The results also suggest that the oximeter response is dependent on the site chosen for measurement. The different scattering properties of skin at different sites would have a similar affect on the oximeter as the probe fibre separation.

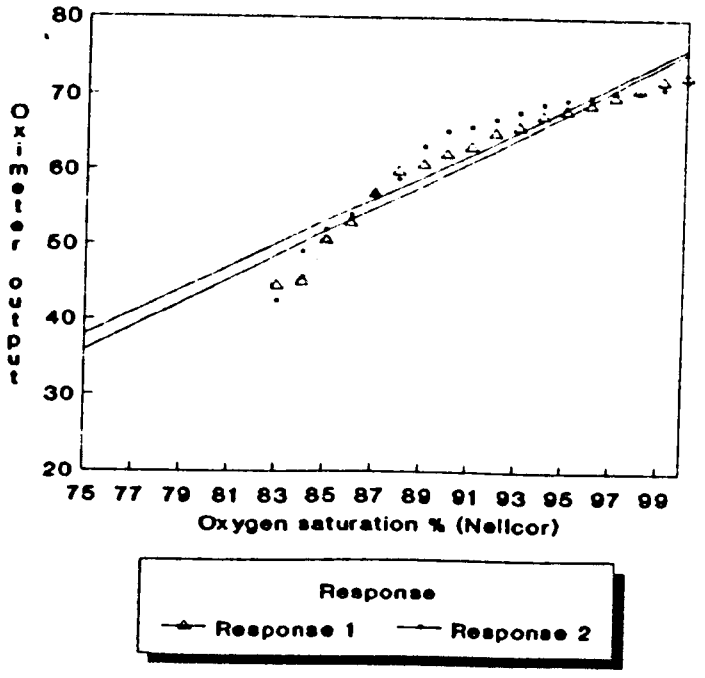

(a)

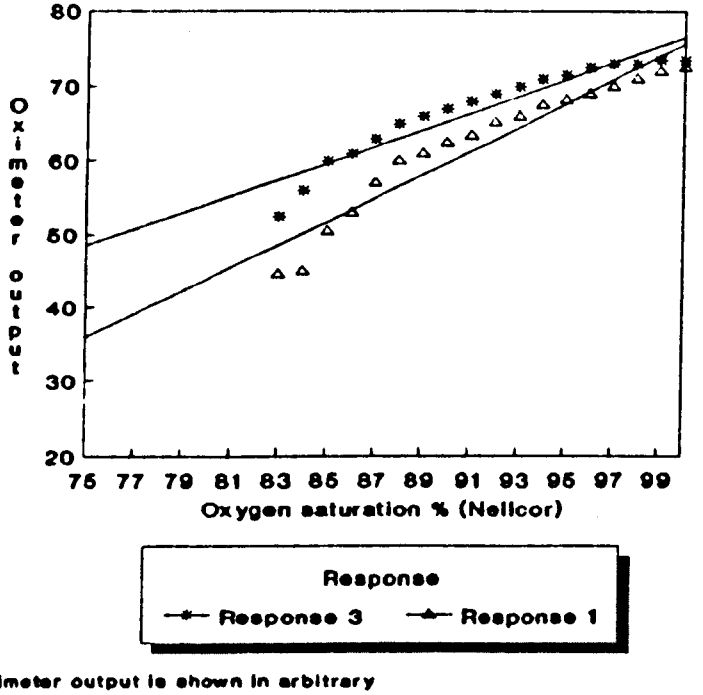

(b)

Figure 7.15 Successive oximeter responses (a) without moving and (b) moving the probe between desaturation procedures.

7.3.3 Study three

A study was performed using the *in vitro* model to observe whether changing the source-detector separation at the probe tip affected the sensitivity of the oximeter response. This was determined by measuring the change in oximeter output voltage for different probe configurations as the blood oxygenation was changed. At the start of each run the blood oxygen saturation was between 95 and 100%. The delivery and collection fibres were placed on the model surface and the blood was slowly reduced by bubbling nitrogen through the blood reservoir. The drop in oxygen saturation was measured by taking blood samples at regular intervals and analysing them with the IL282 CO-oximeter. These results were then compared with the changes in oximeter output voltage.

Results

The results indicating the sensitivity of the oximeter response with different probe configurations are shown in figure 7.16. Measurements were compared for fibre separations of between 0 and 5 mm. As the source-detector separation was increased the sensitivity of the oximeter gradually increased.

Discussion

The results from this study indicate that the oximeter calibration depends on probe configuration. Similar probe dependency has been reported for backscattered light measurements from whole blood (Schmitt et al., 1986). Generally the oximeter became more sensitive as the source and detector fibres were moved further apart. However, the separation distance between the source and detector fibres was limited by the need to detect a strong pulsatile signal which is essential for pulse oximetry processing.

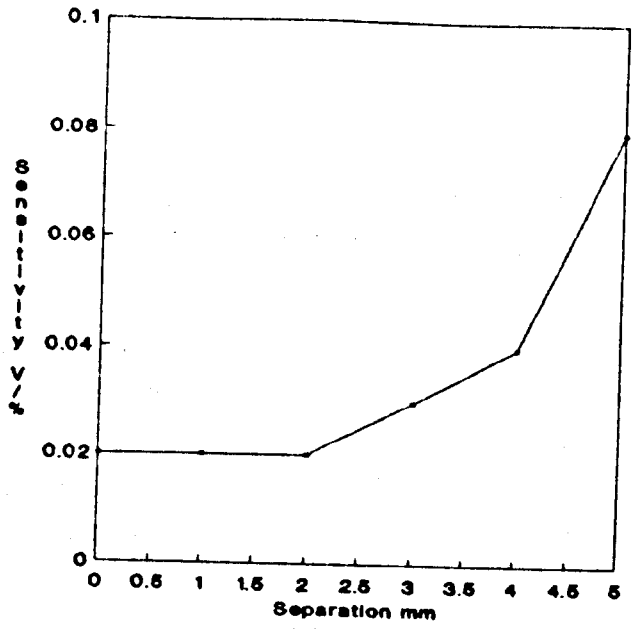

Figure 7.16 Sensitivity of the oximeter response with different probe configurations.

7.4 *In Vivo Testing*

In vivo studies were carried out using the reflection pulse oximeter both on human subjects and anaesthetised dogs.

Human studies

Preliminary measurements of oxygen saturation were obtained from the human hand with the reflection oximeter probe placed on the subject's forefinger. Several breathing exercises were performed by the subject including prolonged breath holding and hyperventilating. The oximeter response was continually traced on a chart recorder and a selection of traces are presented in figure 7.17.

Prolonged breath holding produced characteristically shaped oxygenation responses that have been reported elsewhere (Strohl and Altose, 1984). Early in the breath-hold oxygen saturation decreased slowly but the gradient of the decrease became rapidly steeper. As soon as breathing was resumed the oxygen saturation quickly recovered to its previous level (≈96-98%). Hyperventilating produced a noticeable increase in oxygenation over the period of intervention but this gradually returned to the previous level as the breathing rate was reduced.

In another study both the ratio R and the dc ratio response of the oximeter were compared with the recordings obtained using a Nellcor N-100 transmission pulse oximeter. The reflection probe was placed on a finger and the transmission probe on the thumb of the same hand. A sample of the typical responses obtained for different breathing interventions are shown in figure 7.18.

There was a strong correlation between the Nellcor recordings and both the outputs from the reflection oximeter ($r = 0.982$, $p<0.001$ and $r = 0.542$, $p<0.001$ for the R ratio and dc ratio respectively), figure 7.19. The dc ratio had a smaller correlation coefficient than the pulse oximeter ratio R. This was expected since the dc response cannot

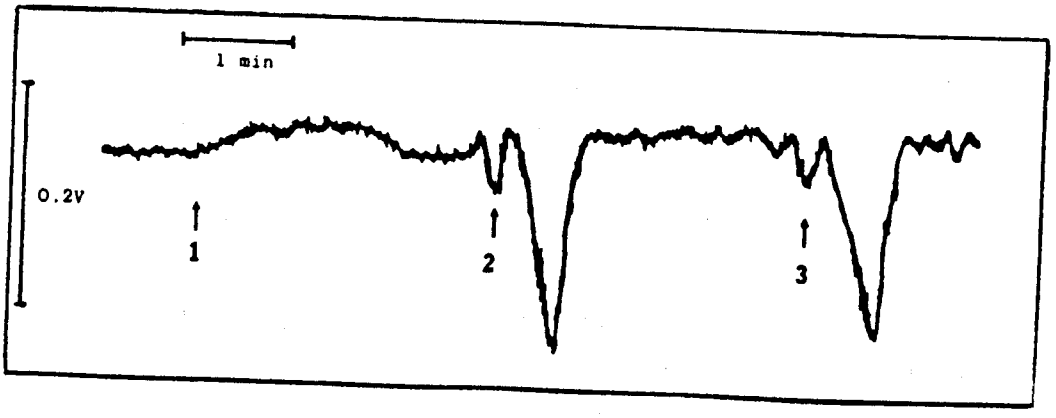

Figure 7.17 Tracing of the oximeter response to (1) hyperventilation and (2 and 3) breath -holding exercises.

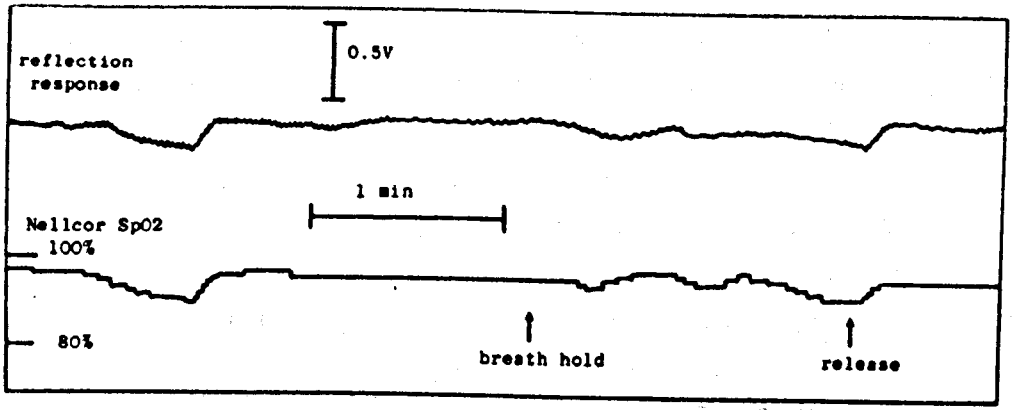

Figure 7.18 Comparison between reflection oximeter and Nellcor responses during breath-holding exercises.

distinguish between arterial and venous blood whereas the Nellcor oximeter and the reflection pulse oximeter indicate the oxygen saturation of arterial blood alone.

Animal studies

An anaesthetised dog model was used to investigate the reproducibility of the oximeter response and the effect of source-detector separation on the instrument sensitivity. Male beagle dogs 12 - 17 kg were anaesthetised with an intravenous injection of Sagatal (30 mg kg^{-1}) and anaesthesia maintained with a continuous perfusion of a Sagatal-saline mixture (Sagatal : saline = 1:12). The left femoral vein and artery were cannulated, the former for maintenance of anaesthesia and the latter for blood pressure measurement and arterial blood samples. A tracheal cannula was inserted to respire the animal using a respirator pump (Harvard Apparatus, model 613A). In each case the tail was shaved to enable the oximeter probes to be positioned on the skin surface (figure 7.20). Pulsatile flow was detected from the caudal artery and arterioles leading from it. The reproducibility of the oximeter response was tested by performing repeated desaturations by altering the respiration rate of the mechanical respirator. Arterial blood samples were taken from the femoral artery and immediately analysed using a blood gas machine (STAT Profile, Nova Biomedical). The respiration rate was then increased again and the oxygenation allowed to increase to its previous baseline level. The desaturation procedure was then repeated and the oximeter responses compared for each case. Figure 7.21 demonstrates the reproducibility of consecutive responses obtained from the tail of a dog at a single measuring site.

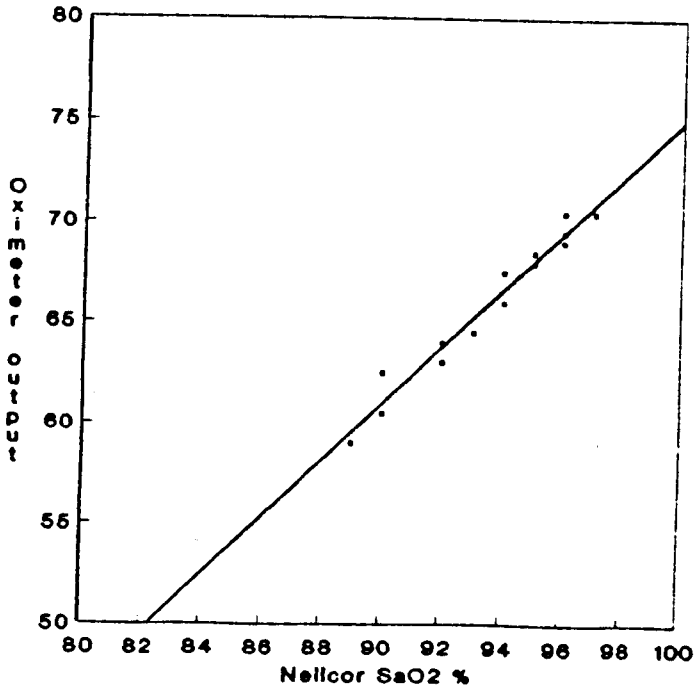

(a)

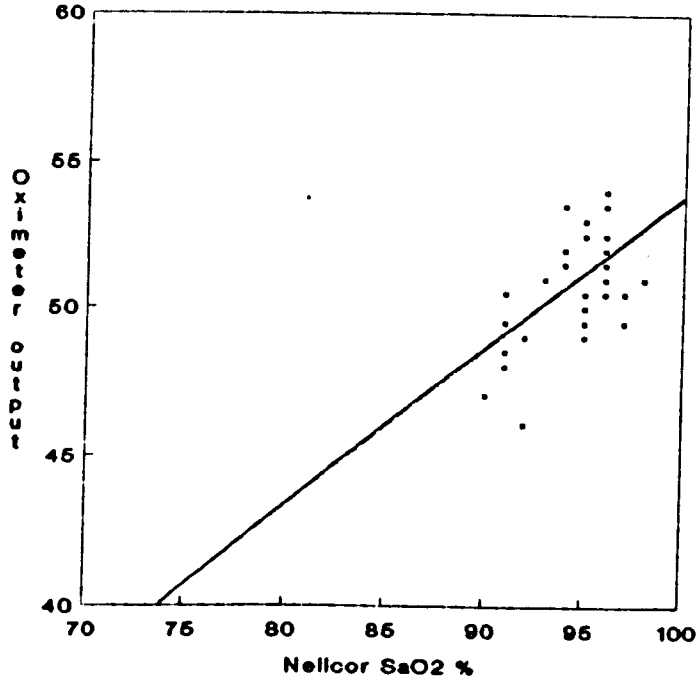

(b)

Figure 7.19 *In vivo* comparison between the Nellcor response and (a) the ratio R and (b) the DC ratio.

A series of desaturation responses were then performed for different source-detector separations. The Nellcor probe was placed on the distal end of the tail and the reflection probes were positioned approximately 5 cm further towards the body. Changes in levels of oxygen saturation were monitored continuously by the two instruments during periods of induced hypoxia. The sensitivity of the reflection oximeter was investigated for various source-detector separations over a range from 0 to 4 mm. This was achieved by comparing changes in output voltage of the reflection oximeter during each desaturation with the percentage change in oxygen saturation as recorded by the Nellcor N-100. The results, shown in figure 7.22, are similar to those found *in vitro* indicating that the oximeter response is more sensitive when the probe separation is increased.

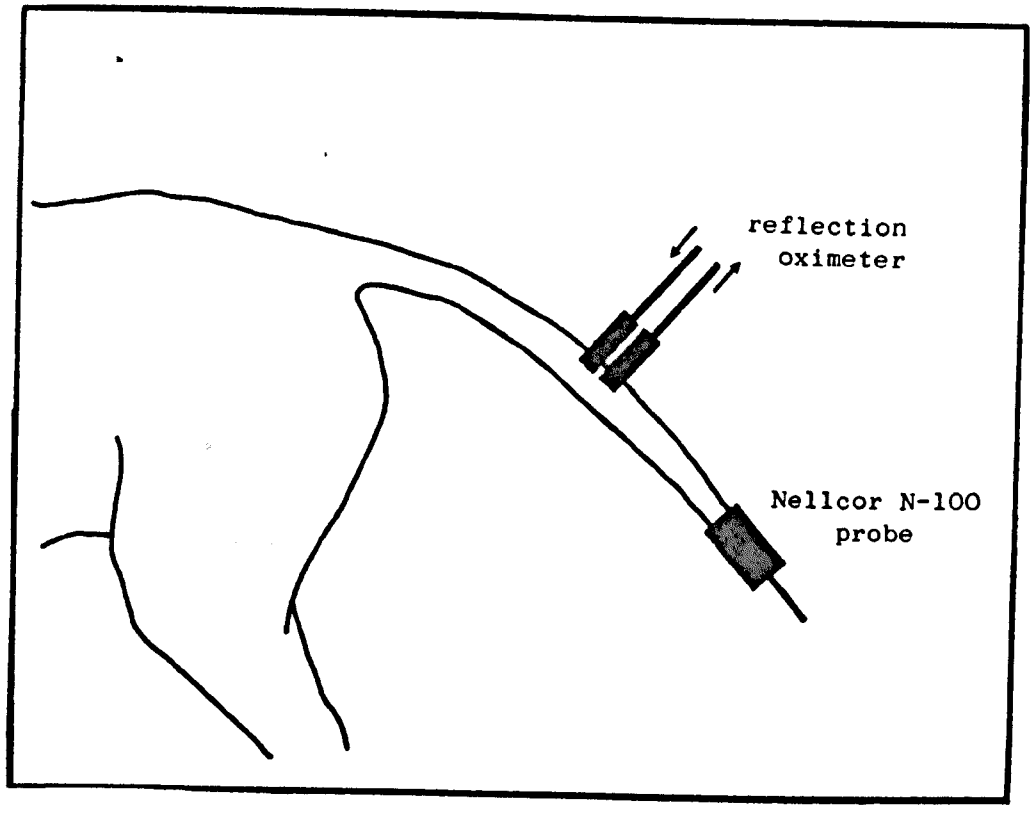

Figure 7.20 Positioning of the oximeter probes on the tail of an anaesthetised dog.

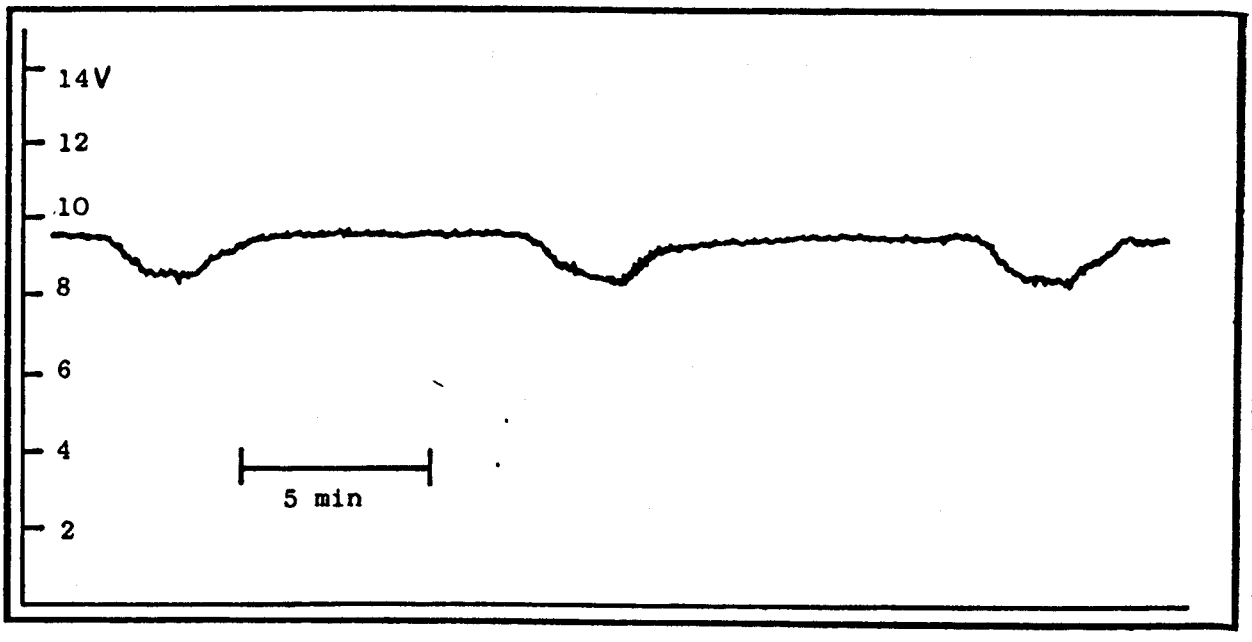

Figure 7.21 Repeated desaturation responses using the reflection oximeter.

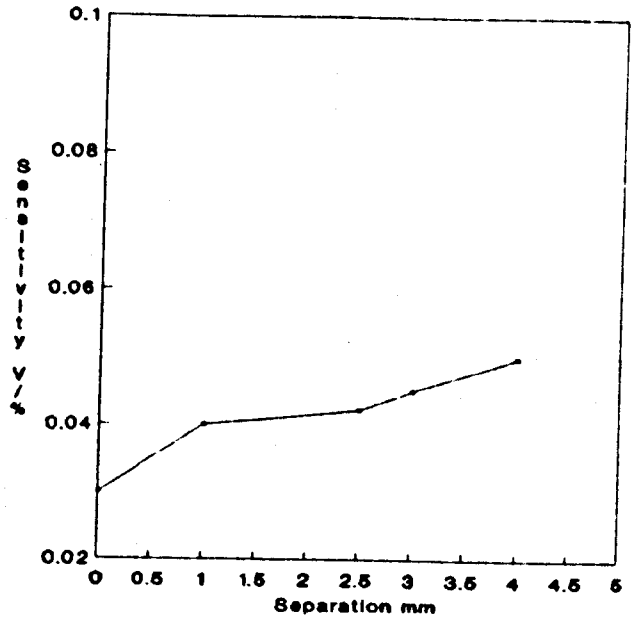

Figure 7.22 Sensitivity of the *in vivo* responses for different probe configurations.

Discussion

The *in vivo* measurements demonstrated that the reflection oximeter can be used as a noninvasive monitor for changes in blood oxygenation. The measurements correlated strongly with the commercial transmission pulse oximeter and characteristic responses were obtained for breath holding exercises performed by human subjects.

The response of the reflection oximeter was highly dependent on the probe configuration. The oximeter was shown to produce reproducible responses to changes in saturation when monitoring at a single site but as the probe was moved to different sites on the tail a range of different oximeter voltages were produced for a fixed oxygen saturation. The sensitivity of the response was found to depend on the source-detector separation which was probably due to the increased volume of tissue sampled as the fibres are moved apart.

In a recent study Almond et al. (1988) considered the optimum source-detector separation for quality photoplethysmograms. It was concluded in their studies that a separation of 5 mm produced the highest quality pulses. The oximeter response also became more sensitive as the separation was increased. However as the separation was increased the detected signal strength was greatly reduced. A major limitation of the reflection oximetry method is the low level photoplethysmogram typically recorded from the skin. There were difficulties obtaining a pulsatile signal from many locations on the skin surface of the anaesthetised dog. These difficulties severely restricted measurements using the backscattered technique to specific highly perfused skin sites.

The oximeter response was shown to be reproducible for successive desaturations at any single location. However as the oximeter probe was moved from location to location on the skin surface several different values of output voltage were obtained corresponding to the same level of oxygen

saturation. The interpretation of these findings is that the instrument can be calibrated for use at any one skin site but not if it is moved between different sites. In general use only relative changes in blood oxygenation can be monitored. The reasons for the site dependency of the oximeter readings are not fully understood but are probably due to different scattering properties of the skin tissue at different locations.

7.5 Conclusions

An oximeter operating by detecting laser light backscattered from the skin has been developed and evaluated both *in vitro* and *in vivo*. Choice of wavelengths was limited by the present availability of laser sources. Using lasers operating at wavelengths of 633 nm and 810 nm a linear and sensitive response to changes in oxygen saturation was predicted.

Both the pulse oximeter and dc oximeter response were demonstrated to have strong correlations with measurements using a blood\gas machine, CO-oximeter and a commercial pulse oximeter. Then characteristic desaturation responses were obtained for human breath-holding exercises and induced hypoxia in a dog model. The reproducibility of the responses was demonstrated at individual skin sites but there was a large variation in the oximeter response from site to site. This indicates that the reflection oximeter could be calibrated if measurements were always taken from the same sample site on any one subject. The calibration would be achieved by obtaining two data points at known levels of oxygen saturation. However if the oximeter were to be used at several different sites on different subjects then it could only follow trends in oxygen saturation. The sensitivity of the oximeter was shown to depend to a great extent on the design of the oximeter probe.

It was initially envisaged that the reflection oximeter would permit oxygen saturation measurements from many skin

sites where a transmission system cannot be applied. However, application of the reflection pulse oximeter was found to be limited to specific skin sites where there was a large pulsatile element to the blood flow.

CHAPTER 8

Combining Blood Flow And Oxygenation Measurements

8.1 Introduction

Researchers have previously attempted to combine different monitoring techniques to simultaneously monitor blood flow and oxygenation (Donahoe, 1984).
In this thesis non-invasive optical monitoring techniques have been investigated. Chapters 2, 3, 4 and 5 were mainly concerned with measurements of skin blood flow using the laser Doppler technique. Chapters 6 and 7 were concerned with blood oxygen measurements and an oximeter was described using laser light backscattered from the skin. The techniques described have individually been demonstrated to provide useful physiological data but more detailed information may be provided by combining the techniques to permit simultaneous measurements from a single instrument. In this chapter a system combining oximetry and laser Doppler flowmetry has been developed measuring blood flow and oxygenation from the same tissue sample.

8.2 Instrument Design

8.2.1 Front end optics

The oximeter described in Chapter 7 was designed to be used in parallel with a laser Doppler flowmeter by using laser light sources operating in continuous output mode. At this stage in the study the oximeter was modified. The infrared channel was kept the same as in the original oximeter design using a semiconductor diode at 810 nm (Sharp LTO10MC0) and a filtered photodiode (EG&G Photon devices). But the red channel was altered by replacing the HeNe gas laser with a 5 mW laser diode emitting light at 670 nm (Toshiba TOLD9211) powered by a laser diode driver (model LD92-03, Laser Drives

Inc.). Detection of the red wavelength was performed by a sensitive photodiode (BPW21, R.S. Components Ltd.) through an optical interference filter with a centre wavelength of 671 nm and a bandwidth of 10 nm (Edmund Scientific, scribed interference filter). Photodiode current-to-voltage conversion was obtained using an op-amp (AD647JH, low noise op-amp) circuit configuration shown in figure 8.1. In this photoconductive mode the resultant output voltage was linearly related to the incident radiation level. The small capacitance in combination with the resistor R_L limited the signal bandwidth to 12.4 kHz. Following current-to-voltage conversion the output voltage of the infrared channel was used for both oximetry and laser Doppler processing. The red channel was used for oximetry processing alone, figure 8.2. The circuit diagram is presented in Appendix 4.

8.2.2 Laser Doppler circuit design

Laser Doppler signal processing was performed using the Stern (ω^2-weighted) algorithm described in Chapter 2. The output from the infrared channel current-to-voltage converter was filtered into ac and dc components. The dc component was used for both oximetry processing and as an indicator of laser light intensity in the laser Doppler processing. The ac signal was selected using a high pass filter then amplified and passed through an eight-pole low pass filter that set the processing bandwidth to 12 kHz. The signal was then differentiated before passing through a process of rms-to-dc conversion. The output was corrected for amplifier and shot noise by subtracting a dc voltage proportional to these noise components. Finally the Doppler output was normalised by dividing by a dc voltage proportional to the detected light intensity. The circuit diagram is presented in Appendix 4.

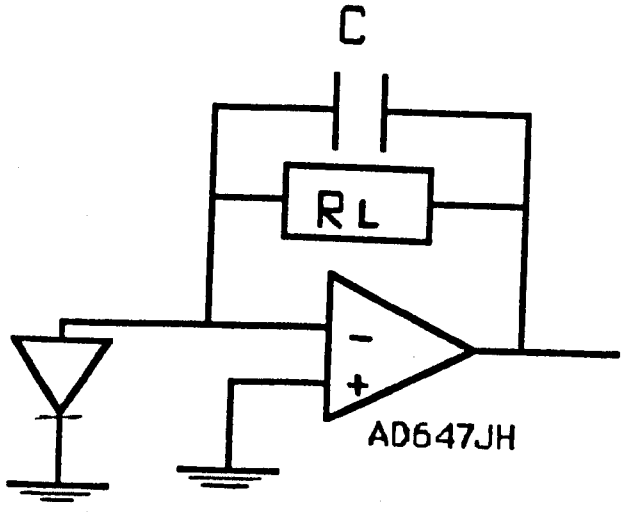

Figure 8.1 Photodiode current to voltage conversion.

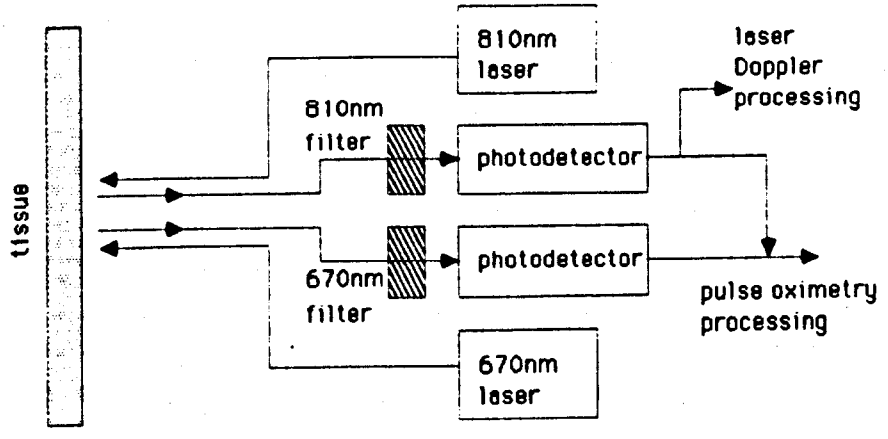

Figure 8.2 Block diagram of the combined oximeter/ flowmeter front-end processing.

8.3 *In Vivo* Measurements

Human study

The combined monitoring system was tested by obtaining measurements from the light backscattered from the thumb of a human subject. Breath holding exercises were performed while continuously recording the laser Doppler flux and oximeter output voltages. The oximeter measurements were not calibrated but displayed relative changes in blood oxygenation.

An example of the combined traces are shown in figure 8.3. The subject performed a Valsalva manoeuvre by taking a deep inspiration and forcing expiration against a closed glottis. This manoeuvre increases the pressure in the chest, which obstructs the venous return to the heart and causes a reduction in the stroke output of the heart. It follows that a reduction in skin blood flow is also observed. It was observed that the Doppler flux measurement decreased for a few seconds. In time the venous pressure builds up and blood flow increases. At the end of the manoeuvre a deep breath is usually taken, the blood enters the thorax and fills the empty lung vessels. This causes another drop in skin blood flow for a few seconds. The blood oxygen saturation was seen to gradually decrease as the subject held his breath but as soon as breathing was resumed the oxygenation rapidly increased to the level prior to the manoeuvre.

These simple tests show the pulse oximeter operating in parallel with the laser Doppler flowmeter. But the combined instrument could only be used where pulsatile blood flow was detected. In many circumstances oxygen measurements may be required when the blood flow has been occluded or when a pulsatile flow cannot be obtained. In these cases the dc oximeter response may be used as a blood oxygen indicator. The dc oximeter provides an indication of arteriovenous blood oxygenation rather than arterial blood alone.

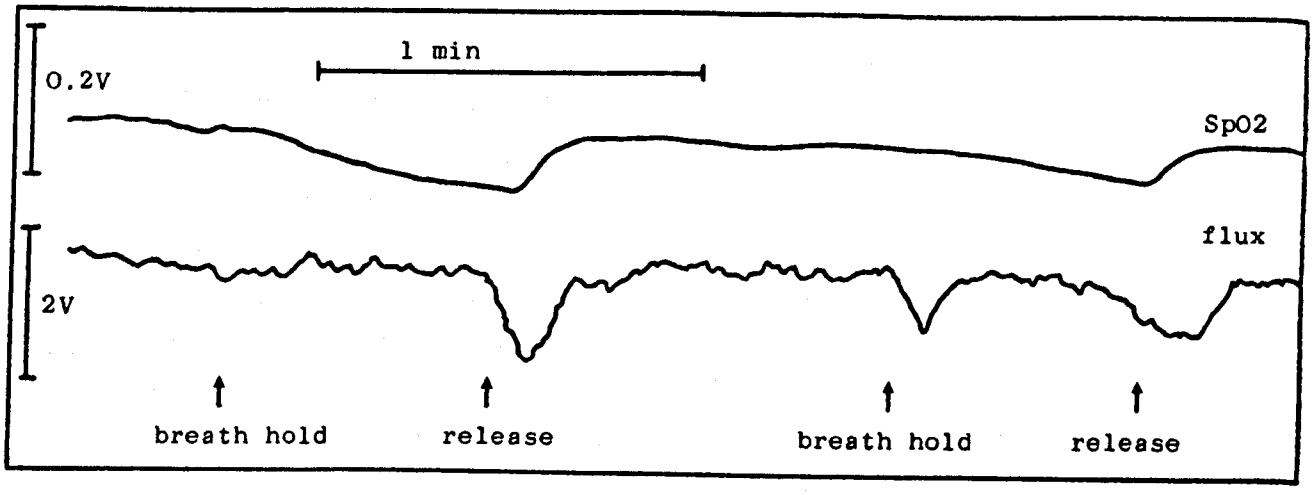

Figure 8.3 Combined oxygen saturation and blood flux measurements during breath-holding exercises.

Rat model

A rat model was used to demonstrate the application of the combined oximeter and flowmeter. Oxygen saturation measurements in laboratory rats have previously been used by Decker et al. (1989) but in that study a transmission pulse oximeter was used. The study reported here combines a dc reflection oximeter and a laser Doppler flowmeter.
Female Alderley Park Wistar rats (n = 4) weighing approximately 200g were anaesthetised with 2% Halothane and respired artificially through a tracheal cannula. A femoral artery was cannulated for the measurement of blood pressure and heart rate using a pressure transducer connected to a chart recorder (Devices MX2). The unaffected hind limb was shaved and loosely restrained using adhesive tape. By exposing the descending aorta and placing a cotton tie loosely around it hind limb occlusions were simply achieved. The optical fibre probe was carefully positioned on the surface of the hind leg so that it was just touching the skin (figure 8.4). Occlusions were performed by lifting the cotton tie for a period of 4 minutes then releasing the tension. The results for all the animals were pooled together and are presented in figure 8.5. Characteristic blood flow and oxygenation responses were obtained. The blood flow decreased dramatically as the aorta was occluded and rapidly increased as the occlusion was released. On the other hand occlusion caused the blood oxygenation to decrease slowly as the oxygen was slowly released to the surrounding tissue. Then, as the occlusion was released, the blood oxygen level was quickly restored as fresh oxygenated blood moved into the tissue microvessels.

8.4 Discussion

The results from the two *in vivo* studies demonstrate how blood flow and oxygenation measurements can be obtained simultaneously from the same sample volume of tissue.
However the information provided by the two monitoring techniques is limited and several problems were encountered during the *in vivo* studies. Both the laser Doppler flowmeter and oximeter were only able to provide measurements of relative changes in blood flow and oxygenation. The operation of the pulse oximeter was limited to specific skin sites where the detected light contained a fluctuating component due to pulsatile blood flow. The DC oximeter response was suitable for most measurement sites but care had to be taken when positioning the oximeter probe. Any movement between the probe tip and the skin surface produced a shift in the oximeter output as the light was then directed onto a different area of tissue with different structural and optical properties.
A fixed probe geometry was used throughout the *in vivo* studies. The delivery and collection fibres were separated by 2 mm. Probe design is critical in the development of a combined blood flow/oxygenation system. It is not a trivial problem since there are many trade-offs to be considered. For the laser Doppler technique, the source-detector separation has to be close enough to ensure an adequate signal-to-noise ratio but not so close that the instrument becomes susceptible to movement artefact. The separation also determines to some extent the depth of the blood flow measurement. The flux measurement tends to originate from deeper layers within the skin as the source-detector separation is increased. For the oximeter the separation should be large enough to ensure reasonable sensitivity to changes in oxygenation but should not significantly decrease the signal-to-noise ratio. Optimizing the probe design would be an important project in further research on a combined monitoring system.

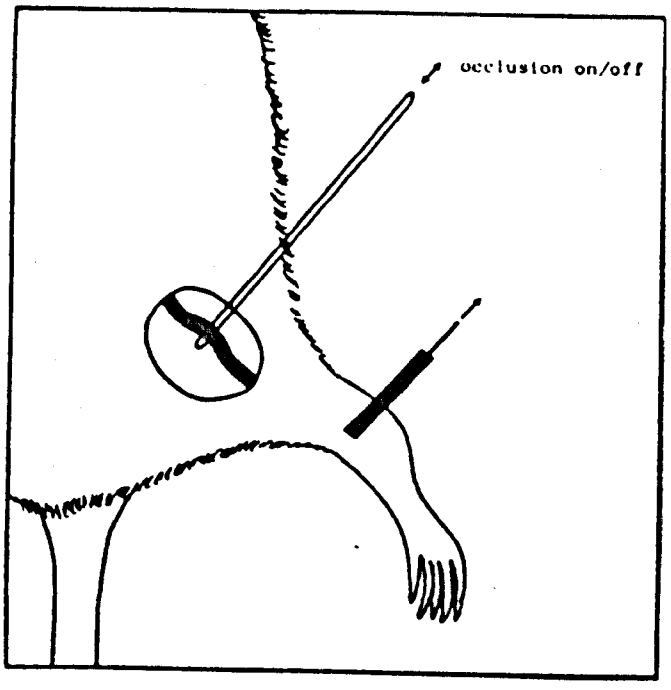

Figure 8.4 Position of probe for measurements using the anaesthetised rat model.

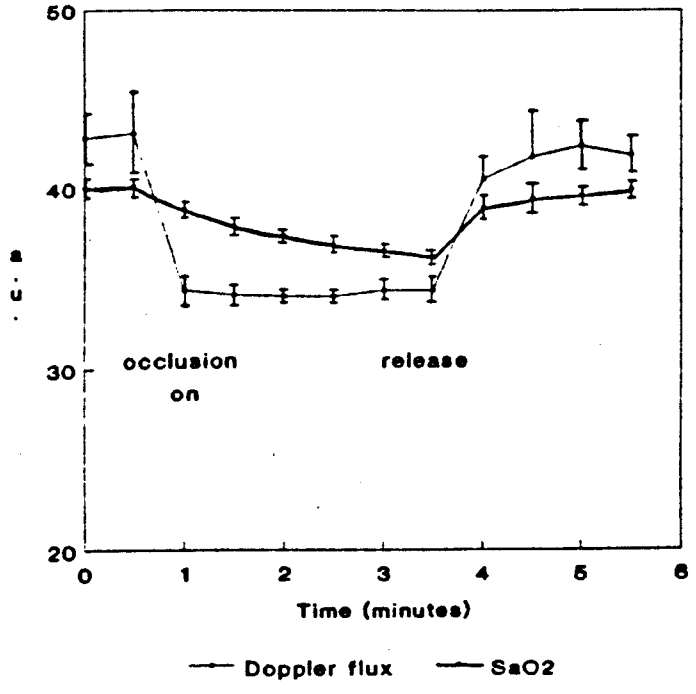

Figure 8.5 Combined oxygen saturation and blood flux measurements for rat femoral occlusions.

8.5 Conclusions

A monitoring system combining pulse oximetry with laser Doppler flowmetry has been developed and demonstrated to record trends in blood oxygenation and flow. The dc oximeter response was also shown to follow changes in blood oxygenation in a combined blood flow/oxygenation system that can be used even when there is no pulsatile element to the blood flow. The dc oximeter responds to changes in the oxygen saturation of both the arterial and venous blood within the sample volume of tissue. Probe design was indicated as being critical in the further development of a combined instrument.

CHAPTER 9

Conclusions And Recommendations

9.1 Conclusions

In this thesis, several studies were performed to investigate the non-invasive monitoring techniques of laser Doppler flowmetry and oximetry.

A comparison between two commercial laser Doppler flowmeters using an *in vitro* flow model showed that measurements of blood flux depend on the signal processing bandwidth employed. By selecting the wideband mode the flowmeters were shown to reliably cover the majority of flow conditions expected in the skin. But reliable measurements using narrowband mode are restricted to situations where only slow moving rbcs (< 1 mms^{-1}) are expected.

Choice of laser source was also shown to affect the measured flux. The HeNe gas lasers used in the laser Doppler studies required a long warm-up time for the output intensity to stabilize whereas systems incorporating laser diodes demonstrated improved light stability which significantly reduced the flowmeter warm-up time. The choice of laser wavelength was demonstrated to affect the volume of skin sampled by the blood flow monitor. Results from several *in vivo* animal models indicated that the infrared wavelength light sampled from a larger volume than the red light. Further studies suggested that a flowmeter using a green wavelength laser would obtain flow measurements predominantly from the capillary vessels. However a green laser suitable for use with an analogue flowmeter is not available at present. Low signal-to-noise ratios are obtained using green HeNe lasers whereas the more powerful Nd-YAG lasers, which also operate in the green, are expensive.

Laser Doppler measurements are usually restricted to measuring dynamic responses at a single site or to discrete measurements at multiple sites. The introduction of a dual channel device enables dynamic responses to be simultaneously monitored at two different skin sites. A dual channel system was evaluated using an *in vitro* flow model which demonstrated that the two channels responded in very similar ways for changes in blood flow. Dual channel measurements were performed *in vivo* to demonstrate how the system may be used to monitor blood flux responses at a drug site as compared to a control site. The instrument provides a simple method of comparing flux responses at other skin sites such as areas of diseased and healthy tissue. In some applications further channels may be useful to map flux changes at several different sites during a blood flow intervention.

A study investigating the effect of applied pressure on Doppler measurements suggested that great care should be taken when positioning the optical fibre probes. It is recommended that in many situations right angled probes should be used. In this case the only pressure at the measurement site is due to the weight of the probe head.

A working prototype oximetry system using backscattered laser light was developed and evaluated using both *in vitro* and *in vivo* models. The oximeter was demonstrated to provide a good indication of changes in blood oxygen saturation but it suffered from a number of limitations.
Ideally, the oximeter should reliably perform quantitative measurements of oxygen saturation but it was found that the response varied from site to site and that one calibration could not be used at all skin sites. Specific single site calibration may be achieved by obtaining reflectance data at two known values of oxygen saturation while the probe was placed at the skin site. However in these studies the oximeter remained uncalibrated and was used to monitor

trends in blood oxygen saturation.
In vivo studies indicated that application of the reflection oximeter was limited to highly perfused skin sites. In order for the oximeter to operate the detected light had to contain a fluctuating component produced by pulsatile blood flow in the underlying tissue.

Blood flow and oxygenation measurements were accomplished by combining a laser Doppler system and oximetry system in a single instrument. The instrument was shown to monitor blood flow and oxygenation during breathing exercises performed by a human subject. The pulse oximeter was limited in its application by the requirement of the presence of a pulsatile flow component within the sampled tissue volume. However in cases where there is no detectable pulse signal the dc oximeter response can be used to monitor changes in blood oxygen saturation. This mode of operation was demonstrated by observing blood flow and oxygen changes during hind limb occlusions in a rat model. The dc oximeter response differed from the pulse oximeter as it cannot differentiate between arterial and venous blood. Instead it provided an indicator of the combined arteriovenous oxygen saturation.

9.2 Recommendations

The instrumentation developed in this thesis has provided a method of simultaneously monitoring blood flow and oxygenation in the skin. However there are several ways in which the instrumentation may be improved.

Further studies are required to understand the optical processes involved as light is scattering through the skin tissue. Combining these findings with further probe designs may reduce the site variability of the oximeter response and lead to a calibrated system.

Many laser Doppler investigations use fibre probes that sample a localised area of tissue and in these applications a fibre system would be required for both the blood flow and oxygen measurements. But it is envisaged that a fibreless probe system could be developed using laser diodes and photodiodes integrated into a small optical head that can be placed directly on the skin surface. This would find some application in large area tissue studies.

The pulse oximeter is limited in its application because the detected light has to contain a fluctuating component due to the pulsatile arterial blood flowing through the tissue. This is not a requirement for the dc oximeter which suggests that this technique may be better for combining with the laser Doppler technique. Further investigations should be undertaken to combine laser Doppler flowmetry with a multiwavelength dc oximeter.

APPENDIX 1

Autocorrelation And Power Spectrum Analysis Of The Photdetector Current

Fluctuations in the backscattered light intensity can be detected using a photodetector. Analysis of the corresponding photocurrent fluctuations provide information about the motion of the perfusing rbcs. The photocurrent can be analysed in the time domain using an autocorrelation function or in the frequency domain using the power spectrum. The autocorrelation is formed by measuring the light intensity at time t and multiplying that value by the intensity at a time $t+\tau$. This is performed many times to produce the autocorrelation function $\langle i(t)i(t+\tau)\rangle$. When there is no movement in the illuminated tissue volume the average intensity at time t will equal that at any other time and the correlation between these two times will be high. If there is any movement the intensity will change with time, the rate at which the intensity becomes uncorrelated depends on the rate at which the scatterers move.

The photocurrent may be defined as the probability per unit time of photoelectron emission. The probability of an electron being emitted from a detector as a result of being illuminated by an optical field is given by (Cummins, 1974),

$$W_1(t) = nE^*(t)E(t)$$

where n is the quantum efficiency.

The joint probability of an electron being emitted at time t and $t+\tau$ is,

$$W_2(t,t+\tau) = nE^*(t)E(t)E^*(t+\tau)E(t+\tau)$$

The autocorrelation function of the photocurrent is,

$$C(\tau) = \langle i(t)\,i(t+\tau)\rangle$$

$$= e^2\langle W_1(t)\,W_2(t,t+\tau)\rangle$$

$$= e\langle i\rangle\delta(\tau) + \langle i\rangle^2 g^{(2)}(\tau)$$

where,

$\delta(\tau)$ is an autocorrelation function describing the quantum mechanical nature of a single electron.

$g^{(2)}(\tau)$ is a second order autocorrelation function.

$$g^{(2)}(\tau) = \frac{\langle E^*(t)E(t)E^*(t+\tau)E(t+\tau)\rangle}{\langle E^*E\rangle^2}$$

This can be expressed in terms of a first order autocorrelation function using the Siegert relation (Jakeman, 1974)

$$g^{(2)}(\tau) = 1 + |g^{(1)}(\tau)|^2$$

Then the autocorrelation function becomes,

$$C = e\langle i\rangle\delta(\tau) + \langle i\rangle^2(1+|g^{(1)}(\tau)|^2)$$

By applying the Wiener-Khintchine transform the autocorrelation function can be converted to a power spectrum in the frequency domain.

$$S(\varpi) = \frac{1}{2\pi}\int_{-\infty}^{\infty} C(\tau)\,\exp(i\varpi\tau)\,d\tau$$

By substituting the autocorrelation function into this equation and changing the limits of the integration for positive frequency terms, the power spectrum becomes,

$$S(\varpi) = \frac{e\langle i\rangle}{\pi} + \langle i\rangle^2\delta(\varpi) + \frac{\langle i\rangle^2}{\pi}\int_0^{\infty} |g^{(1)}(\tau)|^2 \exp(i\varpi\tau)\, d\tau$$

$$= \frac{e\langle i\rangle}{\pi} + \langle i\rangle^2\delta(\varpi) + P(\varpi)$$

The first term is a dc component, the second term a noise component and the third term is the Doppler light beating spectrum.

APPENDIX 2

Bonner And Nossal Model

This appendix encases the theory developed by Bonner and Nossal to demonstrate that the normalized first moment of the spectrum is proportional to the rms speed of the moving rbcs.

Bonner and Nossal (1981) developed an extensive theory relating light scattering from the tissue to blood flow within the tissue. The model predicts how the photocurrent power spectra depends on the rbc speed and concentration.

Blood flow through the vascular bed is assumed to be percolating through a randomly directed network of capillaries and is assumed to consist of identical, spherically symmetric particles illuminated by a light source which has been totally randomized in direction.

Two cases are defined, one in which the tissue has low level of perfusion, and the other where the tissue is highly perfused.

The total light intensity backscattered onto the photodetector is defined as i_0, the portion scattered by moving rbcs is defined as i_{sc} . The normalized photon autocorrelation function is then given as,

$$g^{(2)}(\tau) = \frac{\langle n(t)\,n(t+\tau)\rangle}{\langle n\rangle^2}$$

where n is the number of photons counted at the photodetector.

$$g^2(\tau) = 1 + \frac{\beta\ i_{sc}{}^2 |I(\tau)|^2}{i_0} + \frac{2 i_{sc}(i_0 - i_{sc})\, I(\tau)}{i_0{}^2}$$

where,

β is an instrumentation factor

$I(\tau)$ is the intermediate scattering function for the Doppler shifted light

$$I_1(\tau) = \langle E_{sc}^*(t) E_{sc}(t+\tau) \rangle$$

For low perfusion states where there is a majority of heterodyne events involving single scattering from a moving rbc, it was shown that,

$$I_1(\tau) = \frac{2\varepsilon}{2\varepsilon + T^2}$$

where,

$$T = \frac{\langle v^2 \rangle^{1/4} \tau}{(6a)^{1/4}}$$

ε is a factor depending on the structure of the rbcs
v is the mean velocity of the rbcs
a is the radius of an average spherical scatterer

Accounting for multiple scattering:

For high perfusion states homodyne scattering processes increase and the detected photons are predominantly Doppler shifted. In this case a different autocorrelation function applies,

$$g^{(2)}(\tau) = 1 + \beta(\exp(2m[I_1(\tau)-1]) - \exp(-2m))$$

where m is the average number of collisions of photons with moving rbcs before emerging from the tissue (proportional to the blood volume).
When $m < 1$, the average number of collisions between photons and moving rbcs is less than one, ie. the majority of photons are not Doppler shifted. In this low perfusion heterodyne state the amplitude of the autocorrelation function decreases approximately linearly with decreasing m. However when multiple scattering events occur the amplitude of the autocorrelation function decreases at a rate proportional to $(m)^{1/4}$.

Spectral analysis of the photocurrent signal produces a power spectrum,

$$S(\varpi) = \langle i\rangle^2\delta(\varpi) + \frac{e\langle i\rangle}{\pi} + \langle i\rangle^2 P(\varpi)$$

The Doppler information is contained in the spectrum $P(\varpi)$. The relationship between $P(\varpi)$ and the autocorrelation function is given by,

$$P(\varpi) = \frac{1}{\pi}\int_0^\infty \cos \varpi t \; [g^{(2)}(\tau) - 1]\; dt$$

It was observed that there is a general analytical relationship between m, rbc size and speeds and the width of the spectrum. The first moment of the Doppler power spectrum was defined as,

$$\int_{-\infty}^{\infty} \varpi P(\varpi)\; d\varpi = \langle\varpi\rangle \int_{-\infty}^{\infty} P(\varpi)\; d\varpi$$

and it was demonstrated that the expression for $\langle\varpi\rangle$ could be rewritten as,

$$\langle\varpi\rangle = \frac{\langle v^2\rangle^{1/4}}{(12\varepsilon)^{1/4}a}\beta f(m)$$

where f(m) is a function depending only on m.
Using this equation it can be seen that for low perfusion the first moment of the spectrum varies directly with relative blood flow (ie. the product of rbc concentration (proportional to m) and the rms rbc speed). For higher states of perfusion the first moment of the spectrum is still sensitive to changes in flow. It varies linearly with $\langle v^2\rangle^{1/4}$ but as the square root of m.

APPENDIX 3

Cramer's Rule

Cramer's rule allows the solution of a system of n linear equations in n unknowns to be evaluated in terms of determinants.

Consider a system of m linear equations in the n variables $x_1, x_2, \ldots\ldots, x_n$ has the general form,

$$
\begin{aligned}
&a_{11}x_1 + a_{12}x_2 + \ldots\ldots\ldots\ldots\ldots\ldots\ldots\ldots\ldots\ldots + a_{1n}x_n = k_1\\
&a_{21}x_1 + a_{22}x_2 + \ldots\ldots\ldots\ldots\ldots\ldots\ldots\ldots\ldots\ldots + a_{2n}x_n = k_2\\
&\ldots\ldots\ldots\ldots\ldots\ldots\ldots\ldots\ldots\ldots\ldots\ldots\ldots\ldots\ldots\ldots\ldots\ldots\\
&\ldots\ldots\ldots\ldots\ldots\ldots\ldots\ldots\ldots\ldots\ldots\ldots\ldots\ldots\ldots\ldots\ldots\ldots\\
&a_{m1}x_1 + a_{m2}x_2 + \ldots\ldots\ldots\ldots\ldots\ldots\ldots\ldots\ldots\ldots + a_{mn}x_n = k_m
\end{aligned}
$$

Define the matrices,

$$
\mathbf{A} = \begin{vmatrix} a_{11} & a_{12} & \ldots\ldots\ldots & a_{1n} \\ a_{21} & a_{22} & \ldots\ldots\ldots & a_{2n} \\ . & . & \ldots\ldots\ldots & . \\ . & . & \ldots\ldots\ldots & . \\ a_{m1} & a_{m2} & \ldots\ldots\ldots & a_{mn} \end{vmatrix} \quad \mathbf{X} = \begin{vmatrix} x_1 \\ x_2 \\ . \\ . \\ x_m \end{vmatrix} \quad \mathbf{K} = \begin{vmatrix} k_1 \\ k_2 \\ . \\ . \\ k_m \end{vmatrix}
$$

Now the system can be written as,

$$\mathbf{AX} = \mathbf{K}$$

This can be rearranged to give,

$$\mathbf{X} = \mathbf{A}^{-1}\mathbf{K}$$

x_i, the $_i$th element of the solution vector X is given by,

$$x_i = \frac{1}{|A|}(k_1A_{1i} + k_2A_{2i} + \ldots\ldots\ldots + k_mA_{mi})$$

for $_i = 1, 2, \ldots\ldots, n$ where A_{ij} is the cofactor of A corresponding to the element a_{ij}.

It can be shown using Laplace's expansion theorem that the numerator is the expansion of $|A_i|$ where A_i denotes the matrix derived from **A** by replacing the $_i$th column of **A** by the column vector **K**.

Then,

$$x_i = \frac{|A_i|}{|A|} \qquad \text{for } i = 1, 2, \ldots, n$$

which expresses the elements of the solution vector X in terms of determinants.
The rule is demonstrated using an example.
Solve equations,

$$\begin{aligned} 3x + 2y - z &= -1 \\ x - 2y + 2z &= 7 \\ 2x + y + z &= 3 \end{aligned}$$

$$\delta = \begin{vmatrix} 3 & 2 & -1 \\ 1 & -2 & 2 \\ 2 & 1 & 1 \end{vmatrix} = -11$$

$$\delta 1 = \begin{vmatrix} -1 & 2 & -1 \\ 7 & -2 & 2 \\ 3 & 1 & 1 \end{vmatrix} = -11$$

$$\delta 2 = \begin{vmatrix} 3 & -1 & -1 \\ 1 & 7 & 2 \\ 2 & 3 & 1 \end{vmatrix} = +11$$

$$\delta 3 = \begin{vmatrix} 3 & 2 & -1 \\ 1 & -2 & 7 \\ 2 & 1 & 3 \end{vmatrix} = -22$$

$$x = \frac{\delta 1}{\delta} = 1, \quad y = \frac{\delta 2}{\delta} = -1, \quad z = \frac{\delta 3}{\delta} = 2$$

APPENDIX 4

Circuit Diagrams

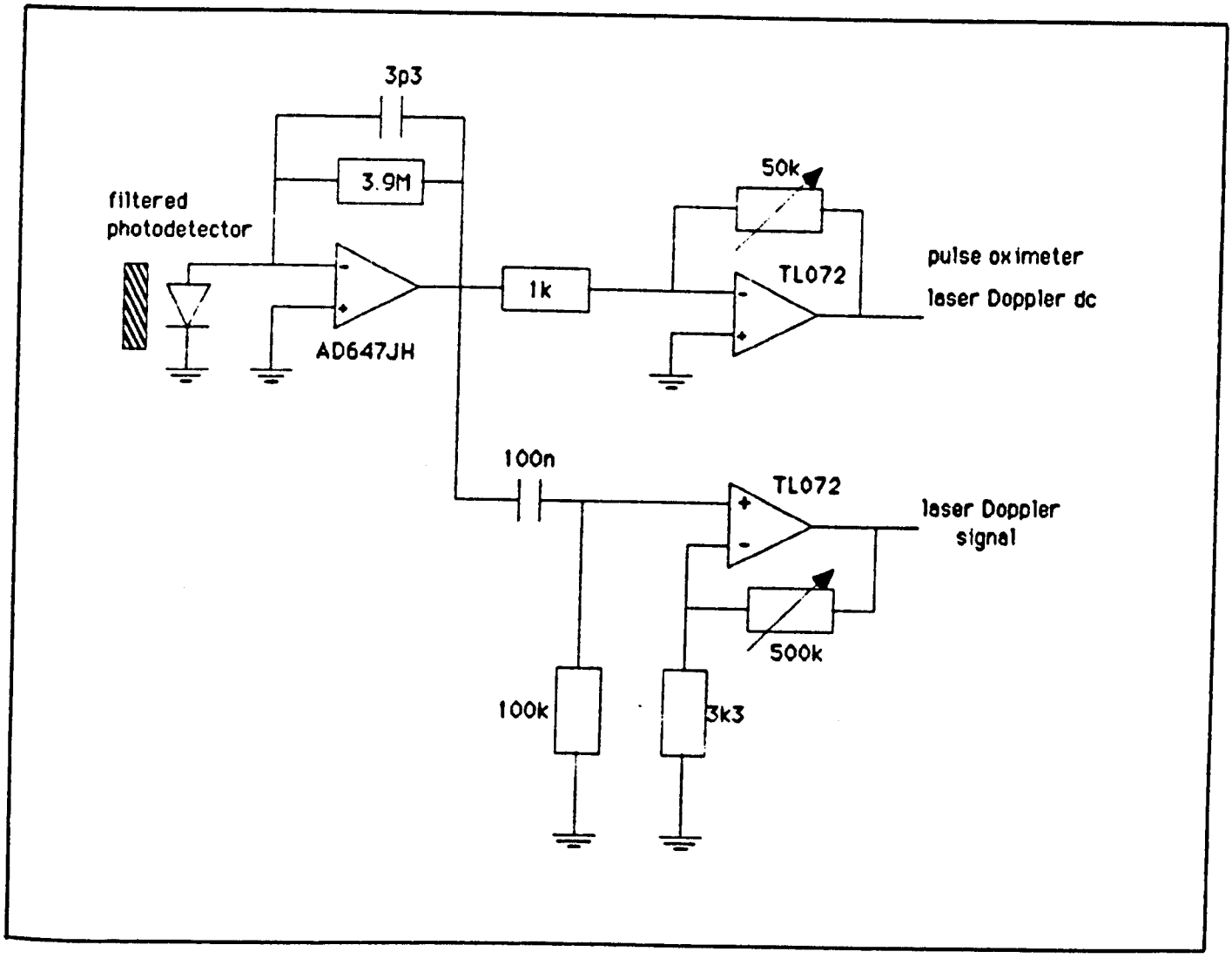

Circuit diagram of the front-end combined oximeter/ flowmeter.

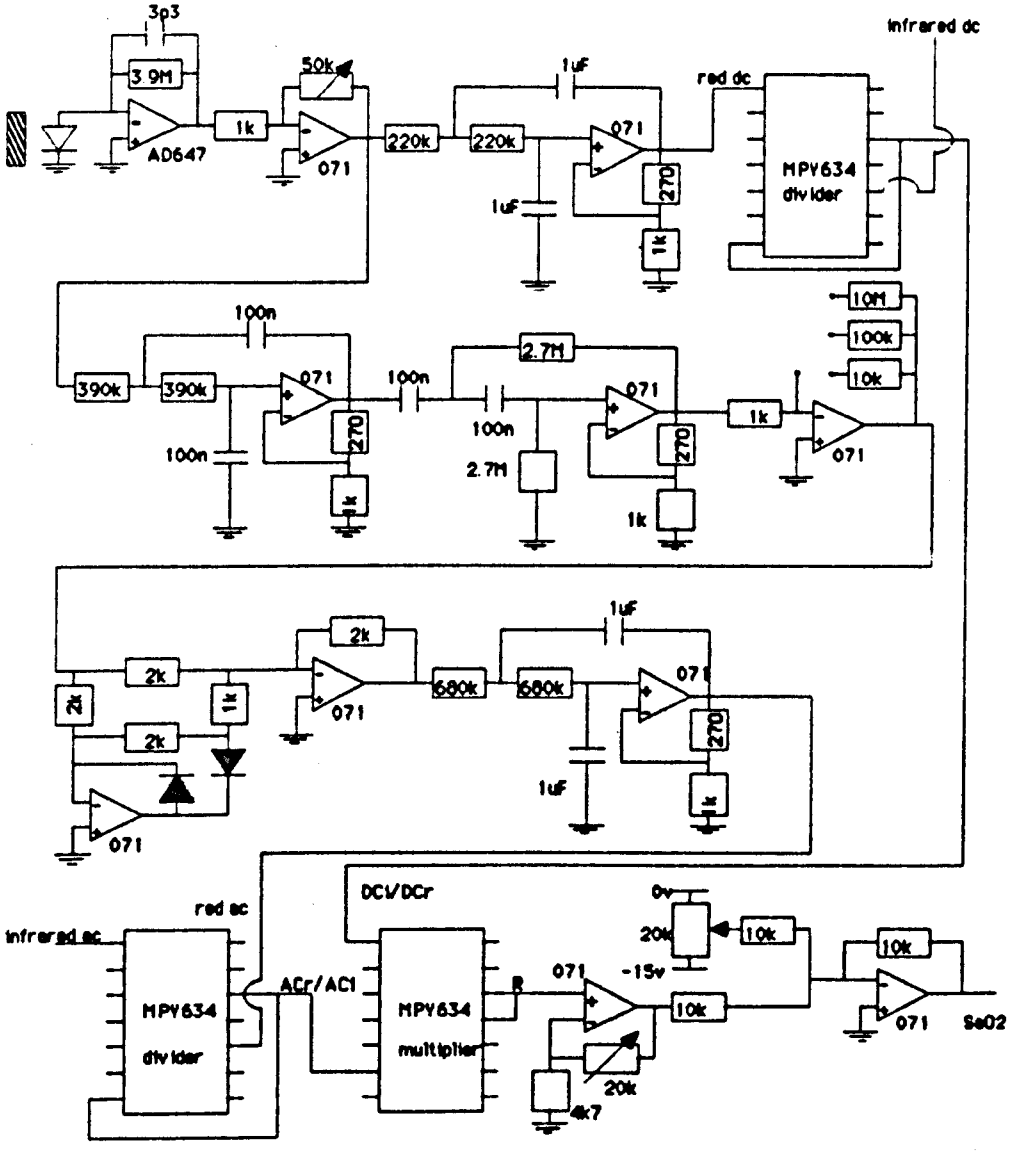

Oximeter circuit diagram.

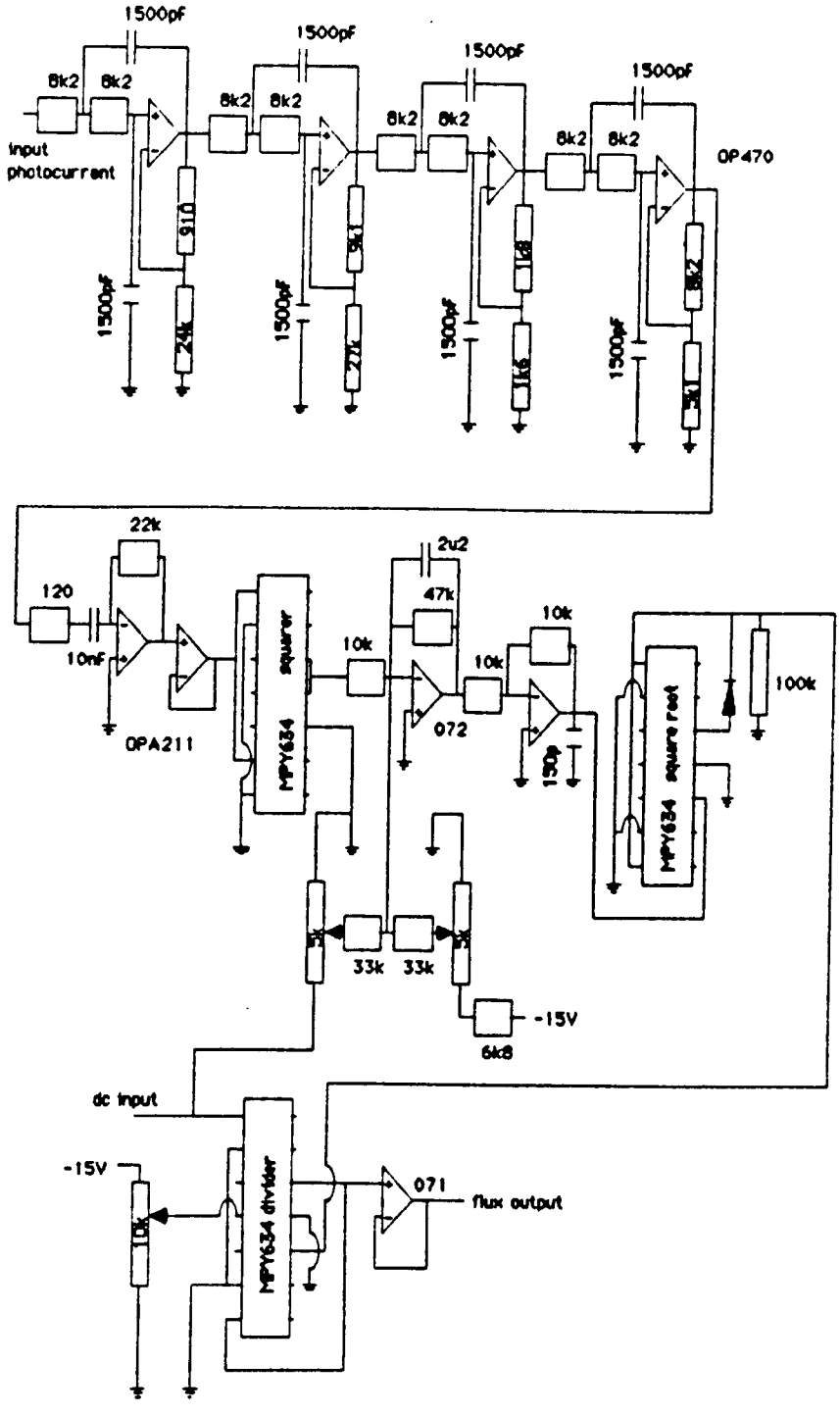

Laser Doppler circuit diagram (based on the Stern algorithm).

APPENDIX 5

Laser Safety

The Health and Safety at Work Act, 1974 places various duties on employers, designers and installers to secure the health and safety of persons at work and others who may be affected by the work.
In 1984 British Standard BS4803 was introduced classifying laser products into one of five classes depending on the level of laser radiation to which access is possible.

Class 1 laser products

These lasers are safe under all viewing conditions. Either the output beam is of very low power (eg. HeNe laser with output < 6.7 μW) or the laser is totally enclosed.

Class 2 laser products

These are low power devices emitting radiation in the visible region. The maximum output power is limited to 1 mW. Safety is improved due to the eye's aversion response (blink reflex) which limits the exposure to the eye to less than 0.25 seconds.

Class 3a laser products

The output radiation is restricted to the visible region of the spectrum. The output power is restricted to 5 mW and a maximum irradiance of 25 Wm^{-2}.

Class 3b laser products

These lasers emit radiation at any wavelength within the electromagnetic spectrum and are hazardous when the beam is directly viewed. Lasers in this class are restricted to a

maximum output power of 0.5 W for CW lasers or up to 10^5 Jm^{-2} for short pulsed lasers.

Class 4 laser products

These include any lasers exceeding the power output from the class 3b lasers. These are hazardous to the eye or skin either by direct exposure or reflection and should be used with extreme caution.

REFERENCES

Ahn H, Lindhagen J, Nilsson GE, Salerud EG, Jodal M and Lundgren O (1985) Evaluation of laser Doppler flowmetry in the assessment of intestinal blood flow in cat. *Gastroenterology*, V.88, p.951-957.

Ahn H, Johansson K, Lundgren O, and Nilsson GE, (1987) In vivo evaluation of signal processors for laser Doppler tissue flowmeters. *Medical & Biological Engineering & Computing*, V.25, p.207-211.

Ahn H, Ivarsson LE, Johansson K, Lindhagen J and Lundgren O (1988) Assessment of gastric blood flow with laser Doppler flowmetry. *Scandanavian J. Gastroenterol.*, V.23, p.1203 -1210.

Almond NE, Jones DP and Cooke ED (1988) High quality photoplethysmograph signals from a laser Doppler flowmeter: preliminary studies of two simultaneous outputs from the finger. *J. Biomedical Engineering*, V.10, October, p.458-462.

Anderson NM and Sekelj P (1967) Light absorbing and scattering properties of non-haemolised blood. *Physics in Medicine and Biology*, Vol.12, p.173-182.

Anderson RR, Hu J and Parrish JA (1981) Optical radiation transfer in the human skin and applications in in vivo remittance spectroscopy, Proceedings of the Symposium on Bioengineering and the Skin, Cardiff, Wales, July 19-21, 1979. Eds. Marks R and Payne PA, MTP Press Ltd., London. Ch.28, p.253-274.

Anderson RR, and Parrish JA (1981) The optics of human skin. *Journal of Investigative Dermatology*, V.77, p.13-19.

Arbit E, DiResta GR, Bedford RF, Shah NK and Galicich JH (1989) Intraoperative measurement of cerebral and tumor blood flow with laser Doppler flowmetry. *Neurosurgery*, V.24, p.166-170.

Asano M and Branemark PI (1970) Cardiovascular and microvascular responses to smoking in man. *Adv. Microcirc.*, V.3, p.125-158.

Asari M and Kenmotsu O (1976) Application of a pulse-type earpiece oximeter in the field of anesthesiology. *Jpn. J. Anesthesiology*, V.26, p.205-207.

Bader DL and Gant CA (1988) Changes in transcutaneous oxygen tension as a result of prolonged pressures at the sacrum. *Clin. Phys. Physiol. Meas.*, V.9, N.1

Barker SJ, Tremper KK and Gamel DM (1986) A clinical comparison of transcutaneous pO2 and pulse oximetry in the operating room. *Anesth. Analg.*, V.65, p.805-8.

Barker SJ, Tremper KK and Hyatt J (1989) Effects of methemoglobinemia on pulse oximetry and mixed venous oximetry. *Anesthesiology*, V.70, p.112-117.

Barnett NJ, Dougherty G and Pettinger SJ (1990) Comparative study of two laser Doppler flowmeters. *J. Medical Engineering and Technology*, V.14, No.6, Nov-Dec., p.243-249.

Belcaro G, Vasdekis S, Rulo A, Nicolaides AN (1989) Evaluation of skin blood flow and venoarterial response in patients with diabetes and peripheral vascular disease by laser Doppler flowmetry. *Angiology*, November, p.953-957.

Bisgaard H, Kristensen JK, Sondergaard J (1986) A new technique for ranking vascular corticosteroid effects in humans using laser Doppler velocimetry. *J. Invest. Dermatol.*, V.86, p.275 -278.

Boggett D, Obeid A, Blond J and Rolfe P (1986) Calibration of a laser Doppler skin blood flow meter using a He-Ne laser and a laser diode. *IEEE Proc. Eng. Med. & Biol. Soc.*, V.1, p.224 -227.

Bollinger A., Butti P., Barras J.P., Trachsler H., and Siegenthaler W. (1974) Red blood cell velocity in nailfold capillaries of man measured by a television microscopy technique. *Microvascular Research*, V.7, p.61-72.

Bonner R and Nossal R (1981) Model for laser Doppler measurements of blood flow in tissue. *Applied Optics*, V.20 No.12 p.2097 -2107

Bonner RF, Clem TR, Bowen PD and Bowman RL (1981) Laser Doppler continuous real-time monitor of pulsatile and mean blood flow in tissue microcirculation. In Scattering Techniques Applied to Supramolecular and Non-equilibrium systems. Ed. S Chen, B Chu and R Nossal. NATO Advanced study institutes series, Series B physics, Plenum Press, New York, p.685-701.

Brahams D (1989) Anaesthesia and the law. *Anaesthesia*, V.44, p.606-7.

Brinkman R and Zijlstra WG (1949) Determination and continuous registration of the percentage oxygen saturation in small amounts of blood. *Arch. Chir. Neerl.*, V.1, p.177-183.

Britton NF, Barker JR and Ring EFJ (1984) A mathematical model for a thermal clearance probe. *IMA J. Maths Appl. Med. Biol.*, V.1, p.95.

Bucher HA, Fanconi S, Baeckert P and Duc G (1989) Hyperoxemia in newborn infants : Detection by pulse oximetry. *Pediatrics*, V.84, No.2, August, p.226-230.

Carrier EB and Rehberg PB (1923) Capillary and venous pressure in man. *Scand. Arch. Physiol.*, V.44, p.20.

Castronuovo JJ, Pabst TS, Flanigan DP, Foster LG (1987) Noninvasive determination of skin perfusion pressure using a laser Doppler. *J. Cardiovasc. Surg.*, V.28, p.253-7.

Challoner AVS (1979) Photoelectric plethysmography for estimating cutaneous blood flow. In Non-Invasive Physiological Measurements. Ed. P Rolfe (London: Academic) Ch.6.

Chapman KR, Liu FLW, Watson RM, Rebuck AS (1986) Range of accuracy of two-wavelength oximetry. *Chest*, V.89, p.540 -542.

Christoforidis EC, Hovendal C, Bjerring P and Kruse A (1989) Continuous measurement of gastric blood flow by laser Doppler flowmetry during gastroscopy. *Scand. J. Gastroenterol.*, V.24, p.16-20.

Chu B (1974) Laser light scattering. Quantum electronics: principle and application. Academic Press p.273.

Clark LC (1956) Monitor and control of blood and tissue oxygen tension. *Trans. Am. Soc. Art. Int. Org.*, V.2, p.41-8.

Cochrane T, Sheriff SB, Boulton AJM, Ward JD and Atkins RM (1986) Laser Doppler flowmetry: in the assessment of peripheral vascular disorders? A preliminary evaluation. *Clin. Phys. Physiol. Meas.*, V.7, No.1, p.31-42.

Cohen A and Wadsworth N (1972) A light emitting diode skin reflectance oximeter. *Med. & Biol. Engng.*, V.10 p.385-391.

Comroe JH and Bothelho S (1947) The unreliability of cyanosis in the recognition of arterial anoxemia. *Am. J. Med. Sci.*, V.214, p.1-6.

Cope M, Delpy DT (1988) System for long term measurements of cerebral blood and tissue oxygenation on newborn infants by near infrared transillumination. *Med. Biol. Eng. Comput.*, V.26, p.289-94.

Cummins HZ, Knable N and Yeh Y (1964) Observation of diffusion broadening of Rayleigh scattered light. *Phys. Rev. Lett.*, V.12, p.150-153.

Cummins HZ (1974) Light beating spectroscopy. In Photon Correlation and Light Beating Spectroscopy. Ed. HZ Cummins and ER Pike (Plenum Press: New York) p.225-236.

Daly CH, Chimoskey JE, Holloway GA, Kennedy D (1976) The effect of pressure loading on the blood flow rate in human skin. In Bedsore Biomechanics Eds. Kenedi RM, Cowden JM and Scales JT. London: Macmillan Press p.69-77.

Damber JE, Lindahl O, Selstam G and Tenland T (1982) Testicular blood flow measured with a laser Doppler flowmeter: acute effects of catecholamines. *Acta Physiol. Scand.*, V.115, p.209-215.

DeBakey ME, Burch G, Ray T and Ochsner A (1947) The "borrowing -lending" hemodynamic phenomenon (hemometakinesia) and its theraputic application in peripheral vascular disturbances. *Ann. Surg.*, V.126, p.850-65.

Decker MJ, Conrad KP and Strohl KP (1989) Noninvasive oximetry in the rat. *Biomed. Instrum. Technol.*, V.23, No.3, p.222 -228.

Delpy DT, Cope M, van der Zee P, Arridge S, Wray S and Wyatt J (1989) Estimation of optical pathlength through tissue from direct time of flight measurement. *Phys. Med. Biol.*

de Mul FFM, van Spijker J, van der Plas D, Greve J, Aarnoudse JG and Smits TM (1984) Mini laser Doppler blood flow monitor with diode laser source and detection integrated in the probe. *Applied Optics*, V.23, No.17, p.2970-2973.

de Trafford J and Lafferty K (1984) What does photoplethysmography measure? *Med. Biol. Eng. Comput.*, V.22, p.479-80.

Dimitroff JM, Jacquez JA and Kuppenheim HF (1955) Spectral reflectance of the skin of rats and rabbits in the region 420-1000 nm. *J. Applied Physiology*, V.8, p.292-296.

Dirnagl U, Kaplan B, Jacewicz M and Pulsinelli W (1989) Continuous measurement o cerebral cortical blood flow by laser Doppler flowmetry in a rat stroke model. *J. Cerebral Blood Flow and Metabolism.*, V.9, p.589-596.

Donahoe TM (1984) Development of an instrument for measuring blood oxygenation and blood flow. Ph.D. thesis, Carnegie-Mellon University, Pittsburgh, Pennsylvania. May 1984.

Dorlas JC and Kuipers AHM (1987) Pulse oximetry - principle and first experiences during anesthesia. *Acta Anaesthesiologica Belgica.*, V.38, No.2, p.133-138.

Douglas NJ, Brash HM, Wraith PK, Calverley PMA, Leggett RJE, McElderry L and Flenley DC (1979) Accuracy sensitivity to carboxyhaemoglobin and speed of response of the Hewlett -Packard 47201A ear oximeter. *Am. Rev. Resp. Disease.*, V.119, p.311-313.

Dowd GSE (1982) Assessment of the skin viability with special reference to transcutaneous oxygen monitoring. MD Thesis, Liverpool.

Dowd GSE, Linge K and Bentley G (1983) Measurements of transcutaneous oxygen pressure in normal and ischaemic skin. *J. Joint Bone Surg.*, V.65B, p.79-83.

Duteil L, Bernengo JC and Schalla W (1985) A double wavelength laser Doppler system to investigate skin microcirculation. *IEEE Trans. Biomed. Eng.*, V.BME-32, No.6, p.439-447.

Eikhoff JH and Jacobson E (1980) Correlation of transcutaneous oxygen to blood flow in heated skin. *Scand. J. Clin. Invest.*, V.40, p.761-65.

Einav S, Berman HJ, Fuhro RL, DiGiovanni PR, Fridman JD and Fine S (1975a) Measurement of blood flow in vivo by laser Doppler anemometry through a microscope. *Biorheology*, V.12, p.203-205.

Einav S, Berman HJ, Fuhro RL, DiGiovanni PR, Fine S and Fridman JD (1975b) Measurement of velocity profiles of red blood cells in the microcirculation by laser Doppler anemometry (LDA). *Biorheology*, V.12, p.207-210.

Elling A and Hanning CD (1986) Oxygenation during preoperative transportation. In Pulse Oximetry, Eds. Payne JP and Severinghaus JW, Dorchester, Springer-Verlag, p.161-164.

Ellis CG, Ellsworth ML and Pittman RN (1990) Determination of red blood cell oxygenation in vivo by dual video densitometric image analysis. *Am. J. Physiol.* V.258, p.H1216-H1223.

Ellsworth ML, Pittman RN and Ellis CG (1987) Measurement of haemoglobin oxygen saturation in capillaries. *Am. J. Physiol.* V. 252 (Heart Circ. Physiol. 21): p.H1031-H1040.

Ellsworth ML, Popel AS, Pittman RN (1988) Assessment and impact of heterogeneities of convective oxygen transport parameters in capillaries of striated muscle: Experimental and theoretical . *Microvascular Research* V.35, p.341-362.

Engel RR, Delpy DT, Parker D (1979) The effect of topical potassium cyanide on transcutaneous gas measurements. In Continuous Transcutaneous Blood Gas Monitoring. Eds. Huch et al. New York, AR Liss, Ch.15, p.117-21.

Enkema L, Holloway GA, Piraino DW, Harry D, Zick GL and Kenny MA (1981) Laser Doppler velocimetry vs heater power as indicators of skin perfusion during transcutaneous O2 monitoring. *Clin. Chem.* V.27, No.3, p.391-396.

Fagrell B, Fronek A and Intaglietta M (1977) A microscope -television system for studying flow velocity in human skin capillaries. *Am. J. Physiol.*, V.233(2), p.H318-H321.

Fagrell B and Ostergren J (1987) Capillary flow measurement in human skin. In Clinical Investigation of the Microcirculation. Eds. JE Tooke and LH Smaje (Boston: Martinus Nijhoff) p.23-34.

Fairley HB (1989) Changing perspectives in monitoring oxygenation. *Anaesthesiology*, V.70, p.2-4.

Fairs S.L.E. (1988) Observations of a laser Doppler flowmeter output made using a calibration standard. *Medical & Biological Engineering & Computing*, V.26, p.404-406.

Fasano VA, Urciuoli R, Bolognese P and Mostert M (1988) Intraoperative use of laser Doppler in the study of cerebral microvascular circulation. *Acta Neurochir.*, V.95, p.40-48.

Feke GT and Riva CE (1978) Laser Doppler measurements of blood velocity in human retinal vessels. *J. Opt. Soc. Am.*, V.68, No.4, p.526-531.

Feld AD, Fondacaro JD, Holloway GA, Jacobson ED (1982) Measurement of mucosal blood flow in the canine intestine with laser Doppler spectroscopy. *Life Sci.*, V.31, p.1509 -1517.

Fischer JC, Parker PM, Shaw WW (1983) Comparison of two laser Doppler flowmeters for the monitoring of dermal blood flow. *Microsurgery*, V.4, p.164-170.

Flynn MD, Williams SA and Tooke JE (1989) Clinical television microscopy. *J. Med. Eng. & Tech.*, V.13, No.6, p.278-284.

Forrester DW, Spence VA, Bell I, Hutchinson F and Walker WF (1980) The preparation and stability of radiodinated antipyrine for use in local blood flow determination. *Eur. J. Nucl. Med.*, V.5, p.145.

Frew HS and Giblin RA (1985) The choice of ultrasound frequency for skin blood flow measurement. *Bioengin. Skin*, V.1, p.193.

Fujii H, Asakura T, Nohira K, Shintomi Y and Ohura T (1985) Blood flow observed by time-varying laser speckle. *Optics Letters*. V.10, No.3, p.104-106.

Galdun JP, Paris PM and Stewart RD (1989) Pulse oximetry in the emergency department. *Am. J. Emerg. Med.*, V.7, No.4, p.422-425.

Gebuhr P, Jorgensen JP, Vollmer-Larsen B,Nielsen SL and Alsbjorn B (1989) Estimation of amputation level with a laser Doppler flowmeter. *J. Bone & Joint Surg.*, V.71, p.514-517.

Gillespie JS and Muir TC (1967) A method of stimulating the complete sympathetic outflow from the spinal cord to blood vessels in the pithed rat. *Br. J. Pharmac. Chemother.*, V.30, p.78-87.

Gillespie JS, Maclaren A and Pollock D (1970) A method of stimulating different segments of the autonomic outflow from the spinal column to various organs in the pithed cat and rat. *Br. J. Pharmac.*, V.40, p.257-267.

Giltvedt J, Sira A and Helme P (1984) Pulsed multifrequency photoplethysmography. *Med & Biol. Eng. & Comput.*, V.22, p.212-215.

Goldie EAG (1942) Device for continuous indication of oxygen saturation of circulating blood in man. *J. Sci. Instrum.*, V.19, p.23.

Graham B, Paulus DA and Caffee HH (1986) Pulse oximetry for vascular monitoring in upper extremity replantation surgery. *J. Hand. Surg.*, V.11A, p.687-692.

Gratti JE, LaRossa DD, Silverman DG and Hartford CE (1983) Evaluation of the burn wound with perfusion fluorometry. *J. Trauma*, V.23, No.3, p.202.

Gush RJ, King TA and Jayson MIV (1984) Aspects of laser light scattering from skin tissue with application to laser Doppler blood flow measurement. *Phys. Med. Biol.*, V.29, No.12, p.1463-1476.

Gush RJ and King TA (1987) Investigation and improved performance of optical fibre probes in laser Doppler blood flow measurement. *Med. Biol. Eng. Comput.*, V.25, p.391 -396.

Haberl R.L., Heizer M.L., and Ellis E.F. (1989) Laser-Doppler assessment of brain microcirculation: effect of local alterations. *American Journal of Physiology.*, V.256, (Heart Circ. Physiology 25) p.H1255-H1260.

Hamilton DV, Palmer GR and Sattelle DB (1982) Laser light scattering of peripheral blood flow in renal patients with arterio-venous fistulae. In Biomedical Applications of Laser Light Scattering. Ed. DB Sattelle, WI Lee and BR Ware. Elsevier Biomedical Press, p.349-354.

Hariri RJ, Flamengo SA, Ghajar JBG, Cohen DS, Shepard SR, McKeever M and Tan KS (1990) Cerebral cortical oxygenation assessed by reflectance infrared pulse oximetry in Yucatan minipigs. *Anesth. Analg.*, V.70, p.S145.

Hardy JD, Hammell HT and Murgatroyd D (1956) Spectral transmittance and reflectance of excised human skin. *J. Appl. Physiol.*, V.9, p.257-264.

Hay WW, Brockway J, Eyzaguirre M (1987) Application of the Ohmeda Biox 3700 pulse oximeter to neonatal oxygen monitoring. *Adv. Exp. Med. Biol.*, V.220, p.151-158.

Hay WM, Brockway JM and Eyzaguirre M (1989) Neonatal pulse oximetry: Accuracy and reliability. *Pediatrics*, V.83, No.5, May, p.717-722.

Henderson HD and Hackett MEJ (1978) The value of thermography in peripheral vascular disease. *Angiology*, V.29, p.65.

Hertzman AB and Speakman CR (1937) Observation on the finger volume pulse recorded photoelectrically. *Am. J. Physiol.*, V.119, p.334-5.

Hirkaler G.M. and Rosenberger L.B. (1989) Simultaneous two-probe laser Doppler velocimetric assessment of topically applied drugs in rats. *J. Pharmacological Methods*, V.21, p.123-127.

Holloway GA and Watkins DW (1977) Laser Doppler measurement of cutaneous blood flow. *J. Invest.Dermatol.*, V.69, No.3, p.306-309.

Holloway GA (1980) Cutaneous blood flow responses to injection trauma measured by laser Doppler velocimetry. *J. Invest. Dermatol.*, V.74, No.1, p.1-4.

Holloway GA (1983) Laser Doppler measurement of cutaneous blood flow. In Non-Invasive Measurements:2, (Academic:London) Ch.6, p.219-249.

Holstein P and Lassen NA (1977) Selection of amputation level. In Vascular Surgery. Ed. Rutherford RB. Pub. WB Saunders, Philadelphia.

Holstein P, Nielsen PE, Barras JP (1979) Blood flow cessation at external pressure in the skin of normal human limbs. *Microvasc. Res.*, V.17, p.71-9.

Holti G and Mitchell KW (1978) Estimation of the nutrient skin blood flow using a segmental thermal clearance probe. *Clin. Exp. Dermatol.*, V.3, p.189-198.

Huch R, Huch A, Lubbers DW (1973) Transcutaneous measurement of blood pO2 (tcpO2): method and application in perinatal medicine. *Perinatal Med.*, V.1, p.173-91.

Hull SM, Goodfield M, Wood EJ, Cunliffe WJ (1989) Active and inactive edges of psoriatic plaques: Identification by tracing and investigation by laser Doppler flowmetry and immunocytochemical techniques. *J. Invest. Dermatol.*, V.92, p.782-785.

Imbriani M, Melotti A and Ghittori S (1987) Methemoglobin and carboxyhemoglobin levels in smokers and non smokers. *G. Ital. Med. Lav.*, V.9, p.11-14.

Intaglietta M, Pawula RF and Tompkins WR (1970) Pressure measurements in the mammalian microvasculature. *Microvasc. Res.*, V.2, p.212-220.

Jakeman E (1974) In Photon Correlation and Light Beating Spectroscopy. Ed. HZ Cummins and ER Pike (Plenum Press: New York)

Jacquez JA and Kuppenheim HF (1954) Spectral reflectance of human skin in the region 235-1000 nm. *J. Appl. Physiol.*, V.7, p.523-28.

Jobsis-VanderVliet FF (1977) Non invasive infrared monitoring of cerebral and myocardial oxygen sufficiency and circulatory parameters. *Science*, V.198, p.1264-7.

Johansson K, Ahn H, Kjellstrom CH and Lindhagen J (1989) Laser Doppler flowmetry in experimental mesenteric vascular occlusion. *Int. J. Microcirc: Clin. Exp.*, V.8, p.183-190.

Kagle DM, Alexander CM, Berko RS, Giuffre M and Gross JB (1987) Evaluation of the Ohmeda 3700 pulse oximeter: Steady-state and transient response characteristics. *Anesthesiology*, V.66, p.376-380.

Karanfilian R.G., Lynch T.G., Lee B.C., Long J.B., and Hobson R.W. (1984) The assessment of skin blood flow in peripheral vascular disease by laser Doppler velocimetry. *The American Surgeon*, December 1984, V.50, p.641-644.

Keifer JC, Russell GB, Snider MT (1989) Pulse oximetry inaccuracy with sickle hemoglobin. Is it due to different absorption spectra? *Anesthesiology*, V.71, No.3a, p.A370.

Kelleher JF (1989) Pulse oximetry. *J. Clin. Monitor*, V.3, No.1, January, p.37-62.

Kim JM, Arakawa K, Benson KT and Fox DK (1986) Pulse oximetry and circulatory kinetics associated with pulse volume amplitude measured by photoelectric plethysmography. *Anesth. Analg.*, V.65, p.1333-9.

Kolari PJ (1985) Penetration of unfocused laser light into the skin. *Archives of Dermatological Research*, V.277, p.342-344.

Knopp JA and Longmuir IS (1972) Intracellular measurement of oxygen by quenching of fluorescence of pyrene butyric acid. *Biochim. Biophys. Acta.*, V.279, p.393-397.

Kramer K (1935) Ein verfahren zur fortlaufenden messung des sauerstoffgehaltes im stromenden blute an uneroffneten gefassen. *Z. Biol.*, V.96, p.61-75.

Kramer K, Elam JO, Saxton GA and Elam WN (1951) Influence of oxygen saturation, erythrocyte concentration and optical depth upon the red and near-infrared light transmittance of whole blood. *Am. J. Physiol.*, V.165, p.229-246.

Kristensen JK, Engelhart M and Nielsen T (1983) Laser Doppler measurement of digital blood flow regulation in normals and in patients with Raynaud's phenomenon. *Acta Dermatovener*, V.63, p.43-47.

Kvernebo K, Slasgsvold CE, Stranden E, Kroese A and Larsen S (1988) Laser Doppler flowmetry in evaluation of lower limb resting skin circulation. A study in healthy controls and arterosclerotic patients. *Scand. J. Clin. Lab. Invest.*, V.48, p.621-626.

Kvernebo K, Slasgsvold CE and Stranden E (1989) Laser Doppler flowmetry in evaluation of skin post-ischaemic reactive hyperaemia. *J. Cardiovasc. Surg.*, V.30, p.70-75.

Kvietys PR, Shepherd AP, Granger DN (1985) Laser Doppler, H_2 clearance, and microsphere estimates of mucosal blood flow. *Am. J. Physiol.*, V.249, p.G221-G227.

Lange K and Boyd LJ (1942) The use of fluorescein to determine the adequacy of the circulation. *Med. Clin. North Am.*, V.26, p.943.

Lawson D, Norley I, Korbon G, Loeb R and Ellis J (1987) Blood flow limits and pulse oximeter signal detection. *Anesthesiology*, V.67, p.599-603.

Leonardo G, Arpaia MR and Guercio RD (1986) Evaluation of the effects of vasoactive drugs on cutaneous microcirculation by laser Doppler velocimetry. *Angiology*, January, V.37, p.12-20.

Li Kam Wa TC, Almond NE, Cooke ED and Turner P (1989) Effect of captopril on skin blood flow following intradermal bradykinin measured by laser Doppler flowmetry. *Eur. J. Clin. Pharmacol.*, V.37, p.471-475.

Linge K, Roberts DH and Dowd GSE (1987) Indirect measurement of skin blood flow and transcutaneous oxygen tension in patients with peripheral vascular disease. *Clin. Phys. Physiol. Meas.*, V.8, No.4, p.293-302.

Lipowsky HH and Zweifach BW (1977) Methods for the simultaneous measurement of pressure differentials and flow in single unbranched vessels of the microcirculation for rheological studies. *Microvasc. Res.*, V.14, p.345-361.

Lipowsky HH, Usami S and Chien S (1980) In vivo measurements of "apparent viscosity" and microvessel hematocrit in the mesentery of the cat. *Microvasc. Res.*, V.19, p.297-319.

Love TJ (1980) Thermography as an indicator of blood perfusion. *Ann. N. Y. Acad. Sci.*, V.335, p.429-37.

Lunde OC, Kvernebo K and Larsen S (1988) Evaluation of endoscopic laser Doppler flowmetry for measurement of human gastric blood flow. *Scand. J. Gastroenterol.* V.23, p.1072-1078.

Manson JRT, Abd-Alrazzai MM, Ausobsky J, Matthews PA and Kester RC (1985) The use of microwave emission thermography in peripheral vascular disease-a preliminary study. In Practical Aspects of Skin Blood Flow Measurements (London: Biological Engineering Society) p.69-72.

Matthes K (1935) Untersuchungen uber die sauerstoffsattigungen des menschlichen arterienblutes. *Arch. Exp. Path. Pharmakol.*, V.179, p.698-711.

McCollum PT, Spence VA, Walker WF, Murdoch G, Swanson AJG and Turner MS (1985) Antipyrine clearance from the skin of the foot and the lower leg in critical ischaemia. In Practical Aspects of Skin Blood Flow Measurements (London: Biological Engineering Society) p.47-51.

Mendelson Y, Cheung PW, Neuman MR, Fleming DG and Cahn SD (1983) Spectrophotometric investigation of pulsatile blood flow for transcutaneous reflectance oximetry. *Oxygen Transport Tissue*, V.4, p.93-102.

Mendelson Y, Cheung PW and Neuman MR (1984) Noninvasive monitoring of arterial blood oxygen saturation. *IEEE/NSF Symposium on Biosensors*, 1984, p.40-43.

Mendelson Y and Ochs BD (1988) Noninvasive pulse oximetry utilizing skin reflectance photoplethysmography. *IEEE Trans. BME*, V.35, No.10, October, p.798-805.

Mendelson Y and Kent JC (1989) Variations in optical absorption spectra of adult and fetal hemoglobins and its effect on pulse oximetry. *IEEE Trans. Biomed. Eng.*, V.36, No.8, p.844-847.

Merrick EB and Hayes T (1976) Continuous, non-invasive measurements of arterial blood oxygen levels. *Hewlett -Packard J.*, V.28, p.2-10.

Micheels J., Alsbjorn B., and Sorensen B. (1984) Laser Doppler flowmetry. A new non-invasive measurement of microcirculation in intesive care? *Resuscitation*, V.12, p.31-39.

Millikan GA, Pappenheimer JR, Rawson AJ and Hervey JP (1941) Continuous measurement of oxygen saturation in man. *Am. J. Physiol.*, V.133, p.390.

Millikan GA (1942) The oximeter : an instrument for measuring continuously oxygen saturation of arterial blood in man. *Rev. Sci.Instrum.*, V.13, p.434-444.

Mindt W and Eberhard P (1982) Electrochemical sensors for invasive and non-invasive monitoring of blood gases. *Med. Progr. Technol.*, V.9, p.105-111.

Mishina H, Asakura T and Nagai S (1974) A laser Doppler microscope. *Optics Communications*, V.11, No.1, p.99-102.

Mishina H, Ushizaka T and Asakura T (1976) A laser Doppler microscope. Its optical and signal-analysing systems and some experimental results of flow velocity. *Optics and Laser Technology*, p.121-127.

Myers B and Donovan W (1985) An evaluation of 8 methods of using fluorescein to predict the viability of skin flaps in the pig. *Plast. Reconstr. Surg.*, V.75, p.245-50.

Nakajima S, Hirai Y, Takase H et al. (1975) Performances of new pulse wave earpiece oximeter. *Respir. Circ.*, V.23, p.41-45.

Newson TP, Obeid A, Wolton RS, Boggett D and Rolfe P (1987) Laser Doppler velocimetry: The problem of fibre movement artefact. *J. Biomed. Eng.*, V.9, April, p.169-172.

Nickerson BG, Sarkisian C,Tremper K (1988) Bias and precision of pulse oximeters. *Chest*, V.93, p.515-517.

Nicolai L (1932) Uber sichtbarmachung verlauf und chemische kinetik der oxyhemoglobinreduktion im lebenden gewebe besonders in der menschlichen haut. *Arch. Ges. Physiol.*, V.229, p.372.

Nilsson GE, Tenland T and Oberg PA (1980a) A new instrument for continuous measurement of tissue blood flow by light beating spectroscopy. *IEEE Trans. BME-27*, p.12-19.

Nilsson GE, Tenland T and Oberg PA (1980b) Evaluation of a laser Doppler flowmeter for measurement of tissue blood flow. *IEEE Trans. BME-27*, p.597-604.

Nilsson G.E. (1984) Signal processor for laser Doppler tissue flowmeters. *Medical & Biological Engineering and Computing*, V.22, p.343-348.

Obeid AN, Boggett DM, Barnett NJ, Dougherty G and Rolfe P (1988) Depth discrimination in laser Doppler measurement using different lasers. *Med & Biol. Eng. & Comput.*, V.26, p.415-419.

Obeid AN (1989) The measurement of blood flow in the microcirculation using lase Doppler flowmetry. PhD Thesis, Biomedical Instrumentation Group, School of Engineering, Oxford Polytechnic, Oxford, U.K.

Obeid A.N., Barnett N.J., Dougherty G., and Ward G. (1990) A critical review of laser Doppler flowmetry. *Journal of Medical Engineering & Technology*, (in press).

Oishi CS, Fronek A and Golbranson FL (1988) The role of non-invasive vascular studies in determining levels of amputation. *J. Bone and Joint Surg.*, V.70-A, No.10, p.1520-1530.

Opitz N and Lubbers DW (1984) Increased resolution power in pO2 analysis at lower pO2 levels via sensitivity enhanced optical pO2 sensors (pO2 optodes) using fluorescence dyes. *Adv. in Exptl. Med. Biol.*, V.180, p.261-267.

Ostergren J. and Fagrell B. (1986) Skin capillary blood cell velocity in man. Characteristics and reproducibility of the reactive hyperemia response. *International Journal of Microcirculation: Clin. Exp.*, V.5, p.37-51.

Ostergren J, Schops P and Fagrell B (1988) Evaluation of a laser Doppler multiprobe for detecting skin microcirculatory disturbances in patients with obliterative arteriosclerosis. *Internat. Angiol.*, V.7, No.1, p.37-41.

Palmer GR, Hamilton DV and Sattelle DB (1980) Changes in the peripheral microcirculation monitored by photon correlation spectroscopy. In Photon Correlation Techniques in Fluid Mechanics, Ed. WT Mayo and AE Smart. Stanford University, California, Ch.24, p.1-7.

Patel BT, Delpy DT, Hillson PJ, Parker D (1989) A topical metabolic inhibitor to improve transcutaneous estimation of arterial oxygen tension in adults. *J. Biomed. Eng.* V.11, Sept, p.381-83.

Payne PA, Faddoul RY and Jawad SM (1985) A single channel pulsed Doppler ultrasound instrument for measurement of skin blood flow. In Practical Aspects of Skin Blood Flow Measurement (London: Biological Engineering Society).

Payne JP and Severinghaus JW (1986) Pulse Oximetry. Springer -Verlag, Berlin Heidelberg.

Periflux PF3 User's Handbook, March 1988, Perimed.

Piantadosi CA, Hemstreet TM, Jobsis-VanderVliet FF (1986) Near infrared spectrophotometric monitoring of oxygen distribution to intact brain and skeletal muscle tissues. *Crit. Care Med.* V.14, p.698-706.

Piraino DW, Zick GL, and Holloway GA (1979) An instrumentation system for the simultaneous measurement of transcutaneous oxygen and skin blood flow. In Frontiers of Engineering in Health Care, IEEE Press, New York, NY, p.55-58.

Pittman RN and Duling BR (1975a) A new method for the measurement of percent oxyhaemoglobin. *J. Appl. Physiol.*, V.38(2), p.315-320.

Pittman RN and Duling BR (1975b) Measurement of percent oxyhaemoglobin in the microvasculature. *J. Appl. Physiol.*, V.38(2), p.321-327.

Pologe JA (1987) Pulse oximetry : Technical aspects of machine design. In Advances in Oxygen Monitoring, edited by Tremper KK and Barker SJ. *Int. Anesth. Clinics* V.25, No.3, p.137-153.

Rayman G, Hassan A and Tooke JE (1986) Blood flow in the skin of the foot related to posture in diabetes mellitus. *British Medical Journal.*, V.292, January, p.87-90.

Rendell M, Bergman T, O'Donnell G, Drbny E, Borgos J and Bonner RF (1989) Microvascular blood flow, volume, and velocity measured by laser Doppler techniques in IDDM. *Diabetes*, V.38, July, p.819-824.

Riva C, Ross B and Benedek GB (1972) Laser Doppler measurements of blood flow in capillary tubes and retinal arteries. *Invest. Opth.*, V.11, p.936-944.

Riva CE, Feke GT, Eberli B and Bernary V (1979) Bidirectional LDV system for absolute measurement of blood speed in retinal vessels. *Applied Optics*, V.18, No.13, p.2301-2306.

Roberts VC (1982) Photoplethysmography - fundemental aspects of the optical properties of blood in motion. *Trans. Inst. M. C.*, V.4, No.2, p.101-106.

Rosenfield K, Kelly SM, Fields CD, Pastore JO, Weinstein R, Palefski P, Langevin RE, Kosowsky BD, Razvi S and Isner JM (1989) Noninvasive assessment of peripheral vascular disease by color flow Doppler/two-dimensional ultrsound. *Am. J. Cardiol.*, V.64, p.247-251.

Rumsey WL, Vanderkooi JM and Wilson DF (1988) Imaging of phosphorescence: A novel method for measuring oxygen distribution in perfused tissue. *Science*, V.241, p.1649 -1651.

Ryan TJ (1973) Structure, pattern and shape of the blood vessels of the skin. In The Physiology and Pathophysiology of the Skin. V.2. Ed. A Jarrett (London: Academic) Ch.16.

Ryan TJ (1985) Dermal vasculature. In Methods in Skin Research. Ed. D Skerrow and CJ Skerrow. Pub. Wiley. Ch.20. p.528-558.

Salerud EG and Nilsson GE (1986) Integrating probe for tissue laser Doppler flowmeters. *Med. & Biol. Eng. & Comput.*, V.24, p.415-419.

Salerud EG and Oberg PA (1987) Single-fibre laser Doppler flowmetry: A method for deep tissue perfusion measurements. *Med & Biol. Eng. & Comput.*, V.25, p.329-334.

Sandage AR (1956) The red-shift. *Scientific American*, September, V.195, No.3, p.170-182.

Sarnquist FH, Todd C and Whitcher C (1980) Accuracy of a new non-invasive oxygen saturation monitor. *Anesthesiology*, V.53, p.S163.

Schawlow AL and Townes CH (1958) Infrared and optic lasers. *Phys. Rev.* V.112, p.1940.

Schmitt JM, Mihm FG and Meindl JD (1986) New methods for whole blood oximetry. *Annals of Biomedical Engineering*, V.14, p.35-52.

Schubert V and Fagrell B (1989) Local skin pressure and its effects on skin microcirculation as evaluated by laser Doppler fluxmetry. *Clinical Physiol.*, V.9, p.535-545.

Sejersen P (1969) Blood flow in cutaneous tissue in man, studies by washout of radioactive xenon. *Circ. Res.*, V.25, p.215-29.

Sendak MJ, Harris AP and Donham RT (1988) Accuracy of pulse oximetry during arterial oxyhaemoglobin desaturation in dogs. *Anesthesiology*, V.68, p.111-114.

Severinghaus JW and Astrup PB (1986) History of blood gas analysis. VI. Oximetry. *J. Clin. Monit.*, V.2, p.270-288.

Severinghaus JW and Naifeh KH (1987) Accuracy of response of six pulse oximeters to profound hypoxia. *Anesthesiology*, V.67, p.551-558.

Shapiro BA, Cane RD, Chomka CM et al. (1989) Preliminary evaluation of an intra-arterial blood gas system in dogs and humans. *Crit. Care Med.*, V.17, p.455.

Shepherd AP, Kiel JW and Riedel GL (1984) Evaluation of light-emitting diodes in whole blood oximetry. *IEEE Trans BME-31*, No.11, November, p.723-725.

Shepherd A.P., Riedel G.L., Kiel J.W., Haumschild D.J., and Maxwell L.C. (1987) Evaluation of an infrared laser-Doppler blood flowmeter. *American Journal of Physiology*, V.252 (Gastrointest. Liver Physiology 15): p.G832-G839.

Shimada Y, Yoshiya I, Oka N, and Hamaguri K (1984) Effects of multiple scattering and peripheral circulation on arterial oxygen saturation measured with a pulse-type oximeter. *Med. & Biol. Eng. & Comput.*, V.22, p.475-478.

Shippy MB, Petterson MT, Whitman RA, Shivers CR (1984) A clinical evaluation of the BTI Biox II ear oximeter. *Resp. Care.*, V.29, p.730-735.

Silverman DG, Lahossa DD, Barlow CH, Bering TG, Popky LM and Smith TC (1980) Quantification of tissue fluorescein delivery and prediction of flap viability with the fibreoptic dermofluorometer. *Plast. Reconstr. Surg.*, V.66, p.545.

Silverston P (1989) Pulse oximetry at the roadside : a study of pulse oximetry in immediate care. *British Medical J.* V.298, 18th March, p.711-713.

Smaje LH, Fraser PA, Clough G (1980) The distensibility of single capillaries and venules in the cat mesentery. *Microvasc. Res.*, V.20, p.358-370.

Smits TM and Aarnoudse JG (1984) Variability of fetal scalp blood flow during labour: continuous transcutaneous measurement by the laser Doppler technique. *British Journal of Obstetrics and Gynaecology*, June, V.91, p.524 -531.

Smits TM, Aarnoudse JG and Zijlstra WG (1989) Fetal scalp blood flow as recorded by laser Doppler flowmetry and transcutaneous pO2 during labour. *Early Human Development*, V.20, p.109-124.

Spence VA, Walker WF, Troup IM and Murdoch G (1981) Amputation of the ischaemic limb: selection of the optimum site by thermography. *Angiology*, V.32, p.65.

Spence VA, McCollum PT, McGregor IW, Sherwin SJ and Walker WF (1985) The effect of transcutaneous electrode on the variability of dermal oxygen tension changes. *Clin. Phys. Physiol. Meas.*, V.6, p.139.

Spence VA, McCollum PT, and Walker WF (1985) Comparative studies of cutaneous haemodynamics in regions of normal and reduced perfusions. In Practical Aspects of Skin Blood Flow Measurement (London: Biological Engineering Society) p.1-10.

SPSS/PC Base Manual (1988), SPSS International B.V., The Netherlands. Ch.11.

Squire JR (1940) Instrument for measuring quantity of blood and its degree of oxygenation in the web of the hand. *Clin. Sci.*, V.4, p.331-339.

Staberg B and Serup J (1988) Allergic and irritant skin reactions evaluated by laser Doppler flowmetry. *Contact Dermatitis*, V.18, p.40-45.

Stern MD (1975) In vivo evaluation of microcirculation by coherent light scattering. *Nature*, V.254, p.56-58.

Stern MD, Lappe DL, Bowen PD, Chimosky JE, Holloway GA, Keiser HR and Bowman RL (1977) Continuous measurement of tissue blood flow by laser-Doppler spectroscopy. *Am. J. Physiol.*, V.232(4): p.H441-H448.

Stern MD, Bowen PD, Parma R, Osgood RW, Bowman RL and Stein (1979) Measurement of renal cortical and medullary blood flow by laser-Doppler spectroscopy in the rat. *Am. J. Physiol.*, V.236(1), p.F80-F87.

Stevenson WH (1982) Laser Doppler velocimetry: A status report. *Proc. IEEE*, V.70, No.6, p.652-658.

Strohl KP and Altose MD (1984) Oxygen saturation during breath -holding and during apneas in sleep. *Chest*, V.85, No.2, p.181-186.

Stunberg S. and Castren M. (1986) Drug- and temperature -induced changes in peripheral circulation measured by laser-Doppler flowmetry and digital-pulse plethysmography. *Scandanavian Journal of Clinical and Laboratory Investigation*, V.46, p.359-365

Suzukawa M, Fujisawa M, Matsushita F, Suwa K, Yamamura H (1978) Clinical application of fingertip pulse wave oximeter. *Jpn. J. Anesthesiology*, V.27, p.6.

Svensson H., Pettersson H., and Svedman P. (1985) Laser Doppler flowmetry and laser photometry for monitoring free flaps. *Scandanavian Journal of Plastic Reconstructive Surgery*, V.19, p.245-249.

Swain ID and Grant LJ (1989) Methods of measuring skin blood flow. *Phys. Med. Biol.*, V.34, No.2, p.151-175.

Swedlow DB (1989) Monitoring in pediatric anesthesia. *Current Opinion in Anaesthesiology*, V.2, p.323-326.

Tanaka T, Riva C and Ben-Sira I (1974) Blood velocity measurements in human retinal vessels. *Science*, V.186, p.830-831.

Tanaka T and Benedek GB (1975) Measurement of the velocity of blood flow (in vivo) using a fiber optic catheter and optical mixing spectroscopy. *Appl. Optics*, V.14, No.1, p.189-196.

Takatani S, Cheung PW and Ernst EA (1980) A noninvasive tissue reflectance oximeter. An instrument for measurement of tissue haemoglobin oxygen saturation in vivo. *Annals of Biomed. Eng.*, V.8, p.1-15.

Takatani S (1978) On the theory and development of a noninvasive tissue reflectance oximeter. PhD Thesis. Biomedical Engineering Department, Case Western Reserve University, Cleveland, OH.

Taylor MB and Whitwam (1988) The accuracy of pulse oximeters: A comparative clinical evaluation of five pulse oximeters. *Anaesthesia* , V.43, p.229-232.

Tenland T. (1982) Laser Doppler flowmetry. Theory and microvascular applications. Ph.D Thesis, Linkoping, Sweden.

Tenland T., Salerud E.G., Nilsson G.E., and Oberg P.A. (1983) Spatial and temporal variations in human skin blood flow. *International Journal of Microcirculation: Clin. Exp.*, V.2, p.81-90.

Thalayasingam S and Delpy DT (1989) Thermal clearance blood flow sensor - sensitivity, linearity and flow depth discrimination. *Med. & Biol. Eng. & Comput.*, V.27, p.394 -398.

Tooke JE, Ostergren J and Fagrell B (1983) Synchronous assessment of human skin microcirculation by laser Doppler flowmetry and dynamic capillaroscopy. *Int. J. Microcirc: Clin. Exp.*, V.2, p.277-284.

Tooke (1987) The study of human capillary pressure. In Clinical Investigation of the Microcirculation. (Boston: Martinus Nijhoff Publishing). p.3-22.

Tooke JE and Smaje LH (1987) Clinical Investigation of the Microcirculation. (Boston: Martinus Nijhoff Publishing).

Tremper KK and Barker SJ (1987) Transcutaneous oxygen measurement: Experimental studies and adult applications. In Advances in Oxygen Monitoring Ed. Tremper KK and Barker SJ. Pub. Little, Brown and Cmpany. V.25, No.3, p.67-96.

Tremper KK and Barker SJ (1989) The optode: Next generation in blood gas measurement. *Crit. Care. Med.*, V.17, p.481-482.

Tremper KK and Barker SJ (1989) Pulse oximetry (editor Biebuyck JF) *Anesthesiology*, V.70, p.98-108.

Twersky V (1970) Interface effects in multiple scattering by large, low-refracting absorbing particles. *J. Opt. Soc. Am.*, V.60, p.908-914.

van den Brande P and Welch W (1988) Diagnosis of arterial occlusive disease of the lower extremities by laser Doppler flowmetry. *International Angiology*, V.7, p.224 -230.

Veyekemons F, Baele P, Guillaume JE, Willems E, Robert A, Clerbaux T (1989) Hyperbilirubinemia does not interfere with haemoglobin saturation measured by pulse oximetry. *Anesthesiology*, V.70, p.118-122.

Watkins D and Holloway GA (1978) An instrument to measure cutaneous blood flow using the Doppler shift of laser light. *IEEE Trans. Biomed. Eng.*, V.BME-25, No.1, p.28-33.

Waxman K, Lefcourt N and Achauer B (1989) Heated laser Doppler flow measurements determine depth of burn. *Am. J. Surg.*, V.157, p.541-543.

Weinman J, Hayat A and Raviv G (1977) Reflection photoplethysmography of arterial blood volume pulses. *Med. Biol. Engng. Comput*, V.15, p.22-31.

Whiton JT and Everall JD (1973) The thickness of the epidermis. *Brit. J. Dermatol.*, V.89, p.467-476.

Williams PC, Stern MD, Bowen PD, Brooks RA, Hammock MK, Bowman RL and Di Chiro G (1977) Mapping of cerebral cortical strokes in Rhesus monkeys by laser Doppler spectroscopy. *Medical Research Engineering*, V.13, No.2, p.3-5.

Wilson J and Hawkes JFB Optoelectronics : an introduction. Prentice-Hall International Series in Optoelectronics, 1983.

Wilson SB and Spence VA (1989) Dynamic thermographic imaging method for quantifying dermal perfusion: potential and limitations. *Med. & Biol. Eng. & Comput.*, V.27, p.496-501.

Wollersheim H, Reyenga J and Thien T (1988) Laser Doppler velocimetry of fingertips during heat provocation in normals and in patients with Raynaud's phenomenon. *Scand. J. Clin. Lab. Invest.*, V.48, p.91-95.

Wollersheim H and Thein TH (1988) Transcutaneous pO_2 measurements in Raynaud's phenomenon. Value and limitations. *Int. J. Microcirc: Clin. Exp.*, V.7, p.357 -366.

Woolfson AD, McCafferty DF, McGowan KE and Boston V (1989) Non -invasive monitoring of percutaneous local anaesthesia using laser Doppler velocimetry. *Int. J. Pharma.*, V.51, p.183-187.

Wood E, Geraci JE (1949) Photoelectric determination of arterial oxygen saturation in man. *J. Lab. Clin. Med.*, V.34, p.387-401.

Wood EH (1950) Oximetry. In Medical Physics, Ed. Glasser O, V.2, Year Book Publishers, Chicago.

Wukitsch MW, Petterson MT, Tobler DR and Pologe JA (1988) Pulse oximetry : Analysis of theory, technology and practice. *J. Clin. Monit.*, V.4, p.290-301.

Yeh Y and Cummins HZ (1964) Localized fluid flow measurements with an He-Ne laser spectrometer. *Appl. Phys. Letters*, V.4, No.10, p.176-178.

Yelderman M and New W (1983) Evaluation of pulse oximetry. *Anesthesiology* V.59, p.349-352.

Young CMA and Hopewell JW (1983) The isotope clearance technique for measuring skin blood flow. *Brit. J. Plastic Surg.*, V.36, p.222-230.

Yoshiya I, Shimada Y, Tanaka K (1980) Spectrophotometric monitoring of arterial oxygen saturation in the fingertip. *Med. & Biol. Eng. & Comput.*, V.18, p.27-32.

Zijlstra WG and Mook GA (1962) Medical reflection photometry. Van Gorcum's medical library, Assen, The Netherlands. p.1-271.

Zorab JSM (1988) Who needs pulse oximetry ? *British Medical J.*, V.296, p.658-659.

Zweifach BW (1974) Quantitative studies of microcirculatory structure and function. *Circulatory Res.*, V.34, June, p.843-866.